ZooKeys 637: 1–20 (2016)
doi: 10.3897/zookeys.637.9909
http://zookeys.pensoft.net

RESEARCH ARTICLE

A peer-reviewed open-access journal
ZooKeys
Launched to accelerate biodiversity research

Complete mitochondrial genomes of two flat-backed millipedes by next-generation sequencing (Diplopoda, Polydesmida)

Yan Dong[1], Lixin Zhu[1], Yu Bai[1], Yongyue Ou[1], Changbao Wang[1]

1 *College of Biology and Food Engineering, Chuzhou University, Chuzhou 239000, China*

Corresponding author: *Yan Dong* (dongyan_bio@126.com)

Academic editor: *Pavel Stoev* | Received 17 July 2016 | Accepted 17 November 2016 | Published 28 November 2016

http://zoobank.org/A53FB0CA-30EC-4B71-AFD6-D00AE30218F7

Citation: Dong Y, Zhu L, Bai Y, Ou Y, Wang C (2016) Complete mitochondrial genomes of two flat-backed millipedes by next-generation sequencing (Diplopoda, Polydesmida). ZooKeys 637: 1–20. https://doi.org/10.3897/zookeys.637.9909

Abstract

A lack of mitochondrial genome data from myriapods is hampering progress across genetic, systematic, phylogenetic and evolutionary studies. Here, the complete mitochondrial genomes of two millipedes, *Asiomorpha coarctata* Saussure, 1860 (Diplopoda: Polydesmida: Paradoxosomatidae) and *Xystodesmus* sp. (Diplopoda: Polydesmida: Xystodesmidae) were assembled with high coverage using Illumina sequencing data. The mitochondrial genomes of the two newly sequenced species are circular molecules of 15,644 bp and 15,791 bp, within which the typical mitochondrial genome complement of 13 protein-coding genes, 22 tRNAs and two ribosomal RNA genes could be identified. The mitochondrial genome of *A. coarctata* is the first complete sequence in the family Paradoxosomatidae (Diplopoda: Polydesmida) and the gene order of the two flat-backed millipedes is novel among known myriapod mitochondrial genomes. Unique translocations have occurred, including inversion of one half of the two genomes with respect to other millipede genomes. Inversion of the entire side of a genome (*trnF-nad5-trnH-nad4-nad4L*, *trnP*, *nad1-trnL2-trnL1-rrnL-trnV-rrnS*, *trnQ*, *trnC* and *trnY*) could constitute a common event in the order Polydesmida. Last, our phylogenetic analyses recovered the monophyletic Progoneata, subphylum Myriapoda and four internal classes.

Keywords

gene order, mitochondrial genome, Myriapoda, next-generation sequence, Polydesmida

Introduction

The Myriapoda comprise more than 18,000 species worldwide and are a diverse and ecologically important group of terrestrial arthropods (Miyazawa et al. 2014). Four groups have been united as Myriapoda: the Chilopoda (centipedes) and Diplopoda (millipedes), containing the vast majority of species, and the poorly investigated Pauropoda and Symphyla. An ancient group, the myriapods inhabited Pangea, and as a result they occur on all continents today except for Antarctica (Edgecombe 2004, 2010). Diplopoda (millipedes) is the third most diverse class of Arthropoda, with more than 11,000 species described and an estimated diversity of 80,000 species (Sierwald and Bond 2007; Shelley 2007; Zhang 2011; Brewer et al. 2012; Enghoff et al. 2015). Millipedes are an important component of modern terrestrial ecosystems and play a major role in the breakdown of organic matter (Hopkin and Read 1992). However, there are few studies documenting aspects of the group's phylogeny, evolution, behavior, physiology, and ecology (Hoffman et al. 2002).

Extant myriapods have not been the subject of extensive molecular phylogenetic study and studies that have been done tend to focus on relationships at the phylum level. Comparative morphological, molecular and higher-level systematic evidence has largely confirmed the monophyly of myriapods (Boudreaux 1979; Ax 1999; Bitsch and Bitsch 2004; Gai et al. 2006; Bäcker et al. 2008; Regier et al. 2008, 2010; Rehm et al. 2014; Fernández et al. 2016), even though this was once a controversial topic (Pocock 1893; Snodgrass 1952; Dohle 1980). The phylogeny of the millipedes is still an open topic regarding their position within the Myriapoda and earliest splits inside the diplopod lineage (Edgecombe 2011; Fernández et al. 2016).

Mitochondrial genomes are used extensively to study phylogeography and phylogenetic relationships (Boore et al. 1998; Gissi et al. 2008; Cameron 2014). In addition to the sequences of mitochondrial genes, the secondary structures of RNAs as well as the mitochondrial gene order have been explored in a phylogenetic context (Boore 1999; Carapelli et al. 2004; Chen et al. 2011; Song et al. 2016). As in most other arthropods, myriapod mitochondrial (mt) genomes are a single circular DNA molecule encoding 13 proteins, 22 transfer RNAs (tRNAs), two ribosomal RNAs (rRNAs), and one A+T-rich region involved in the control of mtDNA replication and transcription.

Gene order in the centipede *Cermatobius longicornis* and the millipede *Prionobelum* sp. is identical to that of *Limulus polyphemus* (Arthropoda: Xiphosura) (Lavrov et al. 2000a; Dong et al. 2012b; Brewer et al. 2013; Gai et al. 2013). However, the arrangement of genes in mt genomes is remarkably variable in *Strigamia maritima* (Chilopoda: Geophilomorpha) and *Symphylella* sp. (Symphyla: Scolopendrellidae) (Gai et al. 2008; Robertson et al. 2015). All millipedes in which the mt genome has been sequenced, except Sphaerotheriida, have *nad6* + *cob* placements that differ from that of *Limulus Polyphemus* and the *nad6* + *cob* pattern was supposed to be sound molecular evidence supporting the Helminthomorpha clade. Dong et al. (2012a) compared nine known myriapod mt genomes and posited that a translocation of *trnT* out of the 5' end of *nad4L* is a common event in derived progoneate lineages. Although taxon sampling is limited, gene synteny has supplied evolutionary evidence relating to Myriapoda phylogenetic and

evolutionary history. Full mitochondrial genomes of sixteen myriapod species have hitherto been sequenced, however, this number is still far from sufficient considering the high species richness of this group (Sierwald and Bond 2007; Budd and Telford 2009; Dong et al. 2012a; Robertson et al. 2015). This lack of mitochondrial genome data is hampering phylogenetic and evolutionary studies within the subphylum Myriapoda.

Compositional heterogeneity and accelerated substitution rates have proven to be major sources of systematic bias in mtDNA based phylogeny (Rota-Stabelli et al. 2011). Avoiding inadequate outgroups, selecting conserved amino acid alignment regions and bolstering taxon sampling are keys to phylogenetic reconstruction using mt genomes (Rota-Stabelli et al. 2011; Chen et al. 2014; Robertson et al. 2015). However, complete representation of the four myriapod classes in many studies is not included (Rota-Stabelli et al. 2011; Brewer et al. 2013) and the mt genomes of class Pauropoda, the presumed sister lineage of millipedes, are available in Genbank but not included in previous studies (Brewer et al. 2013). Relationships among the Myriapoda remain unresolved in Robertson et al. (2015), including among the four classes.

Prior to our study, the mt genomes of one flat-backed millipede representing the family Xystodesmidae: *Appalachioria falcifera* (Keeton, 1959) was sequenced. In this species, the entire side of the mt genome is inverted and all genes are on a single strand. Whole genome shotgun reads sequenced with the Illumina sequencing platform were used to obtain two complete mt genomes from the millipedes *Asiomorpha coarctata* and *Xystodesmus* sp. These species are representatives of the families Paradoxosomatidae and Xystodesmidae and further our understanding of how gene rearrangement occurred in the Polydesmida. Phylogenetic analysis including myriapods, three other arthropod classes and outgroups (species of Onychophora and Priapulida) were also performed to explore the internal relationships within the Myriapoda using sequence alignments from mitochondrial genes.

Methods

Taxon sampling, DNA extraction and PCR

Specimens of *Asiomorpha coarctata* and *Xystodesmus* sp. were collected from Langya Mountain, Chuzhou, Anhui, China (32°16'N, 118°16'E) and stored at the Molecular Biology Laboratory, Chuzhou University, Chuzhou, Anhui, China (MBLCZU). Species identification was performed by Dong Y (first author) and Qian CY (Shanghai Institutes for Biological Sciences, Chinese Academy of Sciences, Shanghai, China). Voucher specimens (MBLCZU000145, MBLCZU000146) were deposited at the MBLCZU. Total genomic DNA was extracted from one individual representing each species using the DNeasy tissue Kit (Qiagen China, Shanghai).

Standard PCR reactions to amplify three different fragments of mtDNA (*cox1*, *cob* and *nad5*) were undertaken for each sample. Primers are listed in Suppl. material 1: Table S1. Amplified PCR products were gel-purified and then analyzed by primer walking on an ABI-PRISM3730 Automated DNA Sequencer.

Genome sequencing and analyses

For Illumina sequencing, double index sequencing libraries with average insert sizes of around 300 bp were prepared. The libraries were sequenced as 250 bp paired-end runs on an Illumina Hi-Seq 2000 (about 2 Gb raw data each species). The resulting bait sequences (*cox1*, *cob* and *nad5*) were subsequently employed as references in the manner detailed below. De novo assemblies were conducted with Geneious v8.1 using the Map to Reference program with the following settings applied: medium-low sensitivity/fast; iterate up to five times; with a maximum of 2% mismatches, a maximum gap size of 3 bp and requiring a minimum overlap of 100 bp; do not trim. After manual inspection, the longest contigs resulting from the respective assemblies were then aligned and ensured for correct translation frames with MEGA v5.0, together with reference protein-coding gene sequences from seven millipedes (*Narceus annularus*, *Thyropygus* sp., *Antrokoreana gracilipes*, *Appalachioria falcifera*, *Abacion magnum*, *Brachycybe lecontii*, *Prionobelum* sp.). The contig ends of *A. coarctata* and *Xystodesmus* sp. overlapped.

Mitochondrial genome annotation and analyses

The assembled consensus sequence of each millipede mtDNA was further annotated and analyzed. Preliminary annotation using MITOS webserver provided overall information on mt genomes (Bernt et al. 2013). Protein-coding genes were annotated by identification of their open reading frames, and alignments of homologous genes of other reported myriapod mt genomes. Blast searches in the National Center for Biotechnology Information also helped to identify and annotate the PCGs. Transfer RNA genes were identified by comparing the results predicted by tRNAscan-SE Search Server v.1.21 and ARWEN based on cloverleaf secondary structure information (Lowe and Eddy 1997; Laslett and Canback 2008). Based on known gene order information, the boundaries of the 16S rRNA (rrnS) gene were assumed to be delimited by the ends of the *trnV* and *trnL2* pair. The 12S rRNA (*rrnL*) gene was assumed to start from the end of *trnV*, and its end was roughly identified by alignment with other published millipede sequences. Nucleotide frequencies and codon usage were determined by MEGA v5.05 (Tamura et al. 2007).

Data sets and sequence alignment

Phylogenetic trees were reconstructed focused on the Arthropoda defining Onychophora and Priapulida as outgroups in the analyses, including 31 taxa (Suppl. material 1: Table S2). Amino acid sequences of 13 mitochondrial protein-coding genes were aligned separately using Clustal X 1.81 based on default settings for each gene (Thompson et al. 1997) then used as guides to align nucleotide sequences. GenBank

accession numbers for taxa used in this study are given in Suppl. material 1: Table S1. Each alignment was analyzed with Gblocks under default settings to select conserved amino acid aligned regions (Castresana 2000).

Phylogenetic analyses

The optimal partition strategy and models were selected by PartitionFinder v1.1.1. We created an input configuration file that contained 13 pre-define partitions by gene. We used the 'greedy' algorithm with branch lengths estimated as 'unlinked' and Akaike Information Criterion (AIC) to search for the best-fit scheme (Suppl. material 1: Table S3). Model selection of the amino acid data set was performed with ProtTest version 2.4 (Abascal et al. 2007), and under AIC, MtRev+I+G was the best-fit model.

Maximum likelihood phylogenetic analysis searches were carried out with RAxML through a web portal (http://phylobench.vital-it.ch/raxml-bb/index.php). Bootstrap values, indicating the robustness of the internal nodes of the gene trees, were set at 100 replicates. Bayesian analyses of nucleotide and amino acid data sets were performed with MrBayes v3.1.2 (Ronquist and Huelsenbeck 2003), using the GTR+I+G model and MtRev+I+G model, respectively. Four Markov chains were run for 2×10^6 generations and sampled every 100 generations to yield a posterior probability distribution of 2×10^4 trees. The first 2000 trees were discarded as burn-in. Three replicates of these Bayesian runs were conducted, retrieving the same topology.

Results

Mitochondrial genome organization

The complete mt genome of *Asiomorpha coarctata* (GenBank accession KU721885) is 15,644 bp long and was assembled with coverage between 54–1062 reads; the genome of *Xystodesmus* sp. (GenBank accession KU721886) is 15,791 bp in length and has a coverage within 86–1392 reads. The sizes of these two mt genomes are within the range reported for those of other myriapods ranging from 14,487–16,833 bp (GenBank accessions NC_016676 and NC_021403).

The two genomes encode 13 protein-coding regions, 22 tRNA and two rRNA genes, consistent with metazoan mitochondrial DNA structure, but contain a number of unique features (Figure 1). Most protein-coding genes start with the codon ATG, with the exception of *nad1*, *nad2*, *nad3*, and *nad4*, which begins with TTG, TTG, GTG, and GTG, respectively. Seven protein-coding genes use the typical termination codons TAG (*cox1*, *cox2*, *nad4L*, *nad4* and *nad5*) and TAA (*atp8* and *nad1*), while others in the mt genome of *A. coarctata* use incomplete stop codons (Table 1). Several genes show complete stop codons, either TAG (as in *cox1*, *cox2*, *nad3*, *nad4L* and *nad5*) or TAG (as in *atp8* and *cytb*) in *Xystodesmus* sp. (Table 2). Incomplete stop

Table 1. Organization of the mitochondrial genome of *Asiomorpha coarctata*.

Feature	From	To	Length (nt)	Codons		Spacer/Overlap(-)
				Start	Stop	
*cox*1	1	1533	1533	ATG	TAG	11
cox2	1545	2222	678	ATG	TAG	8
trnK	2231	2297	67	CTT		1
trnD	2299	2363	65	GTC		0
atp8	2364	2522	159	ATG	TAA	-7
atp6	2516	3182	667	ATG	TA	0
cox3	3183	3967	785	ATG	TA	0
trnG	3968	4031	64	TCC		0
nad3	4032	4381	334	GTG	TA	0
trnA	4382	4443	62	TGC		0
trnR	4444	4509	66	TCG		2
trnN	4512	4579	68	GTT		0
trnS1	4580	4638	69	GCT		0
trnE	4639	4703	65	TTC		0
nad6	4704	5176	473	ATG	AGT	0
cytb	5177	6297	1121	ATG	TA	0
trnS2	6298	6358	61	TGA		0
CR1	6359	7321	963			0
rrnS	7322	8097	776			0
trnV	8098	8162	65	TAC		0
rrnL	8163	9402	1240			0
trnL1	9403	9465	63	TAG		0
trnL2	9469	9533	65	TAA		3
nad1	9534	10460		TTG	TAA	0
trnP	10461	10524	64	CCA		0
nad4L	10525	10806	62	ATG	TAG	0
nad4	10800	12143	1344	GTG	TAG	0
trnT	12144	12206	63	TGT		0
CR2	12207	12393	187			0
trnH	12394	12458	65	GTG		1
nad5	12460	14160	1701	ATG	TAG	3
trnF	14164	14231	68	GAA		0
trnY	14232	14299	68	GTA		1
trnQ	14301	14371	71	TTG		0
trnC	14372	14436	65	GCA		0
trnI	14437	14503	67	GAT		0
trnM	14504	14570	67	CAT		0
nad2	14571	15575	1005	TTG	GGA	0
trnW	15576	15644	69	TCA		0
Total		15644				-7/30

Table 2. Organization of the mitochondrial genome of *Xystodesmus* sp.

Feature	From	To	Length (nt)	Codons		Spacer/Overlap(-)
				Start	Stop	
cox1	1	1533	1533	ATG	TAG	6
cox2	1540	2217	678	ATG	TAG	3
trnK	2221	2287	67	CTT		0
trnD	2288	2351	64	GTC		0
atp8	2352	2513	162	ATG	TAA	-7
atp6	2507	3175	669	ATG	TA	0
cox3	3179	3963	785	ATG	TA	0
trnG	3964	4029	66	TCC		0
nad3	4030	4380	351	GTG	TAG	1
trnA	4382	4445	64	TGC		4
trnR	4450	4514	65	TCG		3
trnN	4518	4579	68	GTT		0
trnS1	4580	4640	61	GCT		2
trnE	4643	4710	68	TTC		2
nad6	4713	5181	469	ATG	T	0
cytb	5182	6303	1122	ATG	TAA	0
trnS2	6304	6360	57	TGA		0
CR1	6361	7392	963			0
rrnS	7393	8172	780			0
trnV	8173	8238	66	TAC		0
rrnL	8239	9465	1227			0
trnL1	9466	9530	65	TAG		51
trnL2	9582	9650	69	TAA		3
nad1	9651	10575	925	TTG	T	0
trnP	10576	10640	65	TGG		2
nad4L	10643	10924	282	ATG	TAG	0
nad4	10918	12264	1347	GTG	TAA	1
trnT	12266	12327	62	TGT		0
CR2	12328	12535	208			0
trnH	12536	12599	64	GTG		1
nad5	12602	14299	1698	ATG	TAG	3
trnF	14303	14369	67	GAA		0
trnY	14370	14434	65	GAT		15
trnQ	14450	14515	66	TTG		2
trnC	14518	14582	65	GCA		3
trnI	14586	14650	65	GAT		0
trnM	14651	14716	66	CAT		0
nad2	14717	15722	1006	TTG	T	0
trnW	15723	15790	68	TCA		1
Total		15791				-7/103

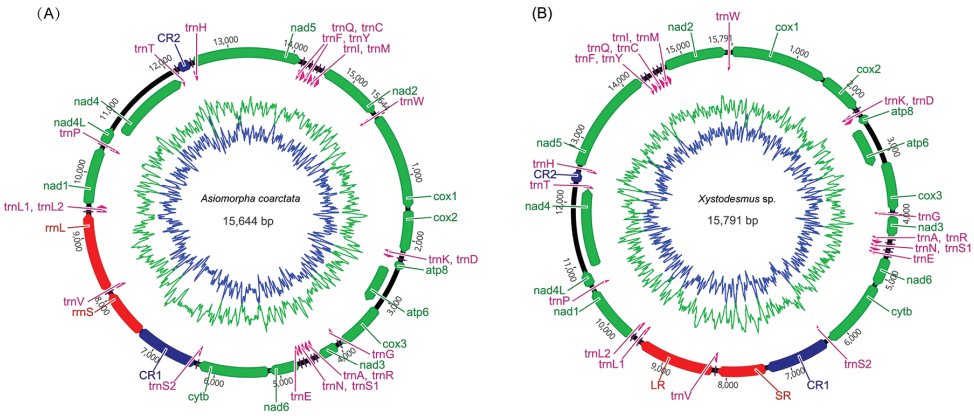

Figure 1. Mitochondrial genomes of the two millipedes sequenced in this study. **A** *Asiomorpha coarctata* **B** *Xystodesmus* sp. Circular maps were drawn with Geneious v9.1.2. Arrows indicate the orientation of gene transcription. Abbreviations of gene names are: *atp6* and *atp8* for ATP synthase subunits 6 and 8; *cox1–3* for cytochrome oxidase subunits 1–3; *cob* for cytochrome b, *nad1–6* and nad4L for NADH dehydrogenase subunits 1–6 and 4L; and lrRNA and srRNA for large and small rRNA subunits. tRNA genes are indicated with their one-letter corresponding amino acids. CR for control region. The GC content was plotted using a green sliding window and the AT content was blue.

codons are frequently found in other myriapod mitochondrial protein-encoding genes (Dong et al. 2012a) and may be completed by polyadenylation after cleavage of the polycistronic transcript (Ojala et al. 1981). Both novel genomes have an overlapping gene region only between *atp8*/*atp6*.

Non-coding regions

Some millipede mt genomes that have been sequenced (e.g. *Antrokoreana gracilipes*) include two major non-coding regions and others contain a single non-coding region, such as *Narceus annularus*, *Prionobelum* sp. and *Appalachioria falcifera* (Figure 5). Of the genomes sequenced here, *Asiomorpha coarctata* and *Xystodesmus* sp. include two major non-coding regions (Table 1 and 2).

The largest non-coding region (CR1, 963 bp) is located between *trnS2* and *rrnS* in *A. coarctata* (Table 1). The non-coding region in *A. coarctata* contains tandemly repeated regions (11.4 × 38 bp), and the repeated unit is 'GTAATAATATAGATA-GAGTAATATAACCTTATATAGGA' (Figure 2).

Transfer RNA

There are 22 potential tRNA genes in *Asiomorpha coarctata* and *Xystodesmus* sp., respectively (Figure 3 and 4), as there are in most other published metazoan mtDNAs (Gissi

```
Consensus pattern (38 bp): GTAATAATATAGATAGAGTAATATAACCTTATATAGGA
                 Repeats: ------------------------------TAATATAACCTTATATAGGA
                          GTAATAATATAGATAGAGTAATATAACCTTATATAGGA
                          GTAATAATATAGATAGAGTAATATAACCTTATATAGGA
                          GTAATAATATAGATAGAGTAATATAACCTTATATAGGA
                          GTAATAATATAGATAGAGTAATATAACCTTATATAGGA
                          GTAATAATATAGATAGAGTAATATAACCTTATATAGGA
                          GTAATAATATAGATAGAGTAATATAACCTTATATAGGA
                          GTAATAATATAGATAGAGTAATATAACCTTATATAGGA
                          GTAATAATATAGATAGAGTAATATAACCTTATATAGGA
                          GTAATAATATAGATAGAGTAATATAACCTTATATAGGA
                          GTAATAATATAGATAGAGTAATATAACCTTATATAGGA
                          GTAATAATATAGATAG--------------------------------------
```

Figure 2. Sequences of the non-coding region in *Asiomorpha coarctata,* primary structures of tandemly repeated regions (11.4 × 38 bp).

et al. 2008). All of these tRNA genes are α-strand-encoded bearing more protein-coding sequence (Figure 1), and the newly sequenced mt genomes show dihydrouridine arm (DHU arm, D-arm) loss in *trnS1* and *trnS2*. According to our analysis based on the ARWEN program, *trnS1* lacks the D-arm in all other millipede species.

Gene order

Gene order arrangements were compared with mt genome organization in other myriapods (Figure 5), including the ancestral gene order of the mitogenome for the Myriapoda shared by *Prionobelum* sp. and *Limulus polyphemus* (Dong et al. 2012b). The overall arrangement of the genes around the *A. coarctata* and *Xystodesmus* sp. mt genomes is unique compared to other myriapod species. All coding regions are on a single strand in *A. coarctata* and *Xystodesmus* sp. which has been reported in the mt genome of the millipede *Appalachioria falcifera* with an entire side of the genome inverted (Brewer et al. 2013). These three flat-backed millipedes are identical but for a single tRNA translocation in *A. coarctata* and *Xystodesmus* sp. The two newly sequenced mt genomes have undergone gene and tRNA translocations compared to other myriapod sequences.

Phylogenetic inference

Bayesian inference and maximum likelihood phylogenetic analysis were performed using conserved blocks of amino acid and nucleotide data sets (Figure 6). The topological pattern obtained using Bayesian inference and maximum likelihood analyses based on both the amino acid and nucleotide data sets were similar.

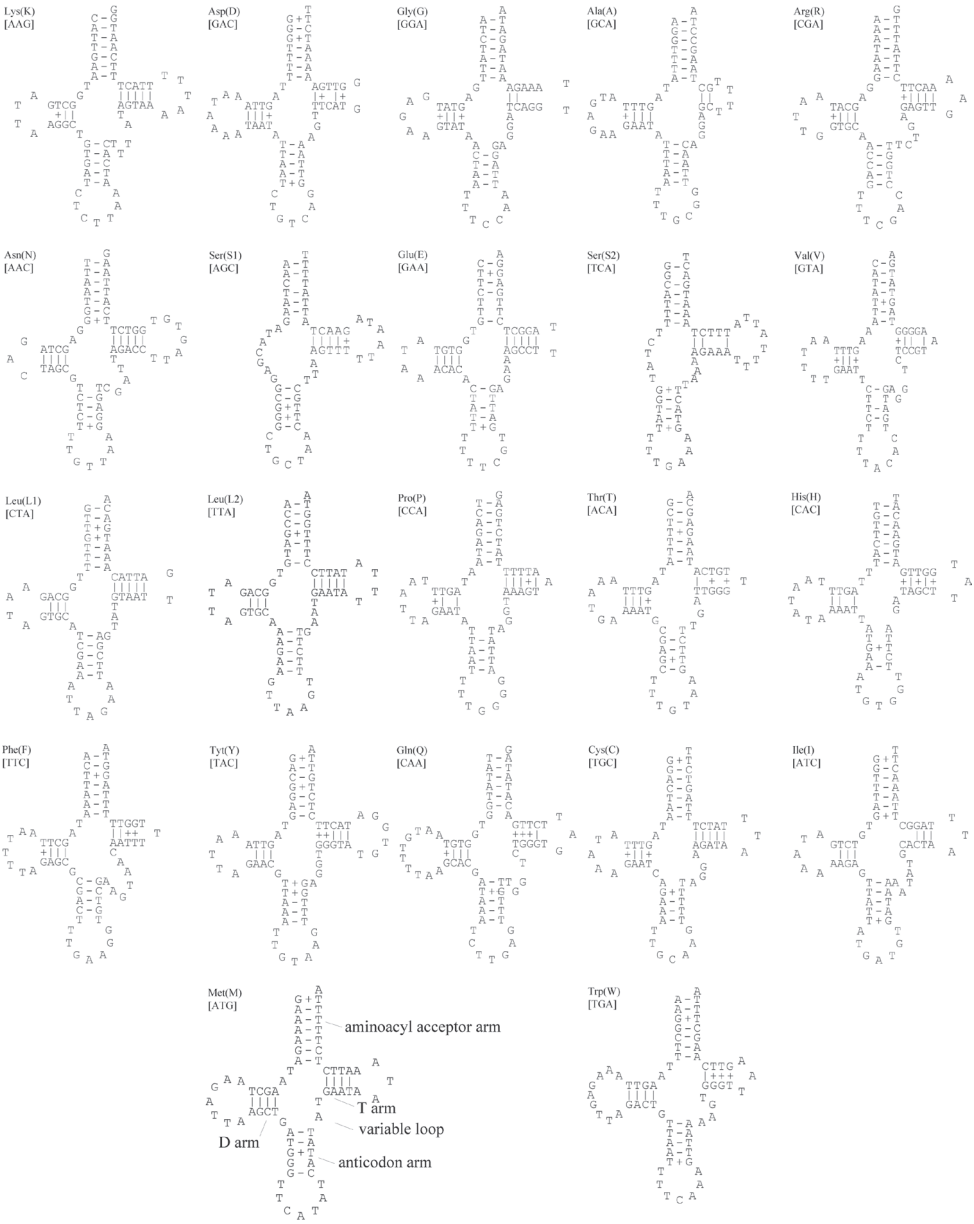

Figure 3. Putative secondary structures of the 22 tRNA genes of *Asiomorpha coarctata.* Watson-Crick base-pairing is indicated by solid lines, and G–T pairs are indicated with plus signs.

Within the Diplopoda, the Polydesmida clade, including *Appalachioria falcifera*, *Asiomorpha coarctata*, and *Xystodesmus* sp. is well supported. A clade consisting of Polydesmida plus Colobognatha (*Brachycybe lecontii*) is also recovered. All millipedes in this study except *Prionobelum* sp. recovered as a monophyletic group, Helminthomorpha.

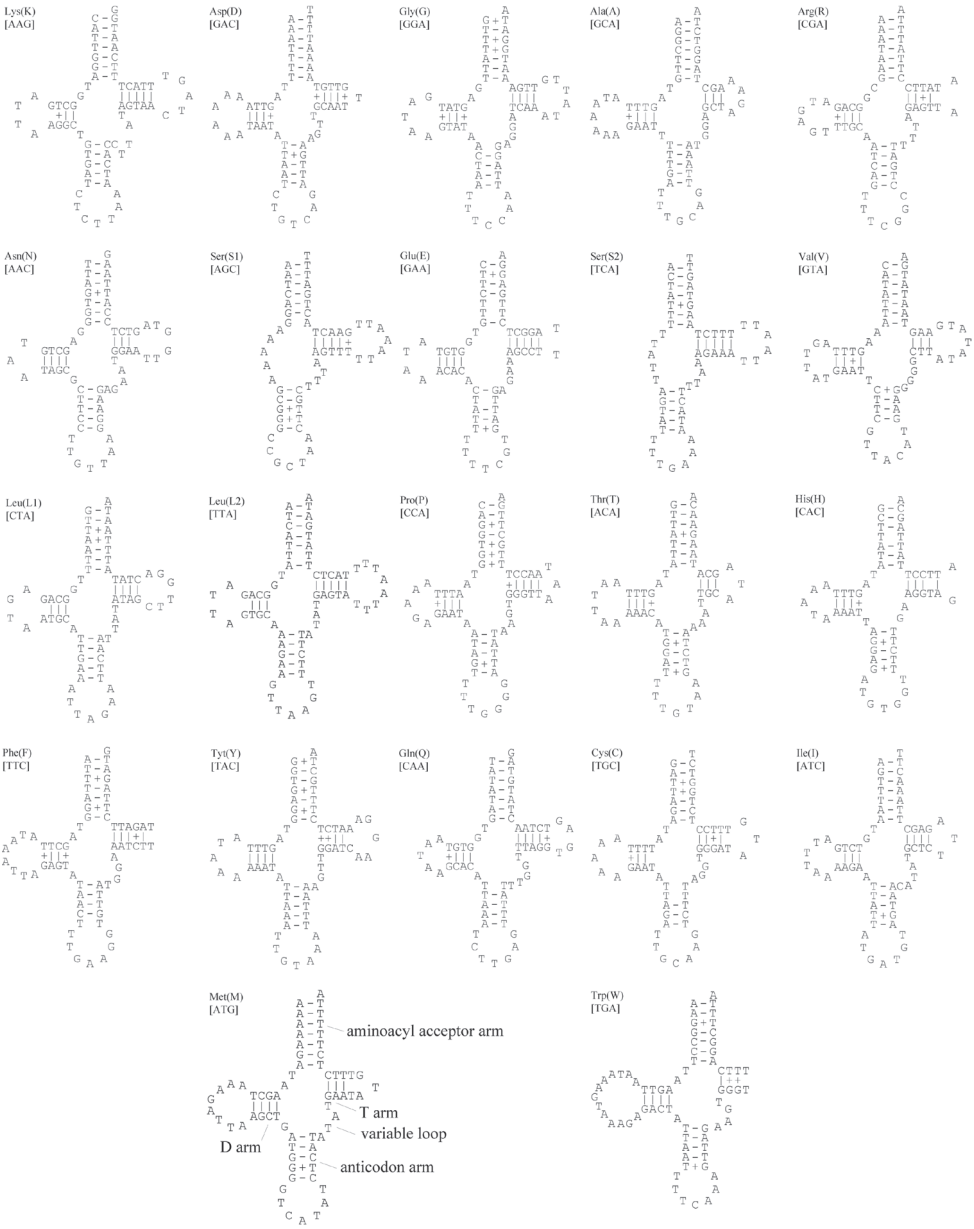

Figure 4. Putative secondary structures of the 22 tRNA genes of *Xystodesmus* sp. Watson-Crick base-pairing is indicated by solid lines, and G–T pairs are indicated with plus signs.

The grouping with Helminthomorpha and Pentazonia (the basal lineage *Prionobelum* sp.) is supported.

Four myriapod clades are resolved, with Chilopoda (BPP = 1.00 and 1.00; MLBP = 99 and 98) as the basal group. A monophyletic Progoneata ("Symphyla + Pauropoda" +

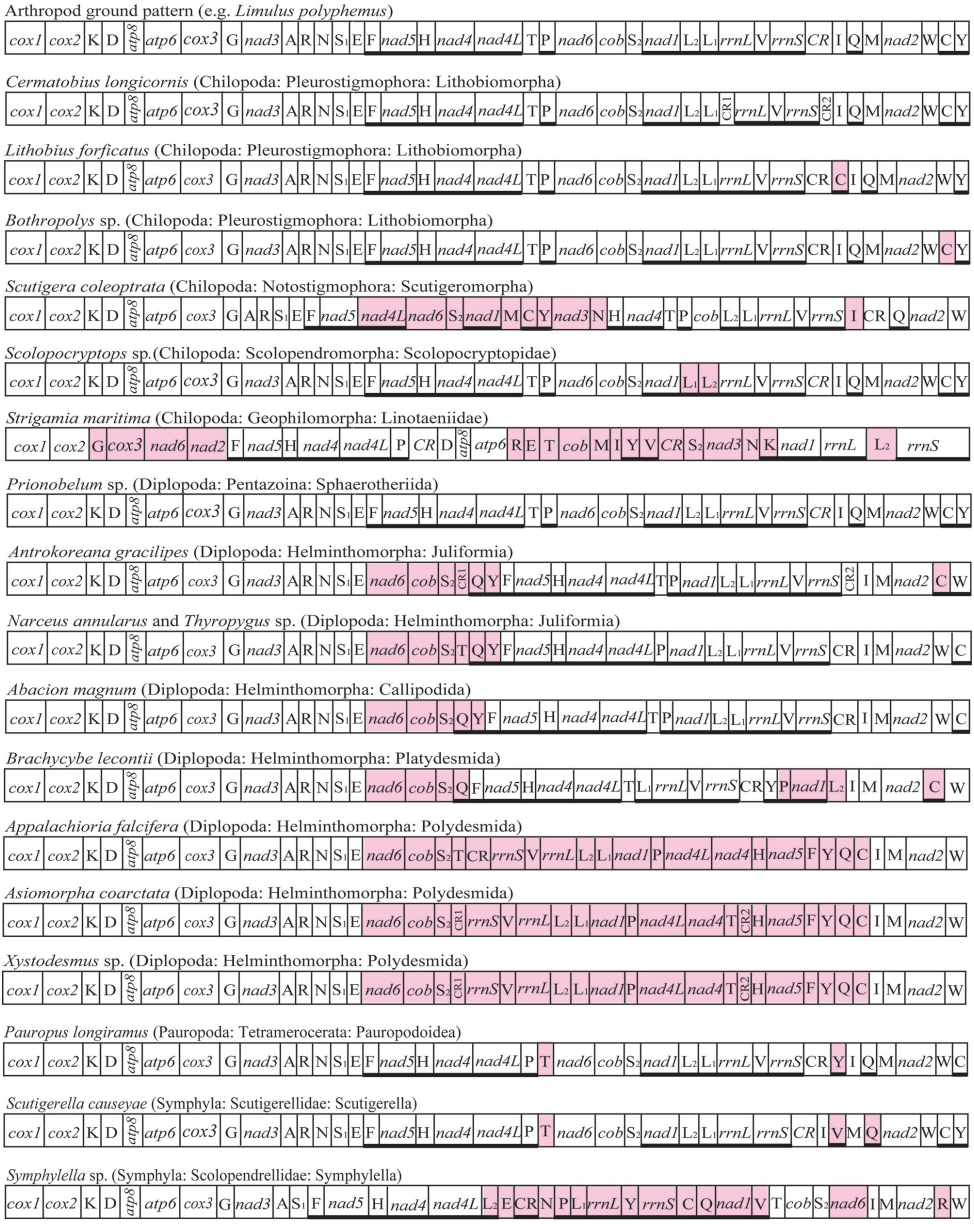

Figure 5. Comparison of gene arrangements in mtDNA of the arthropod ground pattern. Gene segments are not drawn to scale. Genes shaded gray have different relative positions compared to the ground pattern. Underlining indicates the gene is encoded on the opposite strand, and arrows indicate translocation of *trnT*. CR: putative control region. Gene arrangements of two diplopods, *N. annularus* and *Thyropygus* sp. are similar and represented as one.

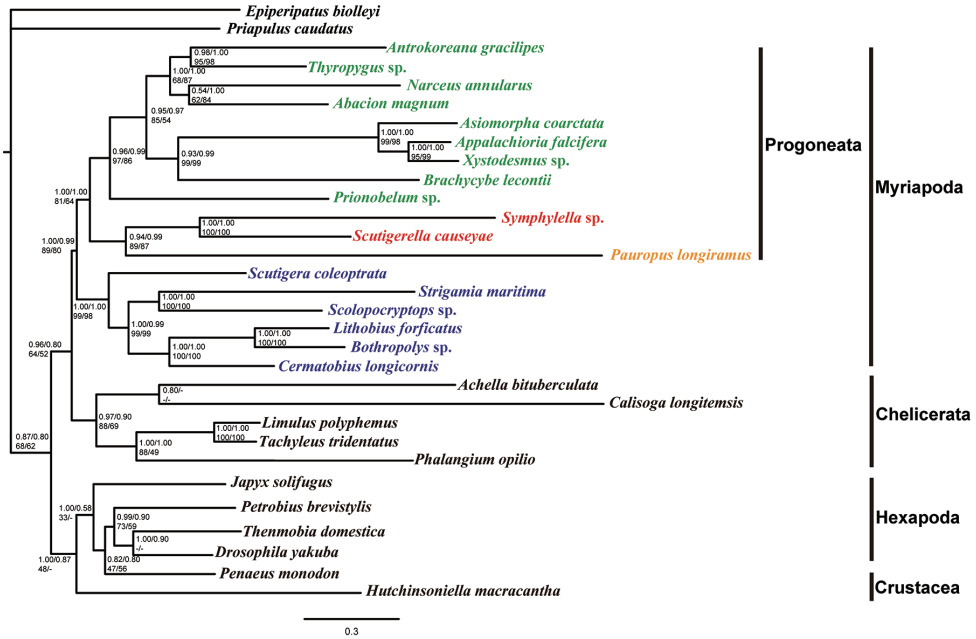

Figure 6. Phylogenetic tree of the Arthropoda, including Myriapoda, Hexpoda, Crustacea and Chelicerata and outgroups reconstructed based on protein-coding genes from mtDNA genomes. Each group of four numbers indicates node confidence values (from top left): Bayesian posterior probabilities in percent (BPP) in amino acid and nucleotide datasets; maximum likelihood bootstrapping values (MLBP) in amino acid and nucleotide datasets.

Diplopoda) is recovered as the sister group of the Chilopoda (BPP = 1.00 and 0.99; MLBP = 89 and 80). Our Bayesian inference analysis recognizes a monophyletic Myriapoda with strong support, while the maximum likelihood analysis is only weakly supported.

Discussion

Next-generation sequencing such as the 454 pyrosequencing, Solexa, and SOLiD provided by Roche, Illumina and Applied Biosystems, has the ability to generate a large number of sequences within a very short time compared to Sanger's method (Chilana et al. 2012). These methods have been fused to rapid generate sequence data and successful de novo sequence assemblies for arthropods (Kirkness et al. 2010) and more recently to the assembly of full mt genomes (Knaus et al. 2011; Ma et al. 2012; Coates 2014; Aguado et al. 2016). Next-generation sequencing results in better assembly, leading to fewer gaps, larger contigs and greater accuracy of the final consensus sequence. It is essential for accurately identifying more complex rearrangements, for example in the order Polydesmida, which has a large inversion in the mt genome in this study.

We found that the genome size was larger in *A. coarctata* (15,644 bp) and *Xystodesmus* sp. (15,791 bp) than other millipede mt genomes (14747–15282 bp; *Antrokoreana gracilipes*, GenBank accession NC_010221; *Appalachioria falcifera*, GenBank accession NC_021933). Intergenic spacer length variation may have arisen through retention of partial duplication, or incomplete multiple deletions of redundant genes (McKnight and Shaffer 1997; Yamauchi et al. 2003) under the duplication-and-deletion mechanism. For this reason, we speculate that multiple intergenic spacers distributed in the two larger mt genomes may serve as a guide in deducing derived gene arrangement.

Most of the tRNAs appear to be truncated and lack one of the arms found in the canonical tRNAs of pauropods and symphylans (Gai et al. 2008; Dong et al. 2012a). One to two nucleotide mismatches could be found in the acceptor arms of the five tRNAs in *A. coarctata,* and in the four tRNAs in *Xystodesmus* sp. Nucleotide mismatch in the arms of tRNAs may also occur in other myriapod groups (Woo et al. 2007; Lavrov et al. 2000b; Gai et al. 2008, 2013; Brewer et al. 2012; Dong et al. 2012a, 2012b).

Compared with other millipedes, the mt gene order in *A. coarctata* and *Xystodesmus* sp. is very similar to that in *Appalachioria falcifera*. These three species belong to the order Polydesmida (Figure 5). There are no differences in the relative position of the protein-coding genes, but the *trnT* gene and non-coding regions of *Appalachioria falcifera* mt genome are translocated with respect to the newly sequenced mt genomes here. Although only nine millipede mt genomes are compared, an extreme variety in gene arrangements is known in millipedes, and inversion of an entire side of the genome (*trnF-nad5-trnH-nad4-nad4L*, *trnP*, *nad1-trnL2-trnL1-rrnL-trnV-rrnS*, *trnQ*, *trnC and trnY*) could be a synapomorphy in the Polydesmida lineage.

Gene arrangement in three flat-backed millipedes is similar to that in other Helminthomorpha sequenced previously in which *nad6* + *cob* placements occurred. We agree with Brewer et al. (2013) that the inversion of the mt genome in flat-backed millipedes is a derived event associated with losing the second non-coding region. The mitochondrial gene arrangements of the order Polydesmida and the infraclass Helminthomorpha lineages are reshuffled regularly. To better understand the evolutionary implications of gene arrangements in the Myriapoda, mt genome research with broader taxon sampling will be required.

This phylogenomic study provides a strongly supported phylogenetic framework for the monophyletic origin of the Myriapoda and the monophyly of the Progoneata and extant myriapod subgroups. Among the Myriapoda, the union of Diplopoda with Pauropoda as a monophyletic group (= Dignatha) was once widely accepted (Dohle 1980, 1998; Enghoff et al. 1993; Blanke and Wesener 2014; Edgecombe 2015), but a number of molecular analyses of nuclear and mitochondrial sequences support the combination of Pauropoda and Symphyla (Gai et al. 2006; Regier et al. 2010; Dong et al. 2012a). Our results strongly support the traditional morphology-based Progoneata (Diplopoda + Pauropoda + Symphyla) defined by the presence of gonopores behind the second pair of legs. The notion of Progoneata recovered here is consistent with that favored by morphology and molecular analyses (Gai et al. 2008; Edgecombe 2010, 2011; Regier et al. 2010; Dong et al. 2012a).

The Polydesmida and Helminthomorpha are recovered as monophyletic. Gene order in *Prionobelum* sp. which is the basal lineage of the millipede mt genome is assumed to represent the millipede or myriapod ground pattern (Dong et al. 2012b), and inversion of the entire side of the genome occurred as a common event in the order Polydesmida lineage proposed in this study. In our gene order comparison of these millipedes, phylogenetic results are mainly concordant with gene arrangement analyses (Figure 5). Combining the implications of phylogenetic analyses and gene arrangement could yield valuable understanding of myriapod evolutionary history.

Polydesmida has been considered the sister group of Juliformia and a 'ring-forming' clade from the perspective of morphology (Enghoff et al. 1993). Polydesmida also unite the Nematophora (including Stemmiulida, Callipodida and Chordeumatida) as sister group for the shared presence of preanal spinnerets (Enghoff 1984; Sierwald et al. 2003; Shear 2008; Blanke and Wesener 2014). The Polydesmida allied with Platydesmida (basal representatives of the subclass Colobognatha) as a clade in our phylogenetic analyses. The combination Polydesmida + Colobognatha has been recovered in previous analyses (Sierwald and Bond 2007; Brewer et al. 2013). More taxa must be sequenced from the Colobognatha and better analysis methods used to test the position of the Polydesmida.

Many internal relationships of the Diplopoda remain unresolved and several groups are paraphyletic. The Bayesian inference tree seems to have better support at shallower nodes with amino acid data sets, whereas the maximum likelihood tree has better support at deeper nodes. The maximum likelihood tree has very low support at most nodes and confuses the relationships of taxa that are confidently placed in monophyletic groups by other studies (Meusemann et al. 2010; Regier et al. 2010; Brewer et al. 2013). Our finding that the Bayesian methods outperformed likelihood-based approaches is consistent with the results reported by Talavera and Castresana (2007).

Acknowledgements

The authors declare no competing interests. Special thanks to Pavel Stoev and three reviewers for constructive comments that improved this paper. This research was supported by the National Natural Science Foundation of China Project (31401971), Anhui Provincial Natural Science Foundation (1408085QC67), and Natural Science Foundation of the Higher Education Institutions of Anhui Province (KJ2013Z245).

References

Abascal F, Posada D, Zardoya R (2007) MtArt: a new model of amino acid replacement for Arthropoda. Molecular Biology and Evolution 24: 1–5. doi: 10.1093/molbev/msl136

Aguado MT, Grande C, Gerth M, Bleidorn C, Noreña C (2016) Characterization of the complete mitochondrial genomes from Polycladida (Platyhelminthes) using next-generation sequencing. Gene 575: 199–205. doi: 10.1016/j.gene.2015.08.054

Ax P (1999) Das System der Metazoa II. Ein Lehrbuch der phylogenetisch en Systematik. Gustav Fischer Verlag, Stuttgart, 384 pp.

Bäcker H, Fanenbruck M, Wägele JW (2008) A forgotten homology supporting the monophyly of Tracheata: the subcoxa of insects and myriapods. Zoologischer Anzeiger 247: 185–207. doi: 10.1016/j.jcz.2007.11.002

Bernt M, Donath A, Jühling F, Externbrink F, Florentz C, Fritzsch G, Pütz J, Middendorf M, Stadler PF (2013) MITOS: improved de novo metazoan mitochondrial genome annotation. Molecular Phylogenetics and Evolution 69(2): 313–319. doi: 10.1016/j.ympev.2012.08.023

Bitsch C, Bitsch J (2004) Phylogenetic relationships of basal hexapods among mandibulate arthropods: a cladistic analysis based on comparative morphological characters. Zoologica Scripta 33: 511–550. doi: 10.1111/j.0300-3256.2004.00162.x

Blankea A, Wesener T (2014) Revival of forgotten characters and modern imaging techniques help to produce a robust phylogeny of the Diplopoda (Arthropoda, Myriapoda). Arthropod Structure & Development 43(1): 63–75. doi: 10.1016/j.asd.2013.10.003

Boore JL (1999) Animal mitochondrial genomes. Nucleic Acids Research 27: 1767–1780. doi: 10.1093/nar/27.8.1767

Boore JL, Lavrov D, Brown WM (1998) Gene translocation links insects and crustaceans. Nature 392(6677): 667–668. doi: 10.1038/33577

Boudreaux HB (1979) Significance of inter segmental tendon system in arthropod phylogeny and a monophyletic classification of Arthropoda. In: Gupta AP (Ed.) Arthropod Phylogeny. Van Nostrand Reinhold Company, New York, 551–586.

Brewer MS, Sierwald P, Bond JE (2012) Millipede Taxonomy after 250 Years: Classification and Taxonomic Practices in a Mega-Diverse yet Understudied Arthropod Group. PLoS ONE 7(5): e37240. doi: 10.1371/journal.pone.0037240

Brewer MS, Swafford L, Spruill CL, Bond JE (2013) Arthropod Phylogenetics in Light of Three Novel Millipede (Myriapoda: Diplopoda) Mitochondrial Genomes with Comments on the Appropriateness of Mitochondrial Genome Sequence Data for Inferring Deep Level Relationships. PLoS ONE 8(7): e68005. doi: 10.1371/journal.pone.0068005

Budd GE, Telford MJ (2009) The origin and evolution of arthropods. Nature 457: 812–817. doi: 10.1038/nature07890

Cameron SL (2014) Insect mitochondrial genomics: implications for evolution and phylogeny. Annual Review of Entomology 59: 95–117. doi: 10.1146/annurev-ento-011613-162007

Carapelli A, Soto-Adames FN, Simon C, Frati F, Nardi F, Dallai R (2004) Secondary structure, high variability and conserved motifs for domain III of 12S rRNA in the Arthropleona (Hexapoda; Collembola). Insect Molecular Biology 13: 659–670. doi: 10.1111/j.0962-1075.2004.00528.x

Castresana J (2000) Selection of conserved blocks from multiple alignments for their use in phylogenetic analysis. Molecular Biology and Evolution 17(4): 540–552. doi: 10.1093/oxfordjournals.molbev.a026334

Chen WJ, Bu Y, Carapelli A, Dallai R, Li S, Yin WY, Luan YX (2011) The mitochondrial genome of *Sinentomon erythranum* (Arthropoda: Hexapoda: Protura): an example of highly dviergent evolution. BMC Evolutionary Biology 11: 246. doi: 10.1186/1471-2148-11-246

Chen WJ, Koch M, Mallatt JM, Luan YX (2014) Comparative analysis of mitochondrial genomes in Diplura (Hexapoda, Arthropoda): Taxon sampling is crucial for phylogenetic inferences. Genome Biology and Evolution 6(1): 105–120. doi: 10.1093/gbe/evt207

Chilana P, Sharma A, Rai A (2012) Insect genomic resources: status, availability and future. Current Science 102: 571–580.

Coates BS (2014) Assembly and annotation of full mitochondrial genomes for the corn rootworm species, *Diabrotica virgifera virgifera* and *Diabrotica barberi* (Insecta: Coleoptera: Chrysomelidae), using next generation sequence data. Gene 542: 190–197. doi: 10.1016/j.gene.2014.03.035

Dohle W (1980) Sind die Myriapoden eine monophyletische Gruppe? Eine Diskussionder Verwandtschaftsbeziehungen der Antennaten. Abhandl. Verhandl. Naturwiss.Ver Hamburg 23: 45–104.

Dohle W (1998) Myriapod–insect relationships as opposed to an insect–crustacean sister group relationship. In: Fortey RA, Thomas RH (Eds) Arthropod Relationships. Chapman and Hall, London, 305–315. doi: 10.1007/978-94-011-4904-4_23

Dong Y, Sun HY, Guo H, Pan D, Qian CY, Hao SJ (2012a) The complete mitochondrial genome of *Pauropus longiramus* (Myriapoda: Pauropoda): implications on early diversification of the myriapods revealed from comparative analysis. Gene 505(1): 57–65. doi: 10.1016/j.gene.2012.05.049

Dong Y, Xu JJ, Hao SJ, Sun HY (2012b) The complete mitochondrial genome of the giant pill millipede,Sphaerotheriidae sp. (Myriapoda: Diplopoda: phaerotheriida). Mitochondrial DNA 23(5): 333–335. doi: 10.3109/19401736.2012.683184

Edgecombe GD (2004) Morphological data, extant Myriapoda, and the myriapod stem-group. Contributions to Zoology Bijdragen Tot De Dierkunde 73: 207–252.

Edgecombe GD (2010) Arthropod phylogeny: an overview from the perspectives of morphology, molecular data and the fossil record. Arthropod Structure & Development 39(2–3): 74–87. doi: 10.1016/j.asd.2009.10.002

Edgecombe GD (2011) Phylogenetic relationships of Myriapoda. In: Minelli A (Ed.) The Myriapoda. Brill, Leiden, 1–20. doi: 10.1163/9789004188266_002

Edgecombe GD (2015) Diplopoda - Phylogenetic relationships. In: Minelli A (Ed.) Treatise on Zoology – Anatomy, Taxonomy, Biology. The Myriapoda, Volume 2, Chapter 2. Brill, Leiden, 353–362. doi: 10.1163/9789004188273_016

Enghoff H, Golovatch S, Short M, Stoev P, Wesener T (2015) Diplopoda – Taxonomic overview. In: Minelli A (Ed.) Treatise on Zoology – Anatomy, Taxonomy, Biology. The Myriapoda, Volume 2, Chapter 2. Brill, Leiden, 363–453. doi: 10.1163/9789004188273_017

Enghoff H, Dohle W, Blower JG (1993) Anamorphosis in millipedes (Diplopoda): the present state of knowledge with some developmental and phylogenetic considerations. Zoological Journal of the Linnean Society 109: 103–234. doi: 10.1111/j.1096-3642.1993.tb00305.x

Fernández R, Edgecombe GD, Giribet G (2016) Exploring phylogenetic relationships within Myriapoda and the effects of matrix composition and occupancy on phylogenomic reconstruction. Systematic Biology 65(5): 871–89. doi: 10.1093/sysbio/syw041

Gai Y, Ma H, Sun X, Ma J, Li C, Yang Q (2013) The complete mitochondrial genome of *Cermatobius longicornis* (Chilopoda: Lithobiomorpha: Henicopidae). Mitochondrial DNA 24(4): 331–332. doi: 10.3109/19401736.2012.760078

Gai Y, Song D, Sun H, Yang Q, Zhou K (2008) The complete mitochondrial genome of *Symphylella* sp. (Myriapoda: Symphyla): Extensive gene order rearrangement and evidence in favor of Progoneata. Molecular Phylogenetics and Evolution 49(2): 574–85. doi: 10.1016/j.asd.2009.10.002

Gai YH, Song DX, Sun HY, Zhou KY (2006) Myriapod monophyly and relationships among myriapod classes based on nearly complete 28S and 18S rDNA sequences. Zoological Science 23: 1101–1108. doi: 10.2108/zsj.23.1101

Gissi C, Iannelli F, Pesole G (2008) Evolution of the mitochondrial genome of Metazoa as exemplified by comparison of congeneric species. Heredity 101: 301–320. doi: 10.1038/hdy.2008.62

Hoffman R, Golovatch S, Adis J, de Morais J (2002) Diplopoda. In: Adis J (Ed.) Amazonian Arachnida and Myriapoda. Pensoft, Sofia-Moscow, 505–533.

Kirkness EF, Haas BJ, Sun W, Braig HR, Perotti MA, Clark JM, Lee SH, Robertson HM, Kennedy RC, Elhaik E, Gerlach D, Kriventseva EV, Elsik CG, Graur D, Hill CA, Veenstra JA, Walenz B, Tubío JM, Ribeiro JM, Rozas J, Johnston JS, Reese JT, Popadic A, Tojo M, Raoult D, Reed DL, Tomoyasu Y, Kraus E, Mittapalli O, Margam VM, Li HM, Meyer JM, Johnson RM, Romero-Severson J, Vanzee JP, Alvarez-Ponce D, Vieira FG, Aguadé M, Guirao-Rico S, Anzola JM, Yoon KS, Strycharz JP, Unger MF, Christley S, Lobo NF, Seufferheld MJ, Wang N, Dasch GA, Struchiner CJ, Madey G, Hannick LI, Bidwell S, Joardar V, Caler E, Shao R, Barker SC, Cameron S, Bruggner RV, Regier A, Johnson J, Viswanathan L, Utterback TR, Sutton GG, Lawson D, Waterhouse RM, Venter JC, Strausberg RL, Berenbaum MR, Collins FH, Zdobnov EM, Pittendrigh BR (2010) Genome sequences of the human body louse and its primary endosymbiont provide insights into the permanent parasitic lifestyle. Proceedings of the National Academy of Sciences of USA 107(27): 12168–12173. doi: 10.1073/pnas.1003379107

Knaus BJ, Cronn R, Liston A, Pilgrim K, Schwartz MK (2011) Mitochondrial genome sequences illuminate maternal lineages of conservation concern in a rare carnivore. BMC Ecology 11: 10. doi: 10.1186/1472-6785-11-10

Laslett D, Canback B (2008) ARWEN: a program to detect tRNA genes in metazoan mitochondrial nucleotide sequences. Bioinformatics 24: 172–175. doi: 10.1093/bioinformatics/btm573

Lavrov D, Boore J, Brown W (2000a) The complete mitochondrial DNA sequence of the Horseshoe Crab *Limulus polyphemus*. Molecular Biology and Evolution 17(5): 813–824. doi: 10.1093/oxfordjournals.molbev.a026360

Lavrov D, Brown W, Boore J (2000b) A novel type of RNA editing occurs in the mitochondrial tRNAs of the centipede *Lithobius forficatus*. Proceedings of the National Academy of Sciences of USA 97: 13738–13742. doi: 10.1073/pnas.250402997

Lowe TM, Eddy SR (1997) tRNAscan-SE: a program for improved detection of transfer RNA genes in genomic sequence. Nucleic Acids Research 25: 955–964. doi: 10.1093/nar/25.5.0955

Ma PF, Guo ZH, Li DZ (2012) Rapid sequencing of the bamboo mitochondrial genome using Illumina technology and parallel episodic evolution of organelle genomes in grasses. PLoS ONE 7: e30297. doi: 10.1371/journal.pone.0030297

Mcknight ML, Shaffer HB (1997) Large, rapidly evolving intergenic spacers in the mitochondrial DNA of the Salamander family Ambystomatidae (Amphibia: Caudata). Molecular Biology and Evolution 14: 1167–1176. doi: 10.1093/oxfordjournals.molbev.a025726

Meusemann K, von Reumont BM, Simon S, Roeding F, Strauss S, Kück P, Ebersberger I, Walzl M, Pass G, Breuers S, Achter V, von Haeseler A, Burmester T, Hadrys H, Wägele JW, Misof B (2010) A Phylogenomic Approach to Resolve the Arthropod Tree of Life. Molecular Biology and Evolution 27: 2451–2464. doi: 10.1093/molbev/msq1

Mora C, Tittensor DP, Adl S, Simpson AGB, Worm B (2011) How Many Species Are There on Earth and in the Ocean? PLoS Biology 9(8): e1001127. doi: 10.1371/journal.pbio.1001127

Ojala D, Montoya J, Attardi G (1981) tRNA punctuation model of RNA processing in human mitochondria. Nature 290: 470–474. doi: 10.1038/290470a0

Pocock RI (1893) On the classification of the tracheate Arthropoda. Zoologische Anzeiger 16: 271–275.

Posada D, Buckley TR (2004) Model selection and model averaging in phylogenetics: advantages of Akaike information criterion and Bayesian approaches over likelihood ratio tests. Systematic Biology 53: 793–808. doi: 10.1080/10635150490522304

Posada D, Crandall KA (1998) MODELTEST: testing the model of DNA substitution. Bioinformatics 14: 817–818. doi: 10.1093/bioinformatics/14.9.817

Regier JC, Shultz JW, Ganley AR, Hussey A, Shi D, Ball B, Zwick A, Stajich JE, Cummings MP, Martin JW, Cunningham CW (2008) Resolving arthropod phylogeny: exploring phylogenetic signal within 41 kb of protein-coding nuclear gene sequence. Systematic Biology 57: 920–938. doi: 10.1080/10635150802570791

Regier JC, Shultz JW, Zwick A, Hussey A, Ball B, Wetzer R, Martin JW, Cunningham CW (2010) Arthropod relationships revealed by phylogenomic analysis of nuclear protein-coding sequences. Nature 463: 1079–1083. doi: 10.1038/nature08742

Rehm P, Meusemann K, Borner J, Misof B, Burmester T (2014) Phylogenetic position of Myriapoda revealed by 454 transcriptome sequencing. Molecular Phylogenetics and Evolution 77C: 25–33. doi: 10.1016/j.ympev.2014.04.007

Robertson HE, Lapraz F, Rhodes AC, Telford MJ (2015) The Complete Mitochondrial Genome of the Geophilomorph Centipede *Strigamia maritima*. PLoS ONE 10(3): e0121369. doi: 10.1371/journal.pone.0121369

Ronquist F, Huelsenbeck JP. (2003) MRBAYES 3: Bayesian phylogenetic inference under mixed models. Bioinformatics 19: 1572–1574. doi: 10.1093/bioinformatics/btg180

Rota-Stabelli O, Campbell L, Brinkmann H, Edgecombe GD, Longhorn SJ, Peterson KJ, Pisani D, Philippe H, Telford MJ (2011) A congruent solution to arthropod phylogeny: phylogenomics, microRNAs and morphology support monophyletic Mandibulata. Proceedings of the Royal Society B-Biological Sciences 278: 298–306. doi: 10.1098/rspb.2010.0590

Shear WA (2008) Spinnerets in the milliped order Polydesmida, and the phylogenetic significance of spinnerets in millipeds (Diplopoda). International Journal of Myriapodology 1: 123–146. doi: 10.1163/187525408X395904

Shelly RM (2007) Taxonomy of extant Diplopoda (Millipeds) in the modern era: Perspectives for future advancements and observations on the global diplopod community (Arthropoda: Diplopoda). Zootaxa 1668: 343–362.

Sierwald P, Bond JE (2007) Current status of the myriapod class diplopoda (Millipedes): Taxonomic diversity and phylogeny. Annual Review of Entomology 52: 401–420. doi: 10.1146/annurev.ento.52.111805.090210

Sierwald P, Shear WA, Shelley RM, Bond JE (2003) Millipede phylogeny revisited in the light of the enigmatic order Siphoniulida. Journal of Zoological Systematics and Evolutionary Research 41: 87–99. doi: 10.1046/j.1439-0469.2003.00202.x

Snodgrass RE (1952) A Textbook of Arthropod Anatomy. Cornell University Press, New York, 363 pp.

Song F, Li H, Shao R, Shi A, Bai X, Zheng X, Heiss E, Cai W (2016) Rearrangement of mitochondrial tRNA genes in flat bugs (Hemiptera: Aradidae). Scientific Reports 6: 25725. doi: 10.1038/srep25725

Talavera G, Castresana J (2007) Improvement of Phylogenies after Removing Divergent and Ambiguously Aligned Blocks from Protein Sequence Alignments. Systematic Biology 56: 564–577. doi: 10.1080/10635150701472164

Tamura K, Dudley J, Nei M, Kumar S (2007) MEGA4: molecular evolutionarygenetics analysis (MEGA) software version 4.0. Molecular Biology and Evolution 24: 1596–1599. doi: 10.1093/molbev/msm092

Thompson JD, Gibson TJ, Plewniak F, Jeanmougin F, Higgins DG (1997) The CLUSTAL_X windows interface: flexible strategies for multiple sequence alignment aided by quality analysis tools. Nucleic Acids Research 25: 4876–4882. doi: 10.1093/nar/25.24.4876

Woo HJ, Lee YS, Park SJ, Lim JT, Jang KH, Choi EH, Choi YG, Hwang UW (2007) Complete mitochondrial genome of a troglobite millipede *Antrokoreana gracilipes* (Diplopoda, Juliformia, Julida), and juliformian phylogeny. Molecules and Cells 23: 182–191.

Yamauchi MM, Miya M, Nishida M (2003) Complete mitochondrial DNA sequence of the swimming crab, *Portunus trituberculatus* (Crustacea: Decapoda: Brachyura). Gene 311: 129–135. doi: 10.1016/S0378-1119(03)00582-1

Supplementary material 1

Supplementary tables

Authors: Yan Dong, Lixin Zhu, Yu Bai, Yongyue Ou, Changbao Wang

Data type: molecular data

ZooKeys 637: 21–31 (2016)
doi: 10.3897/zookeys.637.10148
http://zookeys.pensoft.net

RESEARCH ARTICLE

A peer-reviewed open-access journal
ZooKeys
Launched to accelerate biodiversity research

New synonyms in the highly diverse caddisfly genus *Smicridea* (Trichoptera, Hydropsychidae)

Ernesto Rázuri-Gonzales[1,2], Ralph W. Holzenthal[1]

1 *Department of Entomology, University of Minnesota, 219 Hodson Hall, 1980 Folwell Avenue, St. Paul, Minnesota 55108, USA* **2** *Departamento de Entomología, Museo de Historia Natural, Universidad Nacional Mayor de San Marcos, Apartado 14-0434, Lima 14, Peru*

Corresponding author: *Ernesto Rázuri-Gonzales* (razur001@umn.edu)

Academic editor: *P. Stoev* | Received 10 August 2016 | Accepted 11 November 2016 | Published 28 November 2016

http://zoobank.org/D537C852-FFA4-447C-B324-5CCD099498BA

Citation: Rázuri-Gonzales E, Holzenthal RW (2016) New synonyms in the highly diverse caddisfly genus *Smicridea* (Trichoptera, Hydropsychidae). ZooKeys 637: 21–31. https://doi.org/10.3897/zookeys.637.10148

Abstract

In this paper, *Smicridea* (*Rhyacophylax*) *repula* Oláh & Johanson, 2012 is synonymized with *Smicridea* (*R.*) *lobata* (Ulmer, 1909), and the species *Leptonema islamarga* Botosaneanu, 2002 is transferred to *Smicridea* (*R.*) as a synonym of *S. lobata*. Additionally, we present more detailed illustrations of the male genitalia of *S.* (*R.*) *lobata* and *S.* (*R.*) *signata* (Banks, 1903), and include notes on their distributions to aid in the identification of these two, often-confused species.

Keywords

Synonymy, New combination, Neotropics, Nearctic, Trichoptera

Introduction

The genus *Smicridea* was established by McLachlan (1871) to include the species *Smicridea fasciatella* from Texas. The genus now contains 232 species, making it, by far, the largest Hydropsychidae genus in the Western Hemisphere. The genus occurs from the southwestern USA, through Mexico, Central America, the Caribbean, and all of South America. It is divided into two subgenera: the nominotypical *Smicridea* (130 species) and *Rhyacophylax* Müller 1879 (102 species); the subgenera are based mainly on differences in the wing venation (Flint 1974a).

Table 1. *Smicridea* (*R.*) *signata* species group.

Species name	Author	Distribution
S. (*R.*) *arizonensis*	Flint 1974b	Mexico, USA
S. (*R.*) *bidactyla*	Flint and Reyes 1991	Ecuador, Peru, Venezuela
S. (*R.*) *bifurcata*	Flint 1974a	Costa Rica, Honduras
S. (*R.*) *fogasa*	Oláh and Johanson 2012	Ecuador
S. (*R.*) *hajla*	Oláh and Johanson 2012	Ecuador
S. (*R.*) *inarmata*	Flint 1974b	Mexico
S. (*R.*) *kampoka*	Oláh and Johanson 2012	Peru
S. (*R.*) *leloga*	Oláh and Johanson 2012	Peru
S. (*R.*) *lobata*	(Ulmer 1909)	Costa Rica, El Salvador, Guatemala, Honduras, Mexico, Nicaragua, Panama, Venezuela
S. (*R.*) *nemorosa*	Holzenthal and Blahnik 1995	Costa Rica
S. (*R.*) *nemtompa*	Oláh and Johanson 2012	Ecuador, Peru
S. (*R.*) *pseudolobata*	Flint 1978	Brazil, Suriname
S. (*R.*) *salta*	Flint 1974b	Mexico
S. (*R.*) *signata*	(Banks 1903)	Guatemala, Mexico, USA
S. (*R.*) *singri*	Holzenthal and Blahnik 1995	Costa Rica
S. (*R.*) *tavola*	Oláh and Johanson 2012	Ecuador

In the subgenus *Rhyacophylax*, the *signata* group of Flint (1974a) is characterized by a fixed, tongue-like, ventromesal process on the apex of the phallus, and the presence of a lobe with spinose processes developed in various numbers and positions, arising from the ventrolateral margin of the tenth tergum. Sixteen species distributed from northern South America, throughout Central America, into southwestern USA (Arizona, Colorado, New Mexico, Texas, and Utah) are included in this group (Table 1).

Smicridea lobata (Ulmer 1909, in Ulmer and Thienemann 1909) was described from Las Trincheras (Venezuela), from a single male specimen preserved in alcohol. Ulmer mentioned that the forewing coloration of *S. lobata* resembled that of *S. columbiana* (Ulmer 1905), but he did not compare the genitalia of these two species or those of any of the species in the genus known at the time. Later, Flint (1974b) doubtfully recorded *S. lobata* from Surinam. Even though he did not examine the type, he stated that the specimens he studied agreed with the illustration of the type of *S. lobata* provided by Ulmer. Additionally, after carefully examining the type specimen of *S. lobata*, Flint (1978) concluded that the species he referred to as *S. lobata* in his earlier paper was actually a different species, which he described as *S. pseudolobata*, due to differences in the tenth tergum and the phallus.

Smicridea repula Oláh & Johanson, 2012 was described from Los Tuxtlas area in the state of Veracruz (Mexico). The authors included this species in the *signata* group, stating that it was closely related to the species *S. lobata* from Venezuela and *S. nemtompa* Oláh & Johanson, 2012 from Ecuador and Peru. They indicated that their new

species was easily distinguished from *S. lobata* and *S. nemtompa* by having a lateral wing-shaped process at the mid-length of the phallus.

Leptonema islamarga Botosaneanu, 2002, in Botosaneanu and Viloria 2002, was described from Isla Margarita, Venezuela, and was placed in the *L. davisi* group of Flint, McAlpine and Ross 1987, based on characters of the male genitalia.

The species *Smicridea signata* (Banks, 1903) was originally described as *Pellopsyche signata*, from Fort Collins, Colorado (USA). The description was based on characteristics of the body and wings, with no genitalic characters included (the type is a female). Later, Ross (1944) transferred the species, as *R. signatus*, to *Rhyacophylax*, a separate genus at the time. More recently, Flint (1974a) redescribed the species as *Smicridea* (*R.*) *signata*, and illustrated the male and female genitalia as well as some features of the larva.

We conclude that *S. repula* and *L. islamarga* are synonyms of *S. lobata*, which is a separate species distinct from *S. signata*, based on differences in the tenth tergum as well as in their distributions. Herein, we provide justification for these taxonomic changes as well as more detailed illustrations of *S. lobata* from sites near the type locality (Fig. 1) and of *S. signata* from Utah.

Materials and methods

Specimens were examined with an Olympus SZH dissecting microscope (Olympus Corporation). The illustration of the male genitalia of *S. lobata* was prepared from pencil sketches made with the aid of a drawing tube attached to an Olympus BX41 compound microscope. The pencil sketches were scanned and placed into an Adobe Illustrator CS6 (Adobe Systems, Inc.) document to serve as a template to create a vector graphic illustration. The careful tracing of the original image was accomplished by using a graphic tablet and pen (BAMBOO, Wacom Technology Co.).

We carefully examined specimens from the type series of *S. repula* and *L. islamarga*, borrowed from the Swedish Museum of Natural History (Stockholm, Sweden) and the Naturalis Biodiversity Center (Leiden, The Netherlands), respectively. Further, we examined material of *S. signata* and *S. lobata* identified by Dr Oliver Flint (National Museum of Natural History, Smithsonian Institution, Washington D.C.) and Dave Ruiter (Grants Pass, Oregon, USA) as well as material from the University of Minnesota Insect Collection (St. Paul, Minnesota, USA), and the female type of *S. signata* from the Museum of Comparative Zoology, Harvard University, (Cambridge, Massachusetts, USA). The type of *S. lobata* at the Natural History Museum of Denmark (Copenhagen, Denmark) could not be found (H. Enghoff, pers. comm.).

The material examined is deposited in the following institutions:

DRC Dave Ruiter, personal collection, Grants Pass, Oregon, USA
NBC Naturalis Biodiversity Center, Leiden, The Netherlands
MCZ Museum of Comparative Zoology, Harvard University, Cambridge, Massachusetts, USA

NMNH National Museum of Natural History, Smithsonian Institution, Washington D.C., USA
NRM Swedish Museum of Natural History, Stockholm, Sweden
UMSP University of Minnesota Insect Collection, St. Paul, Minnesota, USA

Material examined

Smicridea (*R.*) *repula*: **MEXICO: Veracruz:** Los Tuxtlas area, Río La Palma, near to the Estación de Biología Los Tuxtlas, 18°33.68'N, 95°02.94'W, 30 mao [meters above ocean], 26.VI.2006, light trap, leg. Espeland & Malm; 1 male holotype (NRM).

Smicridea (*R.*) *signata*: **USA: Colorado:** No further data; 1 female holotype (MCZ, type # 11513). **Arizona:** Clear Cr. Cmp., SE Camp Verde, 17.VI.1968, Flint & Menke; 1 male (NMNH). Greenlee County, light trap, Gila River near Duncan, 32°43.46'N, 109°06.01'W, ca 1120 m, 19.IV.2002, Blinn; 6 males, 6 females (DRC). **New Mexico:** Grant County, Gila River at Forks T13S R13W sec 8, 26.VII.2001, at light, Ruiter; 10 males, 6 females (DRC). **Texas:** Brewster County, Big Bend National Park, Terlingua Creek at Terlingua abaja [Terlingua baja], 29°15'N, 103°37.5'W, 680 m, 1.VI.1993; Gelhaus #607, Nelson & Koenig; 1 male (NMNH). **Utah:** San Juan County, San Juan River, RM 10.6, 37°15'N, 109°51'W, ca 1190 m, light trap, 23.V.2002, Hayden; 6 males, 76 females (DRC). **MEXICO: Chiapas:** Puente Arroyo Viejo, Rt. 200, km 141, 9.VI.1967, Flint & Ortiz; 10 males (NMNH). **Morelia:** Route 95, km 91, nr. Xochitepec, 1.VIII.1965, Flint; 1 male, 28 females (NMNH). Xochitepec, 12-14.VII.1965, Flint & Ortiz; 2 males, 12 females (NMNH). **Oaxaca:** Tehuantepec, 23.VII.1964, Spangler; 3 males, 19 females (NMNH). **San Luis de Potosí:** Palitla, 25.VI.1965, Flint; 3 males, 5 females (NMNH). **Veracruz:** Cordoba, 11-20.XI.1966, Lau, 2 males (NMNH). **GUATEMALA: Escuintla:** Escuintla, 10.VIII.1965, Spangler; 8 males, 10 females (NMNH).

Smicridea (*R.*) *lobata*: **MEXICO: Chiapas:** 7.8 mi E Pichucalco, 7.XII.1975, C. M. & O. S. Flint; 5 males (NMNH). Arriaga, 22.VIII.1965, Spangler; 5 males, 3 females (NMNH). Cascada Misol ha, 20 km S Palenque, 17-18.V.1981, C. M. & O. S. Flint; 3 males (NMNH). Puente Arroyo Viejo, nr. Mapastepec, 7.VIII.1966, Flint & Ortiz; 3 males (NMNH). Río Contento, 7 km N Ocosingo, 20.V.1981, C. M. & O. S. Flint; 1 male (NMNH). Río Tulija, 48 km S Palenque, 17.V.1981, C. M. & O. S. Flint; 8 males, 14 females (NMNH). **Oaxaca:** Dist. Choapan, Bethania, 31 km S San Juan Bautista Tuxtepec, 24.V.1981, C. M. & O. S. Flint; 6 males, 3 females (NMNH). Rancho San Pablo, 17 Km. E Tehuantepec, 23.V.1981, C. M. & O. S. Flint; 2 males (NMNH). Río Valle Nacional, Chiltepec, 25.V.1981, C. M. & O. S. Flint; 3 males, 1 female (NMNH). **San Luis de Potosí:** 1 mi W Tamazunchale, 11.VIII.1972, at black light, G. F. & S. Hevel; 3 males, 2 females (NMNH). **Veracruz:** Barranca de Metlac, Fortín de las Flores, 4.XII.1975, C. M. & O. S. Flint; 3 males, 5 females (NMNH). Barranca de Metlac, 6 km W Fortín, 1.V.1981, C. M & O. S. Flint; 1 male, 1 female (NMNH). Cuitlahuac, 10-12.VIII.1964, Spangler; 1 male (NMNH).

Same, but 24-27.VII.1965, Flint & Ortiz; 1 male (NMNH). La Palma, nr. Sontecomapan, 5.XII.1975. C. M. & O. S. Flint; 9 males (NMNH). Los Tuxtlas area, Los Tuxtlas Biological Station, 31 Km NE of Catemaco, nr. Balzapote, 3-15.V.1981, C. M. & O. S. Flint; 3 males, 6 females (NMNH). Los Tuxtlas area, Los Tuxtlas Biological Station, 31 Km NE of Catemaco, Río Palma, above La Palma, 7-14.V.1981, C. M. & O. S. Flint; 7 males, 3 females (NMNH). Los Tuxtlas area, Los Tuxtlas Biological Station, 31 Km NE of Catemaco, Río Palma, below La Palma, 5.V.1981, C. M. & O. S. Flint; 7 males (NMNH). Los Tuxtlas area, Los Tuxtlas Biological Station, 31 Km NE of Catemaco, seeps at Las Cabañas, 8-15.V.1981, C. M. & O. S. Flint; 5 males, 3 females (NMNH). Los Tuxtlas area, Los Tuxtlas Biological Station, 31 Km NE of Catemaco, Río Máquinas, 4-14.V.1981, C. M. & O. S. Flint; 14 males, 2 females (NMNH). Puente Nacional, 23-24.VII.1965, Flint & Ortiz; 4 males, 5 females (NMNH). Same, but 31.VII.1966, Flint & Ortiz; 4 males, 2 females (NMNH). Pte. [Puente] Tecolapán, E Lerdo de Tejada, 4.XII.1975, C. M. & O. S. Flint; 1 male (NMNH). Río Tecolapan, Rt. 180, km 551, 25-26.VII.1966, Flint & Ortiz; 3 males, 3 females (NMNH). San Andrés Tuxtla, Estación Biológica Tropical "Los Tuxtlas", 18°35.10'N, 95°04.50'W, ca 160 m, 17.V.2015, Kjer; 13 males, 1 female (UMSP). **GUATEMALA: El Progreso:** San Agustín Acasaguastlán, 11-21.VIII.1965, Flint & Ortiz; 4 males, 6 females (NMNH). **Jutiapa:** Laguna Nisquaya, 4.VIII.1965, Spangler; 2 males (NMNH). **Retalhuleu:** Pte. [Puente] El Niño, 16.VI.1966, Flint & Ortiz; 10 males, 6 females (NMNH). **Suchitepequez:** San Antonio de Suchitepequez, 6.VII.1965, Spangler; 1 male, 1 female (NMNH). Cuyotenango, 10-20.VI.1966, Flint & Ortiz, 3 males, 5 females (NMNH). Pte. [Puente] Ixtacapa, 18-19.VI.1966, O. S. Flint & Ortiz; 5 males, 2 females (NMNH). Fca. [Finca] Moca, 12.VI.1966, Flint & Ortiz; 7 males, 2 females (NMNH). **Zacapa:** Río Teculután; 18.VIII.1965; Flint & Ortiz; 1 male (NMNH). **HONDURAS: Choluteca:** 5 mi E Choluteca, 28. VII.1965, Spangler; 1 male (NMNH). **Valle:** Nacaome, 4.VIII.1967, Flint; 3 males, 2 females (NMNH). **EL SALVADOR: El Salvador:** Lago Ilopango, 5.VIII.1967, Flint; 2 males (NMNH). **La Libertad:** Quezaltepeque, 2.II.1965, S. S. & W. D. Duckworth; 2 males (NMNH). **NICARAGUA: Granada:** Reserva Silvestre Privada Domitila, Río cerca de Manantial, 11°42.17'N, 85°57.12'W, ca 60 m, 26.VII.2001, Chamorro & López; 17 males, 5 females (UMSP). **Jinotega:** Río El Tuma, app. 10 kms S of Santa Maura, 11°55.35'N, 86°27.80'W, 1000 m, 30.VII.2000, Chamorro & Chris; 30 males & females (alcohol). **COSTA RICA: Alajuela:** Río Pizote, ca. 5 km N Dos Ríos, 10°56.88'N, 85°17.47'W, 470 m, 9.III.1986, Holzenthal & Fasth; 1 male (UMSP). Laguna Río Cuarto & trib., 2.8 km (road) N Río Cuarto, 10°21.42'N, 84°12.90'W, 400 m, 13.II.1992, Holzenthal, Muñoz & Kjer; 4 males, 2 females (UMSP). **Cartago:** Quebrada Platanillo, ca. 5 km E Moravia de Chirripó, 09°49.27'N, 83°24.42'W, 1130 m, 6.VIII.1987, Holzenthal, Morse & Clausen, 4 males, 1 female (UMSP). **Guanacaste:** Río Tempisquito, ca. 3 km S Route 1, 10°47.40'N, 85°33.12'W, ca 70 m, 6.III.1986, Holzenthal & Fasth, 3 males, 4 females (UMSP). Parque Nacional Santa Rosa, Quebrada San Emilio, 10°51.72'N, 85°36.60'W, 300 m, 27.VI.1986, Holzenthal, Heyn & Armitage; 1 male, 1 female (UMSP). Río Góngora, sulfur mine,

4 km (air) NE Quebrada Grande, 10°53.22'N, 85°28.20'W, 590 m, 21.VII.1987, Holzenthal, Morse & Clausen; 7 males, 1 female (UMSP). Río Poza Salada, 10°47.93'N, 85°39.12'W, 10 m, 24.VII.1987, Holzenthal, Morse & Clausen; 7 males, 7 females (UMSP). Río Cuajiniquil, 10°52.87'N, 85°36.78'W, 250 m, 25.VII.1987, Holzenthal, Morse & Clausen; 6 males, 14 females (UMSP). Parque Nacional Guanacaste, Quebrada Pedregal, El Hacha, 10°58.98'N, 85°32.33'W, 300 m, 27.VII.1987, Holzenthal, Morse & Clausen; 1 male, 2 females (UMSP). **Heredia:** Estación Biológica La Selva, Quebrada El Salto, 10°25.62'N, 84°00.72'W, 50 m, 10.II.1986, Holzenthal; 9 males (UMSP). Río Puerto Viejo, 10°26.40'N, 84°00.72'W, 30 m, 10-11. II.1986, Holzenthal; 1 male (UMSP). Same, but 19.VI.1986, Holzenthal, Heyn & Armitage; 1 male (UMSP). Río Sarapiquí, 7 km W Puerto Viejo, 10°27.12'N, 84°04.02'W, 50 m, 11.II.1986, Morse & Fasth; 8 males, 1 female (UMSP). Río Bijagual, on road to Magsasay, 10°24.48'N, 84°04.57'W, 140 m, 12.II.1986, Holzenthal, Morse & Fasth; 2 males, 1 female (UMSP). Parque Nacional Braulio Carrillo, Río Peje, Est. Magsasay, 10°24.12'N, 84°03.00'W, 130 m, 25-26.VIII.1990, Holzenthal, Blahnik & Huisman; 2 males, females (UMSP). Quebrada Ceiba, 6 km E Cháves, 10°22.92'N, 83°55.32'W, 50 m, 2.VII.1992, Muñoz; 2 males, 2 females (UMSP). Río Bijagual, 3.5 km S Chilamate, 10°26.17'N, 84°03.60'W, 40 m, 1.VII.1992, Muñoz; 1 male (UMSP). **Limón:** Río Barbilla, ca. 8 km W B-Line, 10°04.02'N, 83°22.13'W, 30 m, 31.I.1986, Holzenthal, Morse & Fasth; 21 males, 25 females (UMSP). Río Telire and small trib., SE Suretka, 09°33.23'N, 82°53.52'W, ca 40 m, 1.II.1986, Holzenthal, Morse & Fasth; 2 males (UMSP). Reserva Biológica Hitoy-Cerere, Río Cerere, Est. Miramar, 09°40.27'N, 83°01.68'W, 90 m, 23-24.III.1987, Holzenthal, Hamilton & Heyn; 2 males (UMSP). Río Banano, 16 km WSW Bomba, 09°53.28'N, 83°10.02'W, 150 m, 26.III.1987, Holzenthal, Hamilton & Heyn; 3 males, 4 females (UMSP). Reserva Biológica Barbilla, Río Dantas, 15 km (rd) S Pacuarito, 09°59.63'N, 83°26.58'W, 300 m, 27-30.I.1992, Holzenthal, Muñoz & Kjer, 69 males, 42 females (UMSP). Same, but trib. to Río Dantas, 13 (km) S Pacuarito, 09°59.70'N, 83°28.62'W, 500 m, 1.II.1992, Holzenthal, Muñoz & Kjer; 8 males, 6 females (UMSP). E.A.R.T.H., Río Destierro, Pozo Azul, 10°12.48'N, 83°34.43'W, ca 10 m, 5.II.1992, Holzenthal, Muñoz & Kjer; 6 males, 6 females (UMSP). Same, but 27.VI.1992, Contreras & Muñoz; 9 males, 3 females (UMSP). Río Parismina, 10°14.88'N, 83°34.20'W, 5 m, 4.II.1992, Holzenthal, Muñoz & Kjer; 3 males, 6 females (UMSP). Río Dos Novillos, 10°13.20'N, 83°35.47'W, 20 m, 3.II.1992, Holzenthal, Muñoz & Kjer; 26 males, 34 females (UMSP). **Puntarenas:** Quebrada Pita, ca. 3 km (air) W Golfito, 08°38.52'N, 83°11.58'W, ca 10 m, 15.II.1986, Holzenthal, Morse & Fasth; 1 male (UMSP). Río Bellavista, ca. 1.5 km NW Las Alturas, 08°57.07'N, 82°50.77'W, 1400 m, 18.II.1986, Holzenthal, Morse & Fasth; 1 male, 1 female (UMSP). Reserva Biológica Carara, Río Carara, 4.3 km (rd) E Cost. Sur, 09°48.60'N, 84°34.32'W, 20 m, 12.III.1991, Holzenthal, Muñoz & Huisman, 12 males, females (UMSP). Río Jaba, 2.4 km (air) NW San Vito, 08°49.92'N, 82°59.47'W, 970 m, 13.VI.1986, Holzenthal, Heyn & Armitage; 1 male (UMSP). San Miguel, 08°52.00'N, 82°52.00'W, 14.XI.1991, Muñoz, 8 males; 2 females, 8 males (UMSP). Quebrada Bonita, 09°46.50'N, 84°36.30'W, ca 30

m, 18-20.V.1990, Holzenthal & Blahnik; 9 males, 40 females (UMSP). Same, but 11.III.1991, Holzenthal, Muñoz & Huisman; 4 males, 3 females (UMSP). Río Platanar, 6.5 km NE Buenos Aires, 09°11.70'N, 83°16.87'W, 450 m, 8-9.VII.1992, Muñoz, 12 males (UMSP). San José, Río del Sur, 1.5 km (rd) S Carara, 09°46.13'N, 84°31.87'W, 160 m, 13.III.1991, Holzenthal, Muñoz & Huisman; 3 males, 7 females (UMSP). **PANAMA: Chiriquí:** Dolega, 17.VII.1967. Flint; 1 male (NMNH). **Coclé:** El Valle, ca 820 m, 27.V.1983, Steiner; 1 male (NMNH). **VENEZUELA: Falcón:** Río Ricoa near Dos Bocas, 11°17.32'N, 69°26.07'W, ca 150 m, 8.VI.2001, Holzenthal, Blahnik, Paprocki & Cressa; 25 males, 6 females (UMSP). **Lara:** Parque Nacional Terepaima, Río Sarare nr. Sarare, 09°49.03'N, 69°11.60'W, ca 350 m, 15.VI.2001, Holzenthal, Blahnik, Paprocki & Cressa; 14 males (UMSP). **Miranda:** Río Caruao, 1.6 km S Caruao, 10°35.82'N, 66°20.77'W, 5 m, 26.I.1994, Holzenthal, Cressa & Rincón; 12 males, 14 females (UMSP). **Monagas:** Río Punceres, 09°58.93'N, 63°20.63'W, ca 80 m, 19.VII.2010, Holzenthal, Thomson & Cressa; 15 males, 4 females (UMSP). **Sucre:** Quebrada Zapateral, 1.5 km SE Las Piedras de Cocollar, 10°09.75'N, 63°47.59'W, 810 m, 9.IV.1995, Flint & Holzenthal; 1 male (NMNH), 24 males, 14 females (UMSP). Río Cocollar, 1.5 km SE Las Piedras de Cocollar, 10°09.62'N, 63°47.60'W, 810 m, 7-8.V.1995, Holzenthal & Flint; 11 males, 21 females (UMSP). **Zulia:** Caño Carichuano, 3.4 km SE Carbones del Guasare, 11°00.12'N, 72°17.10'W, 70 m, 12-13.I.1994, Holzenthal, Cressa & Rincón; 14 males, 9 females (UMSP). Los Angeles del Tucuco, 15-16.IV.1991, Menke & Hollenberg; 1 male (NMNH). Río Yasa, ca. 3 km (air) E Kasmera (Estación Biológica), 09°56.47'N, 72°43.20'W, 150 m, 14.I.1994, Holzenthal, Cressa & Rincón; 5 males, 2 females (UMSP).

Leptonema islamarga: **VENEZUELA: Nueva Esparta:** Isla Margarita, Asunción, Río Asunción; 02.VI.2000; Botosaneanu & Viloria; 10 males, 12 females paratypes (NBC).

Discussion

Flint (1974a) stated that *S. signata* was easily recognized by the presence of a lateral serrate process (wing-shaped process of Oláh and Johanson 2012) and a pair of apicodorsal lobes in the phallus. However, after examining the type of *S. lobata*, Flint (1978) considered it and *S. signata* to have nearly identical phalli, including the aforementioned processes and lobes. *Smicridea signata* and *S. lobata* differ in the shape of the tenth tergum. In *S. lobata* the tergites are finger-like and have a bifurcate lobe of varying sizes from the ventral margin (paraproct of Oláh and Johanson 2012) (Fig. 1), whereas in *S. signata* the tergites are broader and the lobe from the ventral margin is rounded (Flint 1974a; fig. 138) (Fig. 2). Flint (1978) also mentioned that the tergites in *S. lobata* were widely separated dorsomesally whereas in *S. signata*, they were closer together. However, in some of the material available to us, the tergites in both species were separated roughly by the same distance. In addition to Fig. 2, the figures of *S. signata* provided by Flint (1974a, figs 137–140) can be used to separate this species from *S. lobata*.

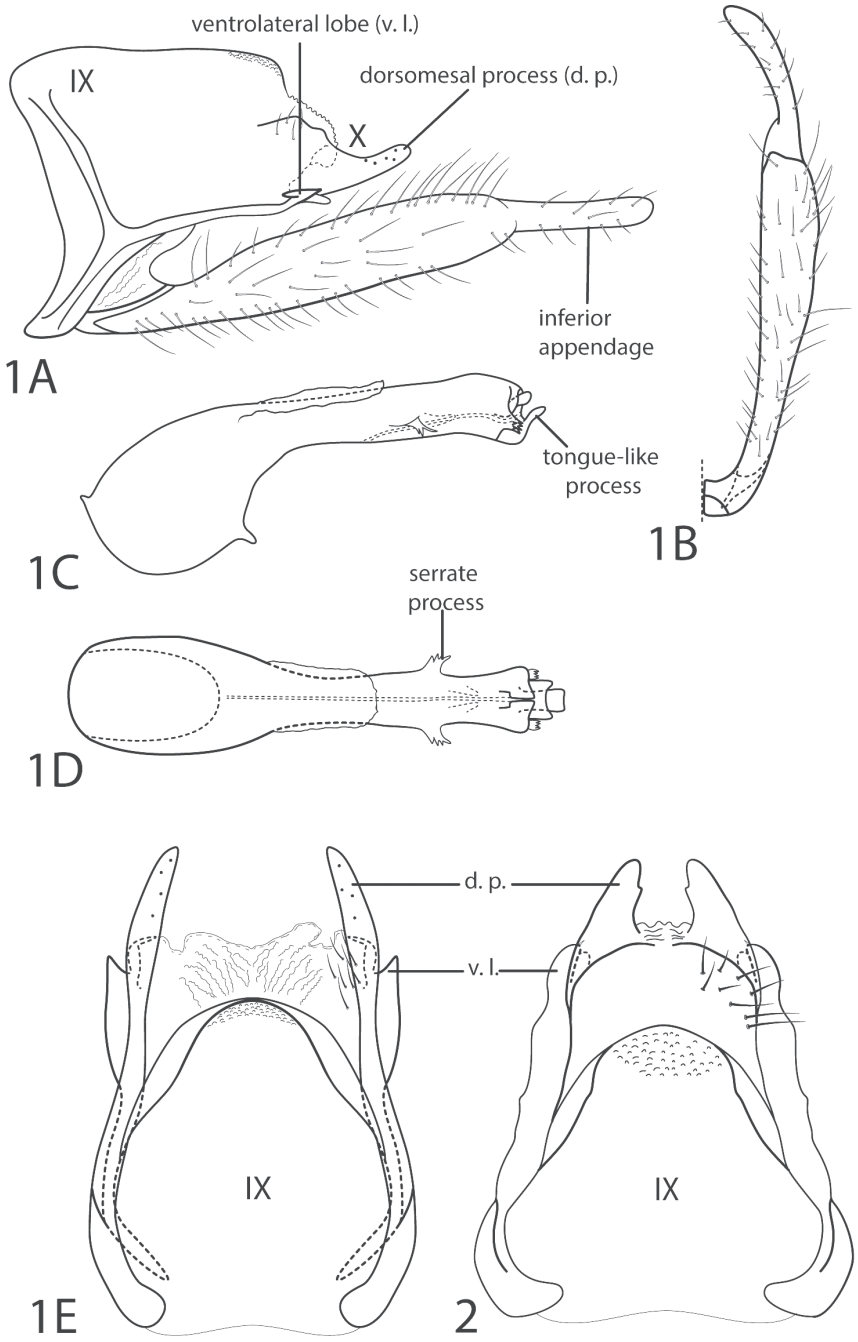

Figure 1–2. *Smicridea* (*R.*) *lobata* (Ulmer, 1909) and *Smicridea* (*R.*) *signata* Banks, 1903, male genitalia. **1A** *Smicridea* (*R.*) *lobata* segments IX and X, lateral **1B** Left inferior appendage, ventral **1C** Phallus, lateral **1D** Phallus, dorsal **1E** Segments IX and X, dorsal **2** *Smicridea* (*R.*) *signata*. Segments IX and X, dorsal. These illustrations were made from specimens of *S. lobata* from Zulia and Sucre States, Venezuela, and specimens of *S. signata* from Utah, USA.

Oláh and Johanson (2012) mentioned that the diagnostic character that separates *Smicridea repula* from its closest relatives, *S. lobata* and *S. nemtompa,* is the presence of lateral serrate processes at the mid-length of the phallus. However, as Flint (1978) noted, both *S. signata* and *S. lobata* also have these processes. Additionally, the illustration accompanying Oláh and Johanson's description for *S. repula* matches Ulmer's *S. lobata* illustration perfectly (Ulmer and Thienemann 1909; fig. 2). Also, the *S. repula* holotype that was loaned to us fits perfectly with the examples of *S. lobata* from Costa Rica, Guatemala, Mexico, Nicaragua, Panama, and Venezuela from the Smithsonian and the University of Minnesota Insect Collection. In these examples, the lateral serrate processes of the phallus vary in size, as noted by Flint (1974a) also for *S. signata*. Finally, since the serrate processes of the phallus are not exclusive to *S. repula*, and all the other characters between *S. repula* and *S. lobata* perfectly match, we consider *S. repula* Oláh & Johanson, 2012 to be a junior subjective synonym of *S. lobata* (Ulmer, 1909), **new synonym**.

Botosaneanu and Viloria (2002) provided a combination of characters for the inclusion of *Leptonema islamarga* in the *L. davisi* species group, along with *L. aterrimum* Mosely, 1933, *L. davisi* Flint, McAlpine & Ross, 1987, and *L. gadzux* Flint, McAlpine & Ross, 1987. However, most of the proposed characters for the inclusion of *L. islamarga* in this group are rather general (e.g., small size, tibial spur formula 1/4/4, middle tibia of females not dilated, and phallus with processes), and they are not exclusive of the group, much less to the genus *Leptonema*. The authors also mentioned that the forewing pattern of *L. islamarga* was extremely distinctive from other members of the genus *Leptonema*. After comparing the forewing color pattern of the paratypes (fig. 7 of Botosaneanu and Viloria 2002), and other specimens, we conclude that this forewing coloration actually corresponds to the color pattern and venation found in many species of *Smicridea* (*Rhyacophylax*). Additionally, Botosaneanu and Viloria (2002) observed a pair of gill-like appendages from the fifth sternite in both sexes. They also hypothesized that these structures replaced the raised, glandular structures of *Leptonema*. However, these structures actually correspond to the anterolateral filaments commonly present in the subgenus *Rhyacophylax* (Flint, 1974b). Finally, the authors recognized that the male genitalia of *L. islamarga* were quite distinct from the other three species in the *Leptonema davisi* group, except for the absence of warts on the tenth abdominal tergum. The illustrations of *Leptonema islamarga* and the specimens in the type series match perfectly with the specimens we have examined of *S. lobata* and with Ulmer's illustration of *S. lobata*. Accordingly, *Leptonema islamarga* Botosaneanu, 2000 is transferred to the genus *Smicridea* (*Rhyacophylax*) and placed as a junior subjective synonym of *Smicridea lobata* (Ulmer, 1909), **new combination, new synonym**.

Based on the material examined, *Smicridea lobata* is distributed in Mexico, Guatemala, Honduras, El Salvador, Nicaragua, Costa Rica, Panama, and Venezuela, and *S. signata* is distributed in southwestern USA, Mexico, and Guatemala. Flint (1974a), in his redescription of *S. signata* included several specimens that were actually *S. lobata*. After re-examining this material, we noted that the distributions of *S. lobata* and *S. signata* overlap in Mexico and Guatemala. Furthermore, we observed that along with the lateral

serrate processes of the phallus, the ventrolateral lobes of the tenth tergum tend to increase in size towards the southern portion of its range. However, as Flint (1974a) stated, these two species can be readily distinguished by the shape of the tenth tergum in dorsal view (Figs 1E–2). The ventrolateral lobes of the tenth tergum are bifurcate in *S. lobata* and rounded in *S. signata*, and the dorsomesal processes are finger-like in *S. lobata* and broad in *S. signata*. Additionally, the ventrolateral lobes of the tenth tergum in *S. signata* present a very small spicule apically, which was not illustrated by Flint (1974a).

Acknowledgements

The authors would like to thank the curators and institutions that loaned the material used in this study: Dr Oliver S. Flint, Jr. (NMNH), Dr Willem Hogenes (NBC), Dr Tobias Malm and Dr Kjell Arne Johanson (NRM), Dr Philip Perkins and Rachel Hawkins (MCZ), and Dave Ruiter (Grants Pass, Oregon, USA). ERG would also like to thank Dr John Luhman for translating the German text in the original description of *Smicridea lobata*. Dave Ruiter and Dr Brian Armitage provided helpful comments to improve the manuscript. This paper was prepared thanks to a doctoral fellowship from Cienciactiva, initiative from Consejo Nacional de Ciencia, Tecnología e Innovación Tecnológica, Peru (contract 277-2015-FONDECYT) awarded to ERG. The research was conducted with the support of Minnesota Agricultural Experiment Station projects MN 17-017 and MN 17-029. This support is gratefully acknowledged.

References

Banks N (1903) Some new neuropteroid insects. Journal of the New York Entomological Society 11: 236–243.

Botosaneanu L, Viloria AL (2002) The caddisflies (Insecta, Trichoptera) of Isla de Margarita (Venezuela) - with description of two new species. Mitteilungen aus dem Museum für Naturkunde in Berlin Deutsche Entomologische Zeitschrift 49: 105–111. doi: 10.1002/mmnd.20020490108

Flint Jr OS (1974a) Studies of Neotropical caddisflies, XVII: the genus *Smicridea* from North and Central America (Trichoptera: Hydropsychidae). Smithsonian Contributions to Zoology 167: 1–65. doi: 10.5479/si.00810282.167

Flint Jr OS (1974b) The Trichoptera of Surinam. Studies of Neotropical caddisflies, XV. Studies on the Fauna of Suriname and other Guyanas 14: 1–151.

Flint Jr OS (1978) Studies of Neotropical Caddisflies, XXII: Hydropsychidae of the Amazon Basin (Trichoptera). Amazoniana 6: 373–421.

Flint Jr OS, McAlpine JF, Ross HH (1987) A revision of the genus *Leptonema* Guerin (Trichoptera: Hydropsychidae: Macronematinae). Smithsonian Contributions to Zoology 450: 1–193. doi: 10.5479/si.00810282.450

Flint Jr OS, Reyes L (1991) Studies of Neotropical caddisflies, XLVI: the Trichoptera of the Río Moche Basin, Department of La Libertad, Peru. Proceedings of the Biological Society of Washington 104: 474–492.

Holzenthal RW, Blahnik RJ (1995) New species of *Smicridea* (*Rhyacophylax*) (Trichoptera: Hydropsychidae) from Costa Rica. Entomological News 106: 213–223.

McLachlan R (1871) On new forms, etc., of extra-European Trichopterous insects. Journal of the Linnean Society of London, Zoology 11: 98–141. doi: 10.1111/j.1096-3642.1870.tb02011.x

Mosely ME (1933) A revision of the genus *Leptonema* (Trichoptera). British Museum (Natural History), London, 1–69.

Müller F (1879) Notes on the cases of some South Brazilian Trichoptera. Transactions of the Royal Entomological Society of London 4: 131–144.

Oláh J, Johanson KA (2012) New species and records of Neotropical Macronematinae and Smicrideinae (Trichoptera: Hydropsychidae). Annales Historico-Naturales Musei Nationalis Hungarici 104: 215–297.

Ross HH (1944) The caddisflies or Trichoptera of Illinois. Bulletin of the Illinois Natural History Survey 23: 1–326.

Ulmer G (1905) Über die geographische Verbreitung der Trichopteren. Zeitschrift fur Wissenschaftliche Insektenbiologie 1: 16–32, 68–80, 119–126.

Ulmer G, Thienemann A (1909) Südamerikanische Trichopteren aus den Kopenhagener Museum. Deutsche Entomologische Zeitschrift 1909: 305–311.

ZooKeys 637: 33–45 (2016)
doi: 10.3897/zookeys.637.9384
http://zookeys.pensoft.net

RESEARCH ARTICLE

A peer-reviewed open-access journal
ZooKeys
Launched to accelerate biodiversity research

Revision of the genus *Ptomaphagus* Hellwig (Coleoptera, Leiodidae, Cholevinae) from the Russian Far East and the Korean Peninsula

Cheng-Bin Wang[1], Jan Růžička[1], Michel Perreau[2], Masaaki Nishikawa[3], Sun-Jae Park[4]

1 *Department of Ecology, Faculty of Environmental Sciences, Czech University of Life Sciences Prague, Kamýcká 129, CZ-165 21 Praha 6, Czech Republic* **2** *IUT Paris Diderot, Université Paris Diderot case 7139 Sorbonne Paris Cité, 5, rue Thomas Mann, 75205 Paris cedex 13, France* **3** *Kashiwagaya 1112–16, Ebina, 243–0402 Japan* **4** *National Institute of Biological Resources, Incheon, Republic of Korea*

Corresponding author: *Jan Růžička* (ruzickajan@fzp.czu.cz)

Academic editor: *B. Guéorguiev* | Received 30 May 2016 | Accepted 11 November 2016 | Published 28 November 2016

http://zoobank.org/401C312B-74D0-4FC8-AD06-3191A6E29979

Citation: Wang C-B, Růžička J, Perreau M, Nishikawa M, Park S-J (2016) Revision of the genus *Ptomaphagus* Hellwig (Coleoptera, Leiodidae, Cholevinae) from the Russian Far East and the Korean Peninsula. ZooKeys 637: 33–45. https://doi.org/10.3897/zookeys.637.9384

Abstract

The conundrum of *Ptomaphagus* (s. str.) *sibiricus* Jeannel, 1934 (Coleoptera, Leiodidae, Cholevinae, Ptomaphagini) is solved, and it is redescribed and newly recorded in South Korea. A new species is also described from the Russian Far East: *P.* (s. str.) *hayashii* **sp. n.** Relevant morphological characters of the concerned species are illustrated with colour plates, and their known distributions are mapped.

Keywords

Leiodidae, Cholevinae, *Ptomaphagus*, taxonomy, new species, the Russian Far East, the Korean Peninsula

Introduction

Ptomaphagus Hellwig, 1795 is the most speciose genus (including 137 known species worldwide) in the tribe Ptomaphagini (Coleoptera, Leiodidae, Cholevinae). However, the nominotypical subgenus, which is limited to the Palaearctic and north Oriental regions has only 29 species (Perreau 2000, Nishikawa 2011, Wang et al. 2016a, 2016b).

In the fauna of the Russian Far East, only one species in the subgenus *Ptomaphagus* s. str. had been recorded before this study, namely *P.* (s. str.) *sibiricus* Jeannel, 1934.

However, when we examined specimens previously identified as *Ptomaphagus* (s. str.) *sibiricus* from various collections, we discovered that three species were identified under this name by different authors. One of them with conspicuous differences from Japan was already described in a previous paper: *P.* (s. str.) *piccoloi* Wang, Růžička, Nishikawa, Perreau & Hayashi, 2016 (Wang et al. 2016a). In this paper, we solve the conundrum of *P.* (s. str.) *sibiricus*, and redescribe it and report it for the first time in South Korea. The third species from the Russian Far East is also new, and is described and illustrated here: *P.* (s. str.) *hayashii* sp. n. Relevant morphological characters of examined species of *Ptomaphagus* are illustrated with colour plates, and their known distributions are mapped.

Material and methods

Specimens were relaxed and softened in a hot saturated solution of potassium hydroxide for 4 minutes (for mounted dry specimens) or 8 minutes (for alcohol-preserved specimens), and then transferred to distilled water to rinse the residual potassium hydroxide off and stop any further bleaching. The softened specimens were moved into glycerin and dissected there to observe morphological details. After examination, the body parts were mounted on a glass slip with Euparal Mounting Medium for future studies. Habitus photographs were taken using a Canon macro photo lens MP-E 65mm on a Canon 550D. Observations, photographs and measurements of morphological details were performed using an Olympus BX53 microscope with an Olympus DP73. The final deep focus images were created with Zerene Stacker 1.04 stacking software. Adobe Photoshop CS6 was used for post processing. Exact label data are cited for specimens examined. Authors' remarks and addenda are placed in square brackets, separate label lines are indicated by a slash (/), and separate labels by a double slash (//). Measurements are averaged over 5 specimens.

The material examined for this study is deposited in the following collections and museums:

BMNH	Natural History Museum (formerly British Museum), London, United Kingdom (M. Barclay)
CCBW	Collection of Cheng-Bin Wang, Chengdu, Sichuan, China
CJRZ	Collection of Jan Růžička, Prague, Czech Republic
CMNE	Collection of Masaaki Nishikawa, Ebina, Japan
CNUIC	Chungnam National University Insect Collection, Daejeon, Korea

MNHN Muséum National d'Histoire Naturelle, France, Paris (T. Deuve, Azadeh Taghavian)
NSMT National Museum of Nature and Science, Tsukuba, Japan (S. Nomura)
SDEI Senckenberg Deutsches Entomologisches Institut, Müncheberg, Germany (L. Behne)

The following abbreviations are used for the measurements in millimetres (mm):

AL (antennal length): length from the antennal base to apex.
BTW (basitarsal width): maximum width of 1st protarsomere.
EBL (extended body length): summation of HL, PL, ELL and length of exposed scutellum, preventing the error introduced by exposed or retracted head.
ELL (elytral length): length from the tail end of scutellum to the elytral apex.
ELW (elytral width): maximum width of the widest portion of two elytra combined together.
EW (eye width): width of a single compound eye in dorsal view.
HL (head length): axial length from the anterior apex of clypeus through the posterior margin of occipital carina.
HW (head width): width of the widest portion of head (usually including eyes).
PL (pronotal length): axial length of the pronotum.
PW (pronotal width): maximum width of pronotum.
TW (tibial width): maximum width of protibia (excluding spines along outer margin etc.).

Results

Genus *Ptomaphagus* Hellwig, 1795

Distribution. Holarctic, north Oriental, north Neotropical.

Subgenus *Ptomaphagus* s. str.

Distribution. Palaearctic, north Oriental.

***Ptomaphagus* (s. str.) *hayashii* sp. n.**
http://zoobank.org/C468947A-D211-4411-B09B-775DFF6A7045
Figs 1B, C; 2; 3

Type material. Holotype: 1♂, USSR: Sadgorod [ca. 43°15'N 132°03'E] / (in forest; trap with / bait), Vladivostok // Primorskyi Kray / 16.VI.1978 / E. Berlov leg. (NSMT).

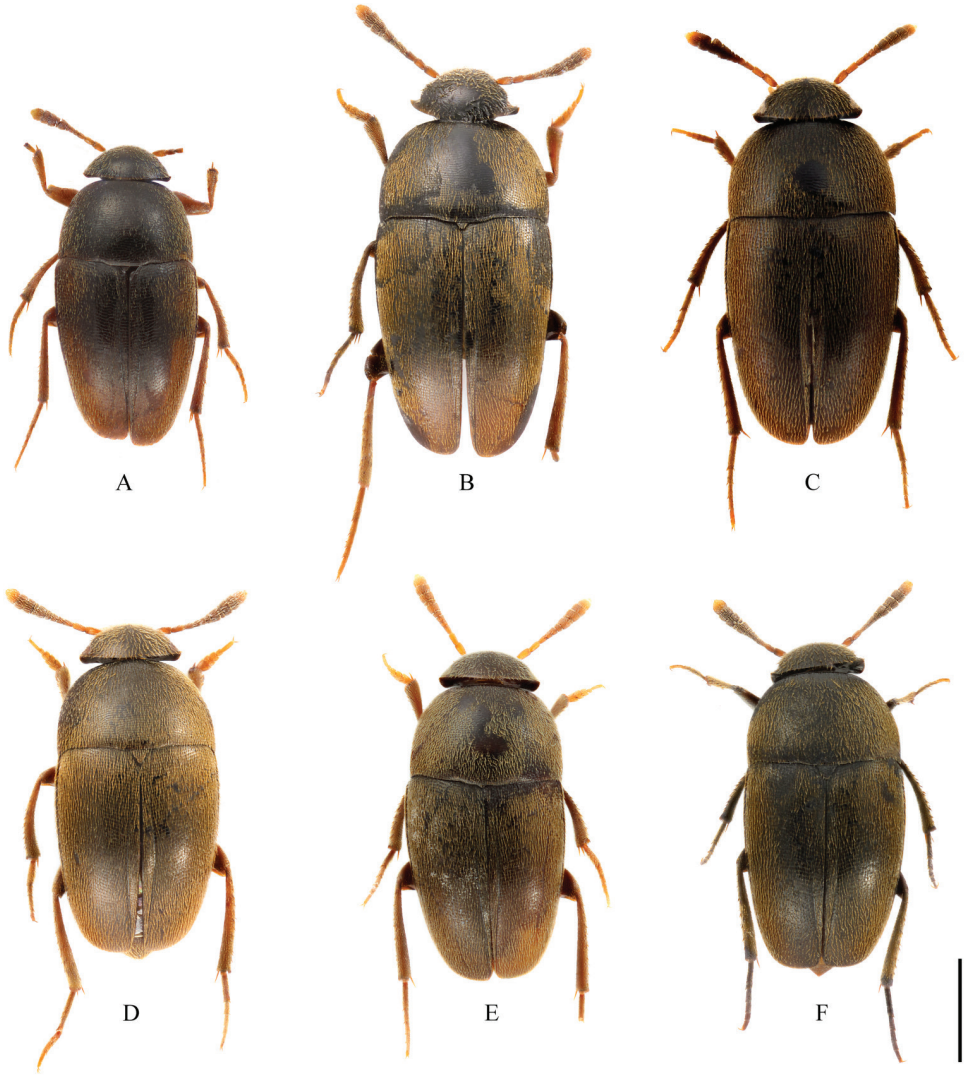

Figure 1. Habitus of *Ptomaphagus* (s. str.) spp. (dorsal view). **A, D–F** *P.* (s. str.) *sibiricus* Jeannel, 1934 **A** ♀ (holotype; Vladivostok) **D** ♂ (Vladivostok) **E** ♂ (Pyeongchang-gun) **F** ♀ (Boeun-gun) **B, C** *P.* (s. str.) *hayashii* sp. n. **B** ♂ (holotype; Vladivostok) **C** ♀ (paratype; Ussuri region). Scale: 1 mm.

Paratypes: 1♂1♀, FE.Russia, SW Khabarovsky / kray reg., Strel'nikova / range Mts., 46°43'N 134°08'E / Samur Riv., 130–550 m alt. / 25.VI.–28.VII.2014 / A. Plutenko leg. (CMNE); 1♀, same data as holotype (CMNE); 1♀, USSR Ussuri reg. / NOVOVARVAROVKA [ca. 43°58'N 132°59'E] / 6–10.VII.1989 / R. Červenka lgt. // Ptomaphagus (s. str.) / sibiricus / Jeannel, 1934 / Jan Růžička det. 2001 // ♀ (CJRZ); 1♂1♀, USSR Ussuri reg. / JASNOE [= Yasnoye, ca. 43°27'N 132°09'E] VII.1989 / St. Bečvář lgt. // Ptomaphagus (s. str.) / sibiricus / Jeannel, 1934 / Jan Růžička det. 2001 (CJRZ); 1♂1♀, USSR Ussuri reg. / JASNOE [= Yasnoye] / VII.1989 12–16 / St. Bečvář

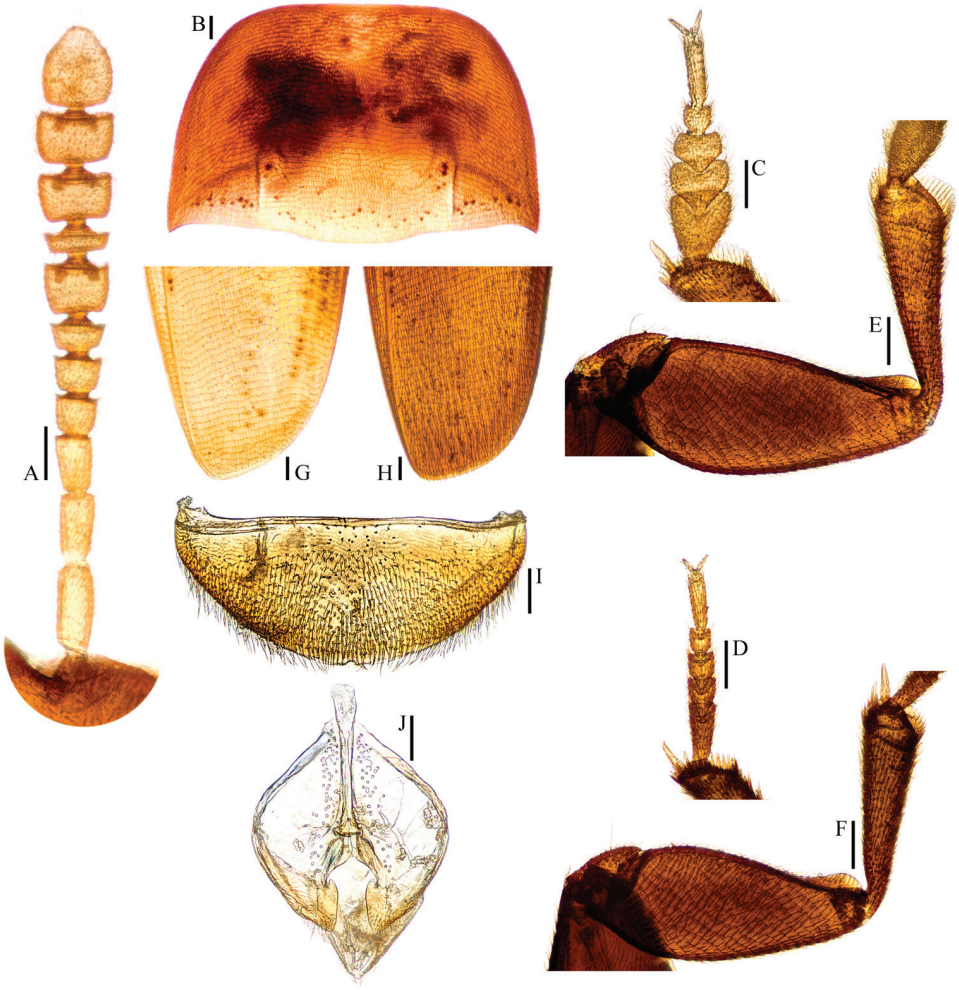

Figure 2. *Ptomaphagus* (s. str.) *hayashii* sp. n. (♂: holotype). **A** antenna ♂ (dorsal view) **B** pronotum ♂ (dorsal view) **C** protarsus ♂ (dorsal view) **D** protarsus ♀ (dorsal view) **E** protibia and profemur ♂ (ventral view) **F** protibia and profemur ♀ (ventral view) **G** elytral apex ♂ (dorsoapical view) **H** elytral apex ♀ (dorsoapical view) **I** ventrite VIII ♂ (ventral view) **J** genital segment ♂ (ventral view). Scales: 0.1 mm.

lgt. // MOUNT. OBLATCHNAJA [= Oblachnaya] / 400–800 m (CJRZ); 1♀, RUSSIA, Far East: / S Primorye region, / LAZO env. [ca. 43°22'N 133°54'E], 2.VII. / 2002 // Ptomaphagus (s. str.) / sibiricus / Jeannel, 1934 / Jan Růžička det 2009 / ♀ (CJRZ); 1♂, RUSSIA: Primorsky / 30 km NE Vladivostok / Tajvaza / 29.VII–5.VIII.1992 / B. D. Gill [leg.] (CJRZ); 1♂, Russian Far East, Primorskii krai / Lazovski Zapovednik, c. 170 km E / Vladivostok, Korpad, 1.–14.v.2001 / 175 m; 43°15'47"N 134°07'44"E / floodplain of Priamushka / Malaise trap 440; / M. Quest coll. BMNH (E) 2009-59 (BMNH); 1♀, same data as previous except: 13.–31.vii.2001 / 43°15'52"N 134°07'45"E; 174 m; / Mountain top, Malaise trap 481 (BMNH).

Description. *Male*. EBL: 3.8–4.3 mm (4.2 mm in holotype). Length of different body parts: HL : AL : PL : ELL = 0.7 : 1.1 : 1.1 : 2.3 mm; width: HW : EW : PW : ELW = 1.1 : 0.1 : 1.6 : 1.8 mm. Proportion of antennomeres from base to tip in μm (length × width): 149 × 75, 109 × 67, 95 × 70, 64 × 79, 58 × 92, 41 × 100, 91 × 128, 39 × 128, 87 × 151, 90 × 156, 161 × 143.

Habitus (Fig. 1B) elongated oval, regularly convex and sublustrous. Well pigmented: mostly blackish brown; mouthparts, antennae (apical half of ultimate antennomere yellowish) and tarsi reddish brown. Dorsum continuously clothed with fine, recumbent, yellowish pubescence. Insertions of pubescence on dorsal surfaces of pronotum, elytra and femora aligned along transverse striolations; interspace between two striolations glabrous.

Head transverse, HW/HL = 1.6. Clypeofrontal suture absent. Clypeus with anterior margin slightly rounded. Compound eyes well developed, EW/HW = 0.11. Antennae (Fig. 2A) slender, AL/HW = 1.0; antennomere III shorter than II; VI with length/width = 0.4; XI peach-shape.

Pronotum (Fig. 2B) transverse, widest just before hind angles, PW/PL = 1.5. Sides gently arched, simply narrowing from posterior to anterior; hind angles slightly projected backwards and acute. Posterior margin widely protruded in middle part, emarginate near hind angles.

Elytra oval, widest at about basal 1/4, ELL/EW = 1.3. Sides weakly arched, gradually narrowing from widest part to apices; apices (Fig. 2G) narrowly rounded. Sutural striae present. Metathoracic wings fully developed.

Prolegs robust, with basal three protarsomeres (Fig. 2C) strongly expanded: TW/BTW = 1.2. Protibiae (Fig. 2E) strongly expanded towards apex. Profemora broad. Mesotibiae arcuate, mesotarsi simply linear. Metatibiae slender and straight.

Abdominal ventrite VIII (Fig. 2I) round at posterior edge and with an inconspicuous median notch. Spiculum gastrale (Fig. 2J) of genital segment with about 1/5 of length protruding beyond anterior edge of epipleurite IX.

Aedeagus (Fig. 3A) long and slender, with median lobe gradually narrowing towards a lanceolate apex and terminated to a widely rounded knob in dorsal view; opening of genital orifice situated on dorsal surface, deeply cut inwards on preapical left margin of median lobe. Ventral surface of the apex of the median lobe (Fig. 3C) inserted with 5 ventrally oriented setae on both sides; parameres narrow, reaching about apical 1/5 of median lobe, each apex (Fig. 3D) with 2 lateral setae and 1 apical seta distinctly shorter. In lateral view (Fig. 3B), median lobe regularly bent ventrad and gradually tapering to a flat apex. Endophallus with stylus quite slender, a subelliptical nodule in middle region, a cheliform complex just below base of stylus, and a circular complex in the basal region.

Female. Similar to male in general appearance (Fig. 1C), including elytral apices (Fig. 2H), but distinguished by the following characteristics: protarsi (Fig. 2D) simply linear; protibiae (Fig. 2F) narrower; abdominal ventrite VIII (Fig. 3E) narrowly rounded at posterior edge; genital segment and ovipositor as shown in Fig. 3F; spermatheca (Fig. 3F) curved in distal part and coiled in proximal part.

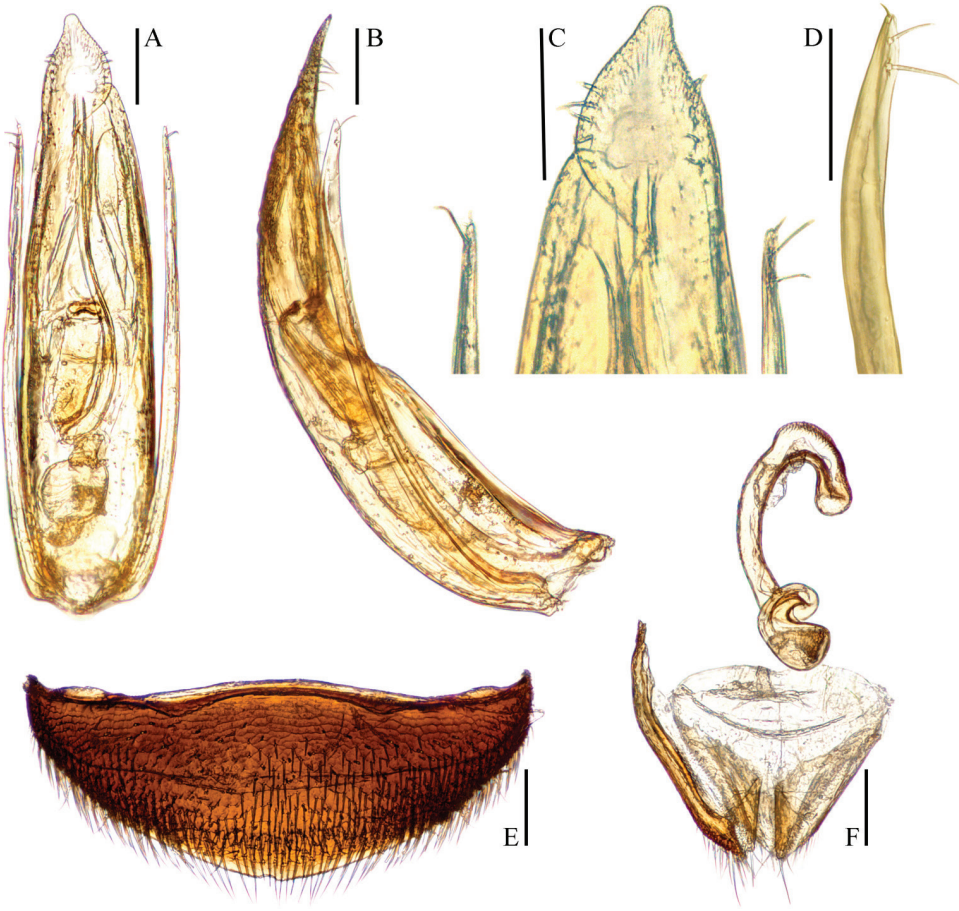

Figure 3. *Ptomaphagus* (s. str.) *hayashii* sp. n. (♂: holotype). **A** aedeagus (dorsal view) **B** aedeagus (lateral view) **C** aedeagal apex (ventral view) **D** paramere apex (lateral view) **E** ventrite VIII ♀ (ventral view) **F** spermatheca, genital segment and ovipositor (ventral view). Scales: 0.1 mm.

Diagnosis. *Ptomaphagus* (s. str.) *sibiricus* is sympatric with *P.* (s. str.) *hayashii* sp. n. in some locations of the Russian Far East, and they are very similar to each other (including spermatheca (Figs 3F; 5F), which is only more roundly curved in the stem part in *P.* (s. str.) *hayashii* sp. n.). For external characters, the body size of *P.* (s. str.) *sibiricus* (Figs 1A, D–F) is a little smaller than *P.* (s. str.) *hayashii* sp. n. (Figs 1B, C). However, their aedeagi provide critical characters to distinguish the two species: in *P.* (s. str.) *hayashii* sp. n., the aedeagus is much larger and more slender (Fig. 3A), the right apicoventral piece of the median lobe is slenderly lanceolate (Fig. 3C), the apical half of median lobe much flatter in lateral view (Fig. 3B); while in *P.* (s. str.) *sibiricus*, the aedeagus is stouter (Fig. 5A), the right apicoventral piece of median lobe is much wider and subpentagonal (Fig. 5C), the apical half of the median lobe thicker in lateral view (Fig. 5B).

Furthermore, based on specimens examined, *P.* (s. str.) *sibiricus* seems to be much more widely distributed, extending southward to South Korea; while *P.* (s. str.) *hayashii* sp. n. is presently known only in the Russian Far East.

Etymology. The specific epithet is dedicated to Mr. Yasuhiko Hayashi (Kawanishi, Japan), a famous independent taxonomist on Staphylinoidea, for his continual generous help to our study.

Distribution. Russia (Far East) (Fig. 6).

Ptomaphagus (s. str.) *sibiricus* Jeannel, 1934

Figs 1A, D–F; 4; 5

Jeannel 1934: 165 (*Ptomaphagus* (s. str.); type locality: [RUSSIA, Far East] Wladiwostok; SDEI); Jeannel 1936: 72, 84 (*Ptomaphagus* (s. str.); in key; distribution); Nishikawa 1983: 1 (*Ptomaphagus* (*Ptomaphagus*); in check-list); Perreau 2000: 364 (*Ptomaphagus* (s. str.); in catalogue); Perreau 2004: 178 (*Ptomaphagus* (*Ptomaphagus*); in catalogue); Zinchenko & Lyubechanskii 2008: 340 (*Ptomaphagus*; distribution); Perreau 2015: 249 (*Ptomaphagus* (*Ptomaphagus*); in catalogue).

Material examined. Type material. Holotype: ♀, [RUSSIA, Far East] Wladiwostok [ca. 43°10'N 132°00'E] // Reitter // Coll. Koltze // Pt. variicornis / Rosenh. // Ptomaphagus sibiricus Jeann. / type / R. Jeannel det. // DEI Müncheberg / Col – 07069 (SDEI).

Additional material. RUSSIA, Far East: 1♀, FE.Russia, SW Khabarovsky / kray reg., Strel'nikova / range Mts., 46°43'N 134°08'E / Samur Riv., 130–550 m alt. / 25.VI.–28.VII.2014 / A. Plutenko leg. (CMNE); 1♀, Vladivostok [ca. 43°10'N 132°00'E] / Christov [leg.] IX.[18]76 // Ptomaphagus sibiricus / Jeannel det. // Ptomaphagus / (Ptomaphagus) sibiricus / Jeannel, 1934 / Ex. M. Nishikawa, 2008 / # MNHN 103377Ch1S ♀ (MNHN); 10♂♂10♀♀, RUSSIA: Primorsky / 30 km NE Vladivostok / Tajvaza / 29.VII–5.VIII.1992 / B. D. Gill [leg.] (CJRZ); 1♀, RUSSIA: Primoryi / Nakhodka [ca. 42°49'N 132°52'E] / 6-8.VIII.1999 / B. D. Gill [leg.] (CJRZ); 1♂, USSR: Sadgorod [ca. 43°15'N 132°03'E]/ (in forest; trap with / bait), Vladivostok // Primorskyi Kray / 16.VI.1978 / E. Berlov leg. (CMNE); 1♂, Primorskiy Kray, Ussuriyskiy Region, Uss. [uriyskiy] Zapov. [ednik, = Reserve], Staraya Baza, 43.64°N, 132.34°E, poch.l. [= pitfall trap], V. Zinchenko & A. Korshunov [leg.], 9.–19.viii.2011 // Ptomaphagus / sibiricus / V. Zinchenko det. 2002 (CCBW). **South Korea:** 1♂, KOREA: Gangwon Prov., / Pyeongchang-gun, Jinbu-myeon, / Dongsan-ri, Mt. Odaesan, Sangwonsa [ca. 37°47'N 128°33'E], / 4.VI.–22.VI.2001, K.-J. Ahn, S.-J. / Park, M.-S. Kim, M.-J. Jeon [leg.], ex FIT // Ptomaphagus / baekamsanensis / n. sp. / det. S.-J. Park 2005 // 1 (CNUIC); 1♂, KOREA: Gangwon Prov., / Hongcheon-gun [ca. 37°41'N 127°50'E], Mt. Baekamsan, / 25.V.–20.VI.2002, K J Ahn, / C W Shin, J S Park, ex FIT // Ptomaphagus koreanus / new species / det. Sun-Jae Park (CNUIC); 1♀, KOREA, Chungbuk Prov., / Danyanggun, Youngchunmyeon,

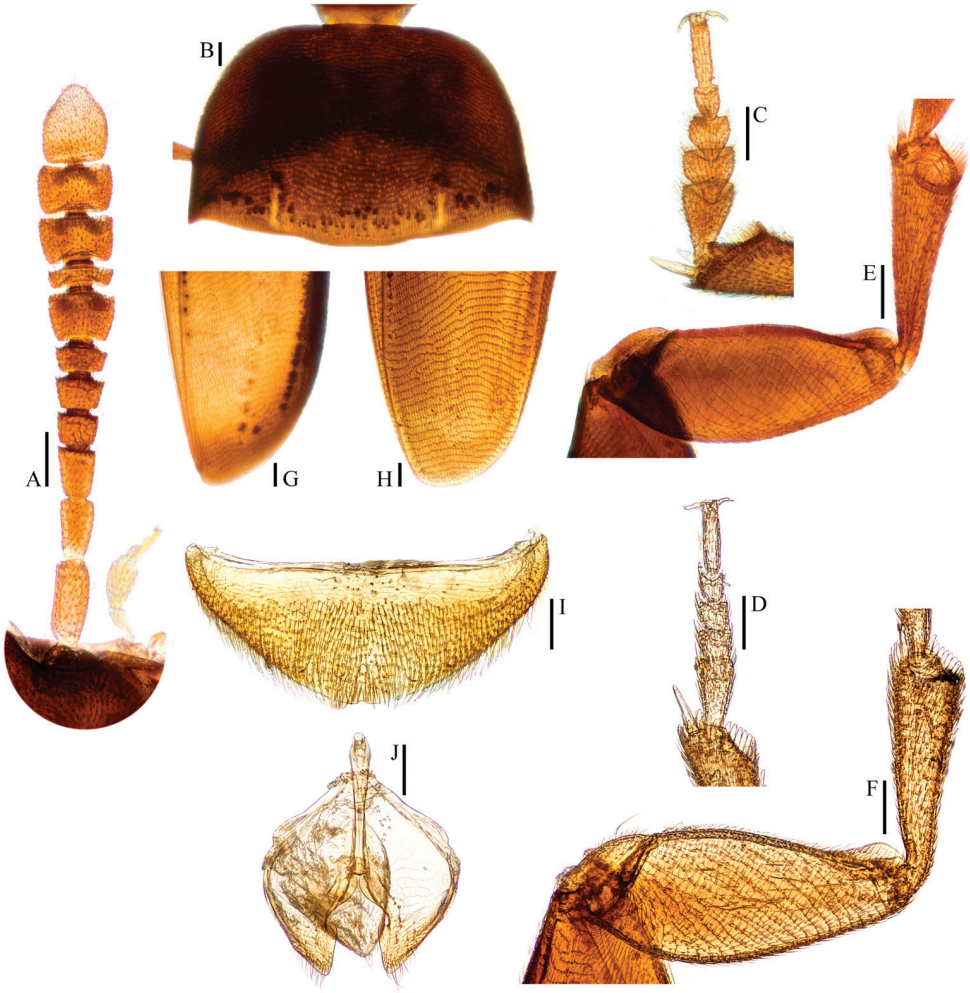

Figure 4. *Ptomaphagus* (s. str.) *sibiricus* Jeannel, 1934 (Vladivostok). **A** antenna ♂ (dorsal view) **B** pronotum ♂ (dorsal view) **C** protarsus ♂ (dorsal view) **D** protarsus ♀ (dorsal view) **E** protibia and profemur ♂ (ventral view) **F** protibia and profemur ♀ (ventral view) **G** elytral apex ♂ (dorsoapical view) **H** elytral apex ♀ (dorsoapical view) **I** ventrite VIII ♂ (ventral view) **J** genital segment ♂ (ventral view). Scales: 0.1 mm.

/ Namcheonri, Namcheon valley, / Mt. Sobaeksan [ca. 36°57'N 128°26'E], (M.T), / 25.V.–6.VII.2006 (CNUIC); 1♂, same data as previous except: 2006.VII.6–VII.28 (CNUIC); 1♀, Korea, Kyungsangbuk-do / Yuongdong-gun / Sangchon-myun, Mulhan-ri / Mt. Minjujisan [ca. 36°02'N 127°50'E] / VI.16–18.2000, / Y.B. Cho / coll. / ex bait trap // ♀ No.9 (CNUIC); 1♀, same data as previous except: ♀ 10 (CNUIC); 4♂♂1♀, Korea, Chonrabukdo / Selchonmyun / Mt. Deokyusan / Baekyeonsa Temple [ca. 35°26'N 126°52'E] // vi.16.1999 / D. S. Kim coll. / ex bait trap // Ptomaphagus / sp. / Det. M. Nishikawa // [5, 6, 13, 14 & 15, respectively] (CNUIC); 1♂2♀♀, KOREA: Chungbuk Prov., / Boeun-gun, Mt. Sokrisan [ca. 36°32'N 127°54'E], / Bubjusa, 2004.VI.1–28, / Y.-B. Cho [leg.], FIT (CMNE).

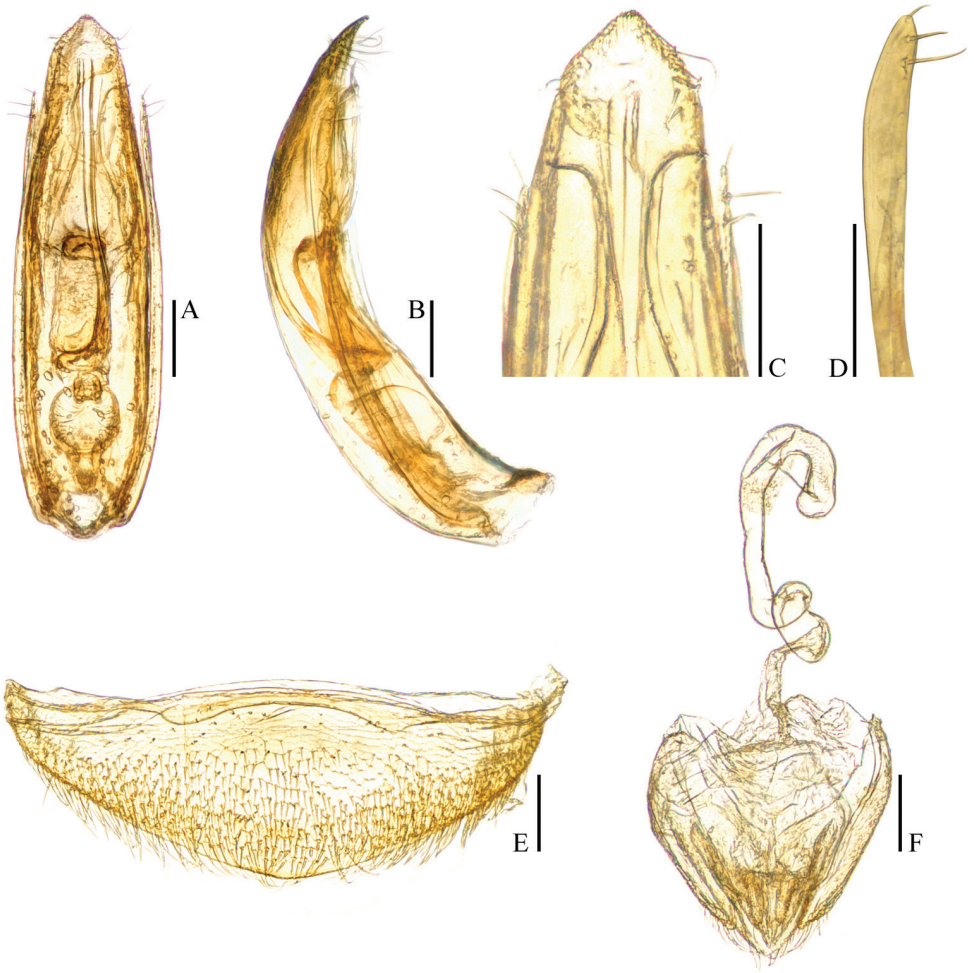

Figure 5. *Ptomaphagus* (s. str.) *sibiricus* Jeannel, 1934 (Vladivostok). **A** aedeagus (dorsal view) **B** aedeagus (lateral view) **C** aedeagal apex (ventral view) **D** paramere apex (lateral view) **E** ventrite VIII ♀ (ventral view) **F** spermatheca, genital segment and ovipositor (ventral view). Scales: 0.1 mm.

Redescription. *Male*. EBL: 3.1–3.8 mm (3.1 mm in holotype). Length of different body parts: HL : AL : PL : ELL = 0.6 : 1.0 : 1.0 : 1.8 mm; width: HW : EW : PW : ELW = 1.0 : 0.1 : 1.5 : 1.6 mm. Proportion of antennomeres from base to tip in μm (length × width): 134 × 66, 107 × 65, 77 × 67, 55 × 81, 54 × 88, 47 × 102, 88 × 125, 35 × 128, 82 × 140, 82 × 140, 147 × 127.

Habitus (Figs 1D, E) elongated oval, regularly convex and sublustrous. Well pigmented: mostly dark brown; mouthparts, basal three antennomeres and apical half of ultimate antennomere, protarsi, and apex of meso- and metatarsi more or less paler. Dorsum continuously clothed with fine, recumbent, yellowish pubescence. Insertions of pubescence on dorsal surfaces of pronotum, elytra and femora align along transverse striolations; interspace between two striolations glabrous.

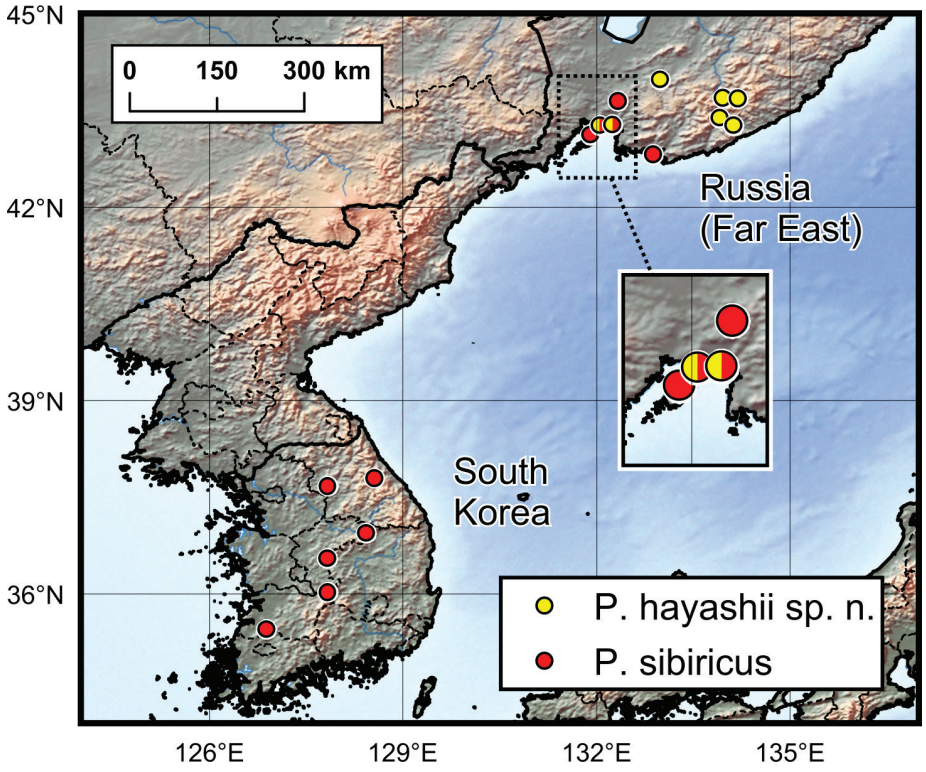

Figure 6. Distribution map of *Ptomaphagus* species from the Russian Far East and the Korean Peninsula.

Head quite transverse, HW/HL = 1.7. Clypeofrontal suture absent. Clypeus with anterior margin almost straight. Compound eyes well developed, EW/HW = 0.1. Antennae (Fig. 4A) slender, AL/HW = 1.0; antennomere III shorter than II; VI with length/width = 0.5; XI peach-shape.

Pronotum (Fig. 4B) transverse, widest just before hind angles, PW/PL = 1.4. Sides gently arched, gradually narrowing from posterior to anterior; hind angles projected backwards and acute. Posterior margin widely protruded in middle part, distinctly emarginate near hind angles.

Elytra oval, widest at about basal 1/3, ELL/EW = 1.2. Sides weakly arched, gradually narrowing from widest part to apices; apices (Fig. 4G) narrowly to widely rounded (all examined specimens from South Korea with wide elytral apices). Sutural striae present. Metathoracic wings fully developed.

Prolegs robust, with basal three protarsomeres (Fig. 4C) strongly expanded: TW/BTW = 1.3. Protibiae (Fig. 4E) distinctly expanded towards apex. Profemora broad. Mesotibiae arcuate, mesotarsi simply linear. Metatibiae slender and straight.

Abdominal ventrite VIII (Fig. 4I) rounded and with an inconspicuous median notch at posterior edge. Spiculum gastrale (Fig. 4J) of genital segment with about 1/5 of length protruding beyond anterior edge of epipleurite IX.

Aedeagus (Fig. 5A) long, slender but relatively strong, with median lobe gradually narrowing towards a wide subpentagonal apex and terminated to a widely rounded knob in dorsal view; opening of genital orifice situated on dorsal surface, deeply cut inwards on preapical left margin of median lobe. Ventral surface of the apex of the median lobe (Fig. 5C) inserted with 6 ventrally oriented setae on the left side and 5 ventrally oriented setae on the rigth side; parameres narrow, reaching about apical 1/6 of median lobe, each apex (Fig. 5D) with 2 lateral setae and 1 apical seta distinctly shorter. In lateral view (Fig. 5B), median lobe thick, regularly bent ventrad, and gradually tapering to a thin apex. Endophallus with stylus quite slender, a cheliform complex just below base of stylus, and a circular complex in the basal region.

Female. Similar to male in general appearance (Fig. 1A, F), including elytral apices (Fig. 4H) and protibiae (Fig. 4F), but distinguished by the following characteristics: protarsi (Fig. 4D) simply linear; abdominal ventrite VIII (Fig. 5E) rounded at posterior edge; genital segment and ovipositor as shown in Fig. 5F; spermatheca (Fig. 5F) curved in distal part and coiled in proximal part.

Diagnosis. See under *P.* (s. str.) *hayashii* sp. n. above. Other remarks on this species see Wang et al. (2016a).

Distribution. Russia (Far East), South Korea (Fig. 6).

Acknowledgements

We would like to express our sincere thanks to Kee-Jeong Ahn (Chungnam National University, Daejeon, Republic of Korea), Maxwell V. L. Barclay (BMNH, London, United Kingdom), Young-Bok Cho (Hannam University, Daejeon, Republic of Korea), Yasuhiko Hayashi (Kawanishi, Japan), Hideto Hoshina (Fukui University, Fukui, Japan), Alfred F. Newton (Field Museum of Natural History, Chicago, USA), Stewart B. Peck (Carleton University, Ottawa, Canada), Vadim Zinchenko (Russian Academy of Sciences, Siberian Branch, Novosibirsk, Russia) and Hong-Zhang Zhou (Institute of Zoology, Chinese Academy of Sciences, Beijing, China) for their considerable help in our study. We are obliged to Pavel Jakubec (Czech University of Life Sciences, Prague, Czech Republic) for helping with habitus photographs with the camera system. All the collectors mentioned in the text are acknowledged for their field work. We thank Maxwell V. L. Barclay for linguistic revision of the text. We are grateful to Leonardo Latella (Verona, Italy) as a reviewer who provided constructive comments on previous version of the manuscript. This study was supported by the Ministry of the Interior of the Czech Republic (no. VI20152018027).

References

Hellwig JCL (1795) Favna etrvsca sistens Insecta qvae in provinciis Florentina et Pisana praesertim collegit Petrvs Rossivs, in Regio Pisano Aethenaeo Publ. prof. et Soc. Ital. Tomus primus. C. G. Fleckeisen, Helmstadii, 457 pp.

Jeannel R (1934) Les *Ptomaphagus* paléarctiques (Col.). Revue Française d'Entomologie 1: 161–170.

Jeannel R (1936) Monographie des Catopidae (Insectes Coléoptères). Mémoires du Muséum National d'Histoire Naturelle (N.S.) 1: 1–433.

Nishikawa M (1983) Family Catopidae. Check-list of Coleoptera of Japan (23). Coleopterists' Association of Japan, Tokyo, 1–6.

Perreau M (2000) Catalogue des Coléoptères Leiodidae, Cholevinae et Platypsyllinae. Mémoires de la Société entomologique de France 4: 1–460.

Perreau M (2004) Family Leiodidae Fleming, 1821. In: Löbl I, Smetana A (Eds) Catalogue of Palaearctic Coleoptera. Volume 2: Hydrophiloidea – Histeroidea – Staphylinoidea. Apollo Books, Stenstrup, 133–203.

Perreau M (2015) Family Leiodidae Fleming, 1821. In: Löbl I, Löbl D (Eds) Catalogue of Palaearctic Coleoptera. Volume 2/1. Hydrophiloidea – Staphylinoidea. Revised and updated edition. Brill, Leiden & Boston, 180–290.

Wang C-B, Nishikawa M, Perreau M, Růžička J, Hayashi Y (2016b) Revision of the genus *Ptomaphagus* Hellwig (Coleoptera, Leiodidae, Cholevinae) from Taiwan Island. ZooKeys 609: 43–62. doi: 10.3897/zookeys.609.9327

Wang C-B, Růžička J, Nishikawa M, Perreau M, Hayashi Y (2016a) Revision of the genus *Ptomaphagus* Hellwig (Coleoptera, Leiodidae, Cholevinae) from Japan. ZooKeys 607: 119–144. doi: 10.3897/zookeys.607.9074

Zinchenko VK, Lyubechanskii II (2008) Notes on the occurrence of round fungus beetles (Leiodidae, Cholevinae) in the Russian Far East. Evraziatskii Entomologicheskii Zhurnal 7(4): 339–340.

ZooKeys 637: 47–59 (2016)
doi: 10.3897/zookeys.637.10202
http://zookeys.pensoft.net

RESEARCH ARTICLE

A peer-reviewed open-access journal
ZooKeys
Launched to accelerate biodiversity research

A new blind species of the cave genus *Oreonectes* from Guizhou, China (Nemacheilinae)

Huaiqing Deng[1,*], Huamei Wen[1,*], Ning Xiao[2], Jiang Zhou[1]

1 *School of Life Sciences, Guizhou Normal University, Guiyang, Guizhou, 550001, China* **2** *Guiyang Nursing Vocational College, Guiyang, Guizhou, 550003, China*

Corresponding author: *Ning Xiao* (armiger@qq.com); *Jiang Zhou* (zhoujiang@ioz.ac.cn)

Academic editor: *M. Bichuette* | Received 17 August 2016 | Accepted 9 November 2016 | Published 28 November 2016

http://zoobank.org/D3F23929-C078-43F3-BE7A-33D13371053D

Citation: Deng H, Wen H, Xiao N, Zhou J (2016) A new blind species of the cave genus *Oreonectes* from Guizhou, China (Nemacheilinae). ZooKeys 637: 47–59. https://doi.org/10.3897/zookeys.637.10202

Abstract

This study aimed to describe a new specimen of cavefish collected from a karst cave in the Daqikong area of Libo County, Guizhou. Twenty-six cavefish specimens were collected and identified as a new species of Balitoridae: Nemacheilinae, and named *Oreonectes daqikongensis* **sp. n.** A genetic analysis was performed and showed that its genetic distances from *Oreonectes shuilongensis* and *Oreonectes platycephalus* are higher than intraspecific distances. Discovery of this species will be helpful to understand the distribution of *Oreonectes*.

Keywords

Cavefish, Libo, new species, *Oreonectes daqikongensis* sp. n.

Introduction

Nemacheilinae are common in tropical Asia. They occur in a great variety of habitats, particularly abundant in swiftly flowing hillside streams. The similar living environment may help explain why many cavefish of Asia belong to this subfamily (Kottelat 1990).

* These authors contributed to the work equally and are regarded as co-first authors.

There are 15 genera and more than 100 species was found belong to the Nemacheilinae subfamily in China so far (Zhu 1995). The *Oreonectes* was first established by Günther (1868) with *O. platycephalus* as the type species. A total of 16 species of Oreonectes are considered valid. Du et al (2008) divide Oreonectes into two groups that including furcocaudalis group and platycephalmus group. The platycephalmus group includes the *O. platycephalus*, *O. Polystigmus*, *O. guananensis* (Yang et al. 2011), *O. luochengensis* (Yang et al. 2011), and *O. anophthalmus* (Zhu 1989). The furcocaudalis group includes the *O. microphthalmus* (Du et al. 2008), *O. macrolepis*, *O. retrodorsalis* (Lan et al. 1995), *O. acridorsalis*, *O. barbatus*, *O. duanensis*, and *O. donglanensis* (Lan et al. 2013), *O. elongates* (Tang et al. 2012), *O. translucens* (Zhang et al. 2006), *O. furcocaudalis* (Zhu 1989), and *Oreonectes* sp. n. (Chen et al. 2011). They all dwell in underground rivers of the karst environment (Yang et al. 2011; Lan et al. 2013). During a cave biodiversity survey on Libo County, Guizhou in 2011, we using seines nets and the bait collected 26 new cavefish specimens at Daqikong area. This study aimed to describe and identify the new specimen of cavefish.

Materials and methods

The holotype was fixed and preserved in 10% formalin, and the paratypes were preserved in anhydrous ethanol. The specimens were stored in the Animal Specimen Room of the School of Life Sciences, Guizhou Normal University (GNUG). All measurements are taken on the left side of the fish specimens. All measurements were taken point to point with digital calipers to 0.1 mm. The new species was identified according to the morphological features, molecular phylogenetic evidence, and distribution regions. Counts and proportional measurements follow Tang et al (2012). The sources of material of other *Oreonectes* species is in Appendix 1.

The tissue sample was extracted from the right side of the specimen no. 25, from which the genomic DNA was extracted using from muscle tissues by standard phenolchloroform methods (Sambrook and Russell 2001). Then the cytb gene segment was amplified using the Cyprinidae universal primers L14724 and H15915 (Rui et al. 2012). Both the amplification and sequencing were completed in Beijing Ruijie Gene Technology Co., Ltd. (Beijing, China).

The Sequence Alignment Editor (BioEdit) software was used to analyze sequencing peaks and delete carrier sequences, and then Seqman v5.51 (DNAStar) was used to perform the sequence assemble and alignment. Complete cytb sequences of other 29 species of Nemacheilinae were obtained from GenBank (Table 1). The cytb gene nucleic acid sequences of all the 30 species were compared with the ClustalW method of MEGA 6.0 software (Tamura et al. 2013), the terminal irregular regions were removed manually. Subsequently, the phylogenetic tree was established using the maximum likelihood (ML) method in MEGA 6.0, while reliability was tested using the Kimma2-Pamameter distance model and bootstrap method by repeating 1000 times.

Table 1. GenBank accession numbers for the analyzed samples included in the phylogenetic analysis.

Genus	Species	Accession
Oreonectes	*shuilongensis*	KF640641
	daqikongensis	KU987436
	platycephalus	DQ105197
Schistura	*fasciolata*	HM010565
	caudofurca	JN837651
	desmotes	GQ174368
	callichroma	JN837652
	latifasciata	JN837653
	bucculenta	JN837654
	macrotaenia	JN837655
	amplizona	JN837656
	cryptofasciata	JF340401
	sikmaiensis	JF340405
	poculi	JF340407
	longa	JF340408
Homatula	*pycnolepis*	KF041000
	acuticephala	HM010527
	longidorsalis	HM010550
	potanini	JF340388
Traccatichthys	*pulcher*	JF340402
Schistura	*shuangjiangensis*	JF340404
Paracobitis	*anguillioides*	HM010582
Triplophysa	*xiangxiensis*	JN696407
	stoliczkai	DQ105249
	siluroides	EF212443
	bleekeri	FJ406605
	stenura	JN837657
	orientalis	DQ105251
Nemacheilus	*maysae*	GQ174377
	ornatus	GQ174363
	pallidus	GQ174370

Results

***Oreonectes daqikongensis* sp. n.**
http://zoobank.org/598D9793-208A-45ED-BCA9-A1C9203003A3

Type materials. The 26 specimens were collected from Daqikong area of Libo County, Guizhou; the overall length of the specimen was 37.82–83.10 mm and the body length was 31.28–70.96 mm.

Holotype. (No. CNGZNU20110128001; Figure. 1a–b) The total length is 77.14 mm and the body length is 61.46 mm. Holotype was collected from a subterranean river of the Daqikong area (N 25°17'05.1", E 107°44'54.3"; H 488 m) in January 2011.

Figure 1. a Holotype of *Oreonectes daqikongensis* sp. n. NO.CNGZNU20110128002. **b** A living *Oreonectes daqikongensis* sp. n.

It was stored in the animal specimen room of the School of Life Sciences, Guizhou Normal University, Guiyang, China.

Paratypes. (25, No. CNGZNU20110128002–CNGZNU20110128026) Paratypes were collected and stored in the same places as the holotype.

Habitat. This species was found only in the Daqikong scenic area. The opening of the cave was halfway up the mountain, and the distance from the opening to the pool was about 15–20 m. The cave got no sunshine because of the twisty pathway. A large number of *Hipposideros armiger* lived in the cave and a thick layer of bat dung was found on the ground. Groundwater extended into the cave, and the water rushed outside the cave in the case of heavy rain. So far, no other fish, shrimps, or aquatic animals were found in the cave. The subterranean river belonged to the Dagou river system, and was the main river of the Libo County, which runs through the whole county, enters Guangxi from the Laocun Xiang, and was the major tributary of the Duliu River system (Figure 2).

Diagnosis. The species has a large head, and the width of the head is larger than its depth. The frontal torso is nearly cylindrical, the backend gradually compresses, and the head is slightly flattened. There is a short distance between the anterior and posterior nostrils, and the anterior nostril forms a short and tubular structure, which is truncated backward. The pectoral fin extends backward to or beyond the starting point of the pelvic fin. The body is naked. The eyes are completely degraded; and eye socket was filled in fat tissue and without any outside remnant indicating their presence. The superior and inferior caudal peduncles have well-developed soft finfolds. No carneous

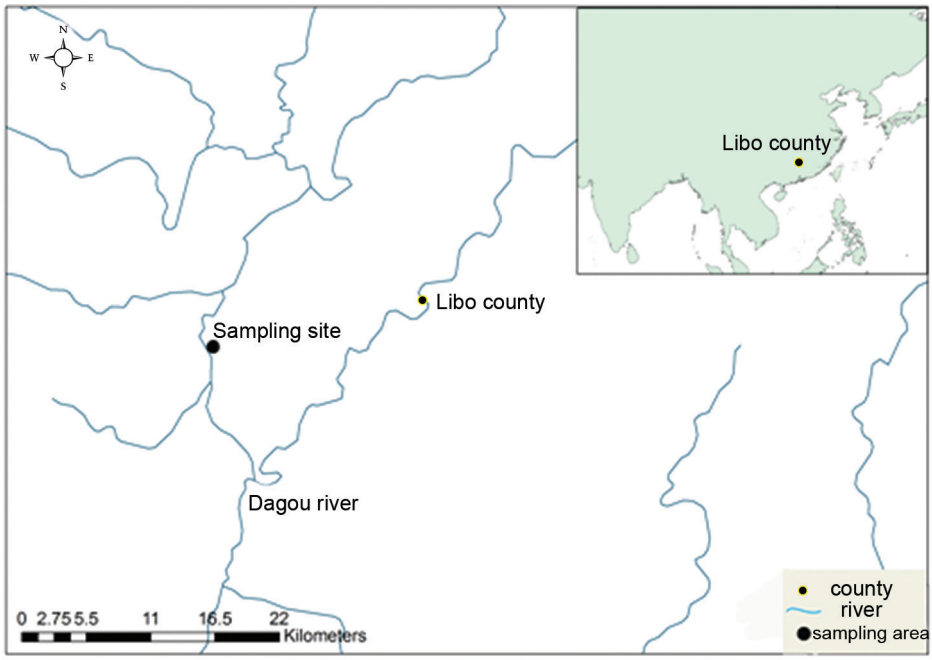

Figure 2. Collection localities of *O. daqikongensis* sp. n.

fin flaps are present in the pelvic fin axilla. The air bladder is wrapped in a bony capsule, and the posterior chamber of the air bladder is developed into a membranous chamber, which is separated from the abdominal cavity and connected to the anterior chamber by a short duct. The whole body is white and transparent, when they are alive, they look a little red because the blood inside, and is unlikely to become black when it is fed in sunlight for a long term.

Description. The species has a slightly elongated body, slightly ridged back, body slightly spindle, and compressed hindquarters, and its widest part is at the gill cover. The main measurable characters of *O. daqikongensis* are shown in Table 2. The head is slightly flattened, lips are rounded, eyes vestigial. Anterior and posterior nostrils well separated. Anterior nostril forms short tubular and posterior nostrils elliptical. The fish has an inferior mouth, and the upper and lower lips are connected at the corner of the mouth. The upper jaw is curved and the lower jaw is spoon shaped. The mouth aperture is U-shaped, and its rear end reaches the bottom part of the posterior edge of the naris. It has three pairs of slim barbels, and one pair each of inner rostral barbels, outer rostral barbels, and mouth corner barbels. The inner rostral barbels are shorter, and the outer rostral barbels extend backward to exceed the rear edge of the posterior naris, while the maxillary barbels extend backward and their ends are appropriate at the center of the rear edge of the opercular bone. The superior and inferior sides of the caudal peduncle have well-developed ridge-like fatty soft fin folds; especially, the soft

Table 2. Main morphometric characters of *O. daqikongensis* sp. n.

Measurements	Holotype	Range	Mean ± SD
Total length (mm)	50.96	41.62~77.14	57.15 ± 10.36
Standard length (mm)	41.68	34.22~61.46	46.49 ± 8.11
Percentage (%) of SL			
Body height	18.04	15.30~23.26	20.43 ± 1.92
Body width (at dorsal fin origin)	13.72	12.42~19.74	15.86 ± 1.77
Predorsal length	50.82	50.79~56.32	53.06 ± 1.74
Length of caudal peduncle	18.67	13.16~19.18	16.50 ± 1.95
Depth of caudal peduncle	7.15	7.15~9.90	8.26 ± 0.82
Percentage (%) of HL			
Body height	60.74	56.94~82.90	70.48 ± 6.93
Head height (at nape)	44.75	44.30~58.84	50.19 ± 4.38
Head width	49.11	49.11~61.73	55.47 ± 4.03
Length of inner rostral barbel	17.12	12.36~17.75	15.03 ± 1.83
Length of outer rostral barbel	24.39	18.42~33.12	25.86 ± 4.29
Length of maxillary barbel	25.85	22.92~30.17	27.04 ± 1.68
Percentage (%) of TL			
Body height	14.76	12.69~18.77	16.43 ± 1.57
Body width(at dorsal fin origin)	11.22	10.30~15.91	12.90 ± 1.36
Head length	24.29	22.29~25.93	23.62 ± 0.93

fin folds between the superior caudal peduncle and the dorsal fin are more apparent than those in the inferior caudal peduncle, where its front end reaches the upper part of the anal fin. The superior soft fin folds originate from the rear edge of the dorsal fin base to one third of the front edge of the caudal fin base, where compressing the dorsal fin backward can reach the origin of the soft fin folds. The inferior soft fin folds originate from the rear edge of the anal fin base to one third of the front edge of the caudal fin base.

The distance from the dorsal fin origin to the rostral end is larger than that from the dorsal fin origin to the caudal fin base, and the outer edge is truncated or slightly concave. The rear end of the dorsal fin can be compressed to reach the soft fin fold origin. The fish has a long pectoral fin, which extends backward to or beyond the pelvic fin base. Also, the pectoral fin has a very special morphology, which does not have branched fin rays. The first and second fin rays are very long, forming a spoke-like shape. The ventral fin originates at a place opposite to the origin of the dorsal fin, and it extends backward to cover the anus and close to the origin of the anal fin. The distance from the anus to the anal fin origin is about 1 mm. The anal fin extends to its base to half of the caudal fin base. The posterior edge of the caudal fin is forked, and the upper lobe is slightly longer than the lower lobe.

The fish is naked, and the intact lateral line is superficially subcutaneously buried, which is flattened from the upper angle of the gill cover and extends backward to the center of the caudal fin base. Sensory tubes are present in the head connecting to the lateral

Oreonectes_daqikongensis																													
Oreonectes_shuilongensis	0.1212																												
Oreonectes_platycephalus	0.1802	0.1682																											
Schistura_fasciolata	0.1865	0.1709	0.1929																										
Schistura_desmotes	0.1870	0.1518	0.2008	0.1927																									
Schistura_callichroma	0.1885	0.1876	0.1987	0.0734	0.1899																								
Schistura_latifasciata	0.1870	0.1827	0.1842	0.0764	0.1847	0.0721																							
Schistura_bucculenta	0.1838	0.1646	0.1904	0.0712	0.1842	0.0764	0.0772																						
Schistura_macrotaenia	0.1849	0.1878	0.1876	0.0733	0.1776	0.0442	0.0774	0.0795																					
Schistura_amplizona	0.1961	0.1914	0.1939	0.0776	0.1834	0.0702	0.0365	0.0773	0.0785																				
Schistura_cryptofasciata	0.1889	0.1708	0.1841	0.0531	0.1764	0.0511	0.0599	0.0540	0.0590	0.0651																			
Schistura_sikmaensis	0.1877	0.1788	0.2225	0.1923	0.1064	0.1930	0.1943	0.1976	0.1957	0.1843	0.1884																		
Schistura_poculi	0.1844	0.1818	0.2162	0.1908	0.0955	0.1881	0.1991	0.1924	0.1857	0.1854	0.1735	0.0892																	
Schistura_longa	0.1832	0.1830	0.2148	0.1895	0.0944	0.1868	0.2004	0.1911	0.1844	0.1866	0.1723	0.0882	0.0009																
Homatula_pycnolepis	0.2143	0.2043	0.2159	0.1531	0.1784	0.1469	0.1516	0.1528	0.1468	0.1531	0.1437	0.1929	0.1980	0.1967															
Homatula_acuticephala	0.1970	0.1898	0.2165	0.1536	0.1642	0.1391	0.1426	0.1497	0.1367	0.1488	0.1348	0.1932	0.1919	0.1907	0.0452														
Homatula_longidorsalis	0.1939	0.1918	0.2165	0.1426	0.1752	0.1354	0.1366	0.1377	0.1353	0.1438	0.1334	0.1959	0.1969	0.1957	0.0996	0.0828													
Homatula_potanini	0.2013	0.1979	0.2076	0.1436	0.1715	0.1340	0.1410	0.1318	0.1386	0.1366	0.1298	0.1919	0.1957	0.1944	0.1036	0.0921	0.0815												
Traccatichthys_pulcher	0.1935	0.1767	0.1993	0.1771	0.1767	0.1671	0.1791	0.1765	0.1686	0.1818	0.1732	0.1959	0.1899	0.1886	0.1895	0.1717	0.1725	0.1860											
Schistura_shuangjiangensis	0.1971	0.1879	0.2189	0.1922	0.0977	0.1882	0.1992	0.2102	0.1833	0.1917	0.1895	0.1231	0.1199	0.1187	0.1981	0.1920	0.1945	0.1772	0.1912										
Homatula_anguillioides	0.1970	0.1898	0.2165	0.1536	0.1642	0.1403	0.1438	0.1509	0.1378	0.1500	0.1359	0.1932	0.1919	0.1907	0.0442	0.0009	0.0839	0.0932	0.1717	0.1920									
Triplophysa_xiangxiensis	0.2077	0.1943	0.2075	0.2046	0.2178	0.2069	0.2030	0.1982	0.2117	0.2040	0.2083	0.2144	0.2290	0.2276	0.2127	0.2044	0.2133	0.2126	0.2252	0.2408	0.2044								
Triplophysa_stoliczkai	0.2534	0.2281	0.2322	0.2428	0.2463	0.2390	0.2404	0.2309	0.2351	0.2530	0.2351	0.2402	0.2420	0.2406	0.2597	0.2538	0.2534	0.2454	0.2393	0.2425	0.2538	0.2277							
Triplophysa_siluroides	0.2546	0.2200	0.2426	0.2286	0.2464	0.2330	0.2233	0.2266	0.2305	0.2259	0.2291	0.2366	0.2255	0.2269	0.2339	0.2281	0.2295	0.2188	0.2354	0.2357	0.2281	0.2135	0.2023						
Triplophysa_bleekeri	0.2478	0.2295	0.2316	0.2612	0.2369	0.2401	0.2459	0.2436	0.2330	0.2612	0.2438	0.2405	0.2395	0.2381	0.2635	0.2533	0.2685	0.2618	0.2514	0.2376	0.2533	0.2249	0.1648	0.2181					
Triplophysa_stenura	0.2497	0.2354	0.2460	0.2482	0.2348	0.2321	0.2412	0.2307	0.2309	0.2371	0.2363	0.2397	0.2276	0.2263	0.2393	0.2278	0.2258	0.2275	0.2261	0.2310	0.2278	0.2000	0.1454	0.1927	0.1712				
Triplophysa_orientalis	0.2383	0.2066	0.2246	0.2287	0.2241	0.2358	0.2194	0.2318	0.2216	0.2260	0.2213	0.2236	0.2316	0.2330	0.2493	0.2404	0.2306	0.2349	0.2273	0.2284	0.2404	0.2114	0.1695	0.1835	0.1791	0.1505			
Nemacheilus_masyae	0.1933	0.1976	0.2130	0.1997	0.1730	0.1984	0.1884	0.2043	0.1900	0.1971	0.1910	0.1879	0.1844	0.1832	0.2191	0.1987	0.2010	0.2031	0.1754	0.1870	0.1987	0.2334	0.2523	0.2528	0.2427	0.2380	0.2327		
Nemacheilus_ornatus	0.1907	0.1895	0.2203	0.1990	0.1840	0.2005	0.2066	0.2003	0.1981	0.1976	0.1894	0.1822	0.1849	0.1837	0.2219	0.2133	0.2042	0.2139	0.1884	0.1943	0.2146	0.2284	0.2482	0.2598	0.2388	0.2404	0.2353	0.1547	
Nemacheilus_pallidus	0.2100	0.2094	0.2210	0.2153	0.1791	0.2153	0.2012	0.2171	0.2066	0.2037	0.2064	0.1917	0.1869	0.1857	0.2178	0.1977	0.2013	0.2084	0.1878	0.2009	0.1977	0.2358	0.2461	0.2455	0.2671	0.2559	0.2418	0.0581	0.1677

Figure 3. Genetic distance between *O. daqikongensis* sp. n. and species of Nemacheilinae.

line at the upper part of the posterior edge of the gill cover, and bifurcate into two lateral lines toward the head. These tubes travel from the supraorbital bone to the inner side of the anterior nostrils and from the infraorbital bone to the outer side of the nostrils, and connect to the two lateral lines via a transverse lateral line at the parietal bone. The whole body is colorless, and the living fish is translucent, where the internal organs are visible. The stomach is U-shaped, and the intestine is in its rear part, which is slightly curved and extends to the anus. The anterior bladder chamber is completely coated by the bony bladder sac, which has a bony posterior wall and no opening. However, the posterior bladder is a well-developed membranous chamber, which is separated from the abdominal cavity and connected to the anterior chamber by a short tube. An oval transparent area exists in the posterior branchial aperture, which is inset in both sides of the body.

Color. The whole body of the living species is pale pink and translucent, where the vertebra, body segment at caudal peduncle, cardinal gill, and internal organs are visible. Its body color is unlikely to change when it is fed in the laboratory under light for a long term.

Phylogenetic findings. In the 25 specimens of *O. daqikongensis* sp. n., the cyt b sequence was at 1140 bp, and the base did not show any difference among them, in which $T = 27.6\%$, $C = 28.7\%$, $A = 28.8\%$, and $G = 14.9\%$, and the overall transition/transversion rate was $R = 0.50$. The genetic distances between the new species and *O. platycephalus* and *O. shuilongensis* were 0.1802 and 0.1212, respectively, which were smaller than the genetic distance among species of other categories. The genetic distance between *Oreonectes* and the other categories of Nemacheilinae ranged from 0.1518 to 0.2546. The interspecific genetic distance of Nemacheilinae was 0.0009–0.2533(Figure 3). The sequence divergence of Cyt b between this species and *O. shuilongensis* was 13.7, and that between this species and *O. platycephalus* was 19.4. Additionally, the divergence ranged from 19.8 to 27 between this species and species of other genus of the Nemacheilinae subfamily (Figure 4). The divergence of *Oreonectes* was smaller compared with the other genus of Nemacheilinae. Since the genetic distances between *O. daqikongensis* sp. n. and the other species of *Oreonectes* were greater than the interspecific distance of each category of Nemacheilinae, *O. daqikongensis* sp. n. was considered as a new species. In the phylogenetic tree (Figure 5), *O. daqikongensis sp. n* was clustered with *O. shuilongensis*

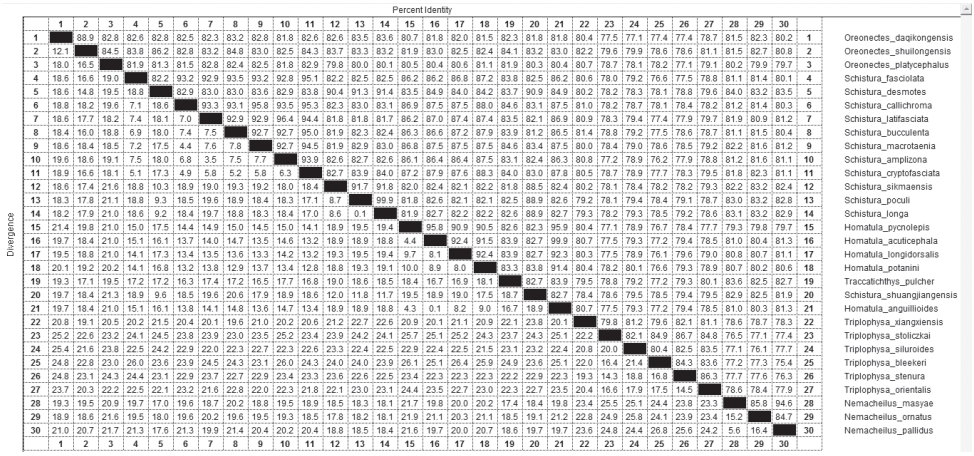

Figure 4. The sequence divergence of Cyt b between *O. daqikongensis* sp. n. and species of Nemacheilinae.

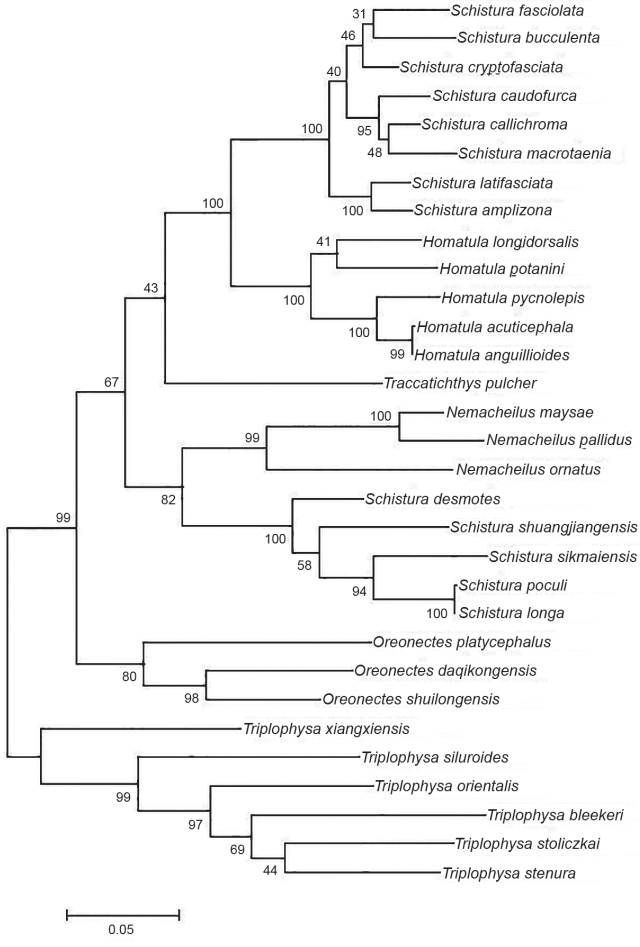

Figure 5. Maximum likelihood phylogenetic trees of Nemacheilinae.

(Bootstrap value (BP) = 99) and *O. platycephalus* (BP = 74). *Oreonectes* with *Schistura*, *Homatula*, and *Nemacheilus* genera was divided into two subsets (BP = 97). This species inhabits in the karst caves. Cave environments were easier to form geographical isolation for the independence of different caves. Therefore, according to the genetic distance, differences in sequences, and phylogenetic tree analysis, *O. daqikongensis* sp. n. belongs to a new species of *Oreonectes*.

Discussion

This species has nearly cylindrical forequarters, gradually compressed hindquarters, and a slightly flat head. The anterior and posterior nostrils are separated by a short distance, and the anterior nostrils form a short and tubular structure with their rear ends extending to become whisker or cusp. It has three pairs of barbels, and naked body. The anterior bladder chamber is completely coated by the bony bladder sac, and the posterior bladder is a well-developed membranous chamber, which is separated from the abdominal cavity and connected to the anterior chamber by a slender duct. Its stomach is U-shaped. All these features are consistent with the typical characteristics of *Oreonectes* described by Zhu (1989).

The new species has completely degraded eyes, without any outside remnant indicating their presence. This feature differed from the features of the following four species: *O. donglanensis* and *T. xiangxiensis* had degraded eyes, with only a small black spot visible, and the eye sockets are filled with loose fat globules; *O. macrolepis* had very small eyes, almost blind; and *O. microphthalmus* had highly degraded eyes, with only eyespots or eye sockets visible. This feature can also be differentiated from the features of the following five species that have normal eyes in appearance: *O. platycephalus*, *O. polystigmus*, *O. luochengensis*, *O. retrodorsalis*, and *O. elongates*.

Forked caudal fins of the new species, so the new species belong to furcocaudalis type. Eyes completely degradation of this new species can be different from other species of furcocaudalis group with eyes nomal. Such as *O. microphthalmus*, *O. macrolepis*, *O. retrodorsalis*, *O. duanensis*, *O. donglanensis* and *O. furcocaudalis*. Lateral line complete of the new species, this characteristic make a distinction between *O. barbatus*, *O. elongatus*, *O. translucens* and *O. acridorsalis* which are lateral line incomplete or no lateral line. The comparison of main traits between the new species and the similarity species of *Oreonectes* (*O. barbatus*, *O. elongatus*, *O. translucens* and *O. acridorsalis*) is in Table 3.

Oreonectes daqikongensis sp. n. and *O. shuilongensis* are both distributed in Guizhou province, but in different county. The two species which have close genetic distance. There are different characteristics as following: a forked caudal fin (vs. truncated or slightly concave belong to platycephalus group), possessing adipose crests of the caudal peduncle (vs. no adipose crests), disappeared eye (vs. eye normal), lateral line is completely (vs. incomplete, 8–10 pores) and body translucence (vs. top of head and body gray and black). *Oreonectes daqikongensis* sp. n. and *O. platycephalus* which have close genetic distance with the new species. However, they can be differs by naked body (vs.

Table 3. Comparison of traits between *O. daqikongensis sp. n.* and the similarity species of *Oreonectes*.

Trait	***O. daqikongensis* sp. n.**	***O. acridorsalis***	***O. barbatus***	***O.elongatus***	***O.translucens***
No.	15	5	8	3	3
Locality of collection	Daqikong area, Libo County, Guizhou	Tian'e County, Guangxi	Nandan County, Guangxi	Huangjiang County, Guangxi	Duan County Guangxi
Dorsal fin rays	iii, 8–9	iii, 7	iii, 8–10	iii, 8–9	iii, 8
Anal fin rays	iii, 6	iii, 5	ii, 5–6	ii, 6–7	iii, 6
Pectoral fin rays	i, 11–12	i, 10–12	i, 10–12	i, 10	i, 11
Pelvic fin rays	i,6–7	i, 5–6	i, 6	i, 6	i, 6
Caudal fin branched rays	13–14	13–14	14	14	16
Pectoral fin rays	Pectoral fin extend to or beyond the origin of the ventral fins	Pectoral fin Fan-shaped, extend to half of the distance between origins of pectoral fin and ventral fin	Pectoral fin extend to approx. two thirds of the distance between origins of pectoral fin and ventral fin	Pectoral fin long and narrow, greater than 1/2 the distance between origins of pectoral and pelvic fins	Pectoral fin long and narrow, almost reaching pelvic-fin origin
Pelvic fin rays	The first and second branched rays of ventral fin are long, but do not form a spiny shape	Pelvic fin is shorter, origin is ahead of dorsal fin origin, extend, but cannot reach anus	Pelvic fin Origin is opposite to the dorsal fin origin, extend but cannot reach the anus	Pelvic fin relatively slender, extending slightly over anus	Pelvic fin extending slightly beyond anus.
Anal fin rays	Anal fin extend to reach half between the anal fin base and caudal fin base	Anal fin truncated outer edge	Anal fin truncated or slightly convex outer edge	Anal fin origin next to anus, tip nearly reaching middle of caudal peduncle	Anal-fin origin just posterior to anus
Lateral line	Lateral line is subcutaneously buried completely, which in the head has three branches	No lateral line in the body, lateral line in the head is not well-developed	No lateral line in the body, lateral line in the head is not well-developed	Lateral line incomplete, with 4 pores behind opercle, connecting to the cephalic lateral-line system.	Lateral line incomplete, with only 3 or 4 lateral pores behind head.
Eyes	Absent	Absent	Absent	Absent	Absent

Table 4. Comparison of traits between *O. daqikongensis* sp. n. and similar species of *Oreonectes*.

Trait	***O. daqikongensis***	***O. shuilongensis***	***O. platycephalus***
No. of specimens	15	16	4
Location	Libo, Guizhou	Sandu, Guizhou	Zhaoping, Guangxi
Dorsal fin rays	iii, 8–9	iii, 7–8	iii, 6–7
Anal fin rays	iii, 6	iii, 6	iii, 5
Pectoral fin rays	i, 11–12	i,11–12	i, 10
Pelvic fin rays	i,6–7	i, 6	i,6–7
Anterior nostril	Anterior nostril in short tubular structure, which is obliquely cut tube	Anterior nostril in short tube extending into relatively long barbel, beyond posterior edge of eye	Anterior nostril in short tube extending into relatively long barbel, beyond edge of posterior nostril
Lateral line	Lateral line is subcutaneously buried completely, which in the head has three branches	Lateral line incomplete, terminates above pectoral fin; 8–10 pores	Lateral line incomplete, terminates above pectoral fin
Caudal fin	caudal fin is forked	Truncated or slightly concave	Rounded
Body color	The whole body of the living species is pale pink and translucent	Top of head and body gray and black in fresh condition; grayish in dorsum and body light brown after preservation in alcohol; fins transparent	In formaldehyde, body light brown; dorsum and side of body with irregular dark gray; dark brown horizontal stripe at end of caudal fin; fins without stains

scaled body), disappeared eye (vs. eye normal) and anterior nostril in a short tubular structure, which is obliquely cut tube (vs. short tube extending into relatively long barbel, beyond edge of posterior nostril) (Table 4).

Both morphological and molecular phylogenetic evidence revealed that *O. daqikongensis* sp. n. is a new species of *Oreonectes*. *Oreonectes* is distributed in the underground rivers in the karst region of Southwest China, of which *O. platycephalus* is most widely distributed. All these areas belong to the Pearl River and the Red River systems. Most of this species is distributed in the Karst regions of Guangxi. Currently, *O. shuilongensisis* and *O. daqikongensis* sp. n. have been discovered in Guizhou, and most are distributed in the southern area of Guizhou. This work is the first time to descript the new species in detail. The discovery of this species will be conducive to comprehensively understand the distribution of *Oreonectes*.

Acknowledgments

The data in this research comes from the Provincial Governor Fund of Guizhou (Qian-Sheng-Zhuan-He-Zi (2010) 14) project and the database of National Digital-Museum of Animal Specimens; this project was supported by key project of Science-technology basic condition platform from The Ministry of Science and Technology of the People's Republic of China (Grant No. 2005DKA21402).

References

Anonymous (2006) Freshwater Fishes of Guangxi, China. Fisheries Institute of Guangxi Zhuang Autonomous Region & Institute of Zoology, Chinese Academy of Science. Guangxi People's Publishing House, 161–163.

Chen P, Han Y, Wu T, Gong Z (2011) The new species of Cobitidae fish in Linyun cave. Journal of Anhui Agricultural Sciences 39: 862–863.

Du L, Chen X, Yang J (2008) A review of the Nemacheilinae genus *Oreonectes* Günther with description of two new species (Teleostei: Balitoridae). Zootaxa 1729: 23–26.

Kottelat M (1990) New species and populations of cave nemacheilines in South and South-east Asia (Osteichthyes: Balitoridae). Memoires de Biospeologie 17: 49–55.

Lan J, Gan X, Wu T, Yang J (2013) Cave fishes of Guangxi, China. Science Press, Beijing, 68–83.

Lan J, Yang J, Chen Y (1995) Two New Species of the Subfamily Nemacheilinae from Guangxi, China (Cypriniformes: Cobitidae). Acta Zootaxonomica Sinica 30: 445–448.

Rui M, Chen X, Yang J, Richard W , Richard L (2012) Phylogenetic relationships of the genus Homatula (Cypriniformes: Nemacheilidae), with special reference to the biogeographic history around the Yunnan-Guizhou plateau. Zootaxa 3586: 78–94.

Rui M, Chen X, Yang J, Richard W , Richard L (2012) Phylogenetic relationships of the genus Homatula (Cypriniformes: Nemacheilidae), with special reference to the biogeographic history around the Yunnan-Guizhou plateau. Zootaxa 3586: 78–94.

Sambrook J, Russell DW (2001) Molecular Cloning: A Laboratory Manual (3rd ed). Cold Spring Harbor Laboratory Press, New York, 2100 pp.

Tamura K, Stecher G, Peterson D, Filipski A, Kumar S (2013) MEGA6: Molecular evolutionary genetics analysis version 6.0. Molecular Biology and Evolution 30: 2725–29. doi: 10.1093/molbev/mst197

Tang L, Zhao Y, Zhang C (2012) A new blind loach, *Oreonectes elongates* sp. nov. (Cypriniformes: Balitoridae) from Guangxi, China. Environmental Biology of Fishes 93: 483–490. doi: 10.1007/s10641-011-9943-7

Yang J, Wu T, Wei R, Yang J (2011) *Oreonectes luochengensis*, a new nemacheiline loach of genus Oreonectes (Balitoridae) from Guangxi, China. Zoological Research 32: 208–211.

Yang Q, Wei M, Lan J, Yang Q (2011) A new species of the genus *Oreonectes* (Balitoridae) from Guangxi, China. Journal of Guangxi Normal University: Natural Science Edition 29: 72–75.

Zhang Z, Zhao Y, Zhang C (2006) A new blind loach, *Oreonectes translucens* (Teleostei: Cypriniformes: Nemacheilinae), from Guangxi. China. Zoological studies 45: 611–615.

Zhu SQ (1989) The Loaches of the Subfamily Nemacheilinae in China (Cypriniformes: Cobitidae). Jiangsu Science, Technology Publishing House, Nanjing, China, 150 pp.

Appendix 1

The source of the material of other *Oreonectes* species.

Species	Number	Standard length (mm)	Distributions locations	River system
O. platycephalus	KIZ200304597–200304600	50.9-58.6	Jinxiu county, Guangxi	Zhujiang
O. polystigmus	KIZ2001060507 (holotype)	57.7	Guilin city, Guangxi	Guijiang
O. microphthalmus	KIZ2004009395 (holotype)	39.0	Du'an county, Guangxi	Red River
O. macrolepis	CLJH91065 (holotype)	54.8	Huanjiang county, Guangxi	Liujiang
O. retrodorsalis	9110001 (holotype)	37.00	Nandan county, Guangxi	Red River
O. acridorsalis	CLJH04100608 (holotype)	48.3	Tian'e county, Guangxi	Red River
O. barbatus	CLJH2009080003(holotype)	54.1	Nandan county, Guangxi	Liujiang
O. duanensis	CLJH2011090302 (holotype)	56.1	Du'an county, Guangxi	Red River
O. donglanensis	CLJH2010010051(holotype)	45.2	Donglan county, Guangxi	Red River
O. elongatus	ASIZB189288(holotype)	78.2	Huanjiang county, Guangxi	Zhujiang
O. guananensis	KIZ2010003067 (holotype)	77.0	Huanjiang county, Guangxi	Xijiang
O. luochengensis	KIZ2010003073 (holotype)	74.9	Luocheng county, Guangxi	Xijiang
O. translucens	ASIZB94785 (holotype)	45.8	Du'an county, Guangxi	Red River
O. furcocaudalis	KIZ9309003, KIZ9309004	58.0-58.7	Du'an county, Guangxi	Red River
O. anophthalmus	KIZ1994001-005	25.3-36.9	Wuming county, Guangxi	Youjiang

ZooKeys 637: 61–79 (2016)
doi: 10.3897/zookeys.637.10276
http://zookeys.pensoft.net

RESEARCH ARTICLE

A peer-reviewed open-access journal
ZooKeys
Launched to accelerate biodiversity research

A new species of *Mastigodiaptomus* Light, 1939 from Mexico, with notes of species diversity of the genus (Copepoda, Calanoida, Diaptomidae)

Martha Angélica Gutiérrez-Aguirre[1], Adrián Cervantes-Martínez[1]

1 *Universidad de Quintana Roo (UQROO), Unidad Cozumel, Av. Andrés Quintana Roo s/n, 77600, Cozumel, Quintana Roo México*

Corresponding author: *Martha Angélica Gutiérrez-Aguirre* (margutierrez@uqroo.edu.mx)

Academic editor: *D. Defaye* | Received 23 August 2016 | Accepted 9 November 2016 | Published 30 November 2016

http://zoobank.org/FADC3B97-FB6F-4559-B71B-EB6F76A3246F

Citation: Gutiérrez-Aguirre MA, Cervantes-Martínez A (2016) A new species of *Mastigodiaptomus* Light, 1939 from Mexico, with notes of species diversity of the genus (Copepoda, Calanoida, Diaptomidae). ZooKeys 637: 61–79. doi: 10.3897/zookeys.637.10276

Abstract

A new species of the genus *Mastigodiaptomus* Light, 1939, named *Mastigodiaptomus cuneatus* **sp. n.** was found in a freshwater system in the City of Mazatlán, in the northern region of Mexico. Morphologically, the females of this new species are distinguishable from those of its congeners by the following combination of features: the right distal corner of the genital double-somite and second urosomite have a wedge-shaped projection, the fourth urosomite has no dorsal projection and its integument is smooth. The males are distinct by the following features: the right caudal ramus has a wedge-shaped structure at the disto-ventral inner corner; the basis of the right fifth leg has one triangular and one rounded projection at the distal and proximal margins, respectively, plus one hyaline membrane on the caudal surface close to the inner margin; the aculeus length is almost the width of the right second exopod (Exp2); and the frontal and caudal surfaces of the right Exp2 are smooth. Furthermore, the analysis of the COI gene of *M. cuneatus* sp. n. has revealed that *M. albuquerquensis* (Herrick, 1895) is its nearest congener, with 18.64% of genetic distance. A key for the identification of the known species of the genus is provided.

Keywords

COI gene, freshwater, Mexico, morphology, taxonomy

Introduction

Diaptomidae G. O. Sars, 1903 is one of the most common families of freshwater copepods worldwide, some genera of this family have restricted distributional patterns and present endemic forms, as the genus *Mastigodiaptomus* Light, 1939. Recent studies of this genus in the Neotropical region have added new species of these diaptomids (Gutiérrez-Aguirre and Cervantes-Martínez 2013) or the morphological and genetic analysis have produced recognition of species such as *M. patzcuarensis* (Kiefer, 1938) (Gutiérrez-Aguirre et al. 2014). Currently ten species of *Mastigodiaptomus* are known: *M. purpureus* (Marsh, 1907), *M. texensis* (M. S. Wilson, 1953), *M. amatitlanensis* (M. S. Wilson, 1941), *M. albuquerquensis* (Herrick, 1895), *M. patzcuarensis* (Kiefer, 1938), *M. montezumae* (Brehm, 1955), *M. nesus* Bowman, 1986, *M. maya* Suárez-Morales & Elías-Gutiérrez, 2000, *M. reidae* Suárez-Morales & Elías-Gutiérrez, 2000, and *M. suarezmoralesi* Gutiérrez-Aguirre & Cervantes-Martínez, 2013.

The fine structural features of the anatomy of the females and males of freshwater copepods are informative for species recognition. Researchers that have developed this idea concerning free-living copepods are Van de Velde (1984) and Hołyńska (2000) in the Cyclopidae genus *Mesocyclops*; and Alekseev et al. (2006) in the Cyclopidae genus *Eucyclops*, particularly the *Eucyclops serrulatus* species complex. Bowman (1986) recognized morphologically similar species within the *Mastigodiaptomus* genus using differences in the integument of prosomal wings and fifth legs of both sexes. Empirical evidence gathered from several species of freshwater crustaceans has shown that these morphological differences are consistent with reproductive isolation (Alekseev et al. 2006), genetic differentiation (Quiroz-Vázquez and Elías-Gutiérrez 2009; Gutiérrez-Aguirre et al. 2014), or both when they are probed (Montiel-Martínez et al. 2008).

In the present work is provided an illustrated description of both sexes of one new species of the genus *Mastigodiaptomus*; it was found in the northern region of Mexico in a field collection carried out in 2014. The analysis was based upon the detailed micro-structure of the antennules, fifth legs, and prosomal integument. In addition, the sequences of the mitochondrial COI gene were used to assess the genetic divergence between the new species and seven congeners to incorporate molecular information into the species description.

Methods

Morphological analysis. The cephalic appendages, swimming legs and urosome of *Mastigodiaptomus cuneatus* sp. n. were examined using light microscopy and illustrated with the aid of a camera lucida. The specimens were dissected and appendages were mounted in glycerine.

The terminology and abbreviations used for the armament of each appendage and structure are based on Huys and Boxshall (1991):

s	setae
sp	spine
sps	spiniform process
ae	aesthetasc
Enp1–Enp^n	first to "n" endopodal segment
Exp1–Exp^n	first to "n" exopodal segment
P1–P5	Legs 1–5

The type material was deposited at the Colección de Referencia de El Colegio de la Frontera Sur (ECOCH-CHZ) Chetumal, México and the Colección Nacional de Crustáceos (CNCR) del Instituto de Biología, Universidad Nacional Autónoma de México.

Molecular analysis. Specimens (2 females, 3 males, and 3 copepodites) were preserved after capture in 96% ethanol and prepared for barcoding following standard methods. DNA was extracted using the HOTSHOT method (Montero-Pau et al. 2008). A segment of the COI gene was amplified using the LCOI490 and HCO2198 primers or the Zplank primers, as suggested by Folmer et al. (1994) and Prosser et al. (2013), respectively. The preparation of the PCR 12.5 μL PCR reaction mixture and visualization of PCR products was performed as described by Gutiérrez-Aguirre et al. (2014) and Montiel-Martínez et al. (2008). Sequence analysis was carried out at the Chetumal Node of the MEXBOL (El Colegio de la Frontera Sur).

Additionally, a search of GenBank and the public data of the Barcode of Life Data System (BOLD) produced sequences of *Mastigodiaptomus albuquerquensis*, *M. patzcuarensis*, *M.* cf. *albuquerquensis* (accession numbers for BOLD and GenBank in Gutiérrez-Aguirre et al. 2014), *M. texensis*, *M.* cf. *nesus*, *M. montezumae*, *M.* cf. *reidae*, and *M. reidae* (accession numbers for BOLD and sampled site are shown in Table 1).

These sequences were downloaded from the BOLD project files *Mastigodiaptomus* of Mexico (MALB), Microcrustacean from Mexico (MCM), and Zooplankton II (ZPII) and compared with our sequence of *M. cuneatus* sp. n., this latter sequence is into the project MCM. In these project files, the electropherograms, sequence data, photographs, primers data, and collection details are available (on the Barcode of Life Data System http://www.boldsystems.org). Fifty-two COI gene sequences > 500 bp were used for the analysis, and BOLD Aligner and the ID Tree using the model Kimura 2 parameter (K2P; Kimura 1980) were utilized to obtain the ID Tree. Two sequences of *Hesperodiaptomus arcticus* (Marsh, 1920) (Calanoida: Diaptomidae) were used as an outgroup.

Table 1. Localities and sequence access for specimens surveyed herein, recorded in Mexico and Canada.

Species	Sample ID BOLD	Locality	Lat N	Long W
Hesperodiaptomus arcticus (Marsh, 1920)	CHU-CRU-0777	Churchill, Manitoba, Canada	58.772	93.844
Hesperodiaptomus arcticus (Marsh, 1920)	BIOUG01701-E09	Churchill, Manitoba, Canada	58.7715	93.844
Mastigodiaptomus cf. *nesus*	Cala039	Minicenote, Quintana Roo, Mexico	18.647	88.412
Mastigodiaptomus cf. *nesus*	Cala041	Minicenote, Quintana Roo, Mexico	18.647	88.412
Mastigodiaptomus cf. *nesus*	ZMXII-508	La Esperanza, Q. Roo, Mexico	19.471	88.029
Mastigodiaptomus cf. *reidae*	ZPLMX581	Kohunlich, Q. Roo, Mexico	18.447	88.825
Mastigodiaptomus cuneatus sp. n.	MAGA-0156	El Camarón, Sinaloa, Mexico	23.236	106.438
Mastigodiaptomus montezumae (Brehm, 1955)	HE-150a	Timilpan, Edo. Mex., Mexico	19.887	99.739
Mastigodiaptomus montezumae (Brehm, 1955)	HE-151a	Timilpan, Edo. Mex., Mexico	19.887	99.739
Mastigodiaptomus montezumae (Brehm, 1955)	HE-154a	Timilpan, Edo. Mex., Mexico	19.887	99.739
Mastigodiaptomus montezumae (Brehm, 1955)	ZPLMX210	km 25, Edo. Mex., Mexico	19.486	99.745
Mastigodiaptomus reidae Suárez-Morales & Elías-Gutiérrez, 2000	ZPLMX224	Kohunlich, Q. Roo, Mexico	18.447	88.825
Mastigodiaptomus reidae Suárez-Morales & Elías-Gutiérrez, 2000	ZPLMX579	Kohunlich, Q. Roo, Mexico	18.447	88.825
Mastigodiaptomus reidae Suárez-Morales & Elías-Gutiérrez, 2000	ZPLMX578	Kohunlich, Q. Roo, Mexico	18.447	88.825
Mastigodiaptomus texensis (M. S. Wilson, 1953)	Cala012	Boca del Puma, Q. Roo, Mexico	20.871	87.055
Mastigodiaptomus texensis (M. S. Wilson, 1953)	Cala016	Boca del Puma, Q. Roo, Mexico	20.871	87.055
Mastigodiaptomus texensis (M. S. Wilson, 1953)	Cala065	Verde Lucero, Q. Roo, Mexico	20.866	87.077
Mastigodiaptomus texensis (M. S. Wilson, 1953)	Cala066	Verde Lucero, Q. Roo, Mexico	20.866	87.077
Mastigodiaptomus texensis (M. S. Wilson, 1953)	Cala069	Verde Lucero, Q. Roo, Mexico	20.866	87.077

Results

Descriptive section

Order Calanoida G. O. Sars, 1903
Family Diaptomidae G. O. Sars, 1903
Subfamily Diaptominae Kiefer, 1932
Genus *Mastigodiaptomus* Light, 1939

***Mastigodiaptomus cuneatus* sp. n.**
http://zoobank.org/FADC3B97-FB6F-4559-B71B-EB6F76A3246F
Figures 1–5

Holotype. One adult female dissected on one slide: ECOCH-Z-09339. Collected 28.VIII.2014. Collectors: A. Cervantes-Martinez, N. Hernández López, M. Bastidas, and J. Aguilar Rubio.

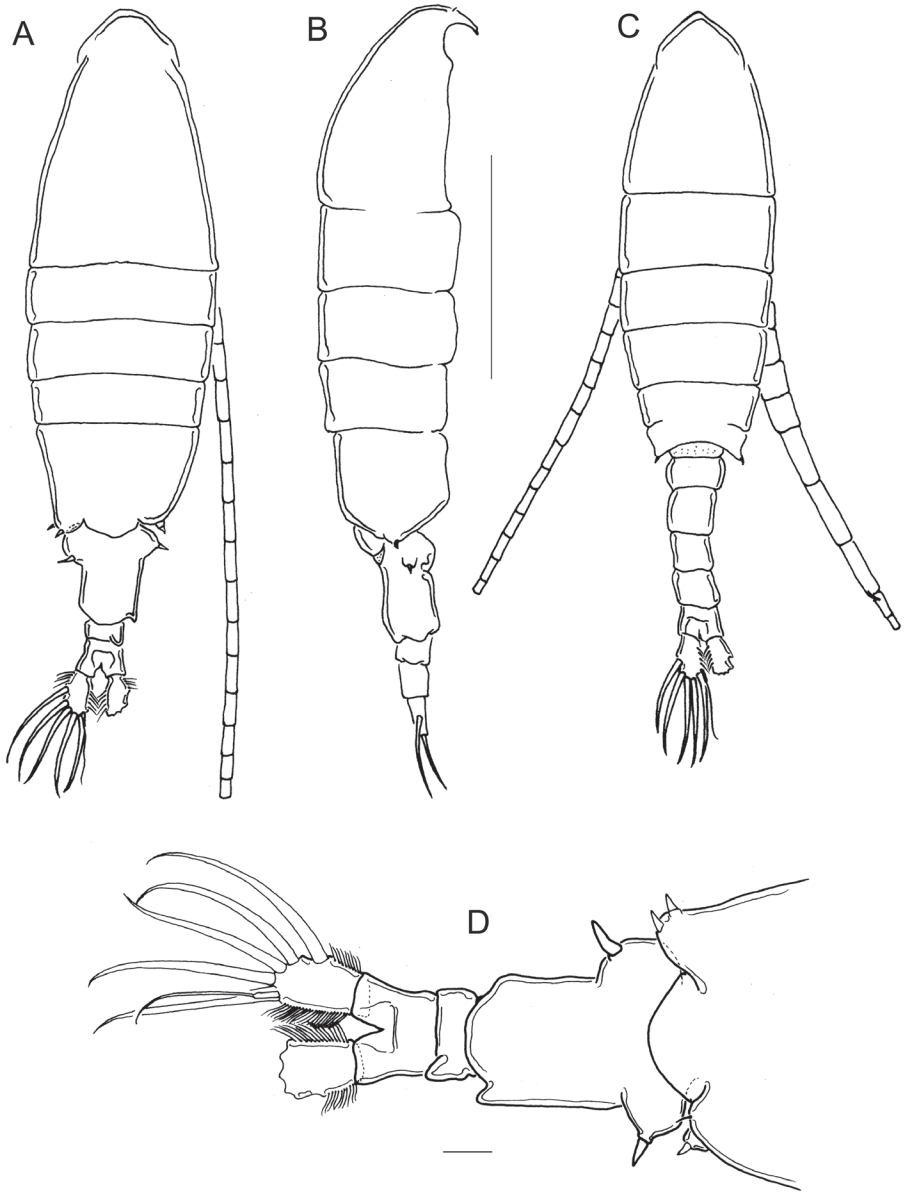

Figure 1. *Mastigodiaptomus cuneatus* sp. n. Adult female, holotype (**A, B, D**) and adult male, allotype (**C**) **A** Habitus, dorsal **B** Habitus, lateral **C** Habitus, dorsal **D** Fifth pediger and urosome, dorsal. Scale bars: 500 μm (**A–C**); 50 μm (**D**).

Allotype. One adult male dissected on one slide: ECOCH-Z-09340. Collected 28.VIII.2014. Same collectors.

Paratypes. Four adult females and five adult males preserved in 90% ethanol with a drop of glycerine. ECOCH-Z-09341. Collected 28.VIII.2014. Same collectors.

Two adult females and two adult males preserved in 90% ethanol: CNCR-31861. Collected 28.VIII.2014. Same collectors.

Type locality. A lagoon called Laguna El Camarón in Avenida Insurgentes, Mazatlán, Sinaloa City, México; 23°14'10"N; 106°26'18"W.

Etymology. The name of the species means "wedged" in Latin and refers to the chitinous protuberance present on the right disto-lateral corner of the first and second urosomites in females, and on the right caudal ramus on the ventral surface in males.

Diagnosis. Adult female: Cuticle surfaces of prosomal somites smooth dorsal and laterally (Fig. 1A, B). Antennules tip reaching beyond the caudal rami. Right wing of fifth pediger with one tiny dorsal spinule plus one stout ventral spine; left wing with two spines (Fig. 1A, D). No dorsal process on the last thoracic somite (Fig. 1B). Genital double-somite and second urosomite with one lateral wedge each on distal margin on the right side (Fig. 1D). Genital double-somite asymmetric and laterally bulbose; each bulb bearing a stout lateral spine (Fig. 1D). Short spines on the rostrum, which are less than 3 times longer than wide (Fig. 2A, B). Endopodite of fifth leg 2-segmented with a row of short spinules (arranged in one oblique line) flanked by 2 larger spinules; Exp3 of the fifth leg bearing 2 apical spines (Fig. 2G).

Adult male: The cuticle surfaces of prosomal somites are smooth dorsally and laterally (Fig. 1C). Right antennule 22-segmented, with one fang-like process on antepenultimate segment, which is less than half the length of the penultimate segment (Fig. 4D). Right antennule with spiniform process on segments 10, 11, and 13 to 16 (Fig. 4D). Inner margin of caudal ramus fringed by long hair-like setae (Fig. 1C). One wedge on distal margin of right caudal ramus on the ventral surface (Fig. 4E). Left and right coxae of the fifth leg have long, acute spines on lateral margins; apical spine of right Exp2 with tiny spinules along medial margin (Fig. 5D). One triangular and one rounded projection located at distal and proximal margins of the right basis, respectively, plus one hyaline membrane on caudal side (Fig. 5D). The aculeus length is almost the width of right Exp2. Left and right endopods one-segmented, with apical spinules (Fig. 5C).

Description adult female. Smooth prosomal somites; body length 1500-1700 μm in paratypes including caudal ramus, $n = 6$ (Fig. 1A, B). Spines on rostrum 2.8-3.0 times longer than wide (Fig. 2B).

Antennule: 25-segmented, extending beyond the caudal ramus (Fig. 1A). Armature details with setae, spines, or aesthetasc in the next order: (1)1s + 1ae; (2)3s+1ae; (3)1s+1ae; (4)1s; (5)1s + 1 ae; (6)1s; (7)1s+1ae; (8)1s +1 sp; (9)2s + 1ae; (10)1s; (11)1s+1ae; (12)1s + 1ae + 1sp; (13)1s; (14)1s+1ae; (15)1s; (16)1s+1ae; (17)1s; (18)1s; (19)1s+1ae; (20)1s; (21)1s; (22)1s + 1ae; (23)1s + 1ae; (24)2s; (25)4s + 1ae.

Antenna: Coxa with one long seta; basis with 2 setae; Exp 7-segmented with 1, 3, 1, 1, 1, 1, 4 setae, respectively. Enp 2-segmented, Enp1 with 2 setae plus a row of spine-like setae. Inner lobe of Enp2 bearing 9 long setae, outer lobe with 7 setae and a group of tiny spinules (Fig. 3A).

Mandible: Eight teeth on gnathobase (6 of these teeth bifid) with a movable seta at tip. Rectangular, nude coxa. Basis with 4 long setae. Enp two-segmented, Enp1 with 4

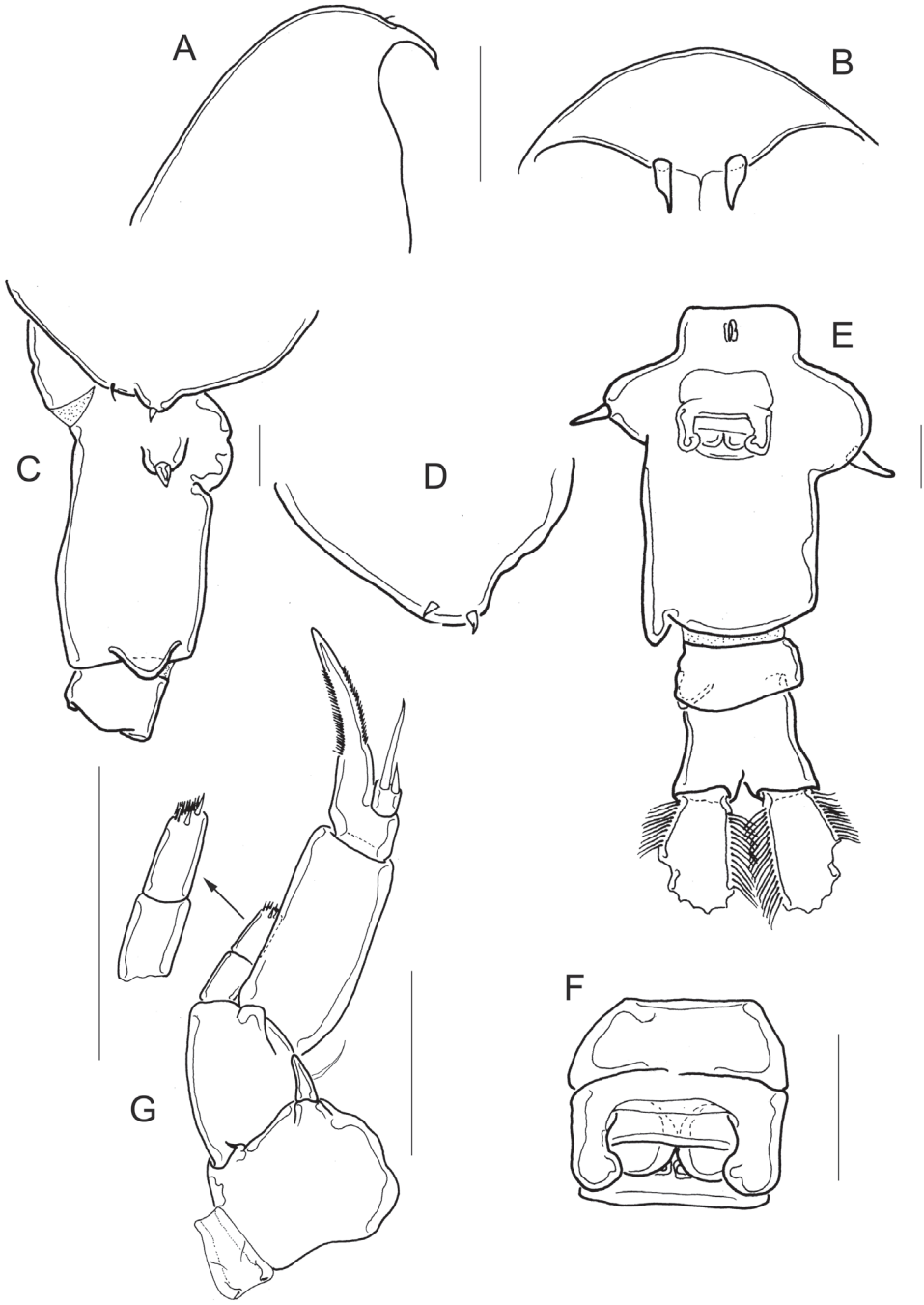

Figure 2. *Mastigodiaptomus cuneatus* sp. n. Adult female, holotype. **A** Rostrum, lateral **B** Rostrum, frontal **C** Wing of fifth pediger, genital double-somite, and second urosomite, lateral right view **D** Wing of fifth pediger, lateral, left view **E** Urosome, ventral **F** Genital field **G** Fifth leg, frontal. Scale bars: 50 μm.

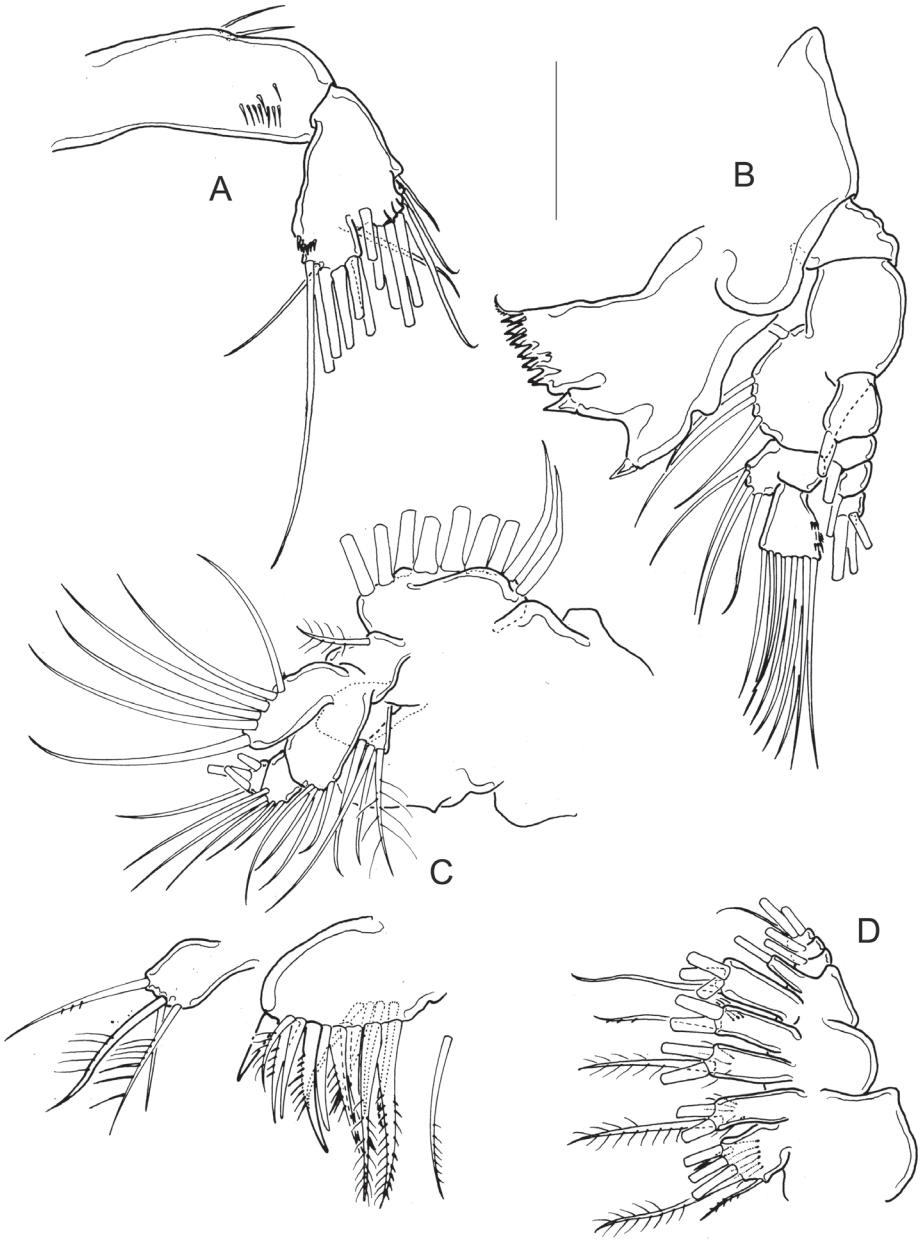

Figure 3. *Mastigodiaptomus cuneatus* sp. n. Adult female, holotype. **A** Enp1 and Enp2 of antenna **B** Mandible **C** Maxillule, coxal endite and praecoxal arthrite separated **D** Maxilla. Scale bar: 50 μm.

setae, Enp2 with 2 distal pectens and 9 long setae. Exp 4-segmented, with 1, 1, 1, and 3 long setae, respectively (Fig. 3B).

Maxillule (Fig. 3C): Coxal epipodite elliptical, bearing 9 long setae. Short basal exite, one-setulated; Exp plate-like with 6 long setae. Enlarged basal endite with 4 setae

and 2-segmented endopodite: Enp1 and Enp2 with 5 and 4 setae, respectively. Basis rectangular with 4 setae; coxal endite quadrangular 4-setulated. Praecoxal arthrite with 15 spiniform setae, 11 anterior, 4 posterior.

Maxilla (Fig. 3D): First praecoxal lobe with 4 long setae and 1 lateral short seta; plus long setules and 1 spinule on posterior side. Second praecoxal lobe 3-setulated. Two coxal lobes with 3 long setae each. All the praecoxal and coxal lobes with long setules located posteriorly. First basal lobe with 4 setae, second basal lobe with 1 seta. Three-segmented Enp, with 1, 1, and 3 setae, respectively.

Maxilliped (not figured): Same structure as described and illustrated for *Mastigodiaptomus albuquerquensis* and *M. patzcuarensis* (see Gutiérrez-Aguirre et al. 2014).

P1-P4: The number of segments on endopods and exopods of P1 to P4, as described for copepods that belong to the Diaptomidae family (Dussart and Defaye 1995). Armature formula of swimming legs as shown in Table 2 including Schmeil's organ on Enp2P2.

Fifth pediger wings and urosome: Right wing of fifth pediger with 2 spines, one dorsal and one ventral (Fig. 2C), left wing with 2 equal spines (Fig. 2D). Genital double-somite and second urosomite each with projections at right distal corner (Fig. 2C); these projections wedge-like in dorsal (Fig. 1D) and ventral views (Fig. 2E). Genital double-somite 1.2 ± 0.1 times longer than wide, lateral margins bulbous and with strong spines; right spine inserted laterally, more proximal than left spine (Fig. 2E). Caudal ramus with long hair-like setules on medial and lateral margins (Fig. 2E). Genital field quadrangular with parallel lateral margins (Fig. 2F).

Fifth leg (Fig. 2G): Coxa with a large spine on distal margin, basis quadrangular with a blunt projection on distal margin and one slender lateral seta. Exp1 1.66 times longer than 2-segmented endopod. Second endopodal segment with a row of spinules at the tip arranged in an oblique line, flanked by 2 larger spinules. Exp2 separated, with one long and one short spine. Exp3 with spinules on distal medial and lateral margins.

Description adult male. Prosomites smooth in dorsal view; left antennule reaching anal somite. Body length 1400-1500 μm in paratypes including caudal ramus, n = 7 (Fig. 1C). Short spines on rostrum 2.7-2.8 times longer than wide (Fig. 4A).

Right antennule (Fig. 4D): 22-segmented, each segment armed with setae, spines, spiniform process, or aesthetasc in the following order: (1)1s+1ae; (2)2s+2ae; (3)1s+1ae; (4)1s; (5)1s+1ae; (6)1s; (7)1s+1ae; (8)1s+1sp; (9)2s+1ae; (10)1s+1sps, (11)1s+1sps; (12)1s+1ae+1sp; (13)1s+1ae+1sps; (14)2s +1ae+1sps; (15)2s +1ae+1sps; (16)2s+ 1ae+1sps; (17)1s+1sp; (18)1s+1sp; (19)1s+1ae; (20)4s; (21)2s; (22)3s+1ae. Segments 17-19 with acuted lamellae on inner margins.

Spiniform process on segment 10 very short, reaching only distal third of its segment; that on segment 11 short, reaching proximal third of the next segment. Convergent spiniform processes on segments 13 and 14. Base of stout spiniform process on segment 13 almost as wide as the length of its segment. Segment 20 is 3.6 times as long as wide, bearing a hook-like projection (less than the half length of penultimate segment) with a smooth hyaline membrane.

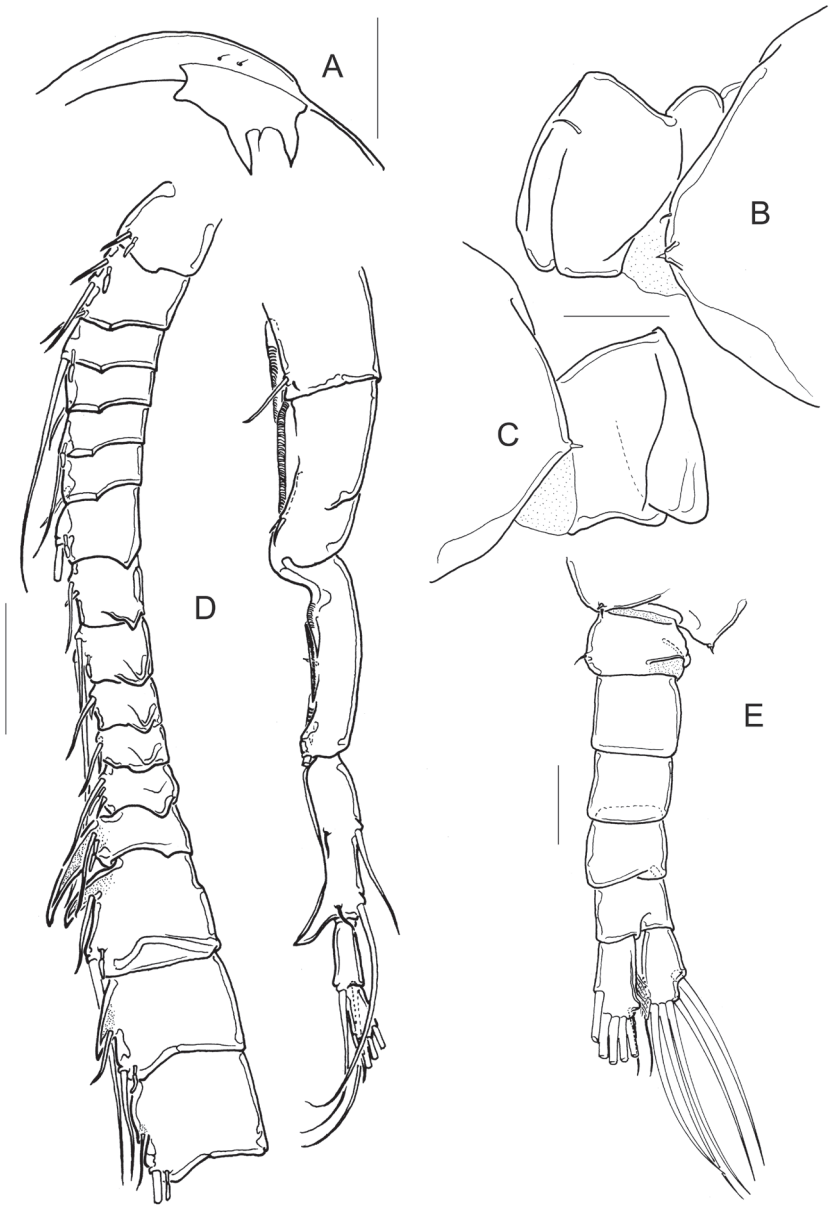

Figure 4. *Mastigodiaptomus cuneatus* sp. n. Adult male, allotype. **A** Rostrum, frontal **B** Wing of fifth pediger and first urosomite, lateral right view **C** Wing of fifth pediger and first urosomite, lateral left view **D** Right antennule **E** Fifth pediger and urosome, ventral. Scale bars: 50 μm (**A–C**); 100 μm (**D, E**).

Antennule, antenna, mandible, maxillule, maxilla, maxilliped, and P1-P4 as described for female.

Right wing of fifth pediger with 1 tiny dorsal spinule and 1 ventral spine (Fig. 4B); left wing bearing 1 small spine (Fig. 4C).

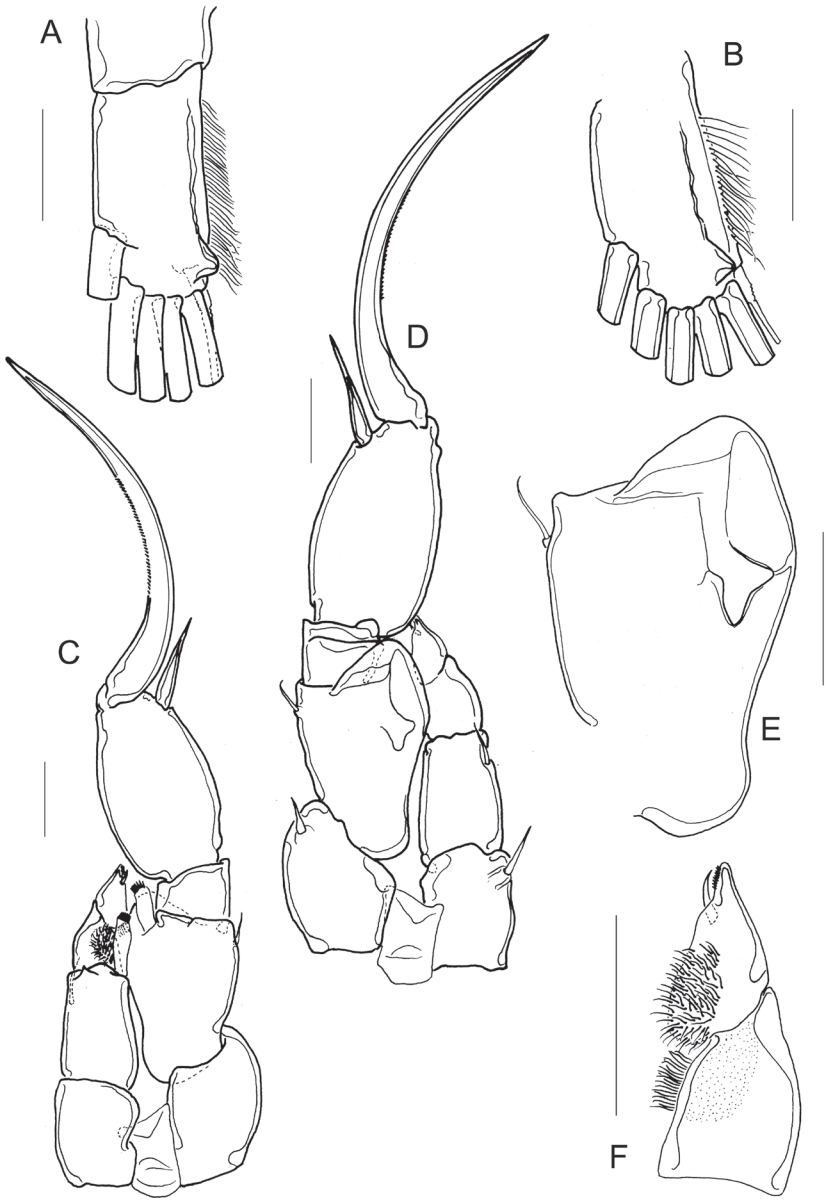

Figure 5. *Mastigodiaptomus cuneatus* sp. n. Adult male, allotype. **A** Right furcal ramus, semi-lateral **B** Right furcal ramus, ventral **C** Fifth leg, frontal **D** Fifth leg, caudal **E** Fifth leg, right basis, caudal **F** Fifth leg, left Exp1 and Exp2. Scale bars: 50 μm.

Urosome: Urosomites nude dorsally and ventrally. First urosomite with thin spine on right side and fold on left side (Fig. 4E). Fourth urosomite slightly projected on right side. Right caudal ramus with wedge-like structure at disto-inner corner of ventral surface; medial margins of rami pilose (Figs 4E, 5A, B).

Table 2. Setation formula of the swimming legs in *Mastigodiaptomus cuneatus* sp. n. (spine in Roman numerals, seta in Arabic numerals).

	Coxa	Basis	Exp	Enp
P1	0-1	0-0	I-1; 0-1; I-3-2	0-1; 1-2-3
P2	0-1	0-0	I-1; I-1; I-3-3	0-1; 0-2; 2-2-3
P3	0-1	0-0	I-1; I-1; I-3-3	0-1; 0-2; 2-2-3
P4	0-1	1-0	I-1; I-1; I-3-3	0-1; 0-2; 2-2-3

P5: Coxal segments with strong spines on caudal view; left and right basis with a lateral seta (Fig. 5D).

Left basis with a triangular protuberance on distal margin of frontal surface (Fig. 5C). Both left Exp1 and Exp2 pilose on medial margins (Fig. 5F), left Exp2 triangular, with its tip adorned with a small inner seta and spinules (Fig. 5F). Left Enp 1-segmented, distally feathered and as long as left Exp1 (Fig. 5C).

Right basis basally and distally projected: basal projection rounded whereas distal projection triangle-shaped; one semi-triangular sclerotization on caudal surface of right basis (Fig. 5D, E). Right Exp1 quadrangular in frontal view (Fig. 5C), one triangular fold and one rounded projection on caudal view (Fig. 5D). Right Exp2 1.6–1.8 times longer than wide and 1.9–2.0 times longer than aculeus, smooth in both frontal and caudal views (Fig. 5C, D). Aculeus inserted at distal third of the segment, pointed, unarmed, short (no longer than the width of the right Exp2). Terminal claw twice the length of Exp2 smoothly bent and ornamented with tiny spinules on inner margin (Fig. 5D). Right Enp one-segmented slightly longer than right Exp1 (Fig. 5C).

Molecular features. The nucleotide sequence (607 bp) obtained for specimen MAGA-0156 (one adult male), identified as *M. cuneatus* sp. n. is shown below:

GGAGCCTGGTCAGGCATAGTAGGAACAGGCCTTAGAATGATTATTCGGATGGAGTTAGGACAAGCCGGGTCTTTAATTGGAGATGACCAAATTTATAATGTAGTAGTTACTGCTCATGCTTTTGTTATAATTTTTTTTTATGGTGATACCTATTTTAATTGGGGGGTTTGGTAATTGGCTTGTTCCGTTAATATTAGGTGCAGCGGATATAGCTTTCCCTCGAATAAATAATATAAGATTTTGATTTTTATTGCCAGCTTTAGTCATATTGTTATCTAGGTCGCTTGTTGAAAGAGGGGCGGGAACAGGGTGAACTGTGTATCCCCCCCTGTCTAGCAACATTGCCCATGCTGGCAGGTCCGTTGATTTTGCTATTTTTTCGCTTCATTTAGCTGGGGTTAGGTCTATTTTGGGCGCAGTAAATTTTATTAGCACATTAGGAAATTTGCGGGCGTTTGGAATAATTTTAGATCGAATACCACTTTTTGCTTGAGCCGTTTTAATCACGGCTATCTTGTTATTGCTTTCTCTTCCTGTTTTAGCCGGGGCGATTACAATGCTTCTTACAGATCGGAACCTCAACTCAAGATTTTATGAT.

The K2P maximum distance between the surveyed species reaching 5.52% (Table 3). The nearest neighbour of *M. cuneatus* sp. n. is *M. albuquerquensis* with 18.64% of genetic distance (Fig. 6).

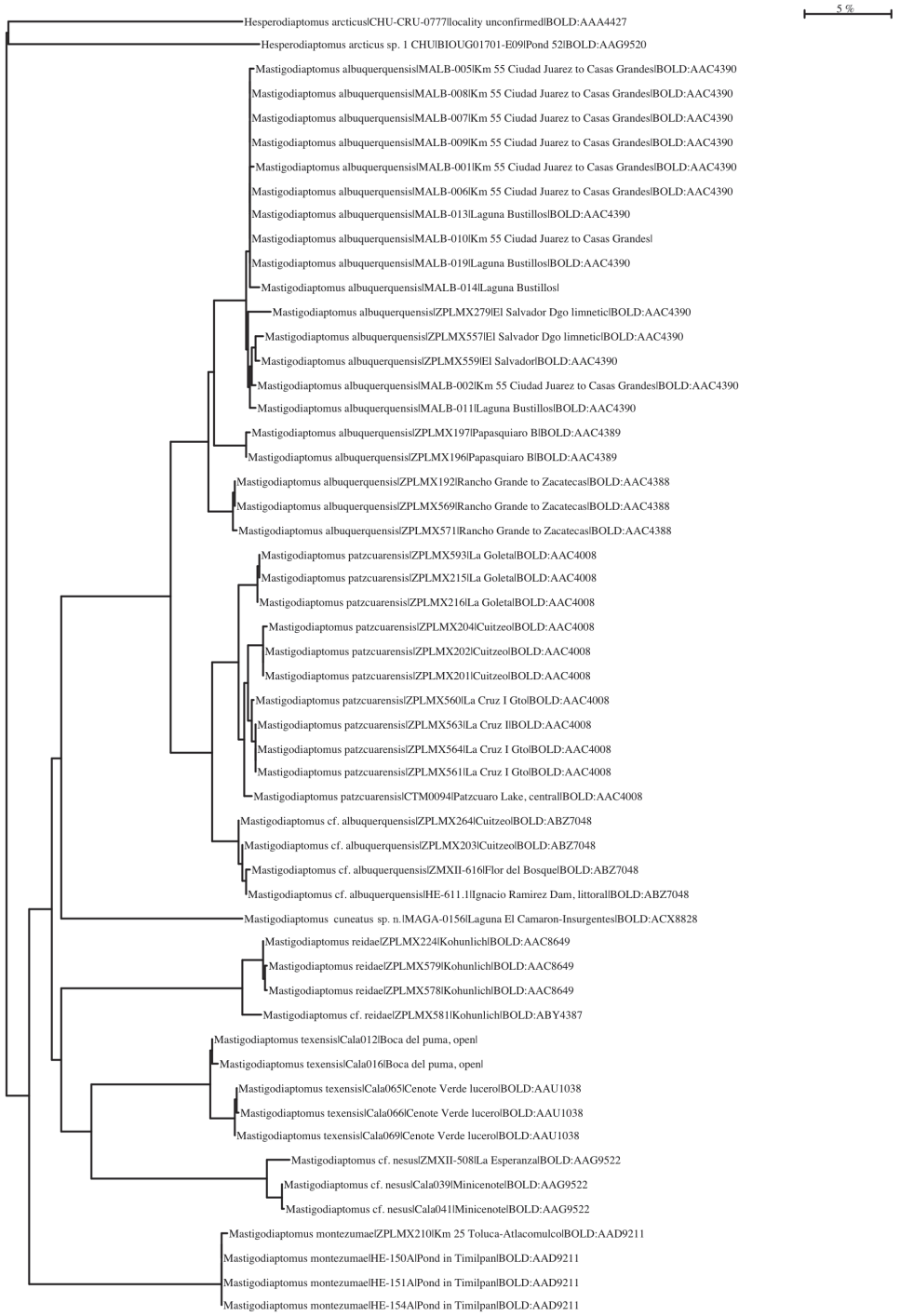

Figure 6. Maximum likelihood tree based on Kimura 2 parameter. The outgroup is *Hesperodiaptomus arcticus*. Numbers represent the specimen ID in BOLD or the GenBank Accession numbers.

Table 3. Sequence divergence (K2P) in the genus and species analysed.

	n	Taxa	Comparisons	Min Dist (%)	Mean Dist (%)	Max Dist (%)	SE Dist (%)
Within species	50	7	273	0	1.94	5.52	0.01
Within genus	54	2	1054	2.34	18.28	28.19	0.01

Discussion

Mastigodiaptomus cuneatus sp. n. is assigned to the genus *Mastigodiaptomus* because it fulfils all the morphological generic criteria as given in Dussart and Defaye (1995), especially the left and right antennules of females and males and the ornamentation of coxa, basis and the endopodal or exopodal lengths of the fifth legs.

Mastigodiaptomus cuneatus sp. n. (from northern Mexico) appeared to be morphologically close to *M. amatitlanensis* (from Lago Amatitlán, Guatemala). Similarities between these species in females include the presence of one protrusion on the second urosomite and the bulbose lateral margins of genital double-somite. The similarities in males are the short aculeus and the lack of hyaline membrane on the right Exp2 of the fifth leg.

However, *M. cuneatus* sp. n. can be separated from *M. amatitlanensis* by the following features: the dorsal projection on the last pediger absent vs. present; the genital double-somite with vs. without a protrusion on the distal right side; on the genital double-somite, the right spine located at a higher level than the left spine vs. both left and right spines placed at same level; and the endopod of fifth leg long and 2-segmented vs. short and 1-segmented.

The males of these species show more morphological differences in the fifth leg: the caudal surface of the right basis is bulbose with the oblique, medial, angulose and curved cuticular process in *M. cuneatus* sp. n. in comparison to the rectangular basis with a transversal, distal, cuneiform lamella in *M. amatitlanensis*. In addition, the distal margins of the left and right endopods bear short setules in *M. cuneatus* sp. n. whereas in *M. amatitlanensis* these distal margins bear one slender seta. The aculeus on the right Exp2 is clearly straight in *M. cuneatus* sp. n. but short, distal and curved in *M. amatitlanensis*. The Exp2 is smooth in *M. cuneatus* sp. n. but in *M. amatitlanensis* an oblique ridge on the caudal surface is present. Finally, we assume that the wedge on the right caudal ramus present in *M. cuneatus* sp. n. is absent in *M. amatitlanensis* because there is no mention of a similar feature in Wilson (1941) or Wilson and Yeatman (1959).

Results related with the COI gene suggested that *M. cuneatus* sp. n. is genetically closest to *M. albuquerquensis* s. str. and the species recorded in Mexico with one sclerotization (similar to the half wing of a butterfly) on the right basis of fifth leg of males such as *M. patzcuarensis*. As previously discussed (see Gutiérrez-Aguirre et al. 2014), this particular sclerotization should not be used as a specific character because actually, it is shared by at least three different species. Therefore, in addition to the genetic distance and the sequences of the COI gene, some morphological features are suggested to separate them.

Whereas the distal margins of prosomites are pilose in females and males of *M. patzcuarensis*, these structures are nude in *M. cuneatus* sp. n and they have tiny spi-

nules on lateral margins in *M. albuquerquensis*. The right Exp2 bearing one curved hyaline membrane and the aculeus is 2-3 times longer than the segment's width in *M. albuquerquensis* and *M. patzcuarensis*; this Exp2 is nude with the aculeus shorter or as long as the segment's width in *M. cuneatus* sp. n. There are no protrusions on the urosomites of males or females of *M. albuquerquensis* or *M. patzcuarensis*, but such structures do occur in *M. cuneatus* sp. n.

Sequences of the COI gene of *M. maya*, *M. suarezmoralesi*, *M. amatitlanensis*, *M. purpureus*, and *M. nesus* from their type localities or areas of their primary distribution, are not yet available for comparison and then the genetic distances between the species showed in Fig. 6 may change when the genetic sequences of the previous species can be added. However, until now, the lowest genetic distance in nearest neighbours of *Mastigodiaptomus* is between *M. patzcuarensis* and *M.* cf. *albuquerquensis* (3.36%), which probably are cryptic species (see Gutiérrez-Aguirre et al. 2014).

Mastigodiaptomus is considered a Neotropical genus and the species with the widest distribution are *M. albuquerquensis* (South of USA and North of Mexico), *M. patzcuarensis*, *M. montezumae* (Central Mexico), *M. nesus* (Caribbean and south eastern Mexico), and *M. texensis* (Texas and south eastern Mexico), whereas the species that are assumed to have restricted distribution or endemics are *M. reidae*, *M. maya*, *M. purpureus*, *M. amatitlanensis*, *M. suarezmoralesi* (see Gutiérrez-Aguirre and Cervantes-Martínez 2013) and, probably, *M. cuneatus* sp. n.

Conclusion

Morphological and genetic differences were found when *M. cuneatus* sp. n. was compared with the ten known *Mastigodiaptomus* species, particularly in the female and male urosomes, the male right antennule and fifth legs, and in the COI gene sequence. This report increases the number of recognized species of *Mastigodiaptomus* to eleven. *Mastigodiaptomus cuneatus* sp. n. appears to be part of the *M. albuquerquensis* complex.

Key to species of *Mastigodiaptomus*

Males

1 Spiniform process on segment 16 of right antennules strongly developed almost as long as its segment width; right basis of P5 with one basal subrectangular protuberance ..... ***Mastigodiaptomus reidae***

– Spiniform process on segment 16 of right antennules reduced or absent; right basis of P5 with basal rounded protuberance or without basal protuberance ... **2**

2 Right basis of P5 with only one lobular protuberance on basal-medial margin, no chitinous lamella or lamellae (on caudal view) **3**

– Right basis of P5 with chitinous lamella or lamellae and with or without rounded protuberance on basal-medial margin (on caudal view) **4**

3 Lobular protuberance of right basis of P5 large; right Exp2 of P5 with two semicircular transverse lamellae, and one longitudinal "Y" shaped ridge; antepenultimate antennular segment with a fang-like process ..... ***M. montezumae***

– Lobular protuberance of right basis of P5 short; right Exp2 of P5 with a low rounded protuberance on outer margin; antepenultimate antennular segment with wide knob-like process ***M. maya***

4 Right basis of P5 with one chitinous lamella **5**

– Right basis of P5 with more than one chitinous lamella **8**

5 Chitinous lamella of right basis of P5 semi-circular, on medial margin **6**

– Chitinous lamella of right basis of P5 cuneiform, transversal; or semi-triangular, on caudal side **7**

6 Right Exp2 of P5 with two short semi-circular lamellae (one medial and one lateral); aculeus with 50% of the length of its segment; short spiniform process on antennular segment 14 ***M. purpureus***

– Right Exp2 of P5 with one long quadrangular lamella (on caudal side) aculeus with 70–90% of the length of its segment; long spiniform process on antennular segment 14 ***M. nesus***

7 Caudal surface of right basis of P5 with one triangular protuberance on distal margin, and one rounded protuberance on basal-medial margin; right Exp2 of P5 nude; right furcal ramus with one wedge-like structure at disto-inner corner of ventral surface ***M. cuneatus* sp. n.**

– Caudal surface of right basis of P5 without protuberances, almost rectangular; right Exp2 of P5 with one straight ridge, obliquely directed..... ***M. amatitlanensis***

8 Left Exp2 of P5 distally truncated and denticulate; aculeus inserted subterminally on Exp2 of P5 ***M. texensis***

– Left Exp2 of P5 distally attenuated (triangular-shape) aculeus inserted on the second third of Exp 2 of P5 ..... **9**

9 Aculeus shorter than the length of right Exp2 of P5 with long spinules on medial margin; two short semi-circular lamellae on medial margin of right Exp2 of P5; second to forth urosomites with denticles on dorsal surfaces..... ***M. suarezmoralesi***

– Aculeus subequal or longer than the length of right Exp2 of P5 with short spinules on medial margin; one long curved hyaline lamella on right Exp2 of P5; dorsal surfaces of urosomites nude **10**

10 Short spines on rostrum: 2.2–3.0 times longer than width; cuticular surfaces of prosomites nude; 1.37–1.82 mm of body length including furcal ramus .. ***M. albuquerquensis***

– Long spines on rostrum: 3.5–5.0 times longer than width; hair-like setae on ventral and distal margins from second to fifth prosomites; 0.92–1.1 mm of body length including furcal ramus..... ***M. patzcuarensis***

Females

1 Hair-like setae only on medial margin of furcal ramus **2**
– Hair-like setae on both, medial and lateral margins of furcal ramus **3**
2 Symmetric genital double-somite, almost parallel lateral margins with short spines on left and right margins ..... ***Mastigodiaptomus purpureus***
– Asymmetric genital double-somite, bulbose lateral margins with short spines on left and right margins..... ***M. reidae***
3 Symmetric genital double-somite, almost parallel lateral margins; two-segmented Enp of P5 bearing one apical spinule longer than the endopodal width **4**
– Asymmetric genital double-somite, bulbose lateral margins; one or two-segmented Enp of P5 bearing two apical spinules shorter than the endopodal width **5**
4 Enp of P5 longer than the inner margin of Exp1 of P5; long lateral sensilla of coxal segment of P5 ..... ***M. texensis***
– Enp of P5 shorter than the inner margin of Exp1 of P5; short lateral sensilla of coxal segment of P5 ..... ***M. maya***
5 One or two urosomites with a chitinous protuberance on the right disto-lateral corner..... **6**
– Urosomites with straight posterior margins, no protuberances are present .. 7
6 Second urosomite with a spine-like protuberance on the right disto-lateral corner; one-segmented Enp of P5 ..... ***M. amatitlanensis***
– Genial double-somite and second urosomite with chitinous protuberance on the right disto-lateral corner; two-segmented Enp of P5..... ***M. cuneatus* sp. n.**
7 Genital double-somite produced, or curved and wrinkled on the right disto-lateral margin..... **8**
– Genital double-somite straight on the right disto-lateral margin **9**
8 Two-segmented Enp of P5, as long as medial margin of Exp1; genital double-somite curved and wrinkled on the right disto-lateral margin .... ***M. suarezmoralesi***
– Two-segmented Enp of P5, shorter than the half length of medial margin of Exp1; genital double-somite produced on the right disto-lateral margin .... ***M. montezumae***
9 One-segmented Enp of P5; left and right spines of genital double-somite inserted at same level; ventral spine of right wing (of last prosomite) directed to the posterior region of the body..... ***M. nesus***
– Two-segmented Enp of P5; right spine of genital double-somite inserted more anteriorly than left spine; ventral spine of right wing (of last prosomite) directed to the dorsal region of the body..... **10**
10 Short spines on rostrum: 1.5–3.6 times longer than width; tiny spines on ventral surface of each prosomites; 1.47–1.87 mm of body length including furcal ramus..... ***M. albuquerquensis***
– Long spines on rostrum: 3.6–4.0 times longer than width; hair-like setae on ventral and distal margins from second to fifth prosomites; 0.9–1.3 mm of body length including furcal ramus..... ***M. patzcuarensis***

Acknowledgements

We received grants from the Universidad de Quintana Roo and National Council of Science and Technology (CONACYT) through the Mexican Barcode of Life (MEXBOL) project CONACyT 271108, Red Temática Código de Barras de la Vida (Continuidad de Redes Temáticas). We are grateful with the academic edition of two native English-speaking editors. We thank professors and students of Instituto Tecnológico de Mazatlán (ITMAZ) for collecting zooplankton samples and making them available to us. We are grateful to Danielle Defaye, Y. Ranga Reddy and an anonymous reviewer who made valuable comments and suggestions to improve the manuscript.

References

Alekseev V, Dumont HJ, Pensaert J, Baribwegure D, Vanfleteren JR (2006) A redescription of *Eucyclops serrulatus* (Fischer, 1851) (Crustacea: Copepoda: Cyclopoida) and some related taxa with a phylogeny of the *E. serrulatus*-group. Zoologica Scripta 35(2): 123–147. doi: 10.1111/j.1463-6409.2006.00223.x

Bowman TE (1986) Freshwater calanoid copepods from the West Indies. Syllogeus 58: 237–246.

Dussart D, Defaye D (1995) Copepoda, Introduction to the Copepoda. SPB Academic Publishing, Belgium, 277 pp. doi: 10.1002/iroh.19960810306

Folmer O, Black M, Hoeh W, Lutz R, Vrijenhoek R (1994) DNA primers for amplification of mitochondrial cytochrome *c* oxidase subunit I from diverse metazoan invertebrates. Molecular Marine Biology and Biotechnology 3: 294–299.

Gutiérrez-Aguirre MA, Cervantes-Martínez A (2013) Diversity of freshwater copepods (Maxillopoda: Copepoda: Calanoida, Cyclopoida) from Chiapas, Mexico with a description of *Mastigodiaptomus suarezmoralesi* sp. nov. Journal of Natural History 47(5–12): 479–498. doi: 10.1080/00222933.2012.742587

Gutiérrez-Aguirre MA, Cervantes-Martínez A, Elías-Gutiérrez M (2014) An example of how barcodes can clarify cryptic species: the case of the calanoid copepod *Mastigodiaptomus albuquerquensis* (Herrick). PLoS ONE 9(1): e85019. doi: 10.1371/journal.pone.0085019

Hołyńska M (2000) Revision of the Australasian species of the genus *Mesocyclops* Sars, 1914 (Copepoda: Cyclopidae). Annales Zoologici 50(3): 363–447.

Huys R, Boxshall GA (1991) Copepod Evolution. The Ray Society, London, 468 pp.

Kimura M (1980) A simple method of estimating evolutionary rate of base substitutions through comparative studies. Journal of Molecular Evolution 16(2): 111–120. doi: 10.1007/BF01731581

Montero-Pau J, Gomez A, Muñoz J (2008) Application of an inexpensive and high-throughput genomic DNA extraction method for the molecular ecology of zooplanktonic diapausing eggs. Limnology and Oceanography-Methods 6: 218–222. doi: 10.4319/lom.2008.6.218

Montiel-Martínez A, Ciros-Pérez J, Ortega-Mayagoitia E, Elías-Gutiérrez M (2008) Morphological, ecological, reproductive and molecular evidence for *Leptodiaptomus garciai*

(Osorio-Tafall 1942) as a valid endemic species. Journal of Plankton Research 30(10): 1079–1093. doi: 10.1093/plankt/fbn067

Prosser S, Martínez-Arce A, Elías-Gutiérrez M (2013) A new set of primers and some methodological improvements for COI amplification in freshwater microcrustaceans. Molecular Ecology Resources 13(6): 1151–1155. doi: 10.1111/1755-0998.12132

Quiroz-Vázquez P, Elías-Gutiérrez M (2009) A new species of the freshwater Cladoceran genus *Scapholeberis* Schoedler, 1858 (Cladocera: Anomopoda) from the Semidesert Northern Mexico, Highlighted by DNA Barcoding. Zootaxa 2236: 50–64. doi: 10.15468/mn7p62

Van de Velde I (1984) Revision of the African species of the genus *Mesocyclops* Sars, 1914 (Copepoda: Cyclopidae). Hydrobiologia 109(1): 3–66. doi: 10.1007/BF00006297

Wilson MS (1941) New species and distribution records of diaptomid copepods from the Marsh collection in the United States National Museum. Journal of the Washington Academy of Sciences 31: 509–515.

Wilson MS, Yeatman HC (1959) Free-living Copepoda. In: Edmonson WT (Ed.) Ward's and Whipple's Freshwater Biology. John Wiley and Sons, New York, 735–861.

ZooKeys 637: 81–88 (2016)
doi: 10.3897/zookeys.637.11001
http://zookeys.pensoft.net

RESEARCH ARTICLE

A peer-reviewed open-access journal
ZooKeys
Launched to accelerate biodiversity research

New South American species of Lamiinae (Coleoptera, Cerambycidae)

Maria Helena M. Galileo[1,3], Antonio Santos-Silva[2]

1 *PPG Biologia Animal, Departamento de Zoologia, Universidade Federal do Rio Grande do Sul, Porto Alegre, RS, Brazil* **2** *Museu de Zoologia, Universidade de São Paulo, São Paulo, SP, Brazil* **3** *Fellow of the Conselho Nacional de Desenvolvimento Científico e Tecnológico (CNPq)*

Corresponding author: *Maria Helena M. Galileo* (galileomh@yahoo.com)

Academic editor: *F. Vitali* | Received 1 November 2016 | Accepted 21 November 2016 | Published 2 December 2016

http://zoobank.org/D453AB53-360A-4893-A52A-43A3C635B288

Citation: Galileo MHM, Santos-Silva A (2016) New South American species of Lamiinae (Coleoptera, Cerambycidae). ZooKeys 637: 81–88. https://doi.org/10.3897/zookeys.637.11001

Abstract

Two new species of cerambycid beetles are described from South America: *Ataxia camiriensis* (Pteropliini), from Bolivia, and *Falsamblesthis uniformis* (Forsteriini), from Peru. The new species are included in previous keys.

Keywords

Key, Neotropical region, taxonomy

Introduction

Increased Cerambycidae collecting in recent decades, in northwestern South America has led to the discovery of many species new to science. Two of the species are included and described herein.

Ataxia Haldeman, 1847 is a relatively large genus of Pteropliini. Currently it includes 41 species, and occurs from the United States of America to southern South America (including Caribbean) (Tavakilian and Chevillotte 2016). Eight species are known from Bolivia (Monné 2016).

Falsamblesthis Breuning, 1959 (Forsteriini) includes nine species occurring only in South America (Monné 2016). The new species described here is the first record of the genus for Peru.

Material and methods

Photographs were taken with a Canon EOS Rebel T3i DSLR camera, Canon MP-E 65mm f/2.8 1–5× macro lens, controlled by Zerene Stacker AutoMontage software. Measurements were taken in "mm" using a micrometer ocular Hensoldt/Wetzlar - Mess 10 in the Leica MZ6 stereomicroscope, also used in the study of the specimen.

The collection acronyms used in this study are as follows:

ACMT	American Coleoptera Museum (James E. Wappes), San Antonio, Texas, USA
FSCA	Florida State Collection of Arthropods, Gainesville, Florida, USA
MNKM	Museo de Historia Natural, Noel Kempff Mercado, Santa Cruz de la Sierra, Bolivia
SLPC	Steven W. Lingafelter Private Collection, Hereford, Arizona, USA

Results

***Ataxia camiriensis* sp. n.**
http://zoobank.org/2E15B030-78CE-45E5-B295-5669AD8E9BC5
Figs 1, 2, 3, 4

Diagnosis. The pronotum without large white pubescence or central band of contrasting pubescence, elytral pubescence not white along suture, and elytral apex widely truncate distinguish this species.

Description. Female. Integument dark brown, almost black, except basal half of antennomeres IV–V, basal third of VI, and basal quarter of VII dark reddish brown. Pubescence obscuring nearly all integument.

Head. Frons finely, sparsely punctate; with dense pale golden pubescence interspersed with sparse, long, erect pale yellow and brown setae. Vertex with pale golden pubescence between antennal tubercles and upper eye lobes (this pubescence slightly projected after posterior edge of upper eye lobes), interspersed with long, erect, sparse pale yellow and brown setae; remaining surface with dense greenish-brown pubescence, less dense along coronal suture. Tempora and gena with dense greenish-brown pubescence (more pale yellow depending on angle of light) interspersed with long, erect, sparse pale yellow setae and some thick, brown setae behind lower eye lobe. Submentum with short, decumbent, moderately sparse pale yellow pubescence, denser close to mentum, interspersed with long, erect, sparse pale yellow setae. Labrum with long, decumbent pale yellow and yellowish-brown setae almost obscuring integument, and dense fringe

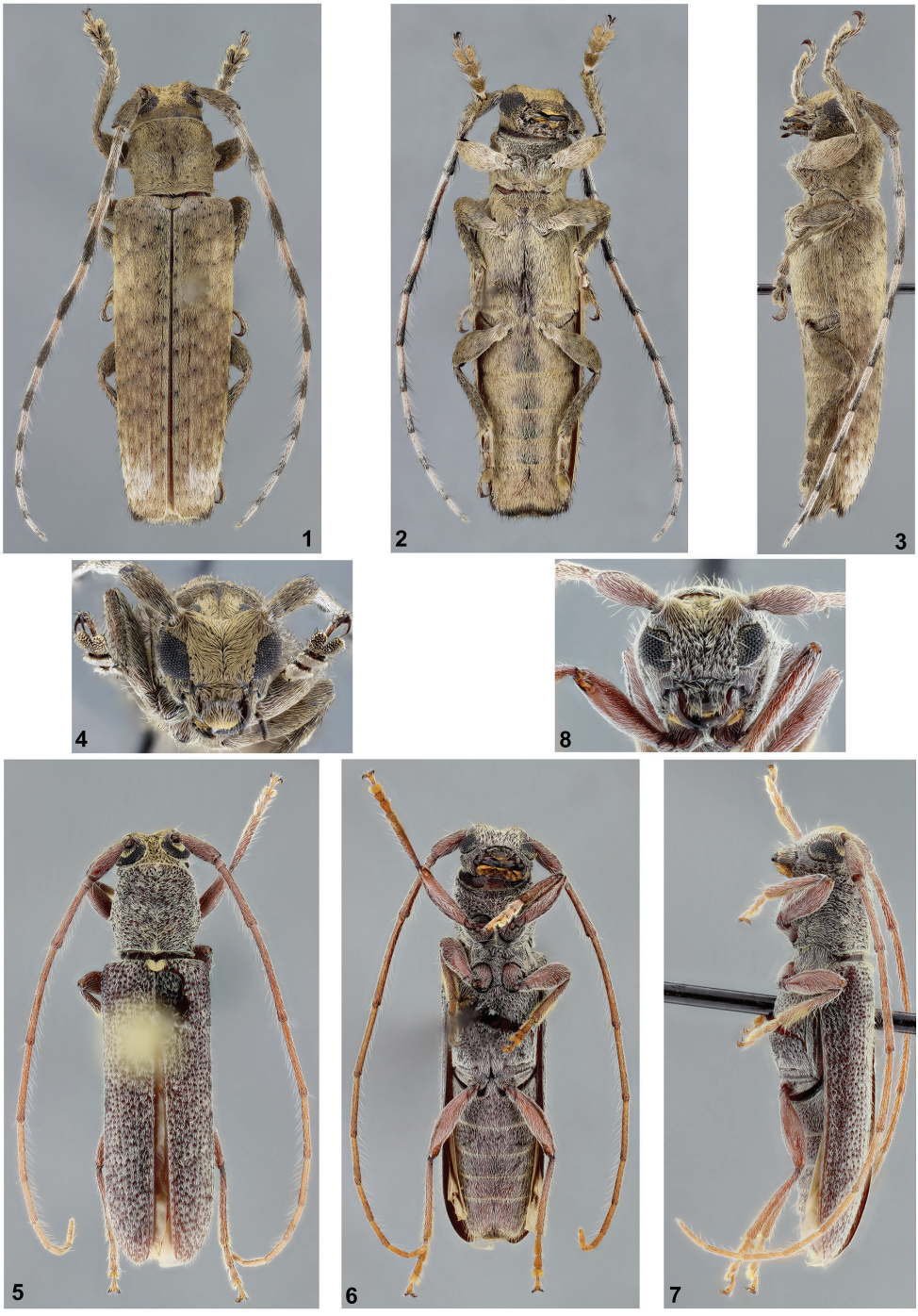

Figures 1–8. 1–4 *Ataxia camiriensis* sp. n., holotype female: **1** dorsal habitus **2** ventral habitus **3** lateral habitus **4** head, frontal view **5–8** *Falsamblesthis uniformis* sp. n., holotype female: **5** dorsal habitus **6** ventral habitus **7** lateral habitus **8** head, frontal view.

of golden pubescence on distal margin. Distance between upper eye lobes 0.45 times length of scape; distance between lower eye lobes in frontal view 0.75 times length of scape. Antennae 1.55 times elytral length, reaching elytral apex at distal quarter of antennomere IX; scape with narrow apical cicatrix, dorsally and laterally with greenish-brown pubescence interspersed with whitish pubescence, ventrally mostly with whitish pubescence, with long, erect, sparse, thick dark brown setae; pedicel and antennomere III with whitish pubescence except pale yellow pubescence exposing integument on dorsal half (not reaching apex); antennomeres IV–X with whitish pubescence on basal area (covering basal half on IV–V, gradually wider toward X); antennomere XI with whitish pubescence; ventral side of antennomeres with long, erect, white setae on basal half, dark brown on distal half (sparser toward XI); dorsal apex of antennomeres III–X with long, erect dark brown setae (gradually shorter toward X); antennal formula (ratio) based on length of antennomere III: scape = 1.04; pedicel = 0.28; IV = 1.42; V = 1.21; VI = 1.06; VII = 0.95; VIII = 0.85; IX = 0.80; X = 0.74; XI = 0.61.

Thorax. Prothorax 1.3 times wider than long (including lateral tubercles); lateral tubercle conical, with blunt apex, placed at about midlength. Pronotum with 5 gibbosities: one on each side of basal half, subcircular, slightly distinct; one on each side of distal half, subcircular, well-marked; one centrally, elongate, slightly distinct. Pronotal surface coarsely, sparsely punctate; basal half with pale yellow pubescence, with some areas more whitish; distal half with greenish-brown pubescence, more pale yellow on some areas; with long, erect, sparse pale yellow setae and thick dark brown setae on distal half. Sides of prothorax coarsely, sparsely punctate close to pronotum, almost smooth toward ventral side; pubescence as on pronotum. Prosternum with yellowish-white pubescence partially obscuring integument, denser, more pale yellow toward apex of prosternal process. Ventral side of meso- and metathorax with pubescence mostly pale yellow, slightly marmorate with greenish-yellow and yellowish-white pubescence; metasternum with long, erect, sparse pale yellow setae; mesosternal process with tubercle slightly projected. Scutellum with greenish-brown pubescence. *Elytra*. Coarsely, sparsely punctate, more so toward apex; slightly longitudinally sulcate along suture; with low, but distinct carina from apex of basal third to near apex, close to margin of longitudinal sulcus; with two other longitudinal carina, less distinct, between the former and lateral curvature; circum-scutellar region with whitish pubescence; basal 4/5 with greenish-brown pubescence marmorate with pale yellow and yellowish-white pubescence, except lateral area of basal third with pale yellow pubescence (not reaching base) and area on basal declivity and circum-scutellar with white pubescence (more silver on declivity and inconspicuous depending on angle of light); distal fifth with large lateral macula with white pubescence; laterodistal apex with dark brown pubescence; with small, sparse glabrous areas, mainly along suture; with thick, sparse, erect dark brown setae; apex widely truncate. *Legs*. Femora with greenish-brown pubescence, pale yellow ventrally on basal third. Tibiae mostly with greenish-brown pubescence, distinctly golden dorsally on transverse sulcus of mesotibiae and distal area of meso- and metatibiae.

Abdomen. Ventrites with pale yellow pubescence (more green or golden depending on angle of light source), except distal area of ventrite V with dark brown pubescence; sides of ventrite with long, decumbent, sparse pale yellow setae.

Male. It differs from female mainly by the antennae distinctly longer (about 1.8 times longer than elytra), surpassing elytral apex at about midlength of antennomere VIII.

Dimensions (mm). Holotype female: Total length, 13.70; prothoracic length, 2.35; basal prothoracic width, 2.55; distal prothoracic width, 2.40; largest prothoracic width (between apices of lateral tubercles), 3.15; humeral width, 3.70; elytral length, 10.10. Paratype male: Total length, 13.00; humeral width, 3.00.

Type material. Holotype female from **BOLIVIA**, Santa Cruz: 20 km N Camiri (road to Eyti, 6–8 km E Hwy 9; 1250 m; 19°5'S / 63°29'W), 26.XI.2013, Wappes & Skillman col. (MNKM). Paratype male from **BOLIVIA**, Santa Cruz: road to Eyti (Cordillera Prov.; 10.5 km NE of Highway 9, 22 km NNE of Camiri; 1140 m; 19°50.56'S / 63°29.05'W), 3–4.XII.2013, Lingafelter col. (SLPC).

Etymology. Named for the city (Camiri) in southern Santa Cruz Department, Bolivia, near where the new species was collected.

Remarks. *Ataxia camiriensis* sp. n. is similar to *A. luteifrons* (Bruch, 1926), but differs as follows: pronotum without large white pubescence areas; elytral pubescence not white along suture; base of elytra without distinct transverse band of white pubescence. In *A. luteifrons* pronotum has a large white pubescent area, elytral pubescence is white along suture, and a distinct transverse band of white pubescence is present along base of elytra.

Ataxia camiriensis sp. n. can be included in the alternative of couplet "21" from Breuning (1961):

21 Elytra coarsely and roughly punctate on basal area. Mexico (Veracruz), Guatemala, Honduras, Nicaragua, Costa Rica, Colombia, Venezuela, French Guiana, Guyana, Peru, Bolivia, Brazil (Amapá, Maranhão) .... ***A. operaria*** **(Erichson, 1848)**

– Elytra very finely punctate on basal area [actually, coarsely, sparsely punctate] ..... **21'**

21' Pronotum with large area with white pubescence; base of elytra with transverse band with white pubescence; elytra with white pubescence along suture. Bolivia (Santa Cruz), Paraguay, Argentina (Catamarca, Santiago del Estero, La Rioja, Mendoza, Santa Fé) ..... ***A. luteifrons*** **(Bruch, 1926)**

– Pronotum lacking large white pubescence areas; base of elytra without distinct white pubescent transverse band; elytra without white pubescence along suture. Bolivia (Santa Cruz) ..... ***A. camiriensis*** **sp. n.**

Falsamblesthis uniformis **sp. n.**
http://zoobank.org/4E1D87C5-5C86-49A0-9D1A-96A0E4CBEBBA
Figs 5, 6, 7, 8

Diagnosis. The vertex with yellow pubescence throughout distinguishes this species of the other of the genus.

Description. Female. Integument black except mouthparts yellowish-brown, antennae dark reddish-brown, gradually lighter toward distal segments, and legs dark reddish-brown.

Head. Frons moderately coarsely, abundantly punctate; with whitish pubescence partially obscuring integument, more pale yellow toward antennal tubercles; with long, erect, sparse pale yellow setae laterally. Vertex moderately coarsely, abundantly punctate; with yellow pubescence obscuring integument, mainly toward prothorax, interspersed with long, erect, sparse pale yellow setae. Area behind upper eye lobes with pubescence and erect setae as on vertex; area behind lower eye lobes coarsely, sparsely punctate, with yellowish-white pubescence not obscuring integument and long, erect, sparse pale yellow setae close to eye. Area on sides of gulamentum moderately finely rugose-punctate. Gulamentum finely, transversely punctate except smooth elevated anterior area; elevated area with short whitish pubescence, not obscuring integument, interspersed with a few long, erect whitish setae. Postclypeus with yellowish-white pubescence not obscuring integument, centrally interspersed with long, erect, sparse yellowish-white setae. Labrum coplanar with anteclypeus on basal half, inclined on distal half; finely, abundantly punctate laterally, smooth centrally; with decumbent, moderately long yellowish-white setae on punctate area, glabrous centrally; with fringe of yellow setae on distal margin. Distance between upper eye lobes 0.30 times length of scape; distance between lower eye lobes 0.75 times length of scape. Antennae 1.95 times elytral length, reaching elytral apex at apex of antennomere VII; with long, erect, moderately sparse pale yellow seta ventrally (sparser, shorter toward distal segment); antennal formula (ratio) based on length of antennomere III: scape = 0.75; pedicel = 0.15; IV = 1.41; V = 1.12; VI = 0.92; VII = 0.74; VIII = 0.63; IX = 0.60; X = 0.54; XI = 0.54.

Thorax. Prothorax 1.1 times wider than long (including lateral tubercles); lateral tubercle small, conical, with acute apex slightly curved backward, placed before midlength. Pronotum coarsely, densely punctate; with yellowish-white pubescence partially obscuring integument (slightly yellower centrally close to basal and distal margins); with long, erect, sparse pale yellow setae throughout. Sides of prothorax and prosternum with sculpture and pubescence as on pronotum. Mesosternum coarsely, moderately sparsely punctate (punctures slightly smaller than on prosternum); with yellowish-white pubescence not obscuring integument. Mesepisternum, mesepimeron and metepisternum smooth; with yellowish-white pubescence partially obscuring integument. Metasternum coarsely, abundantly punctate laterally, gradually sparser toward center; with yellowish-white pubescence not obscuring integument, sparser toward central region; with short, erect, sparse pale yellow setae throughout. Scutellum with dense yellow pubescence. *Elytra*. Coarsely, abundantly punctate on basal third, slightly finer and sparser toward apex; with yellowish-white pubescence partially obscuring integument; with moderately long, erect, sparse pale yellow setae throughout. *Legs*. Femora with yellowish-white pubescence not obscuring integument. Protibiae with pale yellow pubescence not obscuring integument, except on distal half of ventral side, interspersed with long, erect, sparse pale yellow setae; mesotibiae with pale yellow setae, gradually denser and longer toward apex (notably denser and golden on distal half of dorsal side); metatibiae with pale yellow setae, gradually longer toward apex.

Abdomen. Ventrites finely, moderately sparsely punctate (punctures distinctly finer and sparser from I to V); with yellowish-white pubescence not obscuring integument, interspersed with long, erect, sparse pale yellow setae (more abundant on V); ventrite V with small, longitudinal depression on center of base, with distinct, semicircular depression on distal half (notably deeper centrally close to apex); apex of ventrite V truncate, centrally widely, deeply emarginate.

Dimensions (mm), holotype female. Total length, 9.65; prothoracic length, 2.00; basal prothoracic width, 1.75; distal prothoracic width, 1.70; largest prothoracic width (between apices of lateral tubercles), 2.15; humeral width, 2.40; elytral length, 6.70.

Type material. Holotype female from **PERU**, Amazonas: 12 km W Bagua Grande (-5.7257 / -78.5365; 540 m), 14–17.XI.2007, M. E. Irwin & P. D. Parker col. (FSCA).

Etymology. Named for its uniform pubescent appearance.

Remarks. *Falsamblesthis uniformis* sp. n. is similar to *F. ibiyara* Marinoni, 1978, but differs as follows: pronotum convex; distance between upper eye lobes about 1.5 times width of one lobe; pubescence on vertex yellow throughout. In *F. ibiyara* the pronotum is flat, distance between upper eye lobes is wider than twice the width of one lobe, and the pubescence between antennal tubercles and remaining surface of vertex has different color.

Falsamblesthis uniformis sp. n. can be included in the alternative of couplet 5 from Galileo and Martins (1987):

5	Sides of metasternum coarsely and abundantly punctate..... **5'**
–	Sides of metasternum smooth. Ecuador ..... ***F. macilenta*** **(Gounelle, 1910)**
5'	Distance between upper eye lobes about 1.5 times width of one lobe; vertex with yellow pubescence throughout. Peru..... ***F. uniformis*** **sp. n.**
–	Distance between upper eye lobes wider than twice the width of one lobe; pubescence between antennal tubercles and remaining surface of vertex with different color. Brazil (Bahia, Minas Gerais, Espírito Santo, Rio de Janeiro, São Paulo, Paraná, Santa Catarina, Rio Grande do Sul)..... ***F. ibiyara*** **Marinoni, 1978**

Acknowledgments

We express our sincere thanks to our friend James E. Wappes (ACMT) for sending the specimens described in this work. We especially appreciate careful reviews of the manuscript by Steven W. Lingafelter and Francesco Vitali.

References

Breuning S (1961) Révision des Pteropliini (Col. Cerambycidae). Pesquisas, Zoologia (5) 9: 5–61.

Galileo MHM, Martins UR (1987) Sobre Falsamblesthiini (Coleoptera, Cerambycidae, Lamiinae) I. Revisão do gênero *Falsamblesthis* Breuning, 1959. Revista Brasileira de Entomologia 31(3): 447–452.

Monné MA (2016) Catalogue of the Cerambycidae (Coleoptera) of the Neotropical region. Part II. Subfamily Lamiinae. http://cerambyxcat.com/ [accessed November 2016]

Tavakilian GL, Chevillotte H (2016) Titan: base de données internationales sur les Cerambycidae ou Longicornes. Version 3.0. http://titan.gbif.fr/index.html [accessed November 2016]

ZooKeys 637: 89–106 (2016)
doi: 10.3897/zookeys.637.8637
http://zookeys.pensoft.net

RESEARCH ARTICLE

A peer-reviewed open-access journal
ZooKeys
Launched to accelerate biodiversity research

Evaluating the diversity of Neotropical anurans using DNA barcodes

Ruth A. Estupiñán[1], Stephen F. Ferrari[2], Evonnildo C. Gonçalves[3], Maria Silvanira R. Barbosa[3], Marcelo Vallinoto[4], Maria Paula C. Schneider[3]

1 *Instituto Federal da Paraíba, Campus Cabedelo, Cabedelo, Brazil* **2** *Universidade Federal de Sergipe, São Cristóvão, Brazil* **3** *Universidade Federal do Pará, Belém, Brazil* **4** *Universidade Federal do Pará, Campus de Bragança, Bragança, Brazil*

Corresponding author: *Ruth A. Estupiñán* (ruthamanda.estupinan@gmail.com)

Academic editor: *F. Andreone* | Received 27 March 2016 | Accepted 8 October 2016 | Published 2 December 2016

http://zoobank.org/60204385-E2C1-4861-AC2A-7DFF0F3FC6F3

Citation: Estupiñán RA, Ferrari SF, Gonçalves EC, Barbosa MSR, Vallinoto M, Schneider MPC (2016) Evaluating the diversity of Neotropical anurans using DNA barcodes. ZooKeys 637: 89–106. https://doi.org/10.3897/zookeys.637.8637

Abstract

This study tested the effectiveness of COI barcodes for the discrimination of anuran species from the Amazon basin and other Neotropical regions. Barcodes were determined for a total of 59 species, with a further 58 species being included from GenBank. In most cases, distinguishing species using the barcodes was straightforward. Each species had a distinct COI barcode or codes, with intraspecific distances ranging from 0% to 9.9%. However, relatively high intraspecific divergence (11.4–19.4%) was observed in some species, such as *Ranitomeya ventrimaculata*, *Craugastor fitzingeri*, *Hypsiboas leptolineatus*, *Scinax fuscomarginatus* and *Leptodactylus knudseni*, which may reflect errors of identification or the presence of a species complex. Intraspecific distances recorded in species for which samples were obtained from GenBank (*Engystomops pustulosus, Atelopus varius*, *Craugastor podiciferus*, and *Dendropsophus labialis*) were greater than those between many pairs of species. Interspecific distances ranged between 11–39%. Overall, the clear differences observed between most intra- and inter-specific distances indicate that the COI barcode is an effective tool for the identification of Neotropical species in most of the cases analyzed in the present study.

Keywords

Amazon basin, amphibians, COI, DNA barcoding, identification, taxonomy

Introduction

Many amphibian groups are morphologically homogeneous and tend to lack clear diagnostic traits. This means that, while there have been a number of recent advances, the taxonomy of amphibians is poorly resolved in general (see e.g. Darst and Cannatella 2004; Faivovich et al. 2005; Frost et al. 2010; Grant et al. 2006; Roelants et al. 2007; Vences et al. 2003). In particular, the intrageneric diversity of the amphibians appears to be underestimated in most cases (e.g., Bossuyt et al. 2004; Crawford et al. 2010; De la Riva et al. 2000; Fouquet et al. 2007; Vieites et al. 2009). In this context, the accelerating global decline and changes in amphibian populations (Hoffmann, et al. 2010, McCallum, 2007; Stuart et al. 2004; Narins et al. 2014), as well as the cryptic diversity reported for several taxa (Fouquet et al. 2007; Crawford et al. 2013), implies that many still undescribed species may be disappearing from the Neotropical region before they have even been identified (Collins 2010).

The increasing availability of molecular data has reinforced the conclusion that morphological evolution in amphibians is often cryptic, resulting in a revitalization of amphibian taxonomy (e.g. Real et al. 2005; Vieites et al. 2009; Rowley et al. 2010; Stuart et al. 2006; Funk et al. 2012; Xia et al. 2012; Crawford et al. 2013). Rapidly-evolving genes may overwrite the evidence of ancient affinities, but are extremely useful for the understanding of recent divergence among closely-related species. Mitochondrial DNA (mtDNA) has been widely used in phylogenetic studies of animals because it evolves much more rapidly than nuclear DNA, resulting in the accumulation of differences between closely-related species (Brown et al. 1979; Moore 1995; Mindell et al. 1997). The taxonomic reviews at the species level now almost always include some form of analysis of mtDNA divergence. A number of species of the genus *Rana* have been recognized in recent years, based on molecular methods (Newman et al. 2012), for example, and through comparisons with other amphibian species (Channing et al. 2013; Hasan et al. 2014; Biju et al. 2014).

Short DNA sequences from a standardized region of the genome can provide a DNA "barcode" for the identification of species (Hebert et al. 2003), and may provide a substitute for more traditional molecular approaches, which have been used for the identification of amphibian taxa for some time (Larson and Chippindale, 1993). A 648-bp region of the mitochondrial Cytochrome Oxidase I (COI) gene is commonly used as a barcode for the identification of animal species, given that it is easily sequenced and provides excellent resolution for the identification of taxa, especially when combined with the analysis of other traits (Pereyra et al. 2016). This is supported by the considerable divergence in sequences found by Hebert et al. (2003) between 13,000 pairs of closely-related animal species, and reinforces the need for the analysis of more than a single, short sequence of DNA, which may produce inconclusive results (Blotto et al. 2012, Pereyra et al. 2016).

The usefulness of COI as a DNA barcode has been evaluated in Malagasy mantellids and North American plethodontid salamanders (Vences et al. 2005a), Holarctic

amphibians (Smith et al. 2008), and Asiatic salamanders of the family Hynobiidae (Xia et al. 2012). In the Neotropical zone, COI has been tested in amphibians from Panama and the Guianan Shield (Crawford et al. 2010, 2013; Hawkins et al. 2007). Variations in the performance of COI as a DNA barcode have provoked doubts on the effectiveness of the approach for the identification of species (Vences et al. 2005b). The main limitation on the use of COI in amphibians is the lack of a universal primer for the PCR-mediated amplification of the DNA of different species (Vences et al. 2012). In many cases, the overlap found between intraspecific and interspecific distances reduces the reliability of species identification (Vences et al. 2005a; Hawkins et al. 2007). Given this, Vences et al. (2005b) recommended the use of 16S rRNA as a DNA barcode, rather than COI.

Using a combination of primers, COI sequences were used to successfully identify 94% of Holarctic amphibians, and showed that the overlap between intra- and interspecific distances was the result of hybridization, the presence of species complexes or taxonomic problems (Smith et al. 2008). In many cases, there was no overlap in these distances. Overall, then, the COI barcode presented the same problems encountered in the analysis of any other group of animals (Smith et al. 2008; Crawford et al. 2010; Hawkins et al. 2007; Vences et al. 2012).

In this context, the present study evaluated the potential of the mitochondrial COI gene as a barcode, used in combination with other traits, for the identification of Neotropical amphibians from the Amazon basin and other regions of South America. In particular, the study compares the molecular classification of the specimens with the traditional taxonomy of the group.

Material and methods

Study area and samples

In order to establish a reference site for the evaluation of a barcoding approach for Amazonian vertebrates, a field survey was conducted in the BX044 polygon in the southwestern Amazon basin, an area considered to be of the highest importance for the conservation of the biome's biological diversity (Pronabio, 2002). The polygon covers an area of 5270 km^2 and is located between latitudes 08°02'52" and 08°54'46" S, and longitudes 60°50'24" and 62°10'13"W, within the Madeira-Tapajós interfluve (Fig. 1). This interfluve is poorly studied and has few few protected areas, with no more than six percent of its total area located within conservation units of any kind (Ferreira et al. 2001). Notwithstanding, it encompasses a unique complex of habitats including open forests, savanna, forest-savanna transition, and gallery forests (Pereira et al. 2004). This mosaic of habitats reflects the position of the study area within the ecotone marking the transition between the Amazonian Hylea and the Cerrado savannas of central Brazil (Nascimento et al. 1988; Stotz et al. 1997).

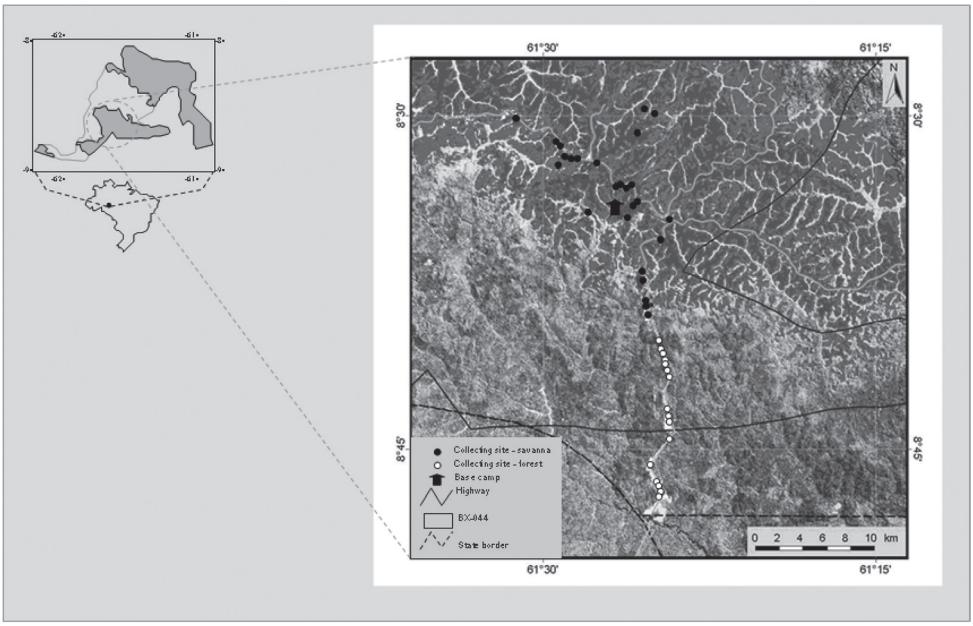

Figure 1. The BX044 priority area for conservation showing the sites at which anuran specimens were collected.

Specimens were collected in January, 2004, at 74 sites located along the Maderinha, Roosevelt, and Jatuarana rivers, and their tributaries. Specimens were collected in open and dense savanna habitats, gallery and flooded forests, rainforest, and ricefields. The specimens were euthanized with a lethal dose of lidocaine (Brasil, 1979). A total of 76 specimens representing 33 species was collected, and 37 sequences were obtained from 17 species, which represent one third of the total number of species analyzed in the present study. The sample was augmented by tissue samples (41 specimens representing 37 species) obtained from other institutions in Brazil and other countries. In addition to these samples, the COI sequences of a number of other amphibian species (see Suppl. material 1) with large sample sizes were obtained from GenBank, to provide a better visualization of the variation in the COI gene in these organisms.

Specimen identification

Following the extraction of tissue samples, the specimens collected during the present study were preserved for identification at the Goeldi Museum in Belém, Brazil, where they were confirmed by M.S.H. Hoogmoed. The accuracy of COI as a barcode for the identification of species was assessed based on the most recent classification of the amphibians (Frost 2016).

Molecular methods

Total DNA was extracted from either muscle or liver tissue by the SDS-proteinase K/phenol-chloroform extraction method (Sambrook and Russell 2001). A partial 680-bp fragment of the COI gene was amplified using the 5-CCTGCAGGAGGAGGAGA-YCC-3′ and 5-AGTATAAGCGTCTGGGTAGTC-3′ primers (Palumbi 1996). The 25 µL polymerase chain reaction (PCR) mixture contained 0.4-1.2 µL of the DNA template, 2.5 µL 10XPCR buffer, 0.5 µL of each primer (10 pM/µL), 0.6-2.0 µL of $MgCl_2$, 1µL dNTPs, and 0.15 µL of *Taq* DNA polymerase. The PCR conditions consistedof 3 min at 94 °C, followed by 35 (or 34) cycles of 50 sec at 94 °C, 50 sec at 55 °C (or 57 and 60 °C), 50 sec at 72 °C and a final extension at 72 °C for 5 min. The DNA was sequenced in both directions using the primers described above in a MegaBace (GE Healthcare) automatic DNA sequencer, using the DYEnamic ET Dye Terminator kit (GE Healthcare).

The sequences obtained were aligned and edited by BIOEDIT v. 7.0.5.3 (Hall 1999). The possible saturation of bases was assessed using a graphic representation of transitions and transversions (Ti-Tv) plotted against Kimura 2 parameters' distance (Kimura 1980). This analysis was run in DAMBE v. 5.3.105 (Xia 2013).

Pairwise comparisons of COI sequences were conducted for three categories: (i) individuals of the same species, (ii) individuals of the same genus (excluding those of the same species), and (iii) individuals of the same family (excluding those of the same genus). The frequency distribution of intra- and interspecific genetic distances was calculated using MEGA 5 (Tamura et al. 2011), as was a neighbor-joining (NJ) tree based on the K2P model (Kimura 1980). The robustness of the nodes of this tree was estimated by a bootstrap analysis, with 1000 pseudo-replications.

The variability of the COI gene between populations of the same species was also tested using the K2P model, for which the species were selected based on the largest possible sample size (number of specimens) in GenBank (*A. varius*, *C. podiciferus*, *D. labialis* and *E. pustulosus*) and the availability of accurate information on their geographic origin. Additional species were included in this analysis (see Suppl. material 1).

Results

COI sequences were recovered from 75% (83/110) of the specimens analyzed. Full-length PCR products (640 bps) were amplified from all of these specimens (see Suppl. material 1). Of the 111 species analyzed, sequences of 56 were obtained during the present study and 58 from GenBank (sequences of *Dendropsophus minutus*, *Rhinella marina*, and *Osteocephalus taurinus* were obtained from both sources). Altogether, 410 sequences were analyzed, of which, 78 were obtained in the present study and 332 from GenBank. No evidence of base saturation was found whatsoever (Fig. 2).

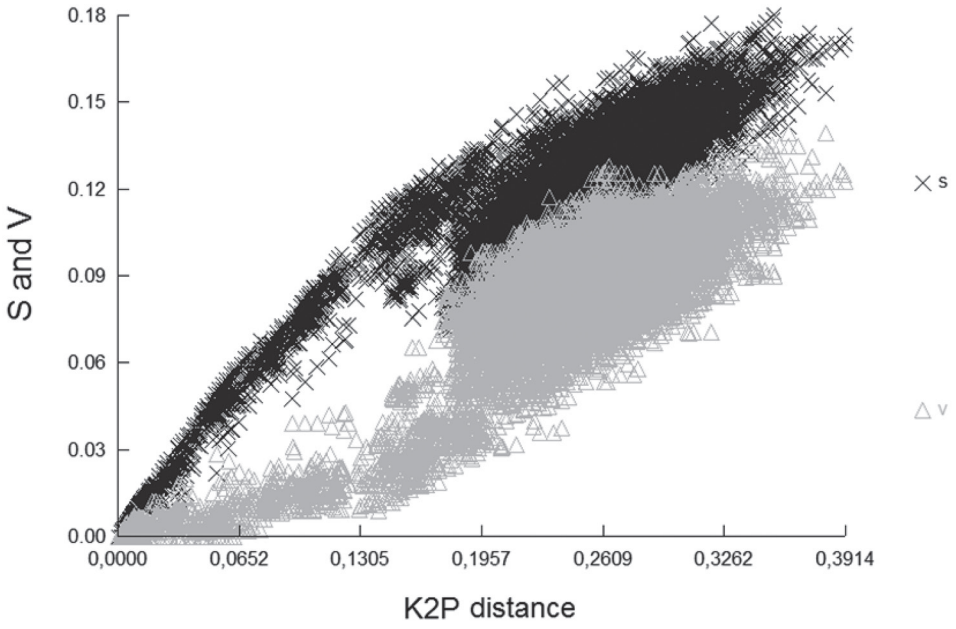

Figure 2. Transition (s) and transversions (v) plotted against the sequence divergence (Kimura 2-parameter distances) for the analyzed anurans.

Species identification

The COI barcode identified correctly the species of 94% of the specimens examined (93 of 109 species). The COI sequences obtained for the 36 species represented by two or more specimens were most similar to one another than to those of any other species. In addition, with a few notable exceptions, which are discussed below, the differences in COI sequences between closely-related species were higher than those within species. The mean K2P distance within species was 3.0% (Fig. 3), whereas that between species was 10.3%.

In most cases, the neighbor-joining (NJ) tree reflected a relatively reduced differentiation within species in comparison with between-species divergence (Fig. 4). Most of the terminal groups include specimens of the same species or genus with bootstrap values of over 85, except for *Ranitomeya*, *Scinax*, *Leptodactylus*, *Osteopilus*, and *Hypsiboas*, which all rendered relatively low bootstrap values. Also, in the Cophomantinae subfamily, the COI barcode generated contradictory clusters, such as *Bokermannohyla alvarengai* being sister group of *Hypsiboas albopunctatus*, *Dendropsophus minutus* and *Hypsiboas multifasciatus*, and *Aplastodiscus callipygius* and *Dendropsophus cachimbo*, and *Aplastodiscus albosignatus.*

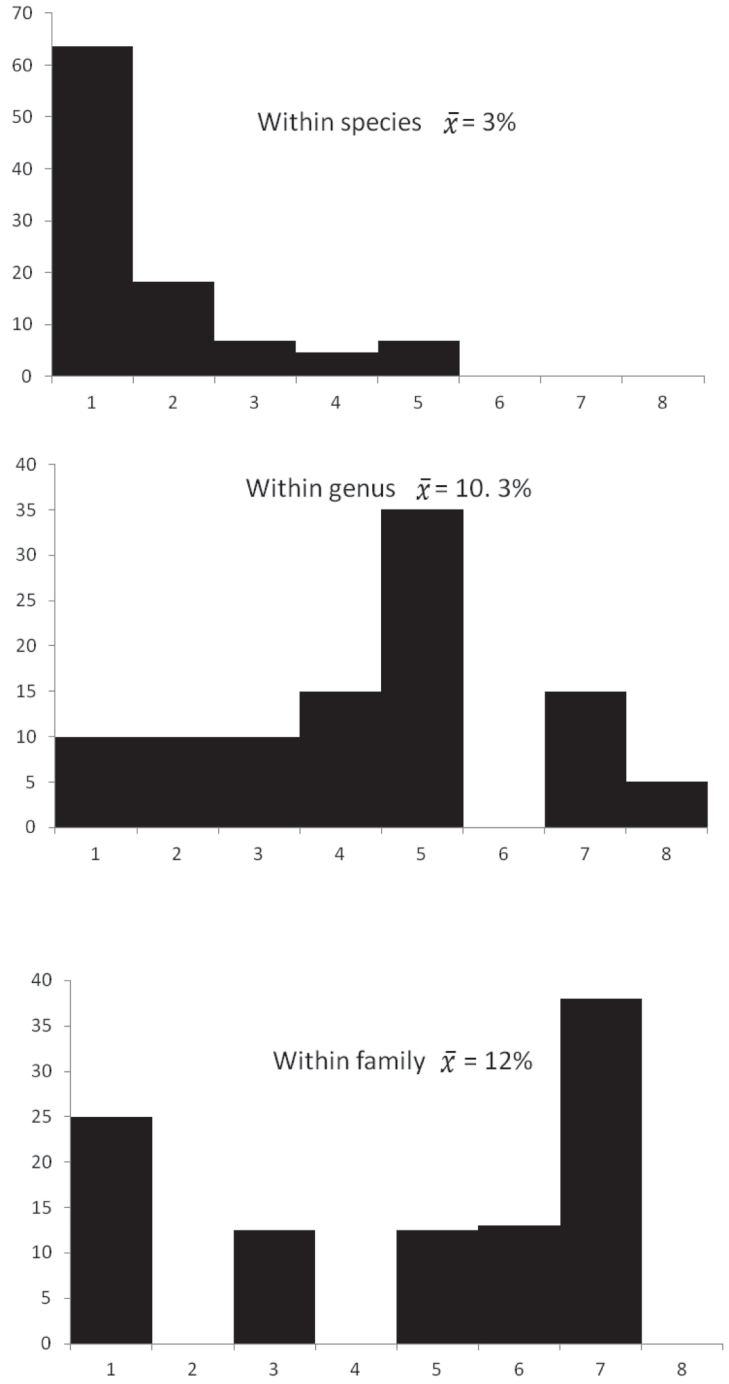

Figure 3. COI sequence divergence (K2P) at various levels of the taxonomic hierarchy for anurans.

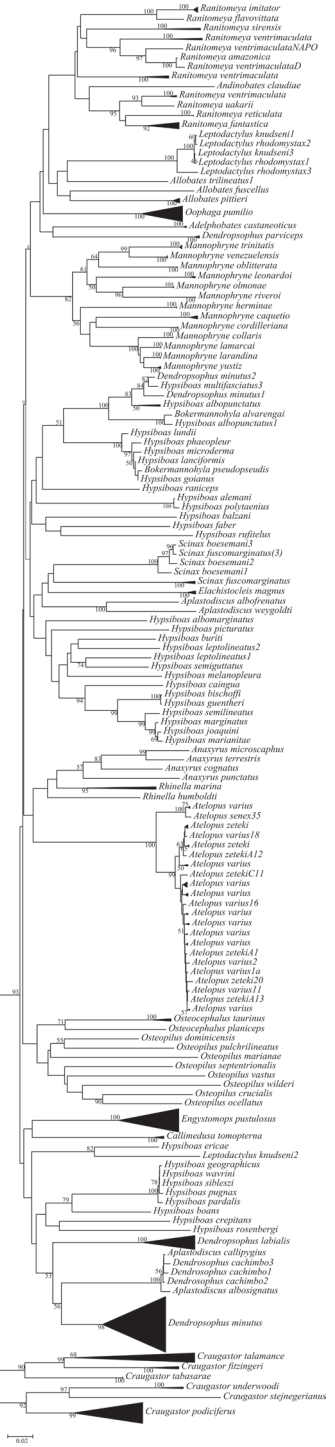

Figure 4. Neighbor-joining (NJ) tree derived from the analysis of COI sequences. The numbers at the nodes represent the percentage bootstrap values.

Table 1. Range of intraspecific and between-taxon divergence values recorded in the present study.

Comparison	Percentage distance
Intraespecific (including GenBank sequences): *Atelopus varius*	0.5–1.2
Craugastor podiciferus	4.1–11.4
Dendropsophus labialis	0.2–9.0
Engystomops pustulosus	0.0–11.4
Intraspecific (only species collected during the present study)	0.0–9.9*
Interspecific	11.0–39.0
Between genera	15.0–31.4
Between families (Bufonidae, Dendrobatidae, Hylidae, Craugastoridae, Leiuperidae, Microhylidae, Aromobatidae, and Leptodactylidae)	23.0–31.0

*Excluding the five outliers (see text).

Intra- and interspecific divergence

All but five of the species collected in the present study were characterized by intraspecific divergence equal to or lower than 9.9% (Suppl. material 1, Table 1). However, higher values were recorded for some taxa, such as *Ranitomeya ventrimaculata* (12.9%), *Hypsiboas leptolineatus*, *Leptodactylus knudseni* (13.3%), and *Scinax fuscomarginatus* with 10.9% (Suppl. material 1).

Interspecific divergence varied considerably (Table 1). The distances between most species (5826 comparisons) were within the 9.9-39% range, whereas a few species (60 comparisons) were in the 0-9.9% range. The distances between populations of *Atelopus varius, Craugastor podiciferus, Dendropsophus labialis*, and *Engystomops pustulosus* exceed the observed intraspecific distances in other species.

Discussion

A single mitochondrial DNA barcode, derived from the COI gene, identified correctly 93 of the 109 Neotropical amphibian species analyzed in the present study. Similar barcodes (sequences) were not observed in different species, and lower distances (generally 0.0–9.9%) were observed within species than between them. The ranges of values recorded in the present study were consistent with those recorded in previous amphibian studies (Table 2). However, relatively high intraspecific variation was recorded between populations in some species, such as *E. pustulosus* (0.0–11.4%), *C. podiciferus* (4.1–11.4%), and *D. labialis* (0.2–9.0%). This indicates the possible presence of additional cryptic species, and supports the development of a standard screening threshold of sequence differentiation that would contribute to the more systematic and effective identification of new animal species.

Lower intra- and interspecific distances have been recorded for the COI barcode in most other animal groups. In butterflies, for example, mean intraspecific distances were 0.46%, while those between species ranged from 2.97% (Hebert et al. 2004b)

Table 2. Within- and between-taxon distances recorded in different groups of amphibians, based on COI sequences.

Taxon or group	Geographic region	Percentage divergence in the COI gene (mean divergence)		Reference
		Within species	Between species	
Mantellidae (frogs)	Madagascar	10.0–18.0 (5.4)	(20.7)	Vences et al. (2005a)
Aneides (Climbing salamanders)	USA	> 7.8 (4.3)	(13.5)	Vences et al. (2005a)
Litoria fallax (two lineages)	Australia	5.0	11–12	James and Moritz (2000)
Ambystoma laterale-jeffesonium complex	Canada	–	9–14	Smith et al. (2007)
Scinax ruber	French Guiana	1.3–14.3	–	Fouquet et al. (2007)
Rhinella gr. *margaritifera*	Brazil, Ecuador, Peru, French Guiana	1.0–5.1	–	Fouquet et al. (2007)
Engystomops pustulosus	Mexico, Guatemala, Nicaragua, Costa Rica, Panama, Colombia, Venezuela	0.0–11.4	–	Data from Weigt et al. (2005) and analyzed in this study
Dendropsophus minutus	French Guiana, Suriname, Guyana	–	9 (uncorrected*p*)	Hawkins et al. (2007)
Hynobiidae (Asian salamanders)	China, Korea, Russia, Iran, Afghanistan, Kazakhstan	0.0–0.061	0.007–0.165	Xia et al. (2012)
Chinese amphibians	China	0–0.101	0.031–0.282	Che et al. (2012)
Eight frog families	Bolivia, Brazil, Colombia, Costa Rica, Ecuador, El Salvador, French Guiana, Guatemala, Guyana Haiti, Jamaica, Mexico, Nicaragua, Panama, Peru, Suriname Trinidad and Tobago, USA, Venezuela	0–9.9	11–39	Present study

to 4.58% (Hajibabaei et al. 2006a). In birds, these distances were 0.43% and 7.93%, respectively (Hebert et al. 2004a), in primates, 0.30% and 5.88% (Hajibabaei et al. 2006b), and in fishes, 0.39% and 9.93% (Ward et al. 2005).

The high COI divergence rates recorded in the present study were nevertheless similar to those recorded in pulmonate snails (Thomaz et al. 1996) and lizards (Harris et al. 2004). In order to evaluate the relative divergence of this gene, Vences et al. (2005a) compared substitution rates in COI with those of two other mitochondrial genes commonly used in studies of amphibians (Cytb and ND4), and concluded that molecular evolution in COI is relatively fast, resulting in considerable variability in comparison with either of the other two genes.

The neighbor-joining tree indicated that most of the species and genera analyzed in the present study form relatively cohesive units. However, the data available on *Dendropsophus minutus* (Hawkins et al. 2007; present study) indicate that this form may include more than one species, and a similarly complex situation was observed in the *Atelopus* species (Lotters et al. 2011). The greatest intraspecific distances were recorded in *Ranitomeya ventrimaculata* (12.9%), *Leptodactylus knudseni*, *Hypsiboas leptolineatus* (13.3%), and *Scinax fuscomarginatus* (10.9%). A similar degree of divergence was found in *R. ventrimaculata* by Symula et al. (2003) and Brown et al. (2011). Likewise, Kok and Kalamandeen (2008) have suggested that *L. knudseni* may represent a species complex. The status of *H. leptolineatus* and *S. fuscomarginatus* is less clear, especially given the taxonomic complexity of *Scinax*, given the large number of known species, its conservative morphology, and the number of undescribed species (Nunes et al. 2012; Duellman et al. 2016).

The greatest intrageneric distances were recorded in *Hypsiboas* (18.2%), *Craugastor* (19.7%), and *Osteopilus* (20.2%). The considerable distances between some *Craugastor* species indicates the existence of a species complex, as indicated previously for *Craugastor podiciferus* by Streicher et al. (2009). In respect to *Osteopilus septentrionalis*, which is widely distributed in Cuba, a similar pattern was observed by the Cyt b gene (Heinicke et al. 2011). According to theses authors, this may be related to ancient marine incursions, which would have isolated different lineages.

The general polytomy observed in the present study may have been the result of the phylogenetic divergence at the family and genus levels, and the relatively reduced number of terminal taxa. This may also be reflected in the considerable variation in the bootstrap values, from 0% to 92%, found in some clades.

The amplification of the COI gene is straightforward in most vertebrates (Clare et al. 2007; Hajibabaei et al. 2006b; Hebert et al. 2004b; Ward et al. 2005). In the present study, however, difficulties were encountered due to the use of universal primers, as reported previously by Vences et al. (2005a; 2012). For instance, in such studies, several modifications were done to perform successful COI amplifications, such as PCR purification and cloning, annealing temperature optimizations, and others. Thus, it may be necessary to formulate a cocktail of primers, with differentiated amplification protocols and annealing temperatures appropriate to the different amphibian species groups, genera or families (Clare et al. 2007; Vences et al. 2012). However, for other

groups, such as Asian Salamanders, Xia et al. (2012) concluded that the high success rate in the sequencing (89%) was due to the reduced variation in the priming regions.

The results of the present study support the use of COI sequences as a DNA barcode for help the identification of Neotropical amphibian species, in particular to ensure the presence of cryptic forms. However, it will still be necessary to identify the factors determining the relatively high rates of divergence observed within the populations of some of the species analyzed in the present study. It will also be important to compile a database of sequences for different molecular markers, in order to better evaluate intra- and inter-specific patterns of variability (Richardson 2012; Luquet et al. 2015; Chambers and Hebert, 2016), addition to update the identification of specimens in the collections.

Acknowledgments

We are grateful to Mariana Lúcio Lyra (UNESP) and Simoni Santos da Silva (UFPA) for their valuable suggestions on the original version of the manuscript, Laíssa de Castro Pontes (LPDNA) for help with the development of the study, and the numerous researchers from Brazil and other countries who contributed samples. We would also like to thank the Brazilian Environment Ministry, which financed the MMA/PROBIO-Brazil project "Diversity of vertebrates on the upper Marmelos River (BX 044)" and CAPES for providing a graduate RAET stipend.

References

Biju SD, Garg S, Mahony S, Wijayathilaka N, Senevirathne G, Meegaskumbura M (2014) DNA barcoding, phylogeny and systematics of Golden-backed frogs (*Hylarana*, Ranidae) of the Western Ghats-Sri Lanka biodiversity hotspot, with the description of seven new species. Contributions to Zoology 83: 269–335. http://www.ctoz.nl/cgi/t/text/getpdf?c=ctz;idno=8304a04

Blotto BL, Nuñez JJ, Basso NG, Úbeda CA, Wheeler WC, Faivovich, J (2012) Phylogenetic relationships of a Patagonian frog radiation, the Alsodes + Eupsophus clade (Anura: Alsodidae), with comments on the supposed paraphyly of Eupsophus. Cladistics 29: 113–131. doi: 10.1111/j.1096-0031.2012.00417.x

Bossuyt F, Meegaskumbura M, Beenaerts N, Gower DJ, Pethiyagoda R, Roelants K, Mannaert A, Wilkinson M, Bahir MM, Manamendra-Arachchi K, NgPKL, Schneider CJ, Oommen, OV, Milinkovitch MC (2004) Local endemism within the western Ghats – Sri Lanka biodiversity hotspot. Science 306: 479–481. doi: 10.1126/science.1100167

Brasil (1979) Lei 6638 de 08 de maio de 1979 Normas para a Prática Didático-científica da Vivissecção de Animais. http://www2.camara.leg.br/legin/fed/lei/1970-1979/lei-6638-8-maio-1979-366514-publicacaooriginal-1-pl.html

Brown JL, Twomey E, Amezquita A, de Souza MB, Caldwell JP, Lotters S, von May R, Melo-Sampaio PR, Mejia-Vargas D, Perez-Pena P, Pepper M, Poelman EH, Sanchez-Rodriguez

M, Summers K (2011) A taxonomic revision of the Neotropical poison frog genus *Ranitomeya* (Amphibia: Dendrobatidae). Zootaxa 3083: 1–120. http://www.mapress.com/zootaxa/2011/2/zt03083p120.pdf

Brown WM, George M Jr ,Wilson AC (1979) Rapid evolution of animal mitochondrial DNA. Proceedings of the National Academy of Sciences of the United States of America 76: 1967–1971. doi: 10.1073/pnas.76.4.1967

Chambers EA, Hebert PDN (2016) Assessing DNA Barcodes for Species Identification in North American Reptiles and Amphibians in Natural History Collections. PLoS ONE 11: e0154363. doi: 10.1371/journal.pone.0154363

Channing A, Schmitz A, Burger M, Kielgast J (2013) A molecular phylogeny of African Dainty Frogs, with the description of four new species (Anura: Pyxicephalidae: Cacosternum). Zootaxa 3701: 518–550. doi: 10.11646/zootaxa.3701.5.2

Che J, Chen HM, Yang J-X, Jin J-Q, Jiang K, Yuan Z-Y Murphy RW, Zhang Y (2012) Universal COI primers for DNA barcoding amphibians. Molecular Ecology Resources 12: 247–258. doi: 10.1111/j.1755-0998.2011.03090.

Clare EL, Lim BK, Engstrom MD, Eger JL, Hebert PDN (2007) DNA barcoding of Neotropical bats: species identification and discovery within Guyana. Molecular Ecology Notes 7: 184–190. doi: 10.1111/j.1471-8286.2006.01657

Collins JP (2010) Amphibian decline and extinction: what we know and what we need to learn. Diseases of Aquatic Organisms 92: 93–99. doi: 10.3354/dao02307

Crawford AJ Lips KR, Bermingham E (2010) Epidemic disease decimates amphibian abundance, species diversity, and evolutionary history in the highlands of central Panama. Proceedings of the National Academy of Sciences of the United States of America 107: 13777-13782. doi: 10.1073/pnas.0914115107

Crawford AJ, Cruz C, Griffith E, Ross H, Ibañez R, Lips KR, Driskell AC, Bermingham E, Crump P (2013) Dna barcoding applied to ex situ tropical amphibian conservation programme reveals cryptic diversity in captive populations. Molecular Ecology Resources 13: 1005–1018. doi: 10.1111/1755-0998.12054

Darst CR, Cannatella DC (2004) Novel relationships among hyloid frogs inferred from 12S and 16S mitochondrial DNA sequences. Molecular Phylogenetics and Evolution 31: 462–475. doi: 10.1016/j.ympev.2003.09.003

De la Riva I, Köhler J, Lötters S Reichle S (2000) Ten years of research on Bolivian amphibians: updated checklist, distribution, taxonomic problems, literature and iconography. Revista Española de Herpetologia 14: 19–164. https://www.researchgate.net/profile/Stefan_Loetters/publication/258507718_Ten_years_of_research_on_Bolivian_amphibians_updated_checklist_distribution_taxonomic_problems_literature_and_iconography/links/0046352861ec6d136d000000.pdf

Duellman WE, Marion AB, Hedges SB (2016) Phylogenetics, classification, and biogeography of the treefrogs (Amphibia: Anura: Arboranae). Zootaxa 4104: 1–109. doi: 10.11646/zootaxa.4104.1.1

Faivovich J, Haddad CFB, García PCA, Frost DR, Campbell JA, Wheeler WC (2005) Systematic review of the frog family hylidae with special reference to Hylinae: phylogenetic analysis and taxonomic revision. Bulletin of the American Museum of Natural History 294: 1–240. doi: 10.1206/0003-0090(2005)294[0001:SROTFF]2.0.CO;2

Ferreira LV, Sá RL, Buschbacher R, Batmanian G, Silva JMC, Arruda MB, Moretti E, Sá LFSN, Falconer J, Bampi MI (2001) Identificação de áreas prioritárias para a conservação da biodiversidade por meio da representatividade das unidades de conservação e tipos de vegetação nas ecorregiões da Amazônia brasileira. In: Capobianco JPR, Veríssimo A, Moreira A, Sawyer D, Santos I, Pinto LP (Eds) Biodiversidade na Amazônia Brasileira: Avaliação e Ações Prioritárias, Uso Sustentável e Repartição de Benefícios. Instituto Socioambiental, São Paulo, 268–289.

Fouquet A, Gilles A, Vences M, Marty C, Blanc M, Gemmell N (2007) Underestimation of species richness in Neotropical frogs revealed by mtDNA analyses. PLoS ONE 2: e1109. doi: 10.1371/journal.pone.0001109

Frost DR (2016) Amphibian Species of the World: an Online Reference. Version 6.0 (05/05/2014 access). Electronic Database accessible at http://research.amnh.org/herpetology/amphibia/index.html. American Museum of Natural History, New York, USA.

Frost DR, Grant T, Faivovich J, Bain RH, Haas A, Haddad CFB, de Sa RO, Channing A, Wilkinson M, Donnellan S.C, Raxworthy CJ, Campbell JA, Blotto BL, Moler P, Drewes RC, Nussbaum RA, Lynch JD, Green DM, Wheeler WC (2010) The Amphibian tree of life. Bulletin of the American Museum of Natural History 297: 1–370. doi: 10.1206/0003-0090(2006)297[0001:TATOL]2.0.CO;2

Funk WC, Caminer M, Ron SR (2012) High levels of cryptic species diversity uncovered in Amazonian frogs. Proceedings of the Royal Society B: Biological Sciences 279: 1806–1814. doi: 10.1098/rspb.2011.1653

Grant T, Frost DR, Caldwell JP, Gagliardo R, Haddad CFB, Kok PJR, Means DB, Noonan BP, Schargel WE, Wheeler WC (2006) Phylogenetic systematics of dart-poison frogs and their relatives (Amphibia: Athesphatanura: Dendrobatidae). Bulletin of the American Museum of Natural History 299: 1–262. doi: 10.1206/0003-0090(2006)299[1:PSODFA]2.0.CO;2

Hajibabaei M, Janzen, DH, Burns, JM, Hallwachs, W, Hebert, PDN (2006a) DNA barcodes distinguish species of tropical Lepidoptera. Proceedings of the National Academy of Sciences of the United States of America 103: 968–971. doi: 10.1073/pnas.0510466103

Hajibabaei M, Singer GAC Hickey DA (2006b) Benchmarking DNA barcodes: an assessment using available primate sequences. Genome 49: 851–854. doi: 10.1139/G06-025

Hall TA (1999) BioEdit: a user-friendly biological sequence alignment editor and analysis program for Windows 95/98/NT. Nucleic Acids Symposium Series 41: 95–98. http://brownlab.mbio.ncsu.edu/JWB/papers/1999Hall1.pdf

Harris DJ, Batista V, Lymberakis P, Carretero MA (2004) Complex estimates of evolutionary relationships in *Tarentola mauritanica* (Reptilia: Gekkonidae) derived from mitochondrial DNA sequences. Molecular Phylogenetics and Evolution 30: 855–859. doi: 10.1016/S1055-7903(03)00260-4

Hasan M, Islam MM, Kuramoto M, Kurabayashi A, Sumida M (2014) Description of two new species of Microhyla (Anura: Microhylidae) from Bangladesh. Zootaxa 3755: 401–418. doi: 10.11646/zootaxa.3755.5.1

Hawkins MA, Sites JW, Noonan BP (2007) *Dendropsophus minutus* (Anura: Hylidae) of the Guiana Shield: using DNA barcodes to assess identity and diversity. Zootaxa 1540: 61–67. http://bnoonan.org/Papers/Hawkinsetal_07.pdf

Hebert PDN, Ratnasingham S, de Waard JR (2003) Barcoding animal life: Cytochrome c oxidase subunit 1 divergences among closely related species. Proceedings of the Royal Society B: Biological Sciences 270: S596–S599. doi: 10.1098/rsbl.2003.0025

Hebert PDN, Stoeckle MY, Zemlak TS, Francis CM (2004a) Identification of birds through DNA barcodes. PLoS Biology 2: e312. doi: 10.1371/journal.pbio.0020312

Hebert PDN, Penton EH, Burns JM, Janzen DH, Hallwachs W (2004b) Ten species in one: DNA barcoding reveals cryptic species in the Neotropical skipper butterfly *Astraptes fulgerator*. Proceedings of the National Academy of Sciences of the United States of America 101: 14812–14817. doi: 10.1073/pnas.0406166101

Heinicke M, Diaz LM, Hedges SB (2011) Origin of invasive Florida frogs traced to Cuba. Biology Letters 7: 407-410. doi: 10.1098/rsbl.2010.1131

Hoffmann M, Hilton-Taylor C, Angulo A et al (2010) The impact of conservation on the status of the World's vertebrates. Science 330: 1503–1509. doi: 10.1126/science.1194442

James CH, Moritz C (2000) Intraspecific phylogeography in the sedge frog *Litoria fallax* (Hylidae) indicates pre-Pleistocence vicariance of an open forest species from eastern Australia. Moleular Ecology 9: 349–358. doi: 10.1046/j.1365-294x.2000.00885.x

Kimura M (1980) A simple method for estimating evolutionary rates of base substitutions through comparative studies of nucleotide sequences. Journal of Molecular Evolution 16: 111–120. http://eclass.uoa.gr/modules/document/file.php/D473/%CE%92%CE%B9%CE%B2%CE%BB%CE%B9%CE%BF%CE%B3%CF%81%CE%B1%CF%86%CE%AF%CE%B1/Phylogeny/Kimura_1980.pdf

Kok PJR, Kalamandeen M (2008) Introduction to the taxonomy of the amphibians of Kaieteur National Park Guyana. Abc Taxa. 5: 1–288. http://www.abctaxa.be/downloads/volume-5-introduction-taxonomy-amphibians

Larson A, Chippindale P (1993) Molecular approaches to the evolutionary biology of plethodontid salamanders. Herpetologica. 49: 204–215. http://www.jstor.org/stable/3892797

Lötters S, van der Meijden A, Coloma LA, Boistel R, Cloetens P, Ernst R, Lehr E, Veith M (2011) Assessing the molecular phylogeny of a near extinct. Systematics and Biodiversity 9: 45–57. doi: 10.1080/14772000.2011.557403

Luquet E, Léna JP,Miaud C, Plénet S (2015) Phenotypic divergence of the common toad (*Bufo bufo*) along an altitudinal gradient: evidence for local adaptation Heredity 114: 69–79 doi:10.1038/hdy.2014.71

McCallum ML (2007) Amphibian decline or extinction? Current declines dwarf background extinction rate. Journal of Herpetology 41: 483–491. doi: 10.1670/0022-1511(2007)41[483:ADOECD]2.0.CO;2

Mindell DP, Sorenson MD, Huddleston CJ, Miranda HC Jr, Knight A, et al (1997) Phylogenetic relationships among and within select avian orders based on mitochondrial DNA. In: Mindell DP (Ed.) Avian molecular evolution and systematics. Academic Press, New York, 214–247. doi: 10.1016/b978-012498315-1/50014-5

Moore WS (1995) Inferring phylogenies from mtDNA variation: Mitochondrial-gene trees versus nuclear-gene trees. Evolution 49: 718–726. doi: 10.2307/2410325

Narins PM, Meenderink SWF (2014) Climate change and frog calls: long-term correlations along a tropical altitudinal gradient Proceedings of the Royal Society B: Biological Sciences 281: 1471–2954. doi: 10.1098/rspb.2014.0401

Nascimento FP, Avila-Pires TCS, Cunha OR (1988) Répteis Squamata de Rondônia e Mato Grosso coletados através do Programa Polonoroeste. Boletim Museu Paraense Emílio Goeldi série Zoologia 4: 21–66.

Newman CE, Feinberg JA, Rissler LJ, Burger J, Shaffer HB (2012) A new species of leopard frog (Anura: Ranidae) from the urban northeastern US. Molecular Phylogenetics and Evolution 63: 445–455. doi: 10.1016/j.ympev.2012.01.021

Nunes I, Kwet A, Pombal Jr JP (2012) Taxonomic revision of the Scinax alter species complex (Anura: Hylidae). Copeia 2012: 554–569. doi: 10.1643/CH-11-088

Pereira JL, Lisboa LS, Thales MC, Lima AS, Ferrari SF (2004) Mapa da cobertura da terra na região do alto rio dos Marmelos. In: Anais do I Simpósio de Ciências Geodésicas e Tecnologias da Geoinformação. I Simpósio de Ciências Geodésicas e Tecnologias da Geoinformação. Recife (Brazil). CD-Rom http://docplayer.com.br/5332509-Mapa-da-cobertura-da-terra-na-regiao-do-alto-rio-dos-marmelos.html

Pereyra MO, Baldo D, Blotto BL, Iglesias PP, Thomé MTC, Haddad CFB, Barrio-Amorós C, Ibañez R, Faivovich J (2016) Phylogenetic relationships of toads of the Rhinella granulosa group (Anura: Bufonidae): A molecular perspective with comments on hybridization and introgression. Cladistics 32: 36–53. doi: 10.1111/cla.12110

Palumbi SR (1996) Nucleic acids II: the polymerase chain reaction. In: Hillis DM, Moritz C, Mable BK (Eds) Molecular Systematics. Sinauer Associates, Sunderland, MA, 205–247.

Pronabio (2002) Programa Nacional da Diversidade Biológica. Ministério do Meio Ambiente Avaliação e identificação de ações prioritárias para a conservação utilização sustentável e repartição dos benefícios da biodiversidade na Amazônia brasileira. MMA/SBF Brasília.

Real R, Barbosa AM, Solano IM, García-París M (2005) Distinguishing the distributions of two cryptic frogs (Anura: Discoglossidae) using molecular data and environmental modeling. Canadian Journal of Zoology 83: 536–545. doi: 10.1139/z05-040

Richardson JL (2012) Divergent landscape effects on population connectivity in two co-occurring amphibian species Molecular Ecology 21: 4437–4451 doi: 10.1111/j.1365-294X.2012.05708.x

Roelants K, Gower DJ, Wilkinson M, Loader SP, Biju SD, Guillaume K, Moriau L, Bossuyt F (2007) Global patterns of diversification in the history of modern amphibians. Proceedings of the National Academy of Sciences of the United States of America 104: 887–892. doi: 10.1073/pnas.0608378104

Rowley J, Brown R, Bain R, Kusrini M, Inger R, Stuart B, Wogan G, Thy N, Chan-ard T, Trung CT, Diesmos A, Iskandar DT, Lau M, Ming LT, Makchai S, Truong NQ, Phimmachak S (2010) Impending conservation crisis for Southeast Asian amphibians. Biology Letters 6: 336–338. doi: 10.1098/rsbl.2009.0793

Sambroo KJ, Rusell DW (2001) Molecular cloning-laboratory manuals. Cold Spring Harbor, New York, 999 pp.

Smith MA, Poyarkov Jr NA, Hebert PDN (2008) COI DNA barcoding amphibians: take the chance. meet the challenge. Molecular Ecology Resources 8: 235–246. doi: 10.1111/j.1471-8286.2007.01964.x

Stotz DF, Lanyon SM, Schulenberg TS, Willard DE, Peterson T, Fitzpatrick J (1997) Avifauna Survey of two tropical forest localities on the middle Rio Jiparaná Rondônia Brazil. Ornithological Monographs 48: 763–781. doi: 10.2307/40157566

Streicher JW, Crawford AJ, Edwards CW (2009) Multilocus molecular phylogenetic analysis of the montane *Craugastor podiciferus* species complex (Anura: Craugastoridae) in Isthmian Central America. Molecular Phylogenetic and Evolution 53: 620–630. doi: 10.1016/j.ympev.2009.07.011

Stuart SN, Chanson JS, Cox NA, Young BE, Rodrigues ASL, Fischman DL, Waller RW (2004) Status and trends of amphibian declines and Extinctions worldwide. Science 306: 1783–1786. doi: 10.1126/science.1103538

Stuart B, Inger R, Voris H (2006) High level of cryptic species diversity revealed by sympatric lineages of Southeast Asian forest frogs. Biological Letters 2: 470–474. doi: 10.1098/rsbl.2006.0505

Symula R, Schulte R, Summers K (2003) Molecular systematics and phylogeography of Amazonian poison frogs of the genus *Dendrobates.* Molecular Phylogenetics and Evolution 26: 452–475. doi: 10.1016/S1055-7903(02)00367-6

Tamura K, Peterson D, Peterson N Stecher G, Nei M, Kumar S (2011) MEGA5: Molecular evolutionary genetics analysis using maximum likelihood evolutionary distance and maximum parsimony methods. Molecular Biological Evolution 28: 2731–2739. doi: 10.1093/molbev/msr121

Thomaz D, Guiller A, Clarke B (1996) Extreme divergence of mitochondrial DNA within species of pulmonate land snails. Proceedings of the Royal Society B: Biological Sciences. 263: 363–368. doi: 10.1098/rpb.1996.0056

Vences M, Kosuch J, Boistel R, Haddad CFB, La Marca E, Lötters S, Veith M (2003) Convergent evolution of aposematic coloration in Neotropical poison frogs: a molecular phylogenetic perspective. Organisms Diversity and Evolution 3: 215–226. doi: 10.1078/1439-6092-00076

Vences M, Thomas M, Bonett RM, Vieites DR (2005a) Deciphering amphibian diversity through DNA barcoding: chances and challenges. Philosophical transactions of the Royal Society of London, Series B Biological Sciences 360: 1859–1868. doi: 10.1098/rstb.2005.1717

Vences M, Thomas M, Van Der Meijden A, Chiari Y, Vieites D (2005b) Comparative performance of the 16S rRNA gene in DNA barcoding of amphibians. Frontiers in Zoology 2: 1–12. doi: 10.1186/1742-9994-2-5

Vences M, Nagy Z T, Sonet G, Verheyen E (2012) DNA barcoding amphibians and reptiles In DNA Barcodes: Methods and Protocols. In: Kress WJ, Erickson DL (Eds) Springer Protocols Methods in Molecular Biology 858: 79–107. doi: 10.1007/978-1-61779-591-6_5

Vieites DR, Wollenberg KC, Andreone F, Kohler J, Glaw F, Vences M (2009) Vast underestimation of Madagascar's biodiversity evidenced by an integrative amphibian inventory. Proceedings of the National Academy of Sciences of the United States of America 106: 8267–8272. doi: 10.1073/pnas.0810821106

Ward RD, Zemlak TS, Innes BH, Last PR, Hebert PDN (2005) DNA barcoding Australia's fish species. Philosophical transactions of the Royal Society of London, Series B Biological Sciences 360: 1847–1857. doi: 10.1098/rstb.2005.1716

Weigt LA, Crawford AJ, Rand AS, Ryan M (2005) Biogeography of the túngara frog. *Physalaemus pustulosus*: molecular perspective. Molecular Ecology 14: 3857–3876. doi: 10.1111/j.1365-294X.2005.02707.x

Xia Y, Gu HF, Peng R, Chen Q, Zheng YC, Murphy RW, Zeng XM (2012) COI is better than 16s rRNA for DNA barcoding Asiatic Salamanders (Amphibia: Caudata: Hynobiidae). Molecular Ecology Resources 12: 48–56. doi: 10.1111/j.1755-0998.2011.03055.x

Xia X (2013) Dambe5: A comprehensive software package for data analysis in molecular biology and evolution. Molecular Biology and Evolution 30: 1720–1728. doi: 10.1111/j.1755-0998.2011.03055.x

Supplementary material 1

Data on the specimens examined in the present study

Authors: Ruth A. Estupiñán, Stephen F. Ferrari, Evonnildo C. Gonçalves, Maria Silvanira R. Barbosa, Marcelo Vallinoto, Maria Paula C. Schneider

Data type: The specimens used in this study, intraspecific distances, locality data and the GenBank association number of the submitted COI sequences. The museum number and reference of each specimen.

Explanation note: Please note that some of the sequences used in the study are incompletely referenced in the GenBank barcode database because they lack some data and we are unable to rectify this because the samples were collected too long ago (1980s or before) for the missing data to be found.

ZooKeys 637: 107–128 (2016)
doi: 10.3897/zookeys.637.10310
http://zookeys.pensoft.net

RESEARCH ARTICLE

A peer-reviewed open-access journal
ZooKeys
Launched to accelerate biodiversity research

Revision of the genus *Heterosmylus* Krüger, 1913 from China (Neuroptera, Osmylidae)

Min Dong[1], Han Xu[1], Yongjie Wang[2], Chunfeng Jia[1], Zhiqi Liu[1]

1 *Department of Entomology, China Agricultural University, Beijing 100094, China* **2** *College of Life Sciences, Capital Normal University, Beijing 100048, China*

Corresponding authors: *Yongjie Wang* (wangyjosmy@foxmail.com); *Zhiqi Liu* (liuzhiqi@cau.edu.cn)

Academic editor: *S. Winterton* | Received 27 August 2016 | Accepted 17 November 2016 | Published 2 December 2016

http://zoobank.org/CB5E8347-7767-49FB-96F4-98E014846775

Citation: Dong M, Xu H, Wang Y, Jia C, Liu Z (2016) Revision of the genus *Heterosmylus* Krüger, 1913 from China (Neuroptera, Osmylidae). ZooKeys 637: 107–128. https://doi.org/10.3897/zookeys.637.10310

Abstract

A new species of osmylid (*Heterosmylus processus* **sp. n.**) is described and the other species in the genus from mainland China are redescribed. *Heterosmylus zhamanus* Yang, 1987, **syn. n.** is identified as a junior synonym of *Heterosmylus yunnanus* Yang, 1986. A key is provided to differentiate Palaearctic and Oriental species of *Heterosmylus*.

Keywords

Heterosmylus, Oriental region, Osmylidae, Palaearctic

Introduction

Heterosmylus Krüger is a relatively small genus of lance lacewing (Osmylidae: Protosmylinae) described by Krüger (1913a) from the Oriental Region. There are presently nine species in the genus, including seven species in mainland China, one species in Taiwan (*Heterosmylus primus* Nakahara) and another species (*Heterosmylus aspersus* Krüger) in northern India. Krüger (1913a) established the genus just based on the comparison with other genera, but the detailed description of the type species *H. aspersus* was given in a subsequent publication (Krüger 1913b). As for the Chinese species, Nakahara (1955) described *Heterosmylus primus* from Taiwan. Subsequently, in a series of

publications, Yang (1986, 1987, 1992, 1997, 1999) described an additional six species from mainland China. However, all the early taxonomists ignored or poorly described the characters of genitalia in osmylids, which result in a vague definition of the genus.

Herein the genus *Heterosmylus* is revised with a focus on the species from mainland China, and detailed descriptions of genitalic structures are provided for the first time. A revised diagnosis of the genus is proposed based on both external morphology and genitalic characters. The new species, *Heterosmylus processus* sp. n., is described and *Heterosmylus zhamanus* Yang, 1987, syn. n. is identified as a junior synonym of *Heterosmylus yunnanus* Yang, 1986. The distribution of the genus in China is also discussed.

Material and methods

All the described specimens are deposited in the Entomological Museum of China Agricultural University (CAU), Beijing. Terminalia preparations were made by macerating the apex of the abdomen in hot 10% KOH for 3–5 min, neutralized with 10% acetic acid. The apex of the abdomen was then transferred to glycerol for further dissection and examination. After examination it was moved to fresh glycerol and stored in a microvial pinned below the specimen. Images of wings were taken with a Nikon D7000 digital camera. Drawings were made under a light microscope. The terminology for wing venation and genitalia follows Winterton and Wang (2016).

Taxonomy

Heterosmylus Krüger, 1913a

Type species. *Heterosmylus aspersus* Krüger 1913a: 37, original designation. Deposited in Stettiner Museum (National Museum Szczecin, Poland).

Type locality. India: Sikkim.

Diagnosis. Head brown or dark brown; compound eyes black; antennae shorter than half length of forewing; prothorax black and length longer than width, with yellow setae; meso- and metathorax dark brown with long setae; legs yellow with short brown setae; forewings oblong and subacute at apex, with few brown spots; nygmata clear surrounded by light brown spot; veins thickened; costal cross-veins simple and occasionally bifurcate; forewing Rs with 8–15 branches, distal to the base of wing; cross-veins among Rs branches forming two or three series of gradates; forewing M branching more basally than the divergence of basal branch of Rs; no more than four cross-veins present between the two branches of M; forewing Cu bifurcating near the base of wing; CuA and CuP with numerous pectinate branches; CuP longer than half length of CuA; hind wings similar to forewings in size and shape without any spot apart from pterostigma; hindwing M branching near the base of wing; hindwing CuA with numerous pectinate branches; CuP simple and shorter than half length of CuA; male

genitalia with 9th tergite narrow, and sternite approximately quadrate; ectoproct relatively large, callus cerci rounded and located at the middle or underside of ectoproct; male genitalia composed of gonarcus, entoprocesses and mediuncus, arched gonarcus similar to other genera of Protosmylinae; mediuncus attached with a membrane below gonarcus, mediuncus bent into C-shape laterally; female genitalia with 9th tergite narrow; spermathecae bent into n-shape with base expanded and apex columniform.

Included species. *Heterosmylus aspersus* Krüger, *H. curvagradatus* Yang, *H. flavidus* Yang, *H. limulus* Yang, *H. primus* Nakahara, *H. processus* sp. n., *H. shennonganus* Yang, *H. wolonganus* Yang, *H. yunnanus* Yang.

Comments. Although the type species of *Heterosmylus* was not described in detail when the genus was established, Krüger provided a detailed description of the type species in a following paper later that year (Krüger 1913a, b). This subsequent work was overlooked by Nakahara (1955), and later Ghosh (2000) presented a brief description for the species without the genitalic characters. Consequently, the systematic status of *Heterosmylus* was not well defined, although it is clear that the monophyly of *Heterosmylus* is well supported in the recent phylogenetic work on Osmylidae by Winterton et al. (in press). *Heterosmylus* also can be distinguished from other genera (*Gryposmylus* Krüger, *Lysmus* Navás, *Paryphosmylus* Krüger) in Protosmylinae based mainly on wing venation. In *Heterosmylus*, the veins are thickened and branches of forewing M have no more than four *ma-mp* cross-veins. In both *Gryposmylus* and *Lysmus* these are slender and the M vein generally five *ma-mp* cross-veins. Moreover, the base of costal-field of forewing of *Heterosmylus* species is narrower compared with that of *Gryposmylus*. *Heterosmylus* differs from *Paryphosmylus* in that the wings are mostly hyaline and single cross-vein presents before the separation of basal branch of Rs (Martins et al. 2016).

Heterosmylus is mainly recorded in the Oriental Region and especially in China (Fig. 1), typically in warmer and humid environments. According to the distribution of the individual species, we find *H. wolonganus*, *H. shennonganus* and *H. yunnanus* with relatively wide distributions. It seems that *H. wolonganus* has a broad geographical distribution from central to western China, occurring in four geographically continuous provinces, Sichuan, Gansu, Shaanxi and Henan. Interestingly, most localities of *H. wolonganus* are along the boundary of Oriental and Palaearctic regions in China. *Heterosmylus shennonganus* is principally distributed in central China, representing a typical Oriental species. *Heterosmylus yunnanus* is another widespread species, distributed in Tibet, Yunnan and Sichuan. Considering the similar environment in these localities, it is estimated that these species might be present in the whole southwest of China. The other five species, *H. curvagradatus*, *H. limulus*, *H. flavidus*, *H. primus* and *H. processus* sp. n., are only recorded in a single region. *Heterosmylus curvagradatus* is restricted to Fujian, while *H. flavidus* is a distinctive species restricted in the west of Yunnan. *Heterosmylus limulus* is limited to Yadong (Tibet) and it could be found at the same altitude as *H. yunnanus*. *Heterosmylus primus* is only recorded in Taiwan. We did not examine this species so we could not compare it with the other species, but *H. curvagradatus* shows the similar appearance with this species, suggesting their potential close relationship. The new species *H. processus* sp. n. is highly distinctive (weakly de-

Figure 1. Distribution of *Heterosmylus* in China. ☆= *H. curvagradatus* ▲= *H. flavidus* ■= *H. limulus* ★= *H. primus* ●= *H. processus* sp. n. △= *H. shennonganus* ◆= *H. wolonganus* ◇= *H. yunnanus*.

fined pterostigma and hyaline and colourless membrane) is found in Shaanxi near the Qinling Mountains.

Key to *Heterosmylus* species (males) in the Palaearctic and Oriental regions

1 Head and thorax with spots or stripes **2**

– Head and thorax without any spot and stripe; pronotum yellowish brown without any stripe, meso- and metanotum dark brown; cross-veins *rs-ma* with lance-shaped brown marks ..... ***H. aspersus***

2 Mediuncus with a process at base (Fig. 4); membrane of wings hyaline and veins not edged with spots (Fig. 2); pronotum with four brown spots along anterior margin, two round brown spots in middle; mesonotum with two brown spots in middle on both sides ..... ***H. processus* sp. n.**

– Mediuncus without any process at base, membrane of wings only with a few spots **3**

3 Forewings with many spots including along the gradate cross-veins **4**

– Forewings with few spots in the membrane (Fig. 21); pronotum with two yellow narrow stripes in middle; metanotum with two brown spots on anterior margin ..... ***H. wolonganus***

4 More than 11 branches of Rs **5**

– 11 or fewer branches of Rs **7**
5 An oblique brown stripe present from pterostigma to the outer margin, Cu with four brown spots; pronotum with two pale yellow longitudinal stripes, mesonotum brown anteriorly ..... ***H. limulus***
– No oblique stripes present from pterostigma to the outer margin **6**
6 Pronotum black with a black longitudinal stripe medially; meso- and metanotum black; Rs with 14–17 branches; Cu edged with 3–4 yellow spots; apex of gonarcus bent upwards and relative long in lateral view ..... ***H. yunnanus***
– Pronotum brown with a yellowish longitudinal stripe medially, meso- and metanotum brown; vertex with a Y-shaped mark ..... ***H. primus***
7 Membrane of wings yellow and gradate cross-veins not edged with spots (Fig. 29); pronotum with a dark brown longitudinal stripe medially ... ***H. flavidus***
– Membrane of wings hyaline and gradate cross-veins edged with brown **8**
8 Apex of mediuncus short, broad and flat in dorsal view (Figs 46–47); ectoproct without any process in lateral view; two yellow longitudinal stripes present from pronotum to mesonotum; mesoscutellum bright yellow, metanotum with a central yellow stripe ..... ***H. curvagradatus***
– Apex of mediuncus long, acute and protuberant in dorsal view (Figs 38–39); ectoproct with a dorsal coniform process in lateral view; pronotum with two narrow longitudinal dark brown marks medially ..... ***H. shennonganus***

***Heterosmylus processus* sp. n.**
http://zoobank.org/18F14A57-CA9C-4329-BA1F-F885461CCCB6
Figs 2–6

Material examined. Holotype Male. CHINA: Shaanxi (Province): Taibai, [33°55'N, 107°43'E] 09.v.1982, leg. Guojun Qi. [Verbatim label data translated from Chinese]: CHINA: Shaanxi, Taibai/ 09.v.1982/ Guojun Qi/ CAU. Terminalia cleared in KOH, and stored in a micro-vial pinned below the specimen.

Diagnosis. Pronotum with four brown spots at anterior margin, two round brown spots in middle and two brown spots at posterior margin; membrane hyaline, pterostigma yellow, without dark spots besides the pterostigma; veins light yellow at base but brown from middle to the end; mediuncus C-shaped in lateral view with a basal process and boat-shaped in dorsal view.

Description. Body length 8.6 mm. *Head*. Vertex yellow with brown setae; ocelli distinctively brown; compound eyes black; antennae yellow with a brown stripe at base; frons with two brown stripes, genae with two round brown spots; maxillary palpi yellow and thick, labium short and brown. *Thorax*. Yellow dorsally and dark brown ventrally; pronotum with four brown spots at anterior margin, two round brown spots in middle and two brown spots at posterior margin linking to the mesonotum; mesonotum with two brown spots in middle on both sides; metanotum similar to the mesonotum, with two spots in middle. *Legs*. Yellow with brown setae; claws brown

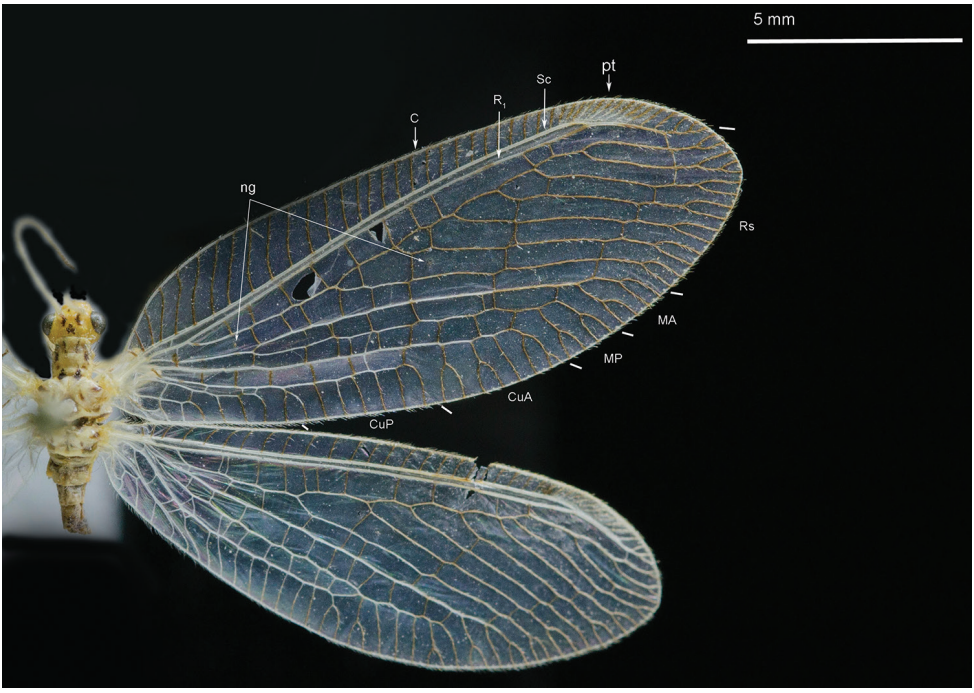

Figure 2. Wings of *Heterosmylus processus* sp. n. Abbreviations: ng, nygmata; pt, pterostigma.

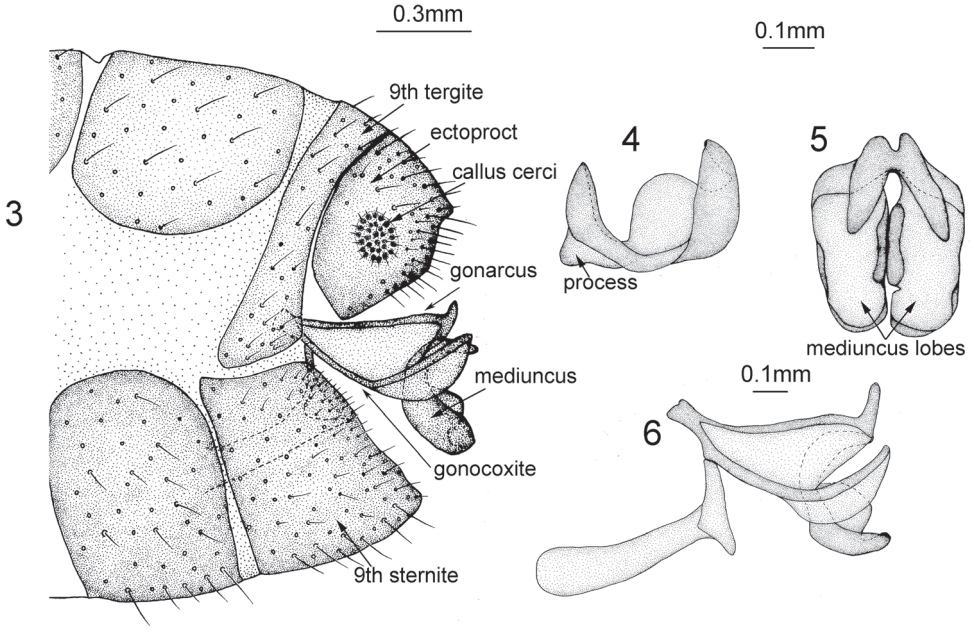

Figures 3–6. *Heterosmylus processus* sp. n. Male: **3** terminalia, lateral view **4** mediuncus, lateral view **5** mediuncus, dorsal view **6** genitalia, lateral view.

with a small tooth. *Wings* (Fig. 2): Forewing length 15.4 mm, width 6.2 mm; membrane hyaline without any spot besides the yellow pterostigma; veins yellow; costal field broad, cross-veins simple without forks. Cross-veins in radial sector few besides the gradate cross-veins. Rs with 8 branches. The basal cross-vein between R_1 and M edged with a brown mark. Hind wing length 14.4 mm, width 5.3 mm; membrane hyaline, veins light yellow at base but brown from middle to the end. Costal field narrow, pterostigma yellow, and Rs with 7 branches. *Abdomen*. Yellow dorsally, dark brown ventrally, covered with yellow setae.

Male Terminalia (Figs 3–6). Ectoproct quadrate in lateral view; callus cerci rounded and small. Distal part of gonarcus bent upwards. Entoprocesses curved in middle and dilated apically. Mediuncus (Figs 4–5) C-shaped in lateral view with a basal process and boat-shaped in dorsal view; two mediuncus lobes fused at base and each one raised on both sides, the inner side larger than the outer one.

Distribution. China (Shaanxi).

Etymology. The specific name refers to the process at the base of the mediuncus.

Remarks. This species is known from its type locality, Shaanxi province. It is easily distinguished from other species in the genus because of the body coloration, morphology and the genital characters. *Heterosmylus processus* sp. n. has a smaller body size and hyaline wings, while the others usually have a patterned membrane. Moreover, the mediuncus within the new species possesses a distinct process at the base whereas it is absent in the other species of *Heterosmylus*.

***Heterosmylus yunnanus* Yang, 1986**

Figs 7–13

Heterosmylus zhamanus Yang, 1988: 195. **syn. n.**

Material examined. Holotype male. CHINA: Yunnan (Province): Lushuixian Gangfang, [25°57'N, 98°52'E], 29.ix.1980, leg. Dejing Zou. [Verbatim label data (translated from Chinese)]: CHINA: Yunnan, Lushuixian, Gangfang, 29.ix.1980/ Dejing Zou. Terminalia cleared in KOH, and stored in a micro-vial pinned below the specimen. 3 males, 1 female (type specimens of *H. zhamanus*), Tibet: Zhangmu, 06.vi.1981, leg. Shengchang Hu; 3 males, 5 females, Tibet: Hanmi, 24.viii.2005, leg. Dakang Zhou; 2 males, Sichuan: Luding, Hailuogou, 26.vi.2006, leg. Xiaoshuan Bai.

Diagnosis. Pronotum black with two yellowish longitudinal stripes at anterior margin; mesonotum with two yellow spots in middle; apex of gonarcus bent upwards and relative long in lateral view.

Redescription. Body length 9–11 mm. *Head*. Vertex dark brown, frons bright yellow; ocelli yellow; compound eyes dark grey; antennae entirely dark; clypeus brownish, maxillary and labial palpi dark brown. *Thorax*. Pronotum black with two yellowish longitudinal stripes at anterior margin; mesonotum with two yellow spots

Figure 7. Wings of *Heterosmylus yunnanus* Yang, 1986.

in middle. *Wings* (Fig. 7). Forewings length 18–21 mm, width 6–7 mm; membrane hyaline, and veins dark brown; pterostigma dark brown with yellowish center. Rs with 15–17 branches; Cu edged with three or four yellow spots. Hind wing length 15–18 mm, width 5–6 mm; membrane hyaline, cross-veins edged with brown marks between Sc and R_1.

Male Terminalia (Figs 8–11). Ectoproct quadrate in lateral view. Gonarcus rod-like in lateral view, the apex bent upwards and relatively long; entoprocesses distally expanded, lobe-shaped; mediuncus fused at base and curved into C-shape in lateral view; each mediuncus lobe raised on both sides, boat-shaped in dorsal view.

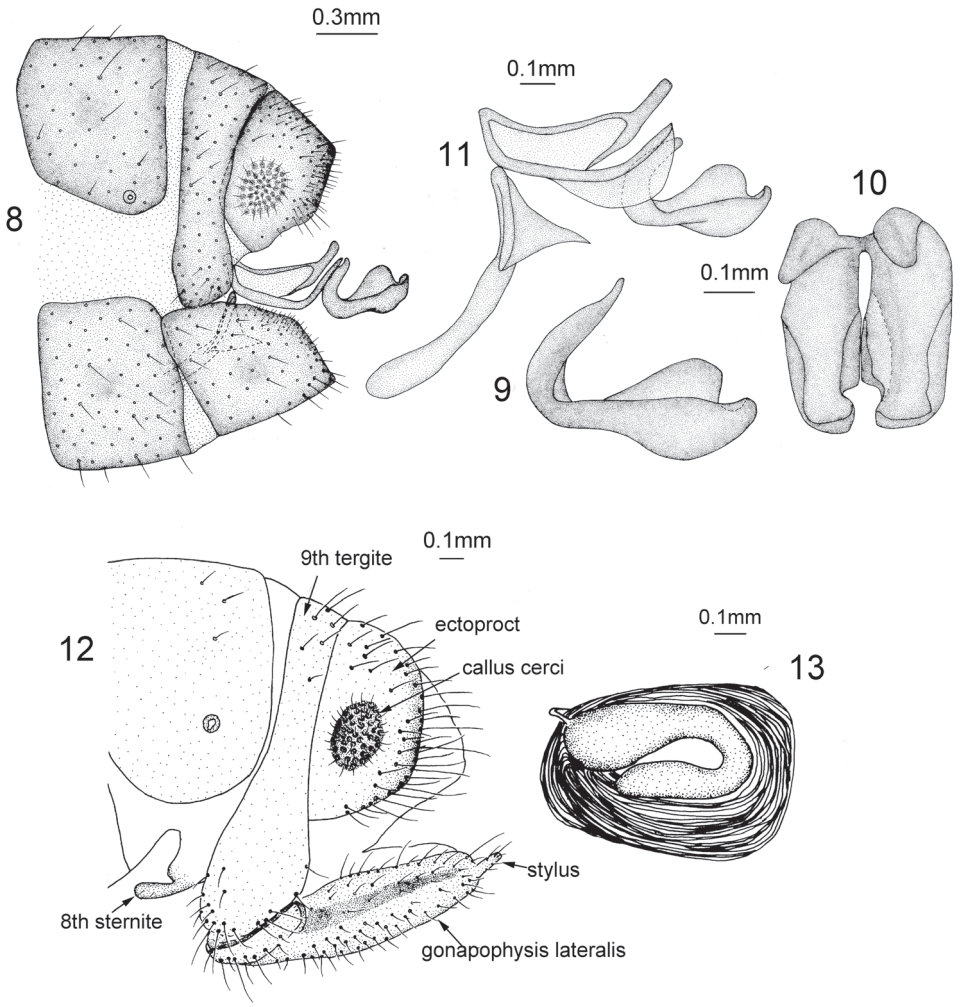

Figures 8–13. *Heterosmylus yunnanus* Yang, 1986. Male: **8** terminalia, lateral view **9** mediuncus, lateral view **10** mediuncus, dorsal view **11** genitalia, lateral view Female: **12** terminalia, lateral view **13** spermatheca, lateral view.

Female Terminalia (Figs 12–13). Ectoproct trapeziform in lateral view; 9th gonocoxite finger-shaped in lateral view, 9th gonostylus brown and long. Spermathecae bent into C-shaped and basal part longer than distal.

Distribution. China (Tibet, Yunnan, Sichuan)

Remarks. Although the original identification of both *H. yunnanus* Yang and *H. zhamanus* Yang was based on the colour pattern of the head, there are no convincing differences to distinguish them after comparison of their genitalic features. So we believe that *H. zhamanus* should be a synonym of *H. yunnanus*.

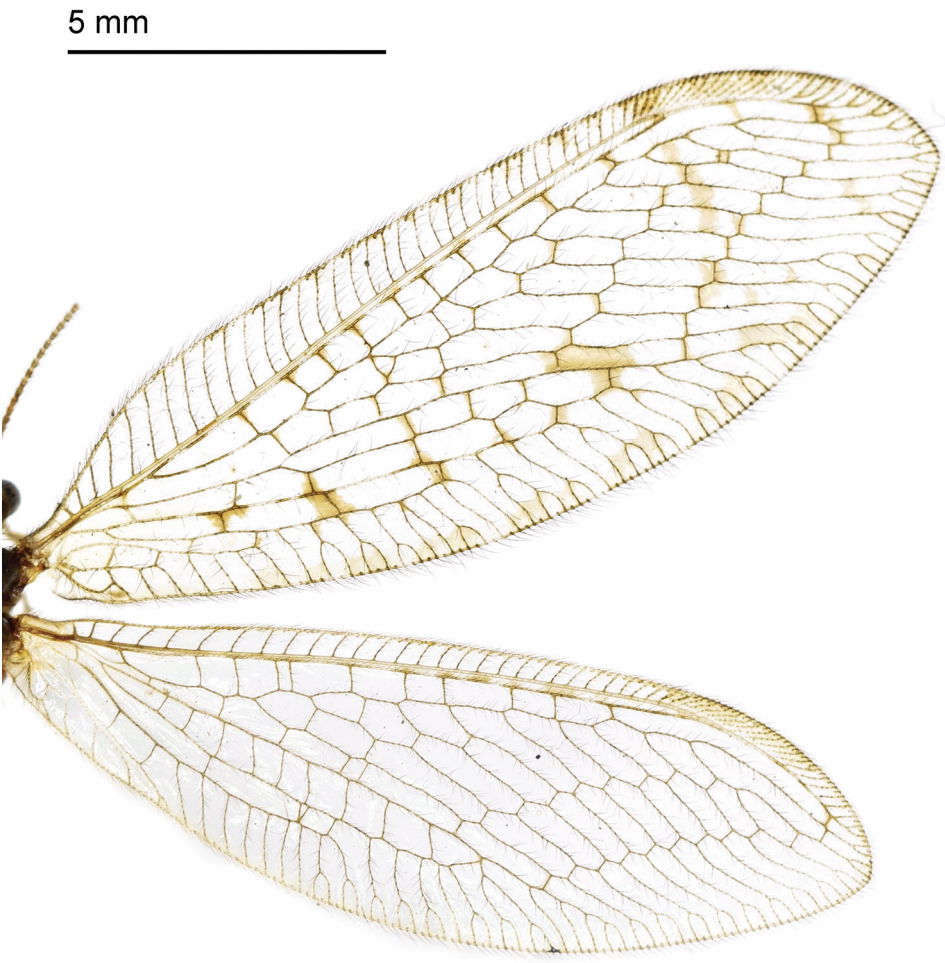

Figure 14. Wings of *Heterosmylus limulus* Yang, 1987.

Heterosmylus limulus Yang, 1987

Figs 14–20

Material examined. Holotype Male, CHINA: Tibet: Yadong, [27°31'N, 88°55'E], 24.viii.1978, leg. Fasheng Li. [Verbatim label data (translated from Chinese)]: CHINA: Tibet, Yadong/ 24.viii.1978/ Fasheng Li/ CAU. 1 male, same data as Holotype. 1 female, China: Tibet: Yadong, 30.viii.1984, leg. Yongxiang Zhao.

Diagnosis. Pronotum with two yellow stripes in middle, an oblique brown mark presenting from the pterostigma to the posterior outer margin of forewing; base of mediuncus slender and apex dilated as lobe-shape in lateral view.

Redescription. Body length 8.0 mm. *Head*. Vertex dark brown, frons brown. Ocelli yellowish, eyes dark grey. Antennae brown, encircled by a yellowish stripe at

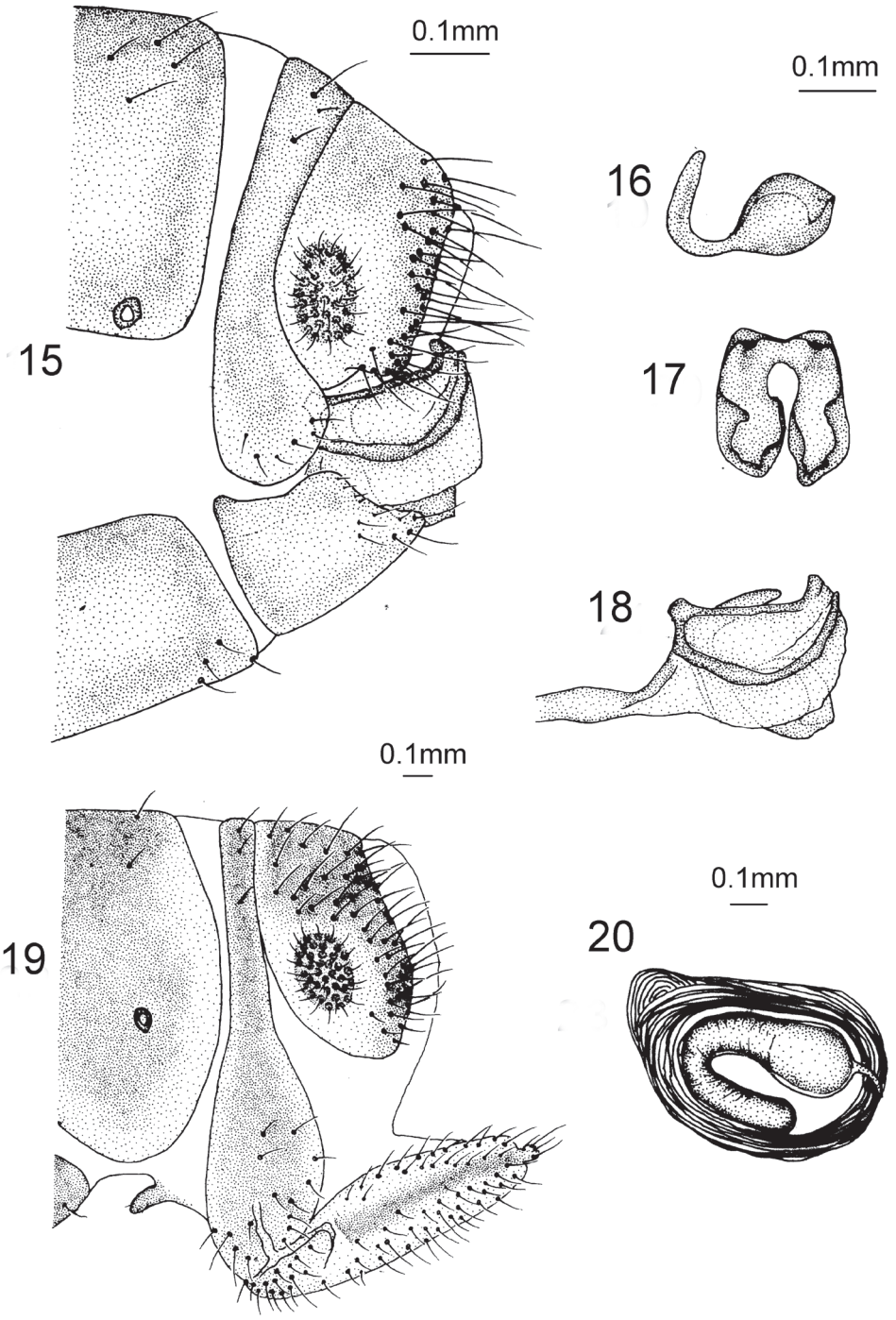

Figures 15–20. *Heterosmylus limulus* Yang, 1987. Male: **15** terminalia, lateral view **16** mediuncus, lateral view **17** mediuncus, dorsal view **18** genitalia, lateral view. Female: **19** terminalia, lateral view **20** spermatheca, lateral view.

base. Clypeus yellow, maxillary palpi and labial palpi dark brown. *Thorax*. Dark brown. Pronotum with two light yellow stripes medially; mesonotum brown at anterior part with black setae. *Wings* (Fig. 14). Forewing length 16–17 mm, width 5–6 mm; membrane hyaline, veins brown; pterostigma yellow, but brown on both sides; an oblique brown stripe presenting from the pterostigma to the posterior outer margin; Cu with four brown spots. Outer gradate series of cross-veins and wing margin bordered with fuscous spots. Rs with 13–15 branches. Hind wing length 13–14 mm, width 4–5 mm; membrane hyaline with some light brown spots between Sc and R_1.

Male Terminalia (Figs 15–18). Ectoproct quadrate in lateral view; gonarcus rod-like in lateral view, distal part upswept and relatively small; mediuncus fused at base and curved into C-shape in lateral view; the base slender and apex dilated as lobe-shape in lateral view.

Female Terminalia (Figs 19–20). Ectoproct approximately oblong in lateral view; 9th gonocoxite fusiform in lateral view; 9th gonostylus brown and small; spermathecae bent into C-shape.

Distribution. China (Tibet).

Heterosmylus wolonganus Yang, 1992

Figs 21–28

Material examined. Holotype Male. CHINA: Sichuan (Province): Wolong, [31°01'N, 103°10'E], 25.vii.1993, leg. Shuyong Wang. [Verbatim label data (translated from Chinese)]: CHINA: Sichuan Prov., Wonglong/ 25.vii.1993/ Shuyong Wang/ CAU. 1 male, CHINA: Shaanxi (Province): Ningshan, 18.vi.1981, leg. Chikun Yang. 1 female, CHINA: Shaanxi (Province): Huangniupu, 15.viii.1981, leg. Weidong Wang. 1 male, CHINA: Shaanxi (Province): Taibaishan, 09.iii.1982, leg. Chikun Yang. 1 male, CHINA: Shaanxi (Province): Taibaishan, 09.v.1982, leg. Guojun Qi. 1 female, CHINA: Shaanxi (Province): Taibaishan, 15.vii.1982, leg. Jingruo Zhou, Lan Liu. 1 male, 1 female, CHINA: Shaanxi (Province): Ningshan, 18.vii.1982, leg. Shenghui Lei. 1 female, CHINA: Shaanxi (Province): Ningshan, Xiangyang, Fengqi, 18.vii.1982, leg. Deqing Wang. 2 males, CHINA: Shaanxi (Province): Nanzheng, Yuanba, 27.v.1983, leg. Dahan He. 1 male, CHINA: Gansu (Province): Wenxian, Bikou, 25.vii.1998, leg. Jun Chen. 2 males, CHINA: Henan (Province): Songxian, Baiyunshan, 19.vii.1996, leg. Xiaocheng Shen. 10 males, 12 females, CHINA: Henan (Province): Songxian, Baiyunshan, 14-18.vii.2004, leg. Bingzhen Yan.

Diagnosis. Pronotum with two yellow narrow stripes in middle; metanotum with two brown spots on anterior margin; gonarcus sclerotized distally and bent upward and hook-shaped in lateral view; base of mediuncus approximately finger-shaped in lateral view.

Redescription. Body length 9–11 mm. *Head*. Vertex yellowish brown; frons yellow with one dark brown spot near antennae; ocelli brown, eyes blackish brown; antennae blackish brown; clypeus yellow, maxillary and labial palpi dark brown

Figure 21. Wings of *Heterosmylus wolonganus* Yang, 1992.

Thorax. Pronotum with two yellow narrow stripes in middle with some dark setae on both sides; mesonotum with two yellow longitudinal spots; metanotum with two brown spots on anterior margin. *Wings* (Fig. 21). Forewing length 18–20 mm, width 6–7 mm; membrane hyaline, veins mostly brown; pterostigma light yellow but brown on both sides; Rs with 10 branches. Four cross-veins present between MA and MP. Hind wing length 16–17 mm, width 5–6 mm; Rs with 11–12 branches, without any distinct spot besides the pterostigma.

Male Terminalia (Figs 22–25). Ectoproct quadrate in lateral view; gonarcus sclerotized distally and bent upwards as hook in lateral view; gonocoxite bent and distally dilated as lobe-shaped in lateral view mediuncus curved into C-shape in lateral view and spoon-shaped in dorsal view; base approximately finger-shaped in lateral view.

Female Terminalia (Figs 26–28). Anterior part of 8th sternite reduced and short finger-shaped, posterior part broad; ectoproct broad and trapezoid in lateral view; 9th

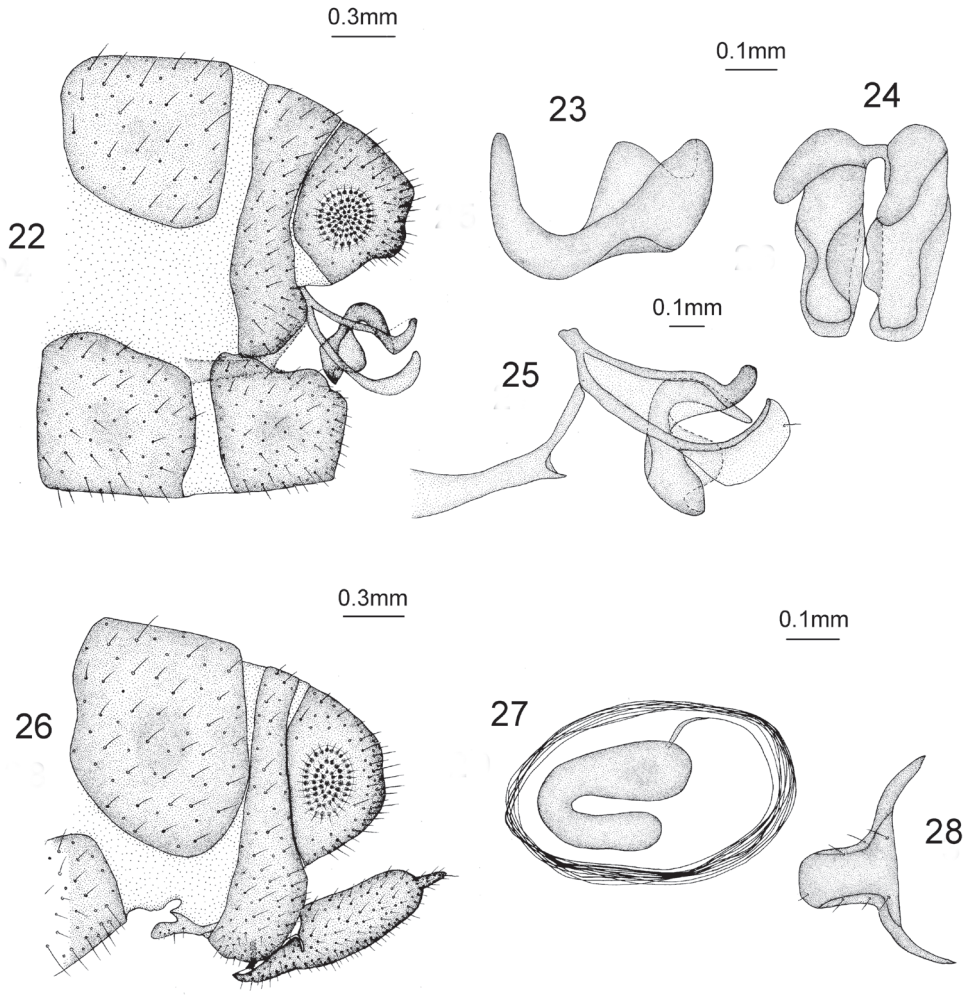

Figures 22–28. *Heterosmylus wolonganus* Yang, 1992. Male: **22** terminalia, lateral view **23** mediuncus, lateral view **24** mediuncus, dorsal view **25** genitalia, lateral view. Female: **26** terminalia, lateral view **27** spermatheca, lateral view **28** 8th sternite, ventral view.

gonocoxite fusiform in lateral view; 9th gonostylus long in lateral view; spermatheca bent into C-shape.

Distribution. China (Sichuan, Shaanxi, Gansu, Henan).

Heterosmylus flavidus Yang, 1992

Figs 29–35

Material examined. Holotype Female. CHINA: Yunnan (Province): Lushui, Yaojiapin, [25°58'N, 98°42'E], 04.vi.1981, leg. Shuyong Wang. [Verbatim label data (translated

Figure 29. Wings of *Heterosmylus flavidus* Yang, 1992.

from Chinese)]: CHINA: Yunnan Prov., Lushui, Yaojiaping/ 04.vi.1981/ Shuyong Wang/ CAU. Paratype Male, CHINA: Yunnan (Province): Lushui, Pianma, 29.v.1981. leg. Xuezhong Zhang. [Verbatim label data (translated from Chinese)]: CHINA: Yunnan Prov., Lushui, Pianma/ 29.v.1981/ Xuezhong Zhang/ CAU.

Diagnosis. Pronotum with a dark brown longitudinal stripe medially; metanotum with a brown spot in middle; forewing light yellow; mediuncus C-shaped in lateral view and scoop-shaped in dorsal view.

Redescription. Body length 7–9 mm. *Head*. Vertex dark brown, frons yellow; ocelli yellowish; Compound eyes brown with some small spots; antennae fuscous except for the yellow scape; clypeus yellow, maxillary and labial palpi black. *Thorax*. Mostly yellow. Pronotum with a brown longitudinal stripe, and with some long setae

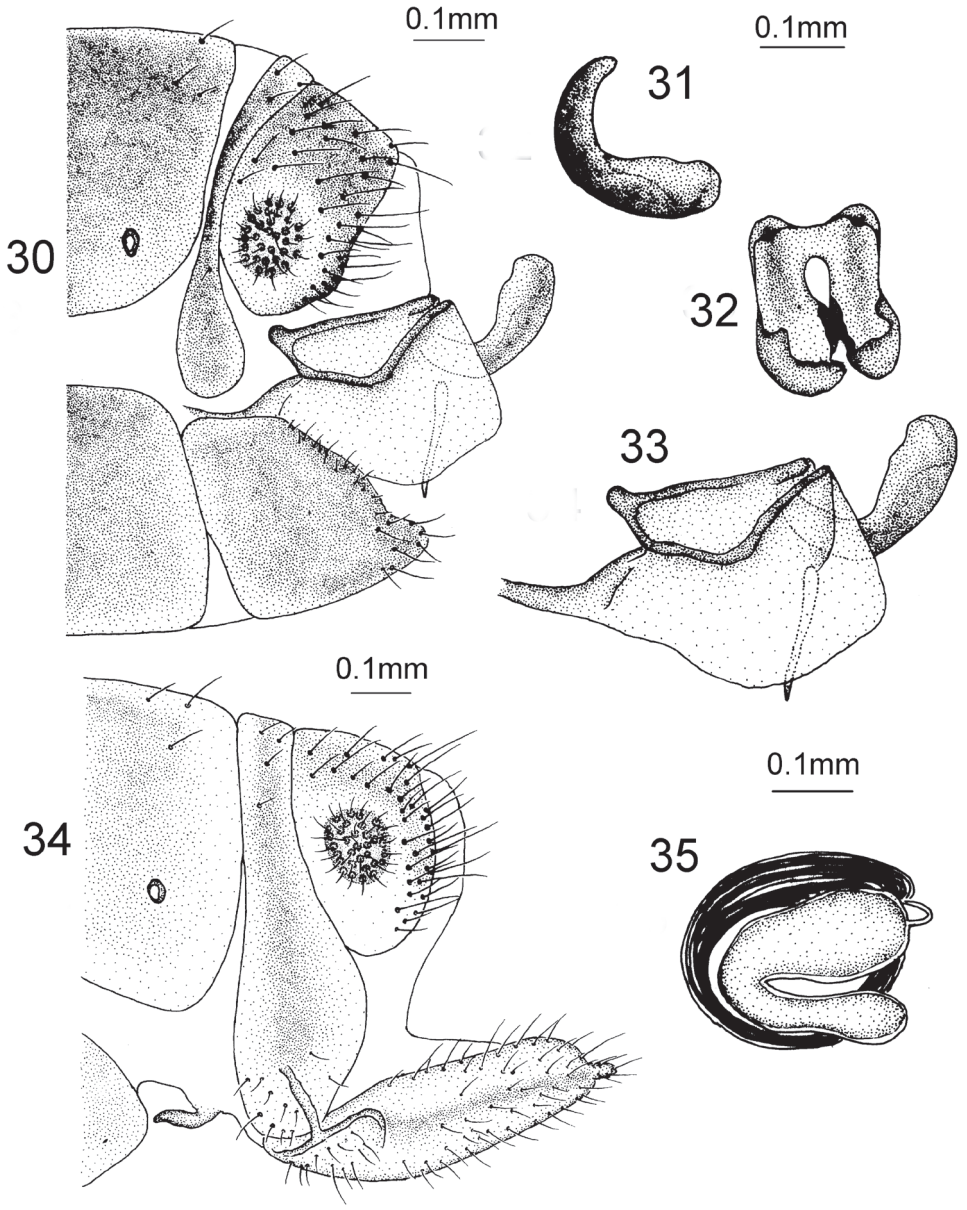

Figures 30–35. *Heterosmylus flavidus* Yang, 1992. Male. **30** terminalia, lateral view **31** mediuncus, lateral view **32** mediuncus, dorsal view **33** genitalia, lateral view. Female: **34** terminalia, lateral view **35** spermatheca, lateral view.

on both sides; mesonotum brown on margin; metanotum dark brown with a brown spot medially. *Wings* (Fig. 29). Forewing length 16–17 mm, width 5–6 mm; membrane light yellow, veins brown and thickened; pterostigma light yellow but brown on

both sides; R_1 edged with some brown spots, Rs with 11 branches, cross-veins among branches of Rs forming three series of gradates. Hind wing length 12–14 mm, width 4–6 mm; membrane hyaline with small spots between Sc and R_1.

Male Terminalia (Figs 30–33). Ectoproct quadrate in lateral view; gonarcus rod-like, but apex not bent upwards in lateral view; gonocoxite bent in the middle; mediuncus C-shaped in lateral view and scoop-shaped in dorsal view.

Female Terminalia (Figs 34–35). 8th sternite finger-shaped in lateral view; ectoproct broad and approximately elliptical in lateral view; 9th gonocoxite finger-shaped in lateral view; 9th gonostylus relatively long and finger-shaped in lateral view; spermathecae bent into C-shape, base thicker than apex.

Distribution. China (Yunnan).

Heterosmyls shennonganus Yang, 1997

Figs 36–43

Material examined. Holotype Male. CHINA: Hubei (Province): Shennongjia, [31°42'N, 110°38'E], 21.viii.1985, leg. Xiaoyuan Mao. [Verbatim label data (translated from Chinese)]: CHINA: Hubei Prov., Shennongjia, 21.viii.1985/ Xiaoyuan Mao/ CAU. Paratype 4 males, 3 females, same data as the holotype. 1 female, Henan: Luanchuan, Longyuwan, 1997.08.14, leg. RLS. 1 male, CHINA: Henan (Province): Luanchuan, Longyuwan, 18.viii.1997, leg. RLS. 1 male, CHINA: Henan (Province): Luanchuan, Longyuwan, 19.vii.2004, leg. Bingzhen Yan. 1 female, CHINA: Henan (Province): Neixiang, Baotianman, 23.vii.2004, leg. Bingzhen Yan. 1 male, CHINA: Henan (Province): Neixiang, Baotianman, 24.vii.2004, leg. Bingzhen Yan. 1 male, CHINA: Chongqing: Jiangjin, Simianshan, 21.ix.2007, leg. Weiwei Zhang. 1 female, CHINA: Shaanxi (Province): Xiangyangba, 24.viii.1982, leg. Shenghui Lei.

Diagnosis. Pronotum with two narrow longitudinal dark brown marks in middle; ectoproct with a dorsal coniform process in lateral view; gonarcus with a short finger-like process distally in lateral view.

Redescription. Body length 8–10 mm. *Head*. Vertex with a brown cross-stripe; frons yellow but brown on both sides; ocelli large and prominent, compound eyes shiny black; antennae dark brown; clypeus fulvous, maxillary and labial palpi brown.

Thorax. Pronotum with two narrow longitudinal dark brown marks in the middle; mesonotum with dark setae; metanotum without spots. *Wings* (Fig. 36). Forewing length 16–17 mm, width 6.4 mm; membrane hyaline, veins mainly brown; pterostigma yellowish but brown on both sides; costal field with three or four brown spots; *r1-rs* edged with brown marks; Rs with 8–9 branches, cross-veins among branches of Rs forming two series of gradates; the outer gradate cross-veins edged with brown spots. Hind wing length 15.5 mm, width 5.4 mm. Membrane hyaline with few spots.

Male Terminalia (Figs 37–40). Ectoproct approximately quadrate with a dorsal coniform process in lateral view; gonarcus approximately rod-like and distally sclerotized with a short finger-like process in lateral view; gonocoxite curved as ancon and distally

Figure 36. Wings of *Heterosmylus shennonganus* Yang, 1997.

dilated as lobe; mediuncus curved and thickened in lateral view and boat-shaped with a cone-shaped apex in dorsal view.

Female Terminalia (Figs 41–43). 8th sternite approximately finger-shaped in lateral view. Ectoproct trapeziform in lateral view; 9th gonocoxite approximately finger-shaped in lateral view; 9th gonostylus finger-shaped and brown; spermathecae bend into C-shape.

Distribution. China (Henan, Shaanxi, Hubei, Chongqing).

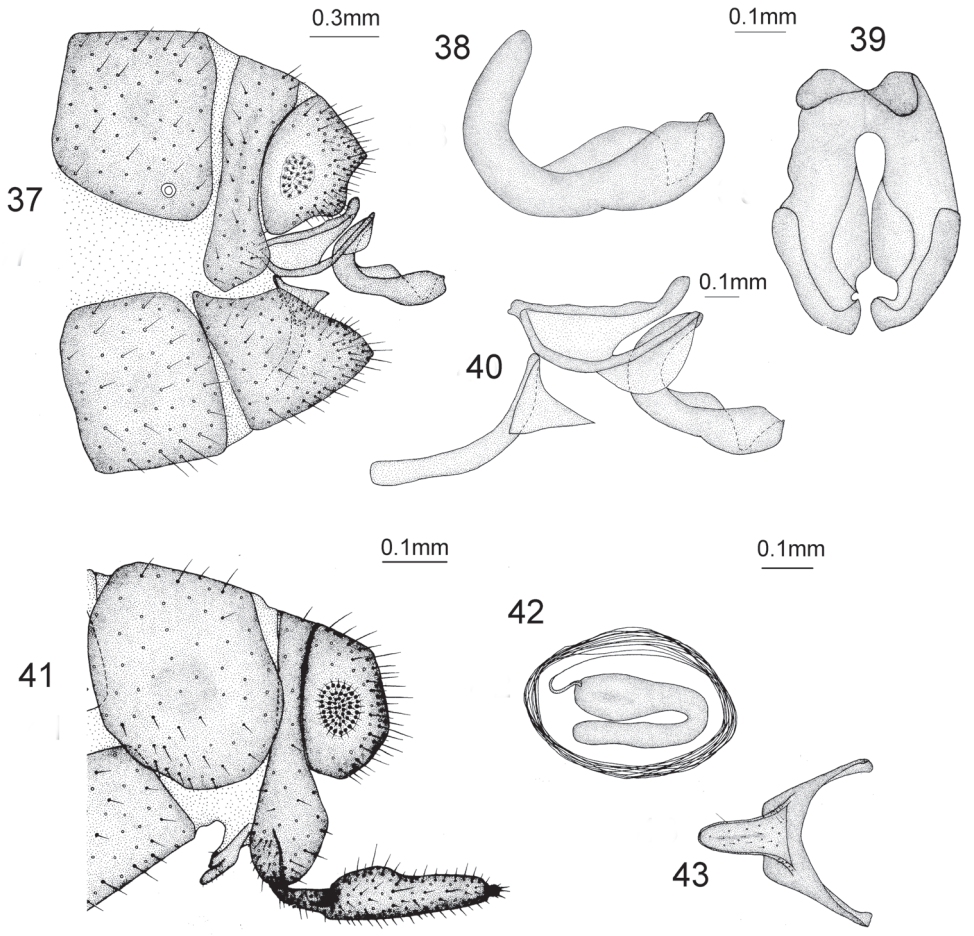

Figures 37–43. *Heterosmylus shennonganus* Yang, 1997. Male **37** terminalia, lateral view **38** mediuncus, lateral view **39** mediuncus, dorsal view **40** genitalia, lateral view. Female: **41** terminalia, lateral view **42** spermatheca, lateral view **43** 8th sternite, ventral view.

Heterosmylus curvagradatus Yang, 1999

Figs 44–50

Material examined. Holotype Male. CHINA: Fujian (Province): Wuyishan, Huanghuacong, [27°48'N, 117°42'E], 13.x.1980, leg. Fan Jiang. [Verbatim label data (translated from Chinese)]: CHINA: Fujian Prov., Wuyishan, Huanghuacong/ 13.x.1980/ Fan Jiang/ CAU. Paratype Female. CHINA: Fujian (Province): Wuyishan, Xianfenling, 19.ix.1987. leg. Jiashe Wang.

Diagnosis. Two yellow longitudinal stripes present from pronotum to mesonotum. mesoscutellum bright yellow, metanotum with a central yellow stripe; apex of gonarcus slightly dilated, short and curved dorsally.

Figure 44. Wings of *Heterosmylus curvagradatus* Yang, 1999.

Redescription. Body length 7–10 mm. *Head*. Vertex shiny yellow with a brown round spot in middle and a greyish yellow transverse band near antennae; frons bright yellow with a black brown stripe; ocelli grey but black at base; compound eyes grey and glossy; antennae black; clypeus yellow, maxillary and labial palpi dark brown. *Thorax*. Dark brown with two yellow longitudinal stripes from pronotum to mesonotum. mesoscutellum bright yellow, metanotum with a central yellow stripe. *Wings* (Fig. 44). Forewing length 15–17 mm, width 5–6 mm; membrane hyaline, veins fuscous with numerous long setae; pterostigma yellow but brown on both sides. Crossveins *r1-rs* edged with dark brown spots. Rs with 8–9 branches, gradates cross-veins with brown marks. Hind wing length 13–14 mm, width 4–6 mm; membrane hyaline without spots besides the pterostigma.

Male Terminalia (Figs 45–48). Ectoproct approximately pentagonal in lateral view; gonarcus rod-like in lateral view, apex slightly inflated, short and curved dorsad; mediuncus fused at base and scoop-shaped in dorsal view and apex flat-bottomed in dorsal view.

Female Terminalia (Figs 49–50). 8th sternite reduced into finger-shape in lateral view; ectoproct approximately trapezoid in lateral view; 9th gonocoxite approximately finger-shaped in lateral view; 9th gonostylus brown and short; spermathecae bend into C-shape.

Distribution. China (Fujian).

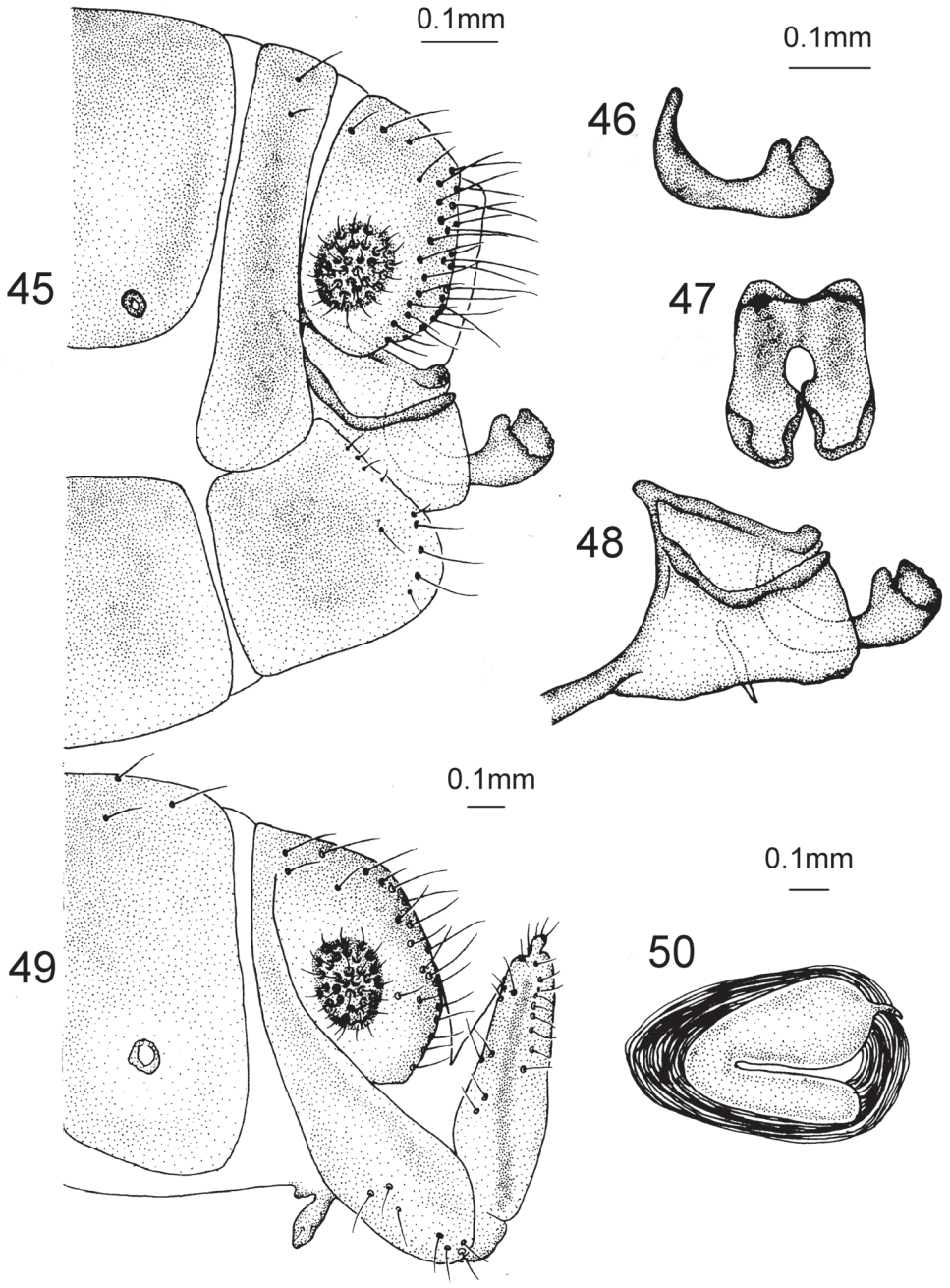

Figures 45–50. *Heterosmylus curvagradatus* Yang, 1999. Male: **45** terminalia, lateral view **46** mediuncus, lateral view **47** mediuncus, dorsal view **48** genitalia, lateral view. Female: **49** terminalia, lateral view **50** spermatheca, lateral view.

Acknowledgements

We wish to express our gratitude to Timothy R. New and Valdimir Makarkin for providing literature necessary to this project. This research was supported by the National Natural Science Foundation of China (Gants 31272352, 31301905 and 41372013), the Beijing Natural Science Foundation (Grant 5132008), and Ph.D. Programs Foundation of Ministry of Education of China (Grant 20131108120005).

References

Adams PA (1969) A new genus and species of Osmylidae (Neuroptera) from Chile and Argentina, with a discussion of Planipennian genitalic homologies. Postilla 141: 1–11. doi: 10.5962/bhl.part.24591

Krüger L (1913a) Osmylidae. Beiträge zu einer Monographie der Neuropteren-Familie der Osmylidaen. II. Charakteristik der Familie, Unterfamilien und Gattungen auf Grund des Geäders. Stettiner Entomologische Zeitung 74: 3–123.

Krüger L (1913b) Osmylidae. Beiträge zu einer Monographie der Neuropteren-Familie der Osmyliden. IV. Beschreibung der Arten. Stettiner Entomologische Zeitung 74: 225–294.

Kuwayama S (1962) A revisional synopsis of the Neuroptera in Japan. Pacific Insects 4: 325–412.

Martins CC, Ardila-Camacho A, Aspoeck U (2016) Neotropical osmylids (Neuroptera, Osmylidae): Three new species of *Isostenosmylus* Krüger, 1913, new distributional records, redescriptions, checklist and key for the Neotropical species. Zootaxa 4149(1): 1–66. doi: 10.11646/zootaxa.4149.1.1

Nakahara W (1955) Formosan Neuroptera collected by the late Dr. T. Kano. Kontyû 23: 6.

New TR (1983) A revision of the Australian Osmylidae: Kempyninae (Insecta: Neuroptera). Australian Journal of Zoology 31: 393–420. doi: 10.1071/ZO9830393

Winterton SL, Wang YJ (2016) Revision of the genus *Gryposmylus* Krüger, 1913 (Neuroptera, Osmylidae) with a remarkable example of convergence in wing disruptive patterning. ZooKeys 617: 31–45. doi: 10.3897/zookeys.617.10165

Winterton SL, Garzón-Orduña IJ, Zhao J, Wang YJ, Liu ZQ (2016) Phylogeny of the lacewing family Osmylidae (Insecta: Neuroptera). Systematic Entomology, (submitted).

Yang CK (1986) Thirty new species and four new genera of Neuroptera from Yunnan, and the family Nemopteridae new to China. Pei ching nung yeh ta hsueh hsueh pao= Acta Agriculturae Universitatis Pekinensis 12: 153.

Yang CK (1987) Neuroptera. In: Zhang S (Ed.) Agricultural insects, spiders, plant diseases and weeds of Xizang. Vol. 1. Xizang Renmin Press House, Tibet, 191–194.

Yang CK (1992) Neuroptera. Insects of the Hengduan Mountains Region Science press, Beijing, 438–454.

Yang CK (1997) Neuroptera: Osmylidae. In: Yang XK (Ed.) Insects of the Three Gorge Reservoir Area of Yangtze River. Chongqing Press, Chongqing, 580–581.

Yang CK (1999) Osmylidae. In: Huang BK (Ed.) Fauna of Insects Fujian Province of China Vol. 3. Fujian Science and Technology Press, Fuzhou, 96–98.

ZooKeys 637: 129–133 (2016)
doi: 10.3897/zookeys.637.10910
http://zookeys.pensoft.net

RESEARCH ARTICLE

A peer-reviewed open-access journal
ZooKeys
Launched to accelerate biodiversity research

Siamothrips balteus, a new species of *Scirtothrips* genus-group from China (Thysanoptera, Thripidae)

Zhaohong Wang[1], Xiaoli Tong[1]

1 *Department of Entomology, College of Agriculture, South China Agricultural University, Guangzhou 510642, China*

Corresponding author: *Xiaoli Tong* (xtong@scau.edu.cn)

Academic editor: *L. Mound* | Received 24 October 2016 | Accepted 22 November 2016 | Published 2 December 2016

http://zoobank.org/4CC9EFAB-F0C4-4FFD-818E-AD58D4C6B5C6

Citation: Wang Z, Tong X (2016) *Siamothrips balteus*, a new species of *Scirtothrips* genus-group from China (Thysanoptera, Thripidae). ZooKeys 637: 129–133. https://doi.org/10.3897/zookeys.637.10910

Abstract

The third species of the genus *Siamothrips* Okajima, *S. balteus* **sp. n.**, is described from China. The new species is characterised by the abdominal tergite II uniformly brown, III–VII with a brown area medially but pale on lateral thirds, tergite VIII smooth medially, tergite X with 3–4 rows of microtrichia medially, and abdominal sternite VII with one pair of discal setae laterally. A key to the three species has been constructed and is presented here.

Keywords

China, new species, *Siamothrips*, thrips, Thripinae

Introduction

Siamothrips is a small genus that was erected by Okajima (1990) based on a single species, *S. argus* Okajima, from Thailand. Subsequently, Ng and Mound (2015) described a second species in the genus, *S. initium* Ng & Mound from Malaysia, and a third species is described here from southern China. Although the generic relationships of the genus are not clear, Okajima (1990) suggested placing it in the tribe Sericothripini, but more recently Masumoto and Okajima (2007) suggested *Siamothrips* might be a member of the *Scirtothrips* genus-group.

Materials and methods

The thrips were collected by beating vegetation over a white plastic tray using a stick, and then sorted and preserved in 90% alcohol. Examined specimens were mounted with Canada balsam using the method outlined by Zhang et al. (2006). Details of the morphological structures were examined with a ZEISS Imager A1 microscope, the photos were taken by the Photometrics CoolSNAP camera, and the figures were subsequently processed with Adobe Photoshop CS6. All type specimens are deposited in the Insect Collection, South China Agricultural University (SCAU).

Taxonomy

Key to species of *Siamothrips* (female)

1 Body and wings uniformly pale; median and submedian setae on mesoscutum not arranged in a transverse line; meso- and metascutum sculpture without inner markings [Thailand] ..... ***S. argus***

– Body and wings bicoloured, pale to brown; median and submedian setae on mesoscutum arranged in a transverse line; sculpture on meso- and metascutum bearing inner markings..... **2**

2 All abdominal tergites pale; tergite VIII with rows of microtrichia extending across segment on anterior half; tergite X smooth medially; abdominal sternite VII without any discal setae and median pair setae arising in front of posterior margin [Malaysia] ..... ***S. initium***

– Abdominal tergite I pale, II uniformly brown, III–VII with brown area medially but pale on lateral thirds; tergite VIII smooth medially; tergite X with 3–4 rows of microtrichia medially; abdominal sternite VII with one pair of discal setae laterally and median pair setae situated at posterior margin [China] ..... ***S. balteus* sp. n.**

***Siamothrips balteus* sp. n.**
http://zoobank.org/E3D023EA-0949-4C85-94A7-FC7D6466AA67
Figs 1–10

Material examined. Holotype. 1 female: **CHINA**, Jiangxi province, Jing'an County, Sanzhualun National Forest Park, Luojiaping (29°01'33"N, 115°17'32"E, alt. 630m), collected from young leaves of *Loropetalum chinense* (Hamamelidaceae), 17.viii.2016, leg. Zhaohong Wang.

Paratypes. 18 females, same data as holotype.

Diagnosis. Body bicoloured, pale to brown; fore wing pale except brown submedianly; abdominal tergite II uniformly brown in contrast to largely pale colouration of the other tergites. Antennal segments III and IV with sense cones forked. Median

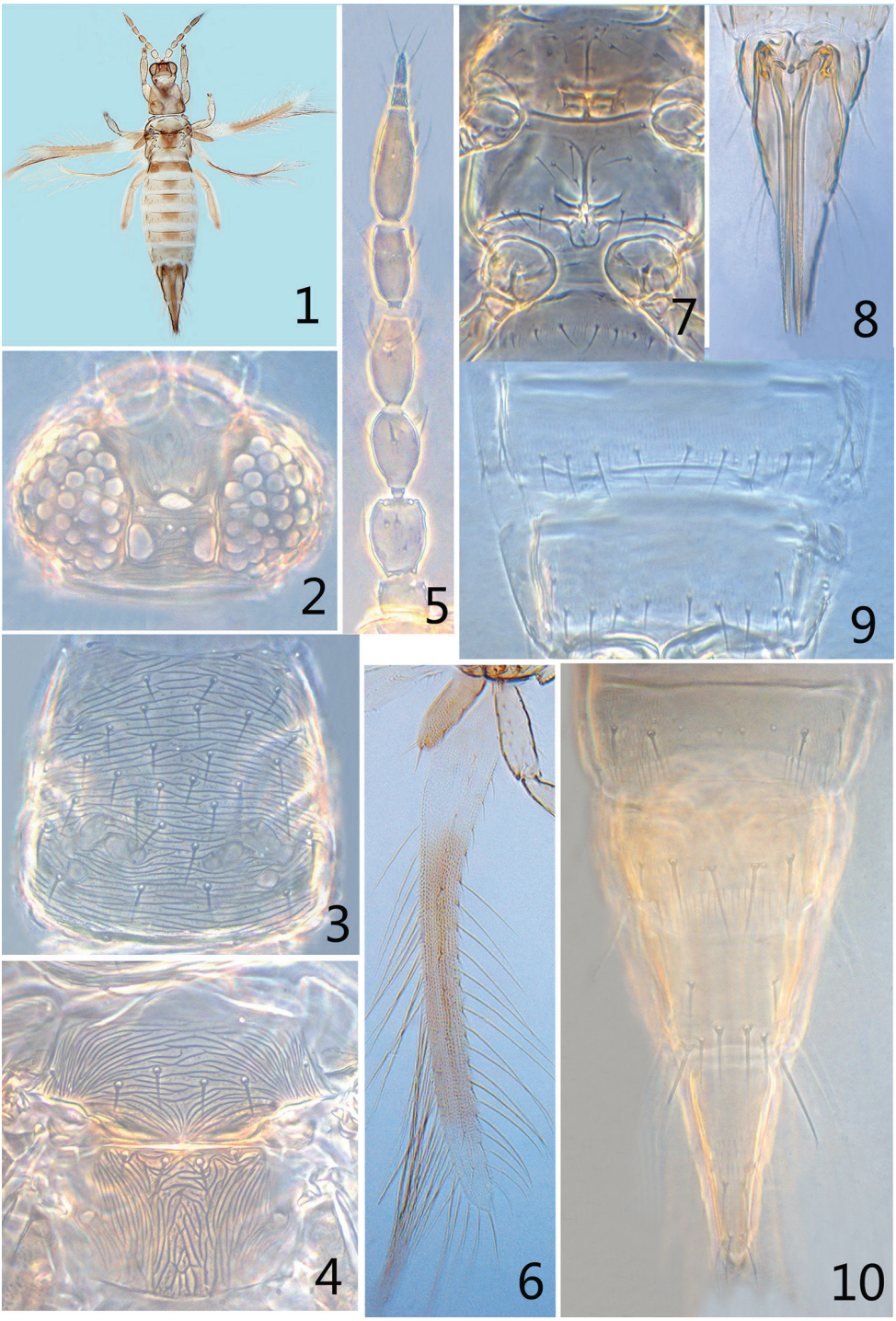

Figures 1–10. *Siamothrips balteus* sp. n. **1** female habitus **2** head **3** pronotum **4** meso- and metanotum **5** antenna **6** fore wing **7** meso- and metasternum 8 ovipsitor **9** abdominal sternites VI–VII **10** abdominal tergites VII–X.

and submedian setae on mesoscutum arranged in a transverse line; sculpture on meso- and metascutum bearing inner markings. Abdominal tergite VIII smooth medially; tergite X with 3–4 rows of microtrichia medially; abdominal sternite VII with one pair of discal setae laterally and median pair setae situated at posterior margin.

Description. Female (*macropterous*) (Fig. 1): Body pale to brown, anterior 3/4 margin of head yellowish brown; antennal segments I–II pale, III light brown, IV–VIII uniformly brown; pronotum uniformly light yellowish brown; posterior half of mesonotum and metanotum brown; all legs pale but tarsi slightly darker at extreme apex; fore wing brown except pale at basal 1/3 and apical 1/7, clavus brown; abdominal tergite I pale, II uniformly brown, III–VII with brown area medially but pale lateral thirds, and antecostal ridges darker medially, VIII–X uniformly yellowish brown; abdominal sternites pale including antecostal ridges.

Head approximately twice as wide as long, widest across eyes, slightly projecting in front of compound eyes; dorsal surface of head including ocellar triangle sculptured with transverse anastomosing striae, but the frons with longitudinal striae (Fig. 2); eyes bulging and pilose without pigmented ommatidia; cheeks very short and almost parallel; three pairs of ocellar setae present, setal pairs I and III subequal in length, pair II longest; pair I situated in front of ocelli, pair II situated on margin or outside of ocellar triangle near eyes, pair III arising on tangent between anterior margins of hind ocelli (Fig. 2); two pairs of postocular setae; mouth-cone long but never extending beyond posterior margin of pronotum; maxillary palps 3-segmented, terminal segment long, slightly shorter than the combined length of other two segments. Antennae 8-segmented (Fig. 5), segment I without dorsal apical setae, II without campaniform sensilla, with four rows of microtrichia dorsally; forked sensoria on III–IV, not reaching more than one-third the length of succeeding segment, V–VI each with an small outer sense cone; III–VI with about four rows of microtrichia on both dorsal and ventral surfaces.

Pronotum (Fig. 3) trapezoidal with approximately 35–40 fine setae including marginal setae, without long posteroangular setae; dorsal surface sculptured with distinctly transverse anastomosing striae but on posterior half, the striae are irregular medially. Mesonotum (Fig. 4) with irregular transverse anastomosing striae bearing inner granules, without campaniform sensilla; median and submedian setae arranging in a transverse line. Metanotum (Fig. 4) sculpture irregular longitudinal reticulate medially with inner markings, lateral area with longitudinal lines bearing feeble inner granules, without campaniform sensilla; median setae usually situated near anterior margin (sometimes at anterior margin), submedian setae situated at anterior margin; median setae slightly shorter than submedian setae. Meso- and metasternum each with approximately 20 long fine setae, meso- and metafurcae with spinula (Fig. 7). Fore wing (Fig. 6) first vein with 11–12 setae, second vein without setae, clavus with three veinal and one discal setae; posteromarginal fringe cilia weakly wavy. Tarsi 2-segmented.

Abdominal tergites II–VII with closely spaced rows of ciliate microtrichia on lateral thirds, S1 setae small, slightly longer than the distance between their bases, but S1 setae on tergites VIII–IX well developed and long, approximately twice as long as distance between their bases; tergites II–VIII smooth medially without any rows of microtrichia, tergite VIII with complete posteromarginal comb (Fig. 10); tergite IX without campani-

form sensilla or microtrichia, but tergite X with 3–4 rows of microtrichia medially (Fig. 10). Abdominal sternites II–VII with rows of ciliate microtrichia across median area, at least on posterior halves, posterior margin with fringe of microtrichia; segment II with three pairs of long posteromarginal setae, III with four pairs of long posteromarginal setae; IV–VII with five pairs of long posteromarginal setae, all primary setae of sternites situated at posterior margins; sternite VII with one pair of discal setae laterally (Fig. 9). Ovipsitor (Fig. 8) straight and elongate, slightly longer than twice the length of pronotum.

Male unknown.

Measurements (holotype female in microns). Distended body length 940. Head, dorsal length 50, ventral length to mouth cone tip 175, width across compound eyes 100; ocellar setae II 16; ocellar setae III 10; postocular setae I 9. Eye length 45. Pronotum length 110, maximum width 125. Metascutal median setae 17, submedian setae 18. Fore wing length 430. Length of median setae on abdominal tergite II–VII 5–10, on tergite VIII–IX 35–45. Antennal segments I–VIII length (width) as follows: 17(20), 26(23), 35(18), 33(18), 34(15), 42(14), 8(6), 12(4). Ovipositor length 240.

Etymology. The specific epithet is from the Latin *balteus*, meaning "belt or waistband," in reference to the abdominal tergite II being entirely brown in contrast to largely pale colouration of the other tergites.

Distribution. China (Jiangxi).

Remarks. This new species is most similar to *S. initium* Ng & Mound, 2015 from Malaysia; however, it can be distinguished from these two species by the key above.

Acknowledgements

This study was supported by the National Natural Science Foundation of China (31372236) and the Key Project for National Groundwork of Science & Technology (No.2013FY111500-5-3). We especially wish to acknowledge Chao Zhao, Baoqiang Pan, and Liangxin Liu for providing help with field work. Thanks are also due to the referees for their advice and constructive comments.

References

Masumoto M, Okajima S (2007) The genus *Scirtothrips* Shull (Insecta, Thysanoptera, Thripidae) and three related genera in Japan. Zootaxa 1552: 1–33. http://biotaxa.org/Zootaxa/article/view/zootaxa.3856.2.6

Ng YF, Mound LA (2015) Genera of the *Scirtothrips* genus-group (Thysanoptera, Thripidae) with a new species of *Siamothrips* from Malaysia. Zootaxa 4021(2): 387–394. https://doi.org/10.11646/zootaxa.4021.2.9

Okajima S (1990) Two thripine species collected on eggplant in Thailand (Thysanoptera, Thripidae). Bulletin of the Biogeographical Society of Japan 45(10): 71–75.

Zhang HR, Okajima S, Mound LA (2006) Collecting and slide preparation methods for thrips. Chinese Bulletin of Entomology 43(5): 725–728.

ZooKeys 637: 135–149 (2016)
doi: 10.3897/zookeys.637.10359
http://zookeys.pensoft.net

RESEARCH ARTICLE

A peer-reviewed open-access journal
ZooKeys
Launched to accelerate biodiversity research

Spatial distribution and seasonal changes of mayflies (Insecta, Ephemeroptera) in a Western Balkan peat bog

Marina Vilenica[1], Andreja Brigić[2], Mladen Kerovec[2], Sanja Gottstein[2], Ivančica Ternjej[2]

1 *University of Zagreb, Faculty of Teacher Education, Petrinja, Croatia* **2** *University of Zagreb, Faculty of Science, Department of Biology, Zagreb, Croatia*

Corresponding author: *Marina Vilenica* (marina.vilenica@gmail.com)

Academic editor: *B. Price* | Received 31 August 2016 | Accepted 9 November 2016 | Published 2 December 2016

http://zoobank.org/F3D151AA-8C93-49E4-9742-384B621F724E

Citation: Vilenica M, Brigić A, Kerovec M, Gottstein S, Ternjej I (2016) Spatial distribution and seasonal changes of mayflies (Insecta, Ephemeroptera) in a Western Balkan peat bog. ZooKeys 637: 135–149. https://doi.org/10.3897/zookeys.637.10359

Abstract

Peat bogs are unique wetland ecosystems of high conservation value all over the world, yet data on the macroinvertebrates (including mayfly assemblages) in these habitats are still scarce. Over the course of one growing season, mayfly assemblages were sampled each month, along with other macroinvertebrates, in the largest and oldest Croatian peat bog and an adjacent stream. In total, ten mayfly species were recorded: two species in low abundance in the peat bog, and nine species in significantly higher abundance in the stream. Low species richness and abundance in the peat bog were most likely related to the harsh environmental conditions and mayfly habitat preferences. In comparison, due to the more favourable habitat conditions, higher species richness and abundance were observed in the nearby stream. Three of the recorded species, *Caenis luctuosa* from the peat bog, and *Eurylophella karelica* and *Leptophlebia marginata* from the stream are new records for the Croatian mayfly fauna. Typical Central European life cycle patterns were confirmed for several species (e.g. *Baetis vernus*, *Nigrobaetis niger*, *Electrogena ujhelyii*), while for several others (e.g. *Habrophlebia fusca*, *Paraleptophlebia submarginata*) some discrepancies were observed. Therefore, these results provide new and valuable information on the ecology of mayflies in peat bog habitats.

Keywords

Environmental factors, life cycle, mayfly assemblages, new records, peat bog

Introduction

Acidic peat bogs dominated by *Sphagnum* species occupy approximately 3 % of the Earth's land surface (Kivinen and Pakarinen 1981) and contain one-third of the world's soil carbon (Joosten and Clarke 2002). Consequently, they play an important role in the global carbon cycle and climate change (Limpens et al. 2008, Battin et al. 2009). Peat bogs are widely distributed in boreal regions of the Northern hemisphere, but in the Western Balkans are in patches of isolated habitat (Spitzer and Danks 2006, Topić and Stančić 2006). These unique and environmentally extreme wetland ecosystems are characterized by diverse aquatic and semiaquatic habitats, high water table and acidity, low oxygen and nutrient levels (Spitzer and Danks 2006).

Peat bogs are amongst the most fragile and endangered ecosystems worldwide (Langheinrich et al. 2004) due to the climate change, agricultural activities (i.e. drainage and peat extraction) and secondary succession (Doyle 1990, Więcek et al. 2013). Even though the conservation values of bogs have been internationally recognized, these wildlife habitats are still understudied in comparison to most other freshwater habitats (Baars et al. 2014). Recent studies have shown that peat bogs are inhabited by unique macroinvertebrate assemblages, often containing rare and threatened species (Hannigan and Kelly-Quinn 2012, Drinan et al. 2013, Baars et al. 2014).

Mayflies are merolimnic insect order (i.e. with aquatic nymphal stages and terrestrial adults) with nymphs inhabiting a wide range of lotic and lentic habitats (Bauernfeind and Soldán 2012). Mayfly assemblages respond to multiple environmental factors, including water temperature (e.g. Bauernfeind and Soldán 2012), water velocity, oxygen content (e.g. Moog 2002; Bauernfeind and Soldán 2012) and pH (e.g. Fiance 1978, Petrin 2011). Mayflies are highly sensitive to habitat alterations (e.g. Zedková et al. 2015, Vilenica et al. 2016) and widely used as indicators in bio-monitoring assessments (Elliott et al. 1988, Sartori and Brittain 2015). Comprehensive data on mayfly life history traits, such as life cycles, habitat and environmental preferences are highly important for the understanding of ecosystem functioning (e.g. Brittain 1990, 1991, Raddum and Fjellheim 1993, Erba et al. 2003).

Aquatic macroinvertebrate (including mayfly) micro-distribution and ecology have primarily been studied in Northern and Central European peat bogs (e.g. Baars et al. 2014, Mieczan et al. 2015), with no comprehensive studies on mayfly assemblages in peat bogs of the Western Balkans. Thus, the aims of this study were to: 1) compare the spatial distribution of mayfly assemblages in two focal habitats: the peat bog and adjacent stream; 2) analyse environmental variables that affect the spatial distribution of mayfly assemblages and 3) determine mayfly seasonal dynamics in studied habitats.

Methods

Study area

The study was conducted in the Đon močvar, one of the largest (10 ha) and oldest peat bogs in Croatia. The peat bog is located in the central part of the country (45°19'4.33"N, 15°54'32.83"E, Fig. 1) at 130 m a.s.l., under the slopes of the Petrova gora Mountain and surrounded by the Danković klada Stream. This region is characterised by a temperate humid climate (Šegota and Filipčić 2003) with an average annual temperature of 10.5 °C and an average annual precipitation of 1 050 mm (Zaninović et al. 2008).

The peat bog is a complex ecosystem, encompassing a mosaic of different habitats from open woodless *Sphagnum* spp. L. sites, deep hollows, and small ponds, to swampy areas dominated by *Rhynchospora alba* (L.) Vahl and *Phragmites australis* (Cav.) Trin. ex Steud. Abandonment of traditional land-management practices, such as mowing and grazing, has led to severe processes of succession at the peat bog. As a result, during the 20th century, the open area on the bog decreased from 40 ha to 10 ha. The peat bog and its surrounding area are protected as a Botanical Reserve and included in the NATURA 2000 network (Alegro and Šegota 2008). The Danković klada Stream is located at the peat bog edge, running through arable land and deciduous forests. It is characterized by high oscillations of water level between the seasons due to oscillations of the rainfall. The stream banks are overgrown with *Alnus glutinosa* (L.) Gaertn. and *Corylus avellana* L. Substrate composition contains mezolithal, microlithal, akal, psammal, argylal, phytal and xylal (Ternjej et al. 2015).

Sampling and identification

Mayflies were sampled together with other aquatic macroinvertebrates at two main habitats: peat bog and stream. Within each habitat type ten replicates were collected once a month, using a benthos net (25×25 cm; mesh size = 500 μm).

In the peat bog, macroinvertebrates were collected from four different types of lentic microhabitats: lake, hollows, ditches and pools. In the stream, all major substrate types were sampled: mezolithal, microlithal, akal, psammal, argylal, phytal and xylal. The study sites differed in physico-chemical water properties, size and vegetation composition (Table 1). The samples were collected during one vegetation season, between March and November 2015.

Species were identified using e.g. Müller-Liebenau (1969), Malzacher (1984) and Bauernfeind and Humpesch (2001). Very young or damaged individuals were identified to the family level. Nomenclature follows Bauernfeind and Sóldan (2012). All voucher specimens are deposited at the Department of Biology, Faculty of Science, Zagreb, Croatia. After identification, total nymphal body length without cerci and antennae was measured using a micrometer on a dissecting stereomicroscope (Stemi 2000-C, Carl-Zeiss).

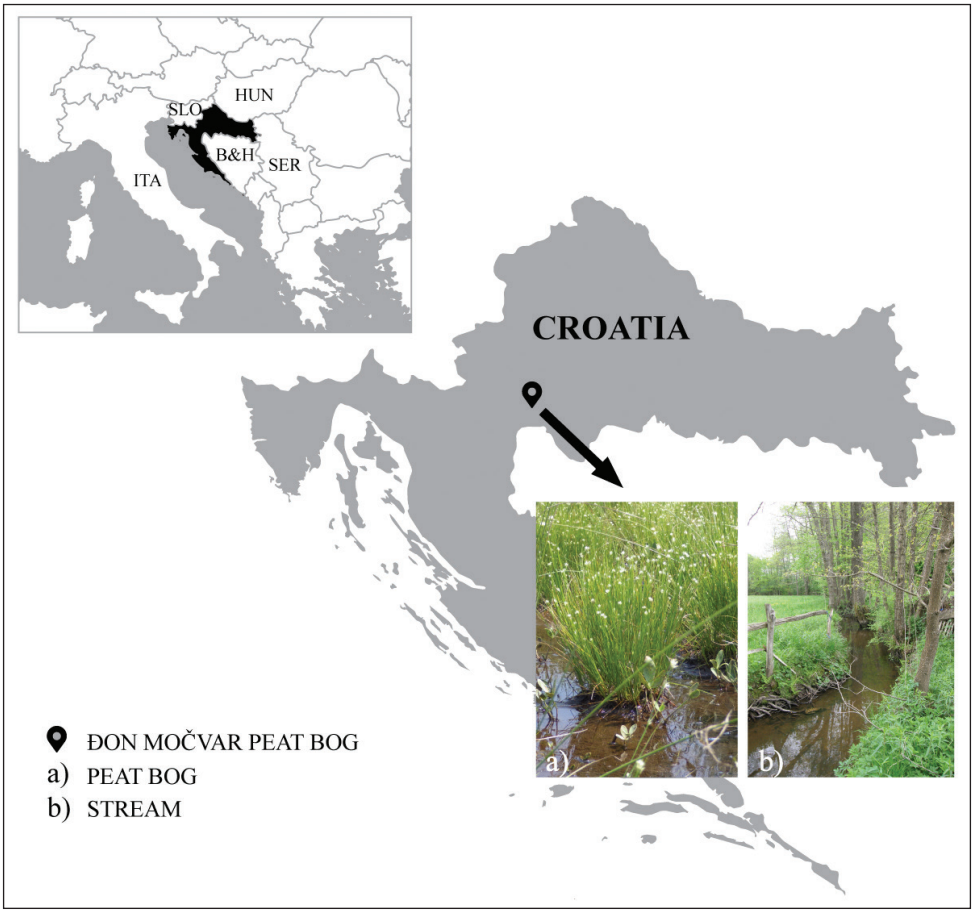

Figure 1. Geographical position of the Đon močvar peat bog, Croatia.

Environmental variables

The physico-chemical water properties (water temperature, pH, dissolved oxygen concentration and conductivity) were measured at each site during each sampling date, with a multiparameter probe (WTW Multi 3430). Alkalinity (concentration of $CaCO_3$ (mg/L)) was measured using Standard Analytical Procedure (APHA). Since the water was brown coloured, distrophic with low turbidity, standard methods (e.g. depth-meter) could not be applied for measuring water depth. Therefore, water depth was measured with a constructed meter.

Data analysis

Dominance was determined according to Bick (1989). Taxa represented by > 10% of individuals are classified as eudominant, taxa with 5–10% of total abundance as

Table 1. Comparison of physico-chemical water properties between the Đon močvar peat bog and adjacent stream using Mann-Whitney U test. Key: *** p<0.001, ** p<0.01, ns non-significant. The values are mean ± standard deviation.

Physico-chemical water properties	Peat bog			Stream			Mann-Whitney U test	
	mean ± SD	min	max	mean ± SD	min	max	U	p
Water pH	5.60 ± 0.36	5.02	6.57	6.76 ± 0.37	6.20	7.25	0.00	***
Alkalinity ($CaCO_3$ mgL^{-1})	17.80 ± 3.50	10.00	22.50	53.75 ± 15.29	25.00	70.00	0.00	***
Conductivity (μScm^{-1})	37.10 ± 47.08	4.98	210.00	99.88 ± 29.81	60.00	128.00	8.00	**
Water depth (cm)	5.00 ± 0.56	3.93	5.60	11.84 ± 4.48	3.50	17.00	8.00	**
Water temperature (°C)	14.90 ± 6.81	5.20	37.00	13.22 ± 3.90	7.30	18.80	23.00	ns
Oxygen (mgL^{-1})	6.90 ± 2.78	1.00	11.83	7.49 ± 2.08	4.71	10.82	22.00	ns

dominant, taxa with 2–5% as subdominant, taxa with 1–2% as recedent and taxa with less than 1% of total share as subrecedent. In order to estimate differences in physico-chemical water properties and mayfly assemblages (number of taxa and number of individuals) between the peat bog and adjacent stream, a Mann-Whitney U test was applied. Prior to the analyses, the data were tested for normality using a Shapiro-Wilk test. These tests are based on pooled microhabitat data both from the peat bog and stream, for physico-chemical parameters and mayfly assemblages. The tests were performed using Statistica 12.0 software package (StatSoft Inc. 2013). For estimation of similarity and differences in mayfly assemblages between the peat bog and stream during the study period, a Bray-Curtis similarity index was used. Prior to analysis, the data were square root transformed. The results of hierarchical cluster analysis were superimposed on Non-metric multidimensional scaling (NMDS) plot. Samples with no mayfly records were excluded from analyses. These analyses were performed using the PRIMER v6 software package (Clarke and Warwick 2001). Life cycle patterns of eudominant and dominant mayfly species were analysed by grouping the nymphs into 1 mm body size classes. All figures were processed with Adobe Illustrator CS6.

Results

In the peat bog, water was highly acidic, differing significantly from the stream (Table 1). Alkalinity and conductivity were three times lower in the peat bog than in the stream. Additionally, water depth was two times lower in the peat bog than in the stream. Water temperature did not differ significantly between the two habitats. However, we observed large variability of water temperature among peat bog microhabitats, particularly in shallow ditches, where summer maximums reached 37 °C. Similar variability was detected for oxygen concentration, with minimum values of only 1 mgL^{-1} in the peat bog (Table 1).

A total of ten mayfly species were recorded in the peat bog and adjacent stream (Table 2). Only two species were collected from the peat bog, *Cloeon dipterum* (Lin-

Table 2. Mayfly taxa and their abundance recorded in the Đon močvar peat bog and adjacent stream. Key: * new mayfly records for the Croatian fauna.

Mayfly taxa	Peat bog	Dominance (%)	Stream	Dominance (%)
Baetidae				
Baetidae juvenile			106	18.40
Baetis rhodani (Pictet, 1843)			6	1.04
Baetis vernus Curtis, 1834			131	22.80
Cloeon dipterum (Linnaeus, 1761)	36	97.30	5	0.90
Nigrobaetis niger (Linnaeus, 1761)			60	10.40
Caenidae				
Caenis luctuosa (Bürmeister, 1839) *	1	2.70		
Heptageniidae				
Electrogena ujhelyii (Sowa, 1981)			89	15.50
Ephemerellidae				
Eurylophella karelica Tiensuu, 1935 *			1	0.17
Leptophlebiidae				
Habrophlebia fusca (Curtis, 1834)			119	20.10
Leptophlebia marginata (Linnaeus, 1767) *			1	0.17
Paraleptophlebia submarginata (Stephens, 1835)			57	9.91
Species richness (S)	**2**		**9**	
Number of individuals (N)	**37**		**575**	

naeus, 1761) and *Caenis luctuosa* (Bürmeister, 1839), while in the stream nine species were recorded. *Cloeon dipterum* was the most abundant species recorded in the peat bog (Table 1), while it was the only subrecedent in the stream. *Caenis luctuosa* was found only in the peat bog with only one specimen (Table 2). In the stream, *Baetis vernus* Curtis, 1834) (22.80% of the total catch) was the most numerous species, followed by *Habrophlebia fusca* (Curtis, 1834) (20.10%) and *Electrogena ujhelyii* (Sowa, 1981) (15.50%) (Table 2).

Three species were recorded for the first time for the Croatian mayfly fauna, namely *Caenis luctuosa*, *Eurylophella karelica* Tiensuu, 1935 and *Leptophlebia marginata* (Linnaeus, 1767) (Table 2).

Species richness ranged from 0 to 2 in the peat bog and from 3 to 7 in the stream. It was significantly lower in the peat bog (mean ± SD, 0.66 ± 0.71; Mann-Whitney U test, $U = 0.00$, $p < 0.001$; Fig. 2a) than in the stream (4.56 ± 1.24). The number of individuals ranged from 0 to 18 in the peat bog and from 11 to 173 in the stream. There was a significant difference between the peat bog (4.11 ± 5.76) and stream (63.89 ± 52.68; $U = 1.00$, $p < 0.001$; Fig. 2b).

The similarity between the peat bog and stream was very low, less than 7%. Moreover, NMDS analysis showed clustering of the samples according to the habitat type: the peat bog and stream clustered separately (Fig. 3).

In the peat bog, mature nymphs of *C. dipterum* (Fig. 4a) were recorded in June and between August and November, with the highest abundance in August. The body length ranged between 2.2 and 7.04 mm.

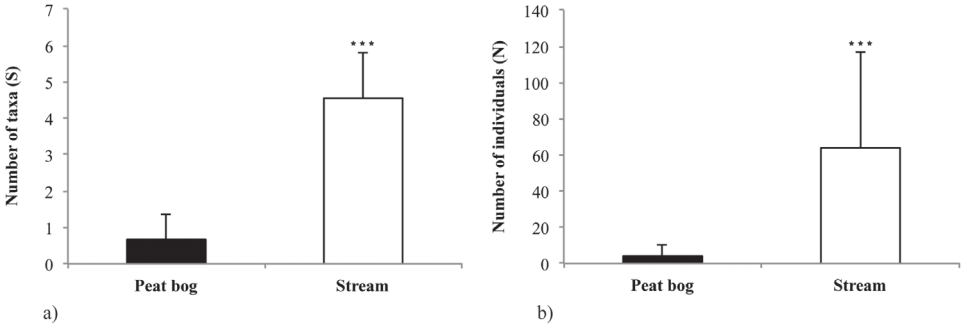

Figure 2. Mayfly taxa: **a** species richness (S) and **b** number of individuals (N) in the peat bog and adjacent stream (mean ± SD). The asterisk indicates significant difference between the habitats (Mann-Whitney U test, $p < 0.001$).

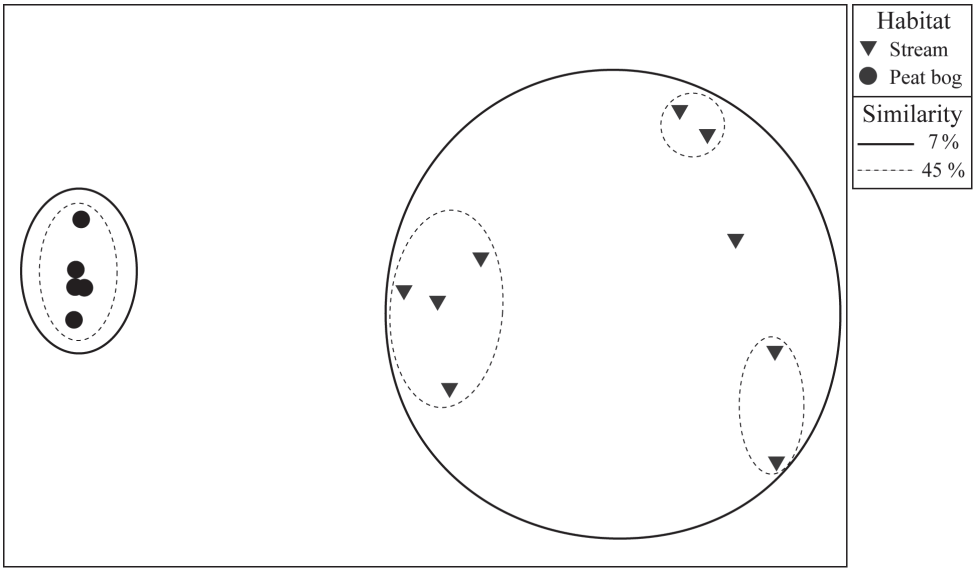

Figure 3. Ordination of non-metric multidimensional scaling of mayfly assemblages based on Bray-Curtis similarity coefficient (group average linking) and their square root transformed abundances, with superimposed data of hierarchical cluster analysis.

In the adjacent stream, the body length of *B. vernus* (Fig. 4b) ranged between 2.56 and 7.76 mm. The species was recorded between March and June and between September and November. Mature nymphs were recorded in both periods of occurrence. The body length of *Nigrobaetis niger* (Fig. 4c) ranged between 2.64 and 6.40 mm. Mature nymphs were recorded in March, June, and October. *Habrophlebia fusca* (Fig. 5a) was recorded between March and July, with mature nymphs present from April. The body length ranged between 1.60 and 7.20 mm. *Paraleptophlebia submarginata* (Fig. 5b) was recorded between August and November. The body length ranged between

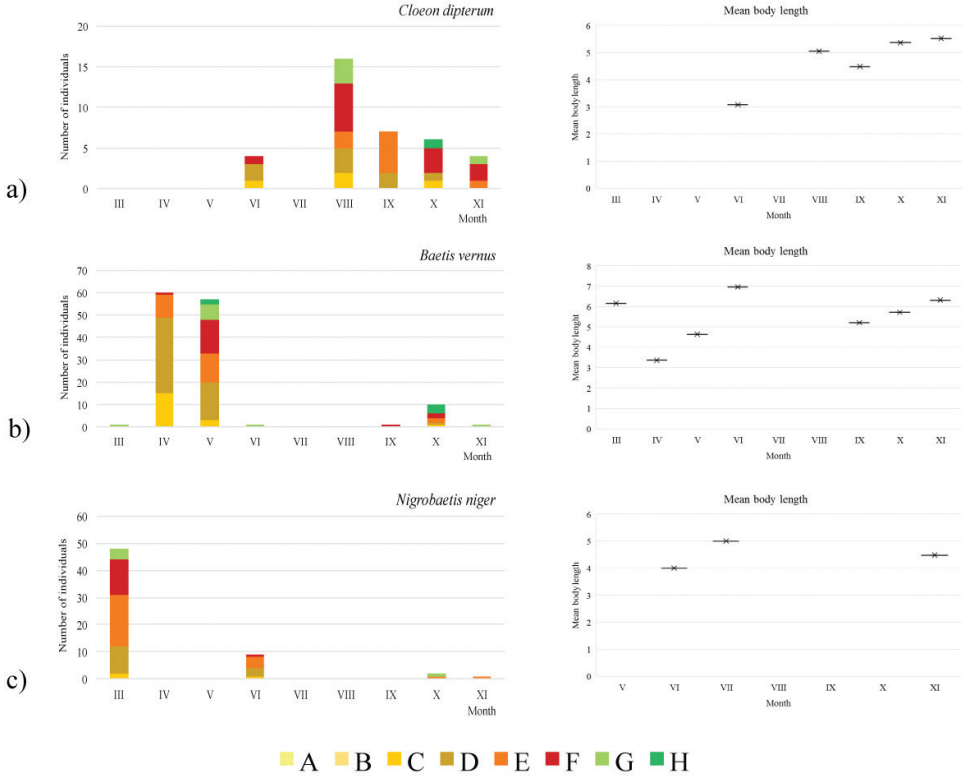

Figure 4. Seasonal dynamics of **a** *Cloeon dipterum* in the Đon močvar peat bog and **b** *Baetis vernus* **c** *Nigrobaetis niger* in adjacent Daković klada Stream between March and November 2015. Legend: Body length category: A = 0.00–0.99 mm; B = 1.00–1.99 mm; C = 2.00–2.99 mm; D = 3.00–3.99 mm; E = 4.00–4.99 mm; F = 5.00–5.99 mm; G = 6.00–6.99 mm; H = 7.00–7.99 mm.

2.00 and 8.16 mm, with mature nymphs present in October and November. The body length of *E. ujhelyii* (Fig.5c) ranged between 0.90 and 10.95 mm, with mature nymphs present in March, April and November.

Discussion

This study shows that mayflies have low species richness and abundance in the peat bog, as already reported by several other studies (e.g. Bauernfeind and Moog 2000, Joniak and Domek 2006, Schartau et al. 2008). Similarly, NMDS analysis showed a low degree of similarity between the peat bog and adjacent stream. The extreme habitat conditions, such as low pH and high water temperatures were most probably the main limiting factors for mayflies. Nevertheless, two species managed to survive in such harsh environment. The eurytopic and eurythermic *C. dipterum*, a typical pioneer species exhibiting traits of invasive behaviour (Bauernfeind and Sóldan 2012) was re-

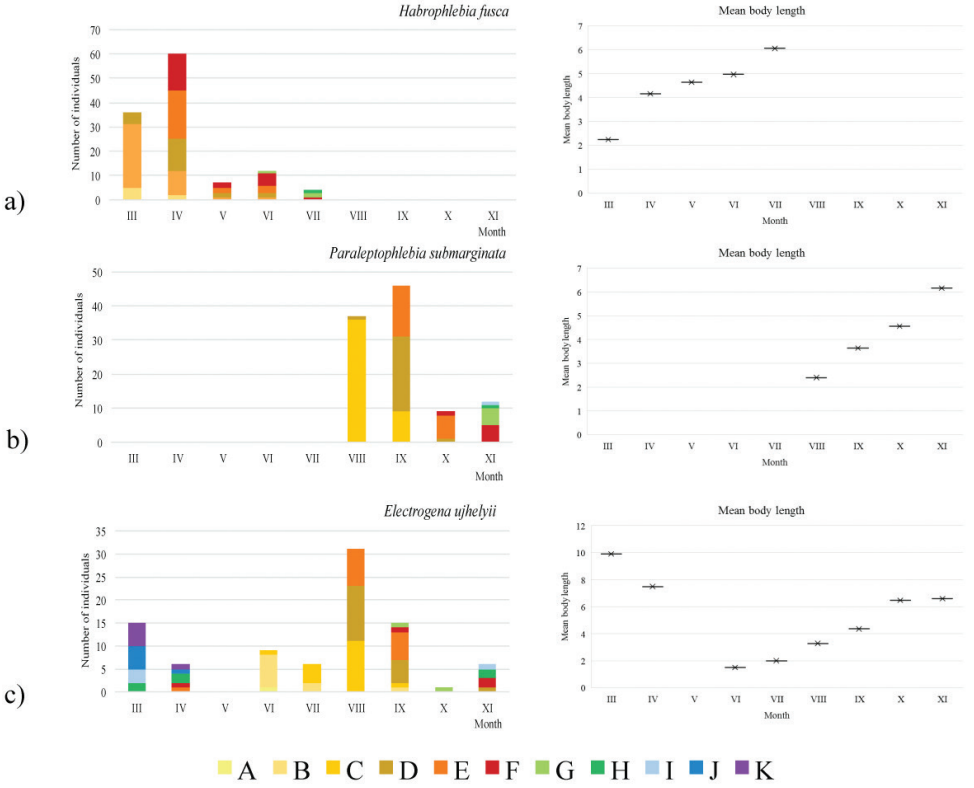

Figure 5. Seasonal dynamics of **a** *Habrophlebia fusca* **b** *Paraleptophlebia submarginata* **c** *Electrogena ujhelyii* in Danković klada Stream between March and November 2015. Legend: Body length category: A = 0.00–0.99 mm; B = 1.00–1.99 mm; C = 2.00–2.99 mm; D = 3.00–3.99 mm; E = 4.00–4.99 mm; F = 5.00–5.99 mm; G = 6.00–6.99 mm; H = 7.00–7.99 mm; I = 8.00–8.99 mm; J = 9.00–9.99 mm; K = 10.00–10.99 mm.

corded at both focal habitat types (i.e. peat bog and stream). Highly tolerant species to eutrophication and high temperatures, *C. luctuosa,* generally inhabits lentic habitats, predominantly lakes (Bauernfeind and Sóldan 2012) and it was recorded only in the peat bog. Surprisingly, some studies show high sensitivity of this species to acidification (e.g. Joniak and Domek 2006, Schartau et al. 2008). However, the pH values at the sites in these studies were even lower (approximately 4) than in Đon močvar peat bog, which could indicate that the species is intolerable to pH values less than 5. Future studies should focus on revealing the pH tolerance of *C. luctuosa*.

The interplay of moderate physico-chemical water properties and a variety of microhabitats in the adjacent stream provided suitable habitat conditions for significantly higher abundances of diverse mayfly species (Bauernfeind and Sóldan 2012). When compared to some other similar streams in that area (e.g. five species recorded in Čatlan, Zeleni dol and Moštanica Streams; see in Vilenica et al. 2015), mayfly species richness recorded from the Danković klada Stream could be considered as relatively high. Mayfly

assemblage composition in the stream is a consequence of the mayfly preferences for lotic habitats (e.g. Bauernfeind and Moog 2000, Bauernfeind and Humpesch 2001, Bauernfeind and Sóldan 2012), combined with neutral pH values and moderately high water temperatures. With the exception of *E. ujhelyii* and *E. karelica*, whose temperature preferences are not recognized yet, all other recorded species are eritherm, with a preference for moderately warm to warm water temperatures (Buffagni et al. 2009, Buffagni et al. 2015). As water temperature was already recognized as one of the most important environmental factors influencing mayfly assemblages (e.g. Brittain 1979, Harper and Peckarsky 2006) and many authors showed that mayflies are very sensitive to low pH values (Fiance 1978, Gerhardt 1990, Petrin 2011), the results of this study are in accordance.

Mayfly adult life is very short, with the individual life span lasting approximately one day depending on the species. Thus, mayflies spend the majority of their life in the nymphal stage in aquatic habitats (Brittain and Sartori 2003, Bauernfeind and Soldán 2012). Life cycles and seasonal dynamics of most of the temperate mayfly species are well known, with about 60% of the species having univoltine, 30% multivoltine, 4% semivoltine and 3% variable life cycle types (Clifford 1982). The proportion of univoltine species in the study area is in accordance with the latter data, while the proportions of the multivoltine and variable species, show certain discrepancies. According to the literature (Clifford 1982, Bauernfeind and Soldán 2012), 60% of the recorded species were previously determined to have univoltine (e.g. *H. fusca*, *P. submarginata*), 20% multivoltine (bivoltine) (*N. niger*, *C. dipterum*) and 20% variable (*B. rhodani*, *B. vernus*) life cycles. Semivoltine species were not recorded. Certain plasticity, i.e. discrepancies from their representative life cycle patterns were already recorded for some species in different climates and different habitats, which often results in unique patterns (e.g. Alba-Tercedor 1990, López-Rodríguez et al. 2008).

For bivoltine *B. vernus*, *N. niger* and univoltine *E. ujhelyii* (Clifford 1982, Bauernfeind and Sóldan 2012, Buffagni et al. 2015), typical life cycle patterns were confirmed. For. *C. dipterum*, species with highly adaptive life cycles (Clifford 1982, Bauernfeind and Soldán 2012, Buffagni et al. 2015), seasonal bivoltine summer life cycle type was recorded. On the other hand, some discrepancies were observed for two Leptophlebiidae species. Some previous studies have shown that *H. fusca* and *P. submarginata* have univoltine life cycles with overwintering in the nymphal stage and mature nymphs present during the early winter season (Bauernfeind and Sóldan 2012). In the Danković klada Stream, mature nymphs of *H. fusca* and *P. submarginata* were successively recorded during the early summer and late autumn, respectively. López-Rodríguez et al. (2010) recorded similar pattern in the life cycles of some other species belonging to the same two genera. These seasonal differences in ecological niche partitioning could be related to the availability of the suitable resources in the habitat.

The current study represents an important contribution to the knowledge of the mayfly fauna in Croatia, with several new records for the country together with some records of rare species. Widely distributed, *C. luctuosa*, recorded only from the peat bog and *L. marginata*, recorded only from the stream, were documented for the first time in Croatian freshwater habitats (Vilenica et al. 2015, Dekić et al. 2016). What is even more interesting, *E. karelica*, the species with a disjunct distribution, so far recorded only from Lithuania,

North European Russia, Poland and Hungary (Bauernfeind and Sóldan 2012, Alain and Belfiore, 2013) was also recorded for the first time (Vilenica et al. 2015, Dekić et al. 2016).

Although the Red list of Croatian mayflies does not exist yet, and none of the species is protected by the law, some recorded species are listed as rare and endangered in European Red lists (e.g. *C. dipterum*, *C. luctuosa*, *N. niger*, *H. fusca*, *L. marginata*, *P. submarginata*, *E. ujhelyii*; see in e.g. Sartori and Landolt 1999, Zabric 2001). Besides newly recorded *C. luctuosa*, *L. marginata and E. karlelica*, all other species are distributed both in Pannonian lowland and Dinaric Western Balkan ecoregions (ER 11 and ER 5, *sensu* Illies 1978) and in freshwater habitats of both Black Sea and Adriatic Sea Basins. *Nigrobaetis niger* and *P. submarginata* were recorded in rivers and streams, *H. fusca* in springs, rivers and streams, *C. dipterum* in rivers, streams and lakes and *E. ujhelyii* in springs and streams (Vilenica et al. 2015). Hence, none of these species is recorded at a critically low number of localities. However, at the localities throughout Croatia where it was previously recorded, *N. niger* was present in low abundances (Vilenica et al. 2015). Yet, in our study, the species was among the dominant taxa in the Danković klada Stream.

In order to evaluate more precise conservation status and threats to each of the species, additional studies are necessary at an even higher number of freshwater habitats in Croatia.

Conclusions

With three new species records for the country, this study showed that our knowledge of the Croatian mayfly fauna is still growing. Mayfly assemblage composition and abundance in the peat bog is very impoverished and rare species can survive in such harsh environments. A number of species recorded in the adjacent stream preferably occur in lentic habitats, but can also be found in slowly flowing streams (e.g. limnophil *E. ujhelyii*, *L. marginata*, limno-rheophil *H. fusca*, *E. karelica*; Buffagni et al. 2015). However, it seems that their dispersion to the peat bog was not possible probably due to harsh environmental conditions (low pH, high oscillations of water level and temperature).

New and rare recorded species highlight the high conservation value of the Đon močvar peat bog and adjacent stream. During the 20th century, the abandonment of traditional land-management practices, such as mowing and grazing, has led to severe processes of succession in the studied peat bog. Many of the lentic habitats have decreased in size or completely disappeared, which endangers inhabiting aquatic and terrestrial assemblages. In order to preserve unique habitats and their biodiversity in the Western Balkan region, it is of a crucial importance to protect Croatian largest peat bog from rapid successional changes.

Studies on distribution, biodiversity and ecology are particularly important for conservation planning e.g. for determining the conservation status of species and defining the factors that affect biodiversity patterns (de Silva and Medellín 2001). Thereby, knowledge of mayfly faunal composition, ecology, and seasonal dynamics could contribute to the classification and protection of the peat bog habitats in Croatia.

Acknowledgements

We would like to thank Antun Alegro, Vladimir Bartovsky, Mirjana Dimnjaković, Marija Ivković, Renata Matoničkin Kepčija, Ivana Pozojević, Ana Previšić, Sandra Slivar and Marija Starčević for the field assistance. Thanks to Miran Katar for help with the artwork. This study was funded by the Institution for protected nature management of Sisak-Moslavina county, grant awarded to IT (No. 402-08/14-01/02).

References

Alain T, Belfiore C (2013) Ephemeroptera, mayflies. Fauna Europaea version 2.6.2. http://www.faunaeur.org [accessed on 20th of June, 2016]

Alba-Tercedor J (1990) Life cycles and ecology of mayflies from Sierra Nevada (Spain). Limnetica 6: 23–34.

Alegro A, Šegota V (2008) Florističke i vegetacijske značajke botaničkog rezervata „Đon močvar" u Blatuši. General technical report. State Institute for Nature Protection, Zagreb, Croatia, 33 pp. [In Croatian]

Baars J-R, Murray DA, Hannigan E, Kelly-Quinn M (2014) Macroinvertebrate assemblages of small upland peatland lakes in Ireland. Biology and Environment: Proceedings of the Royal Irish Academy 2014. doi: 10.3318/BIOE.2014.31

Battin TJ, Luyssaert S, Kaplan LA, Aufdenkampe AK, Richter A, Tranvik LJ (2009) The boundless carbon cycle. Nature Geoscience 2: 598–600. doi: 10.1038/ngeo618

Bauernfeind E, Moog O (2000) Mayflies (Insecta: Ephemeroptera) and the assessment of ecological integrity: a methodological approach. Hydrobiologia 422: 71–83. doi: 10.1023/A:1017090504518

Bauernfeind E, Humpesch UH (2001) Die Eintagsfliegen Zentraleuropas - Bestimmung und Ökologie. Verlag NMW, Wien, 239 pp.

Bauernfeind E, Soldán T (2012) The mayflies of Europe (Ephemeroptera). Apollo Books. Ollerup, Denmark, 783 pp. doi: 10.1163/9789004260887

Bick H (1989) Ökologie: Grundlagen, terrestrische und aquatische Ökosysteme, angewandte Aspekte, Gustav Fischer Verlag, Stuttgart, New York.

Brittain JE (1979) Emergence of Ephemeroptera from Øvre Heimdalsvatn, a Norwegian subalpine lake. In: Pasternak K, Sowa R (Eds) Proceedings of the 2nd International Conference on Ephemeroptera. Panstwowe Wydawnictwo Naukowe, Warszawa-Kraków, 115–123.

Brittain JE (1990) Life history strategies in Ephemeroptera and Plecoptera. In: Campbell IC (Ed.) Mayflies and Stoneflies. Kluwer Academic Publishers, 1–12. doi: 10.1007/978-94-009-2397-3_1

Brittain JE (1991) Life history characteristics as a determinant of the response of mayflies and stoneflies to man-made environmental disturbance (Ephemeroptera and Plecoptera). Proceedings of the 6th International Conference on Ephemeroptera and Plecoptera, Granada, 539–545.

Brittain JE, Sartori M (2003) Ephemeroptera (Mayflies). In: Resh VH, Cardé RT (Eds) Encyclopedia of Insects. Academic Press, Amsterdam, 373–380.

Buffagni A, Cazzola M, López-Rodríguez MJ, Alba-Tercedor J, Armanini DG (2009) Volume 3 – Ephemeroptera. In: Schmidt-Kloiber A, Hering D (Eds) Distribution and Ecological Preferences of European Freshwater Organisms, Pensoft Publishers, Sofia-Moscow, 254 pp.

Buffagni A, Armanini DG, Cazzola M, Alba-Tercedor J, López-Rodríguez MJ, Murphy J, Sandin L, Schmidt-Kloiber A (2015) Dataset "Ephemeroptera". www.freshwaterecology.info - the taxa and autecology database for freshwater organisms, version 6.0 [accessed on 30.03.2016]

Clarke KR, Warwick RM (2001) Change in marine communities: an approach to statistical analysis and interpretation. Primer-E, Lutton, United Kingdom.

Clifford HF (1982) Life cycles of mayflies (Ephemeroptera), with special reference to voltinism. Quaestiones Entomologicae 18(1–4): 15–90.

Dekić S, Ćuk R, Belfiore C (2016) Contribution to Croatian mayfly fauna (Insecta: Ephemeroptera). Natura Croatica 25(1): 101–108. doi: 10.20302/NC.2016.25.6

de Silva HG, Medellín RA (2001) Evaluating completeness of species lists for conservation and macroecology: a case study of Mexican land birds. Conservation Biology 15: 1384–1395. doi: 10.1111/j.1523-1739.2001.00177.x

Doyle G (1990) Ecology and Conservation of Irish Peatlands. In: Doyle G (Ed.) Ecology and Conservation of Irish Peatlands. Royal Irish Academy, Dublin.

Drinan TJ, Foster GN, Nelson BH, O'Halloran J, Harrison SSC (2013) Macroinvertebrate assemblages of peatland lakes: Assessment of conservation value with respect to anthropogenic land-cover change. Biological Conservation 158: 175–187. doi: 10.1016/j.biocon.2012.10.001

Elliott JM, Humpesch UH, Macan TT (1988) Larvae of the British Ephemeroptera: a key with ecological notes. Scientific Publications of the Freshwater Biological Association 49, 145.

Erba S, Melissano L, Buffagni A (2003) Life cycles of Baetidae (Insecta: Ephemeroptera) in a North Italian Prealpine stream. In: Gaino E (Ed.) Research update on Ephemeroptera & Plecoptera. Università di Perugia, Perugia, 177–186.

Fiance SB (1978) Effects of pH on the biology and distribution of *Ephemerella funeralis* (Ephemeroptera). Oikos 31: 332–339. doi: 10.2307/3543659

Gerhardt A (1990) Effects of Subacute Doses of Cadmium on pH-stressed *Leptophlebia marginata* (L.) and *Baetis rhodani* Pictet (Insecta: Ephemeroptera). Environmental Pollution 6: 29–42. doi: 10.1016/0269-7491(90)90170-H

Hannigan E, Kelly-Quinn M (2012) Composition and structure of macroinvertebrate communities in contrasting open-water habitats in Irish peatlands: implications for biodiversity conservation. Hydrobiologia 692(1): 19–28. doi: 10.1007/s10750-012-1090-4

Harper MP, Peckarsky BL (2006) Emergence cues of a mayfly in a high-altitude stream ecosystem: potential response to climate change. Ecological Applications 16(2): 612–621. doi: 10.1890/1051-0761(2006)016[0612:ECOAMI]2.0.CO;2

Illies J (1978) Limnofauna Europaea. Gustav Fischer Verlag. Stuttgart & New York, 532 pp.

Joniak T, Domek P (2006) Influence of humification on biodiversity of lake benthic macroinvertebrates. Acta Agrophysica 7(2): 363–368.

Joosten H, Clarke D (2002) Wise Use of Mires and Peatlands-Background and Principles including a Framework for Decision Making. International Mire Conservation Group, International Peat Society.

Kivinen E, Pakarinen P (1981) Geographical distribution of peat resources and major peatland complex types in the world. Suomalaisen Tiedeakatemian toimituksia Series A III Geologica-Geographica 132: 1–28.

Langheinrich U, Tischew S, Gersberg RM, Lüderitz V (2004) Ditches and canals in management of fens: opportunity or risk? A case study in the Drömling Natural Park, Germany. Wetlands Ecology and Management 12: 429–445. doi: 10.1007/s11273-004-0700-y

Limpens J, Berendse F, Blodau C, Canadell JG, Freeman C, Holden J, Roulet N, Rydin H, Schaepman-Strub G (2008) Peatlands and the carbon cycle: from local processes to global implications, a synthesis. Biogeosciences 5: 1475–1491. doi: 10.5194/bg-5-1475-2008

López-Rodríguez MJ, Tierno de Figueroa JM, Alba-Tercedor J (2008) Life history and larval feeding of some species of Ephemeroptera and Plecoptera (Insecta) in the Sierra Nevada (Southern Iberian Peninsula). Hydrobiologia 610: 277–295. doi: 10.1007/s10750-008-9444-7

López-Rodríguez MJ, Tierno de Figueroa JM, Alba-Tercedor J (2010) Comparative Study of the Nymphal Biology of Two Coexisting Species of Mayflies (Insecta: Ephemeroptera) in a Mediterranean Stream in Southern Europe. International Review of Hydrobiology 95(1): 58–71. doi: 10.1002/iroh.200811197

Malzacher P (1984) Die europäischen Arten der Gattung *Caenis* Stephens (Insecta: Ephemeroptera). The European species of the genus *Caenis* Stephens (Insecta: Ephemeroptera). Stuttgarter Beiträge zur Naturkunde, Serie A (Biologie) 373: 1–48.

Mieczan T, Tarkowska-Kukuryk M, Adamczuk M, Pęczuła W, Demetraki-Paleolog A, Niedźwiecki M (2015) Research of Different Types of Peatbogs: Relationships of Bioceonosis Structures and Physico-Chemical Parameters. Polish Journal of Environmental Studies 24(1): 191–198.

Moog O (2002) Fauna Aquatica Austriaca, Edition 2002, Wassserwirtschaftskataster, Bundesministerium für Land und Forstwirtschaft, Umwelt und Wasserwirtschaft, Vienna.

Müller-Liebenau I (1969) Revision der europäischen Arten der Gattung *Baetis* Leach, 1815. (Insecta, Ephemeroptera). Gewässer und Abwasser 66/67: 95–101.

Petrin Z (2011) Species traits predict assembly of mayfly and stonefly communities along pH gradients. Oecologia 167(2): 513–524. doi: 10.1007/s00442-011-2003-3

Raddum GG, Fjellheim A (1993) Life cycle and production of *Baetis rhodani* in a regulated river in Western Norway: comparison of pre - and post - regulation conditions. Regulated Rivers: Research and Management 8: 49–61. doi: 10.1002/rrr.3450080109

Sartori M, Landolt P (1999) Atlas de distribution des Ephémères de Suisse (Insecta, Ephemeroptera). Fauna helvetica 3. SEG-CSCF Ed., Neuchâtel.

Sartori M, Brittain JE (2015) Order Ephemeroptera. In: Thorp J, Rodgers DC (Eds) Thorp and Covich's Freshwater Invertebrates: Ecology and General Biology, 4th Edition, Academic Press, New York, 873–891. doi: 10.1016/B978-0-12-385026-3.00034-6

Schartau AK, Moe SJ, Sandin L, McFarland B, Raddum GG (2008) Macroinvertebrate indicators of lake acidification: analysis of monitoring data from UK, Norway and Sweden. Aquatic Ecology 42(2): 293–305. doi: 10.1007/s10452-008-9186-7

Spitzer K, Danks HV (2006) Insect biodiversity of boreal peat bogs. Annual Review of Entomology 51: 137–61. doi: 10.1146/annurev.ento.51.110104.151036

Šegota T, Filipčić A (2003) Köppenova podjela klima i hrvatsko nazivlje. Geoadria 8/1: 17-23. [In Croatian]

Ternjej I, Alegro A, Brigić A, Gottstein S, Kerovec M, Matoničkin Kepčija R, Šegota V, Previšić A, Vilenica M, Lajtner J, Antonović I, Starčević M, Bujan J (2015) Revitalizacija cretnog staništa posebnog botaničkog rezervata Đon-Močvar. Croatian Botanical Society, Zagreb, 138 pp. [In Croatian]

Topić J, Stančić Z (2006) Extinction of fen and bog plants and their habitats in Croatia. Biodiversity and Conservation 15: 3371–3381. doi: 10.1007/s10531-005-4874-2

Vilenica M, Gattolliat J-L, Mihaljević Z, Sartori M (2015) Croatian mayflies (Insecta, Ephemeroptera): species diversity and distribution patterns. ZooKeys 523: 99–127. doi: 10.3897/zookeys.523.6100

Vilenica M, Previšić A, Ivković M, Popijač A, Vučković I, Kučinić M, Kerovec M, Gattolliat J-L, Sartori M, Mihaljević Z (2016) Mayfly (Insecta: Ephemeroptera) assemblages of a regulated perennial Mediterranean river system in the Western Balkans. Biologia 71(9): 1038–1048. doi: 10.1515/biolog-2016-0121

Więcek M, Martin P, Gąnka M (2013) Distribution patterns and environmental correlates of water mites (Hydrachnidia, Acari) in peatland microhabitats. Experimental and Applied Acarology 61(2): 147–160. doi: 10.1007/s10493-013-9692-8

Zabric D (2001) Analiza stanja biotske raznovrsnosti enodnevnic (Ephemeroptera). Ekspertne študije za Pregled stanja biotske raznovrsnosti in krajinske pestrosti v Sloveniji. Agencija Republike Slovenije za okolje, Ljubljana, 116–122. [In Slovenian]

Zaninović K, Gajić-Čapka M, Perčec Tadić M, Vučetić M, Milković J, Bajić A, Cindrić K, Cvitan L, Katušin Z, Kaučić D, Likso T, Lončar E, Lončar Ž, Mihajlović D, Pandžić K, Patarčić M, Srnec L, Vučetić V (2008) Klimatski atlas Hrvatske / Climate atlas of Croatia 1961–1990, 1971–2000. Državni hidrometeorološki zavod, Zagreb, 200 pp.

Zedková B, Rádková V, Bojková J, Soldán T, Zahrádková S (2015) Mayflies (Ephemeroptera) as indicators of environmental changes in the past five decades: a case study from the Morava and Odra River Basins (Czech Republic). Aquatic Conservation: Marine and Freshwater Ecosystems 25(5): 622–638. doi: 10.1002/aqc.2529